

**System-oriented approach for catchment characterization
in terms of typical landscape subunits based on
the geophysical models**

Dissertation

der Mathematisch-Naturwissenschaftlichen Fakultät
der Eberhard Karls Universität Tübingen
zur Erlangung des Grades eines
Doktors der Naturwissenschaften
(Dr. rer. nat.)

vorgelegt von
Dipl.-Geoph. Tatiana Feskova
aus Kaliningrad / Russland

Tübingen
2015

Tag der mündlichen Qualifikation:

27.01.2016

Dekan:

Prof. Dr. Wolfgang Rosenstiel

1. Berichterstatter:

Prof. Dr. Peter Dietrich

2. Berichterstatter:

Prof. Dr. Erwin Appel

This dissertation is dedicated to my geophysicist parents

Эта диссертация посвящается моим родителям геофизикам

„To strive, to seek, to find, and not to yield,“ - from “Ulysses” of Alfred, Lord Tennyson

*“Anything that arranges the nature itself is good at any intention.
The whole nature in general is really nothing more than a connection of phenomena
according to rules; and there is no randomness everywhere,“* - Immanuel Kant

“In the living nature nothing happening that is not in the connection with the whole,“ -
Johann Wolfgang von Goethe

“... the loveliest and saddest landscape in the world ...” -
from “The Little Prince” of Antoine de Saint Exupéry

Abstract

Hydrological conditions in a catchment depend on many factors such as climatic, geological, geomorphological, biological and human, which interact with each other and influence water balance in a catchment. This interaction leads to the subordination in the landscape structure, namely the weak elements subordinate to the powerful elements. Thereby, geological and geomorphological factors play an essential role in catchment development and organization, because the main lithological features keep their properties in the landscape structure during a long time. We consequently can allocate a hillslope to one class of the representative units because the important flow processes run at the hillslope. Moreover, we can subdivide a hillslope into stratigraphic subsurface units and significant hillslope areas based on the lithological change of contrasting interfaces. The knowledge of subsurface structures is necessary to understand and predicate complex hydrological processes in a catchment. Geophysical techniques provide a good opportunity to explore the subsurface.

It is impossible to achieve a complete geophysical investigation of subsurface in a catchment with difficult environmental conditions because of large time effort in the field, equipment logistic, and ambiguity in the data interpretation. The research study demonstrates how we can investigate a catchment using geophysical methods in an effective manner in terms of characterization across representative units with respect to a functional role in the catchment. This research study aims to develop combined resistivity and seismic velocity hillslope subsurface models for the distinction of representative functional units.

In order to identify the contrasting interfaces of the hillslope, to localize significant hillslope areas, and to address the ambiguity in the geophysical data interpretation, the research study combined resistivity surveys (vertical electrical soundings and electrical resistivity tomography) with refraction seismic method, and conducted these measurements at one single profile along the hillslope transect and perpendicular to this transect. The measurements along the hillslope transect deliver the two-dimensional hillslope section of resistivity and seismic velocity distribution with contrasting stratigraphic interfaces, whereas the measurements perpendicular to the hillslope transect obtained from vertical electrical soundings survey localize significant hillslope areas indicating existence of two-dimensional features in the subsurface.

To demonstrate the suitability of the suggested approach, we carried out resistivity and refraction seismic measurements at two hillslopes with different environmental conditions (geology, geomorphology, slope inclination, land use). The first hillslope is locating in the forested Weierbach catchment in the Ardennes massif, the mid-western part of the Grand Duchy of Luxembourg. The second hillslope is placing in the grassland Schaefertal catchment in the Lower Harz, the Central Germany. Besides, both hillslopes are characterized by Pleistocene periglacial slope deposits, which plays an important role in the ecosystem functioning.

The obtained resistivity and seismic hillslope models for each study site complement well one another. The hillslope models identify significant hillslope areas along the hillslope called as elementary functional units, and electrical vertical stratigraphic units and seismic vertical stratigraphic units that agree with lithological stratigraphy of these study sites.

Therefore, the suggested geophysical approach is suitable to characterise a hillslope as the representative unit only at a single transect in the efficient manner in contrast to the expensive 3D-measurements.

In conclusions, to amplify the suitability of this approach, we constructed the geophysical hillslope model in the three-dimensional image using an additional cross profile. This three-dimensional image proves the correctness of our approach. Based on the obtained results, we can provide a conceptual hydrogeological model of the representative hillslope.

Zusammenfassung

Die hydrologische Gegebenheiten in einem Flusseinzugsgebiet hängen von verschiedenen Faktoren ab wie klimatischen, geologischen, geomorphologischen, biologischen und menschlich verursachten. Diese Faktoren wirken wechselseitig aufeinander und beeinflussen die komplette Wasserbalance in einem Flusseinzugsgebiet. Diese Wechselwirkungen führen zu einer Unterordnung schwacher Elemente unter energetisch stärkere Elemente in der Struktur einer Landschaft. Geologische und geomorphologische Faktoren spielen dabei eine wesentliche Rolle in der Entstehung, Entwicklung und Organisation eines Flusseinzugsgebiets, weil lithologische Strukturen ihre Eigenschaften in der Landschaft-Struktur über einen längeren Zeitraum erhalten können. Da am Hang wichtige Abflussprozesse ablaufen, kann einen Hang zu einer Klasse der repräsentativen Einheiten zugeordnet werden. Zudem kann ein Hang aufgrund der lithologischen Änderung der Kontrastgrenzen im Untergrund in lithostratigraphische Untergrundeinheiten und spezifische Hangflächen aufgegliedert werden. Die Kenntnisse über Untergrundstrukturen sind bedeutsam für das Verständnis und eine Vorhersage von hydrologischen Prozessen in einem Flusseinzugsgebiet. Geophysikalische Methoden bieten eine gute Möglichkeit, den Untergrund zu erkunden.

Eine komplette geophysikalische Erkundung des Untergrundes in einem Flusseinzugsgebiet mit schwierigen Umweltbedingungen kann aufgrund eines längeren Zeitaufwands im Feld, der Logistik der Ausrüstung und der Mehrdeutigkeit in der Interpretation geophysikalischer Daten niemals vollständig erreicht werden. Die Forschungsarbeit demonstriert, wie ein Flusseinzugsgebiet auf eine effiziente Art und Weise mit geophysikalischen Methoden im Sinne von einer Charakterisierung über typische Landschaftseinheiten in Hinsicht auf eine funktionale Rolle in dem Flusseinzugsgebiet erkundet werden kann. Das Ziel dieser Forschungsarbeit ist, ein geophysikalisches Hangmodell durch die kombinierte Interpretation geoelektrischer und seismischer Daten zur Unterscheidung typischer funktionaler Einheiten zu entwickeln.

Zur Identifizierung der Kontrastgrenzen im Untergrund eines Hanges, zur Lokalisierung der signifikanten Hangflächen und zum Befassen der Mehrdeutigkeit in der Interpretation geophysikalischer Daten wurden geoelektrische Methoden (vertikale elektrische Sondierung und elektrische Widerstandtomographie) mit Refraktionsseismik kombiniert. Die Messungen erfolgten lediglich auf einem Profil entlang des Hanges und quer zum Hang. Die Messung entlang des Hangprofils liefert eine zwei-dimensionale Hangsektion der Verteilung des elektrischen spezifischen Widerstands und der seismischen Geschwindigkeiten. Die Messung quer zum Hangprofil lokalisiert signifikante Hangflächen, die auf die Anwesenheit der zwei-dimensionalen Körper hindeuten.

Zur Demonstration der Eignung des vorgeschlagenen Ansatzes werden geoelektrische und refraktionsseismische Messungen auf zwei Hängen mit unterschiedlichen Umweltbedingungen (Geologie, Geomorphologie, Hangneigung, Landnutzung) durchgeführt. Der erste Hang befindet sich im bewaldeten Weierbach-Flusseinzugsgebiet in den Ardennen im Westen des Großherzogtums

Luxemburg. Der zweite Hang liegt in einer Grass-Landschaft im Schäfertal-Flusseinzugsgebiet im Unteren Harz in Deutschland. Beide Hänge sind durch pleistozänen periglazialen Hangschutt charakterisiert, der eine wichtige Rolle im Funktionieren eines Ökosystems spielt.

Die erhaltenen geoelektrischen und seismischen Hangmodelle für jeden Standort ergänzen sich einander gut. Geophysikalische Hangmodelle identifizieren sowohl signifikante Fläche entlang des Hangs, als auch elektrische und seismische vertikale stratigraphische Einheiten, die mit der lithologischen Stratigraphie beider Standorte übereinstimmen.

Somit ist der vorgeschlagene geophysikalische Ansatz zur Hangcharakterisierung als eine repräsentative Einheit auf nur einem Profil auf eine effiziente Art gut geeignet im Vergleich zu aufwendigen drei-dimensionalen Messungen.

Zum Schluss wird das geophysikalische Hangmodell in der drei-dimensionalen Darstellung mit Hilfe eines zusätzlichen Querprofils erstellt. Somit wird die Zuverlässigkeit des angewendeten Ansatzes geprüft. Die konzeptuellen hydrogeologischen Modelle können basierend auf den erstellten geophysikalischen Modellen aufgebaut werden.

Аннотация

Гидрологические условия речного бассейна зависят от самых различных моментов. Речь идет о климатических, геологических, геоморфологических, биологических, а также об антропогенных факторах, которые взаимодействуют между собой и влияют на водный баланс в речном водоразделе. Такое взаимодействие привело к следующей иерархии в структуре ландшафта: слабые компоненты ландшафта подчиняются наиболее сильному. При этом геологический и геоморфологический факторы выступают как одни из ведущих при формировании, развитии и организации ландшафта, поскольку благодаря им, ландшафт может сохранять свои главные свойства на протяжении длительного времени. По причине того, что основные водные массы стекают по склонам речных долин, мы рассматриваем склон как один из классов ландшафтной иерархии. В довершение всего, на основании литологических изменений, мы можем также подразделить склон на вертикальные и на латеральные структурные единицы. Дабы лучше понять и предсказать гидрологические процессы, протекающие в речном водоразделе, необходима исчерпывающая информация о его подземных недрах с применением геофизических исследований. Подобные исследования целого речного бассейна редко будет иметь подобающий результат, потому как напрямую связаны с временными затратами в процессе длительных полевых работ, с труднореализуемой логистикой геофизического оборудования, а также с частой многозначностью толкования геофизических данных. Данная научная работа предлагает эффективный подход для исследования подземных недр речного бассейна геофизическими методами с точки зрения подразделения его на ландшафтные единицы, несущие важное функциональное значение. Задачей настоящей исследовательской работы является построение комбинированной геофизической склоновой модели, с использованием методов электрического сопротивления и техники преломленных сейсмических волн для обнаружения типичных ландшафтных функциональных единиц.

С целью опознать контрастные границы в вертикальной структуре склона и выделить особые зоны с учетом многозначности геофизических данных, в настоящей научной работе были выполнены комбинированные геофизические исследования с применением вертикального электрического зондирования, электротомографии и сеймики преломленных волн на одном профиле вдоль склона и поперек склона. Геофизические исследования (электротомография и сеймика) вдоль склона представлены в виде двухмерного склонового разреза, иллюстрирующего распределение электрических и сейсмических свойств недр. Вертикальное электрическое зондирование поперек склона дало возможность локализовать особые зоны, указывающие на наличие двухмерных структур в вертикальном разрезе.

Для установления надежности предлагаемого метода, нами были проведены геофизические исследования на двух склонах, характеризующихся разными природными условиями (геология, геоморфология, наклон, землепользование). Первый склон расположен в

лесном речном бассейне Вайербах в Арденнах, Великое Герцогство Люксембург. Второй склон находится в луговом речном бассейне Шэферталь в Нижнем Гарце, в Германии. Следует отметить наличие у обоих объектов плейстоценовых перигляциальных склоновых отложений, играющих немаловажную роль в функционировании экологических систем.

Полученные электрические и сейсмические модели склона для каждого случая хорошо дополняют друг друга. Геофизические склоновые модели определяют особые зоны вдоль склона, а также вертикальные электрические и сейсмические единицы стратиграфической структуры, согласованные с литологическим строением.

Таким образом, предложенный в данной научной работе геофизический метод исследования в целях изучения склоновой структуры в качестве типичной ландшафтной единицы на одном профиле, дает надежные и достоверные результаты. Следует подчеркнуть: вышеприведенное утверждение позволяет считать подобный метод более рациональным по сравнению с трехмерными исследованиями.

В заключение данной работы, мы построили трехмерную структурную геофизическую модель склона, с использованием дополнительного поперечного профиля. На основании этого, нами была также сформирована концептуальная гидро-геологическая модель. Следовательно, можно с достаточной точностью сделать вывод, что такая модель как нельзя лучше подтверждает надежность предложенного метода.

Contents

Abstract.....	I
Zusammenfassung	III
Аннотация.....	V
Contents	VII
List of Figures.....	IX
List of Tables	XIV
List of Figures in Appendix	XV
List of Symbols.....	XVI
List of Abbreviations	XVII
1 Introduction	1
1.1 The Russian landscape school.....	2
1.2 The West landscape school	4
1.3 Ground geophysical application for hillslope characterization	5
1.3.1 The application of geo-electric	6
1.3.2 The application of refraction seismic	6
1.3.3 The combined application of resistivity and refraction seismic surveys.....	7
1.4 Research objectives and structure of this monograph	8
2 Research philosophy of the landscape system and the research.....	11
2.1 State of the art and understanding landscape as complex system	11
2.2 Hillslope as a functional unit to understand processes in catchment	17
2.3 Catchment investigation from geophysical perspectives	21
3 Study sites.....	25
3.1 Weierbach catchment	25
3.2 Schaefertal catchment	27
4 Methodology	31
4.1 Geo-electrical survey.....	33
4.1.1 Vertical electrical soundings	34
4.1.2 Electrical resistivity tomography.....	38
4.1.3 VES versus ERT, and versus Combination.....	40
4.2 Refraction seismic	42
4.2.1 The theoretical background of refraction seismic (RS).....	42
4.2.2 Experimental composition.....	45
4.3 Geo-electric versus refraction seismic, and versus Combination.....	54
4.4 Joint three-dimensional interpretation of the investigated hillslope.....	55

Contents

5 Results and discussions	56
5.1 Geo-electrical investigation.....	56
5.1.1 Application in the Weierbach catchment	56
5.1.2 Application in the Schaeferfetal catchment.....	63
5.2 Refraction seismic investigation	70
5.2.1 Application in the Weierbach catchment	70
5.2.2 Application in the Schaeferfetal catchment.....	79
5.3 Geo-electric versus refraction seismic, and versus combination.....	91
5.3.1 Application in the Weierbach catchment	91
5.3.2 Application in the Schaeferfetal catchment.....	94
5.4 Joint three-dimensional interpretation of the investigated hillslope.....	97
5.4.1 Application in the Weierbach catchment	97
5.4.2 Application in the Schaeferfetal catchment.....	101
6 Discussions of the design of the hydrogeological conceptual model	105
7 Conclusion.....	110
Bibliography	114
Appendix A.....	123
Appendix B	125
Appendix C	127
Appendix D.....	129
Appendix E	131
Acknowledgments	132
Contribution	133
Affidavit.....	134
Biographical sketch.....	135

List of Figures

Figure 2-1: Conceptual diagram representing the landscape as an open interactive system	12
Figure 2-2: Flow chart for multidisciplinary catchment characterization in terms of landscape units	19
Figure 3-1: Location of a representative hillslope (the orange line) at the Weierbach catchment study site in the hydrological observatory Atttert Basin (the red line in the north-west graph), the mid-western part of Grand Duchy of Luxembourg.....	26
Figure 3-2: Digital elevation model of the representative hillslope at the Weierbach catchment study site	27
Figure 3-3 Location of a representative hillslope (the orange line) at the Schaeferfartal catchment study site in the Lower Harz, the Central Germany (the north-west graph)	28
Figure 3-4: Groundwater level (in absolute height) at the TERENO Soil-Network hillslope at the Schaeferfartal catchment study site.....	29
Figure 3-5: Digital elevation model of the representative hillslope at the Schaeferfartal catchment study site	30
Figure 4-1: Measuring layout to combine geo-electrical and refraction seismic techniques for the characterization of a representative hillslope.....	31
Figure 4-2: Flow chart for geophysical investigation of a representative hillslope in a catchment in an effective manner	32
Figure 4-3: Refraction ray paths and travel time curves modified from (Telford, Geldart und Sheriff 1990)	43
Figure 4-4: The principle of the “Plus-Minus” method developed by (Hagedoorn 1959)	50
Figure 5-1: The case study of the Weierbach catchment: Sounding curves of Schlumberger and Half-Schlumberger measurements (the left diagram) at the ERT profile 0 meter presenting an example for lateral homogeneity perpendicular to the ERT profile, and their inversion result with equivalent models (the right graph)	57
Figure 5-2: The case study of the Weierbach catchment: Sounding curves of Schlumberger and Half-Schlumberger measurements (the left diagram) at the ERT profile 75 meter indicating significant shallow heterogeneity perpendicular to the ERT profile, and their inversion results with equivalent models (three graphs at the right site). The central graph of the inversion results presents Schlumberger measurement, whereas the left graph from the central graph is HSB for WNW-site, and the right graph from the central graph is HSB for ESE-site	58
Figure 5-3: The case study of the Weierbach catchment: Geo-electrical investigation using ERT slope profile (the upper diagram) perpendicular to the Weierbach creek, and VES-spreading (the below diagram) parallel oriented to the creek. The VES results for locations with lateral homogeneity perpendicular to the ERT profile are drawn with bold line	59

List of Figures

Figure 5-4: The case study of the Weierbach catchment: Box-whisker plots of resistivity (the left diagrams) and thickness (the right diagrams) distribution downhill as well as over the width of the hillslope in terms of EFU's.....	61
Figure 5-5: The case study of the Weierbach catchment: Interpretation of VES results in terms of ESU's	62
Figure 5-6: The case study of the Weierbach catchment: Comparison of ERT and VES results of the first and second interfaces	63
Figure 5-7: The case study of the Schaeferfalta catchment: Sounding curves of Schlumberger and Half-Schlumberger measurements (the left diagram) at the ERT profile 75 meter presenting an example for lateral homogeneity perpendicular to the ERT profile, and their inversion result with equivalent models (the right graph)	64
Figure 5-8: The case study of the Schaeferfalta catchment: Sounding curves of Schlumberger and Half-Schlumberger measurements (the left diagram) at the ERT profile 15 meter illustrating a light shallow heterogeneity perpendicular to the ERT profile, and their inversion results with equivalent models (three graphs at the right site). The central graph of the inversion results presents Schlumberger measurement, whereas the left graph from the central graph is HSB for West-site, and the right graph from the central graph is HSB for East-site.....	65
Figure 5-9: The case study of the Schaeferfalta catchment: Resistivity results of ERT slope profile (the upper diagram) perpendicular to the Schaeferbach creek, and VES-spreading (the below diagram) parallel oriented to the creek. The VES results for locations with lateral homogeneity perpendicular to the ERT profile are drawn with bold line.....	67
Figure 5-10: The case study of the Schaeferfalta catchment: Box-whisker plots of resistivity (the left diagrams) and thickness (the right diagrams) distribution downhill as well as over the width of the hillslope in terms of EFU's.....	68
Figure 5-11: The case study of the Schaeferfalta catchment: Interpretation of VES results in terms of ESU's	69
Figure 5-12: The case study of the Schaeferfalta catchment: Comparison of ERT and VES results of the first and second interfaces.....	70
Figure 5-13: The case study of the Weierbach catchment: Refraction seismic travel-time data interpretation using Plus-Minus technique of two symmetrical wave fronts. (a) the travel time diagram with slowness slopes; (b) the diagram of calculated Plus-time values; (c) the diagram of calculated Minus-time values with seismic velocity slope. Structural subsurface models for assumed seismic velocity models (d) without topography and (e) with topography	72
Figure 5-14: The case study of the Weierbach catchment: The refraction seismic tomography results of the slope profile perpendicular to the Weierbach creek in terms of seismic velocity (the upper diagram) and slowness (the below diagram).....	73

List of Figures

- Figure 5-15: The case study of the Weierbach catchment: The refraction seismic results of the slope profile perpendicular to the Weierbach creek based on the ray tracing FD modelling using four shots as case of two layer model: (1) the ray paths (coloured lines) with measured (black lines) and calculated (coloured crosses) travel time of the direct wave and the head wave (the upper diagram); (2) the constructed two-layer subsurface model and measured travel time with seismic velocity slopes(the below diagram)75
- Figure 5-16: The case study of the Weierbach catchment: The refraction seismic results of the slope profile perpendicular to the Weierbach creek based on the ray tracing FD modelling using all shots as case of two layer model: (1) the ray paths (coloured lines) with measured (black lines) and calculated (coloured crosses) travel time of the direct wave and the head wave (the upper diagram); (2) the constructed subsurface two-layer model and measured travel time with seismic velocity slopes(the below diagram)77
- Figure 5-17: The case study of the Weierbach catchment: The hillslope refraction seismic subsurface model in terms of SVU's compares results obtained with ray tracing and plus-minus methods.....78
- Figure 5-18: The case study of the Schaeferfalta catchment: Refraction seismic travel time data interpretation using Plus-Minus technique of two symmetrical wave fronts. (a) the travel time diagram with slowness slopes; (b) the diagram of calculated Plus-time values; (c) the diagram of calculated Minus-time values with seismic velocity slope. The structural subsurface models for assumed seismic velocity models (d) without topography and (e) with topography80
- Figure 5-19: The case study of the Schaeferfalta catchment: The refraction seismic tomography results of the slope profile perpendicular to the Schaeferbach creek in terms of seismic velocity (the upper diagram) and slowness (the below diagram)82
- Figure 5-20: The case study of the Schaeferfalta catchment: The refraction seismic results of the slope profile perpendicular to the Schaeferbach creek based on the ray tracing FD modelling using four shots as the case of two-layer model: (1) the ray paths (coloured lines) with measured (black lines) and calculated (coloured crosses) travel time of the direct wave and the head wave (the upper diagram); (2) the constructed two-layer subsurface model and measured travel time with seismic velocity slopes(the below diagram)83
- Figure 5-21: The case study of the Schaeferfalta catchment: The refraction seismic results of the slope profile perpendicular to the Schaeferbach creek based on the ray tracing FD modelling using all shots as case of two-layer model: (1) the ray paths (coloured lines) with measured (black lines) and calculated (coloured crosses) travel time of the direct wave and the head wave (the upper diagram); (2) the constructed subsurface two-layer model and measured travel time with seismic velocity slopes(the below diagram)85
- Figure 5-22: The case study of the Schaeferfalta catchment: The refraction seismic results of the slope profile perpendicular to the Schaeferbach creek based on the ray tracing FD modelling using two shots as case of three-layer model for the upper slope: (1) the ray paths (coloured lines) with measured (black

List of Figures

lines) and calculated (coloured crosses) travel time of the direct wave and the head wave (the upper diagram); (2) the constructed subsurface two-layer model and measured travel time with seismic velocity slopes(the below diagram)	87
Figure 5-23: The case study of the Schaeferfalta catchment: The refraction seismic results of the slope profile perpendicular to the Schaeferbach creek based on the ray tracing FD modelling using all shots as case of three-layer model for the upper slope: (1) the ray paths (coloured lines) with measured (black lines) and calculated (coloured crosses) travel time of the direct wave and the head wave (the upper diagram); (2) the constructed subsurface two-layer model and measured travel time with seismic velocity slopes(the below diagram)	88
Figure 5-24: The case study of the Schaeferfalta catchment: The hillslope refraction seismic subsurface models in terms of SVU's as two-layer model (the upper diagram) and three-layer model (the central diagram). The below diagram demonstrates the depth difference between these models for the lower refractor.....	90
Figure 5-25: The case of the Weierbach catchment: The transparent comparison of layer interface between ERT, VES and RS (the upper diagram). The depth difference between VES and RS (the below diagram)	91
Figure 5-26: The case study of the Weierbach catchment: The hillslope subsurface models as joint geophysical interpretation in terms of ESU's, EFU's and SVU's	93
Figure 5-27: The case of the Schaeferfalta catchment: The transparent comparison of layer interface between ERT, VES and RS (the upper diagram). The depth difference between VES and RS (the below diagram)	95
Figure 5-28: The case study of the Schaeferfalta catchment: The hillslope subsurface models as joint geophysical interpretation in terms of ESU's, EFU's and SVU's	96
Figure 5-29: The case study of the Weierbach catchment: The transparent comparison of layer interfaces between ERT, VES and RS of the hillslope profile parallel to the slope inclination	98
Figure 5-30: The case study of the Weierbach catchment: The refraction seismic model of the second geophysical profile perpendicular to the hillslope inclination in terms of SVU's	98
Figure 5-31: The case study of the Weierbach catchment: The transparent comparison of layer interfaces between ERT, VES and RS of the second geophysical profile perpendicular to the hillslope inclination (the upper diagram). The sounding curves of Schlumberger and Half-Schlumberger measurements (the below diagram) at the hillslope profile 50 meter presenting lateral homogeneity perpendicular to the slope inclination	99
Figure 5-32: The case study of the Weierbach catchment presents the three-dimensional interpretation of the representative hillslope in terms of SVU's	100
Figure 5-33: The case study of the Schaeferfalta catchment: The transparent comparison of layer interfaces between ERT, VES and RS of the hillslope profile parallel to the slope inclination	101

List of Figures

Figure 5-34: The case study of the Schaefertal catchment: The refraction seismic model of the second geophysical profile perpendicular to the hillslope inclination in terms of SVU's	102
Figure 5-35: The case study of the Schaefertal catchment: The transparent comparison of layer interfaces between ERT, VES and RS of the second geophysical profile perpendicular to the hillslope inclination (the upper diagram). The sounding curves of Schlumberger and Half-Schlumberger measurements (the below diagram) at the hillslope profile 50 meter presenting shallow heterogeneity perpendicular to the slope inclination.....	103
Figure 5-36: The case study of the Schaefertal catchment presents three-dimensional interpretation of the representative hillslope in terms of SVU's	104
Figure 6-1: The conceptual hydro-geological model of the representative north-facing hillslope locating in the Weierbach catchment.....	107
Figure 6-2: The conceptual hydro-geological model of the representative north-facing hillslope locating in the Schaefertal catchment for the wet state.....	108
Figure 7-1: Comparison of horizontal and vertical survey scales achievable in 1 day by three-person field team for RS, ERT and VES demonstrates time effort in hours for the complex accessible terrain (like forest with changeable topography) using a single profile	112

List of Tables

Table 1-1: Landscape classification according to the Russian landscape school (Mamaj 2013)	3
Table 2-1: Perspectives on catchments under change described by (Ehret, et al. 2014)	13
Table 2-2: The suggested research program to develop landscape model for the case “catchment”	16
Table 2-3: Landscape classification according to the Nikolaev’s concept (Nikolaev 2006)	18
Table 2-4: Link between Geophysics and Hydrology focused on geo-electrical and seismic surveys....	23
Table 4-1: The acquisition field parameters of geo-electrical investigations at two study sites (explanation see in the chapters 4.1.1 and 4.1.2)	35
Table 4-2: Estimation of the investigated depth (ID) according to the rule of the thumb (Kirsch 2006)	38
Table 4-3: Comparison of ERT and VES techniques (explanation see in the chapters 4.1.1 and 4.1.2)	41
Table 4-4: The acquisition field parameters of refraction seismic at two study sites	46
Table 4-5: Summarization of applied geophysical methods	54
Table 5-1: The case study of the Weierbach catchment: The interpreted ESU’s	62
Table 5-2: The case study of the Schaeferfetal catchment: The interpreted ESU’s	69
Table 5-3: The case study of the Weierbach catchment: Ray parameters and seismic velocities to develop subsurface models using PMM	71
Table 5-4: The case study of the Weierbach catchment: Seismic subsurface parameters obtained with the ray tracing FD modelling for both cases	78
Table 5-5: The case study of the Schaeferfetal catchment: Ray parameters and seismic velocities to develop subsurface models using PMM	81
Table 5-6: The case study of the Schaeferfetal catchment: Seismic subsurface parameters obtained with the ray tracing FD modelling for the scenario of the two-layer model	86
Table 5-7: The case study of the Schaeferfetal catchment: Seismic subsurface parameters obtained with the ray tracing FD modelling for the scenario of the three-layer model applied for the upper slope	89
Table 5-8: The case study of the Schaeferfetal catchment: Comparison of seismic velocity values between two-layer model and three-layer model for the upper slope	89
Table 5-9: The case study of the Weierbach catchment: Comparison of geophysical units	92
Table 5-10: The case study of the Schaeferfetal catchment: Comparison of geophysical units	95
Table 6-1: Description of the conceptual hydro-geological model for the case study the Weierbach catchment (see the Figure 6-1)	107
Table 6-2: Description of the conceptual hydro-geological model for the case study the Schaeferfetal catchment (see the Figure 6-2)	108
Table 7-1: The applied geophysical techniques to develop the system-oriented geophysical approach	111

List of Figures in Appendix

A - 1: The case study of the Weierbach catchment: RMS-fitting of the VES inversion	123
A - 2: The case study of the Schaefertal catchment: RMS-fitting of the VES inversion.....	124
B - 1: The case study of the Weierbach catchment: Unfiltered seismograms for the shot position at the profile meter 0 (the upper diagram) and for the shot position at the profile meter 95 (the middle diagram); and filtered seismogram with band-pass filter: lower cut-off 10 Hz and upper cut-off 75 Hz for the shot position at the profile meter 95 (the below diagram).....	125
B - 2: The case study of the Schaefertal catchment: Unfiltered seismograms for the shot position at the profile meter 1 (the upper diagram) and for the shot position at the profile meter 96 (the middle diagram); and filtered seismogram with band-pass filter: lower cut-off 15 Hz and upper cut-off 120 Hz for the shot position at the profile meter 96 (the below diagram).....	126
C - 1: The case study of the Weierbach catchment: 1D-VSP-modelling for the shot position at profile meter 0 (the upper diagram), 50 (the middle diagram) and 95 (the below diagram) in terms of two layers	127
C - 2: The case study of the Schaefertal catchment: 1D-VSP-modelling for the shot position at profile meter 1 (the upper diagram), 48 and 49 (the middle diagrams), and 96 (the below diagram) in terms of two layers.....	128
D - 1: The case study of the Weierbach catchment: 1D-VSP-modelling for the shot position at profile meter 0 (the upper diagram) and 95 (the below diagram) in terms of three layers.....	129
D - 2: The case study of the Schaefertal catchment: 1D-VSP-modelling for the shot position at profile meter 1 (the upper diagram) and 48 (the below diagram) in terms of three layers for the upslope	130
E - 1: The satellite image presents a possible geological-geomorphological 2D-feature at the Schaefertal study site	131

List of Symbols

A / B	Symmetrical shot point A / B
AB	Spacing between two current electrodes A and B
δ	Delay time
δ_s / δ_r	Delay time at the shot point / geophone
H	Entropy
I_{AB}	Current sending to electrode pair AB
J	Joule
K	Kelvin
k	Geometric or configuration factor
k_B	Boltzmann constant
MN	Spacing between two potential electrodes M and N
Θ_c	Critical angle
Ω	Ohm
p	Ray parameter or slowness
ρ_a	Apparent specific resistivity
p_i	Probability in the i -microstate
Q_{rev}	Reversible transfer of the heat
S/N	signal-to-noise ratio
T	Absolute temperature
T^+ / T^-	Time plus / minus values
t_A / t_B	Observer travel time from the shot point A / B
t_{AB}	Total travel time from the shot point A to B and reverse
$t_{\text{direct wave}}$	Time of direct wave
t_g	Observed refraction time at the geophone
$t_{\text{head wave}}$	Time of head wave
t_i	intercept time
V_n	Seismic velocity for n -layer
V_{MN}	Potential difference or voltage measured at electrode pair MN
x	Offset / distance
x_c	Critical distance
x_{co}	Crossover distance
Δx	Horizontal increment
z	Depth
Δz	Vertical increment

List of Abbreviations

BPL	Basal periglacial layer
CAOS	Catchments As Organised Systems
CATFLOW	Physical-based hydrological model
CMP	Common midpoint
DC	Direct current
DD	Dipole-Dipole array
DFG	National Research Fund of Germany / Deutsche Forschungsgemeinschaft
EFU	Elementary functional unit
EMI	Electro-magnetic induction
ERT	Electrical resistivity tomography
ESU	Electro-stratigraphic unit
FD	Finite difference method
FNR	National Research Fund of Luxembourg
GPR	Ground penetration radar
HGU	Hydro-geomorphic unit
HRU	Hydrological response unit
HSC	Half-Schlumberger array
ID	Investigated depth
IPL	Intermediate periglacial layer
LTLU	Locale topological landscape unit
LTU	Lateral topological unit
LVL	Low velocity layer
MGOS	Multi-Geodes Operation System
NSZ	Near surface zone
PD	Pol-Dipole array
PMM	Plus-Minus Method
PP	Pol-Pol array
PPSDs	Pleistocene periglacial slope deposits
REW	Representative elementary watershed
REV	Representative elementary volume
RMSD	Root-mean-square deviation
RS	Refraction seismic
RST	Refraction seismic tomography

List of Abbreviations

SC	Schlumberger array
SoilNet	Hybrid wireless sensor network
STD	Standard deviation error
STU	Soil-topographic unit
SVU	Seismic velocity unit
TERENO	Terrestrial Environmental Observatories
TOPMODEL	Rainfall-runoff model based on topography
UPL	Upper periglacial layer
VES	Vertical electrical soundings
VSP	Vertical seismic profiling
WF	Wave front
WN	Wenner-Alpha array

1 Introduction

It is the recognized fact that our environmental house known as the Earth planet represents a hierarchical system (Blöschl, Thybo and Savenije 2015), where all elements from micro-levels to macro-levels interact with each other and develop the whole earth landscape structure. Each element has a particular role and function in the landscape structure and developing at the local and regional as well as global scale. The act and the interaction between all these elements occur in compliance with the physical rules. Moreover, the hierarchical principle operates on spatial as well as chronological scales. The citations of Immanuel Kant and Johann Wolfgang von Goethe introducing this monograph also confirm the fact on the nature organisation.

Consequently, we can consider a catchment as a hierarchical system, where climatic, geological, geomorphological, hydrological, biological and human factors interact with each other and create the catchment form and structure. This interaction influences the total water balance in the catchment. Thereby, the lithology-geological and geomorphological factors play a fundamental role in the catchment developing and functioning because of the keeping the main geological features during the long time. The topography and the subsurface structures also control the complex interaction between surface and the subsurface flows (Freeze 1972; Shahedi 2008). Geophysical techniques provide a good opportunity, to explore the underground structures for the understanding of the complex flow processes.

A complete geophysical investigation of the subsurface structures in a catchment with the difficult environmental conditions never will be economical feasible because of large time effort in the field, equipment logistic, and ambiguity in the data interpretation. However, to characterize the catchment in terms of the functional geophysical units with the respect to hydrological functions using geophysical techniques in the efficient manner, we propose a system-oriented geophysical approach based on the combination of electrical resistivity and refraction seismic techniques.

Therefore, let us start with the introduction to the background of the landscape organisation and the existing landscape schools. Afterwards, we will introduce some interesting scientific literature, which used the geophysical techniques (especial, resistivity and seismic surveys) for the hillslope characterisation. Finally, we will clarify the objectives of this research study and overview the monograph structure.

* * *

We begin our research study with the first question: *“Why is our environment an organized system?”* To answer this question in a simple way, we have to look from a window outside. We will find many simple examples indicating on the given organisation in the nature. The simple examples for the nature organisation at the temporal scale are the seasonal change and the change of day and night. We also can consider the turbulence in the atmosphere as a complex organised system. Moreover, a river system represents other example for the complex organised environmental system at the spatial as well as temporal scale. The water in the form of precipitation reaches the stream channel through hillslopes

1 Introduction

in the terms of surface and subsurface flows. These flow processes indicate spatial as well as temporal change. If we destroy the geo-system between the hillslope and the stream channel (for example, by constructing a dam), it follows to the change of the total water balance in this system influencing also the state of other geo-elements in this system. Therefore, the nature itself couples all environmental elements in an array system that functions with the respect to the physical rules. If we take away one element from this system, we destroy it. This destroyed system needs a given relaxation time for the reconstruction.

To understand the earth landscape systems (especial, the catchment system), we need to apply multi-discipline methodology. Here, we have to answer the next question: *“How can we study the complex nature systems like a catchment in the efficient way?”* Multiple studies worldwide attempted successful to categorize a landscape as an organized system, and to develop appropriate concepts and models based on observations, physical laws and conceptual models. With respect to the different research manner, we differ landscape schools in two groups, which developed their research strategies independent of each other for the understanding of the environmental processes in the nature system. Therefore, we will introduce the Russian landscape concepts and the West landscape concepts. The introduction of these landscape concepts makes an interesting contrast to understand the landscape structure from the different perspective.

1.1 The Russian landscape school

The knowledge of the Russian landscape school is not famous in the West scientific world because of the political ideology in the 20th century and the language barrier. However, we will bridge this gap and start our introduction with some scientific works from Russia (former USSR). The Russian landscape school established a landscape research based on observation and application of different methods to characterize a landscape system as hierarchy of small elements (Solncev 1948; Preobrazhensky 1966; Isachenko 1980; and Mamaj 2013).

The Russian landscape science began to develop from different subjects studying different processes through the observation, comparison, and testing of experiments. The main principle of the landscape science is to describe the state, the developing and the functioning of the nature system (Mamaj 2013). The functioning of the landscape system is the results of landscape developing (Mamaj 2013). The main factors creating the form and the structure of the earth landscapes are the gravity and the solar energy (Mamaj 2013). The solar energy is the source for all processes running at the Earth. The gravity sorts out all earth elements and develops the hierarchy in the landscape structure. Moreover, due to the interaction between electro-magnetically and gravitational fields we can split the landscape in micro- and macro-elements. Micro-elements are presented for example by some rock bodies, water mass, etc., whereas macro-elements are represented the mass flows (such as air flow, surface and subsurface flows) and therefore play a crucial role in the landscape organization because they are formed and transformed by gravitational force, which is presented as an energetically factor in the landscape developing (Mamaj

1 Introduction

2013). Therefore, Solncev considered the landscape as a complex of the macro-elements arranging in the sequence with decreased gravity force (B. Solncev 1981). Thereby, lithology plays an essential role in landscape developing and organization. The Solncev's concept considers the subordination of macro-elements under the gravity force known as the concept "gravitational paradigm" (Mamaj 2013). As far as, Nikolaev 2006 analysed and summarized the landscape concepts of (Solncev 1948, Solncev 1981) in appropriate manner. He proves that: *"the main factor of the landscape organization is the geologic-geomorphological factor. Relief and subsurface structures present a special matrix, which develops a landscape pattern. Due to stable lithological base, the spatial organization of regional ecosystem can keep the main features of landscape during a long time"* (Mamaj 2013). Moreover, the weak landscape elements subordinate to the powerful elements (such as lithological base). Such subordination develops a hierarchy in the landscape structure. Each singular hillslope also should have a hillslope gravity centre, which depends on the distribution of lithological mass, surface and subsurface flow (Nikolaev, 2006).

The Russian landscape concept classifies the nature system into three large hierarchical levels that summarize in the Table 1-1 shown the examples for each level. The first level is the landscape level assumed an earth area with the exact geographical coordinates at the global scale. Inside of the landscape level, we designate the local topological landscape units called as landscape subunits and take the places at the regional scale. This second level, we can subdivide into the smallest elementary landscape units known as a facie. The facie is characterised by the homogeneous lithological base, relief, microclimate, soil, flora and fauna at the local scale.

Table 1-1: Landscape classification according to the Russian landscape school (Mamaj 2013)

Hierarchy level	Description	Example
Landscape	A natural terrestrial complex with exact geographical identification and coordinates	A catchment
Landscape subunit	Locale topological landscape unit (LTLU)	A forest massif, a hill, hillslopes, wetlands, oxbow lake
Facie	The smallest elementary landscape unit with homogeneous lithological base, relief, microclimate, soil, flora, fauna	foot slope, upslope

Moreover, (Nikolaev 2006) classified the earth landscape more detailed based on the taxon classification system. We will introduce his landscape classification in the chapter 2, in the Table 2-3 in order to introduce the research philosophy of this work.

Nowadays, many Russian landscape scientists consider the concept of the landscape poly-structure (Mamaj 2013). The concept of Solncev is the special case of the landscape poly-structure concept. The landscape poly-structure concept considers the landscape as the superposition of the independent spatial structures (Mamaj 2013). Geo-systems represent a statistical complex and have to interpret as the poly-systems. The landscape interpretation has to consider the interaction between elements and the influence of the neighbour-landscapes. (Cherkashin, 2007) believes that we cannot study the nature landscape using only a system theory. We have to interpret it in a multi-disciplinary analysis as an object of poly-systems.

1.2 The West landscape school

In this subchapter, we will introduce some famous scientific work representing the West landscape school. The landscape studies of the West landscape school differ in two kind of studies (Reggiani, Sivapalan and Hassanizadeh 1998). One school uses the physical-mathematical principle. Other landscape school describes the landscape system in the conceptual way. Imbeaux presents the earliest study (1897) recognizing the complexity of catchment responses due to spatial structure (Kulasova, Beven, Blazkova, Rezacova, & Cajthaml 2014). The other early example (1933), we can find in the works by Horton (Beven 2004). Additional example is a mathematical model of (Freeze & Kirkby 1978). The conceptual semi-distributed TOPMODEL described by Beven and Kirkby in 1979 (Beven & Freer 2001) is other example for hydrological similarity of points in a catchment. Furthermore, the case study discussed by (Dooge 1986) proves that it is necessary to develop a novel framework to structure an instrumental data for the calibration of existing methods using hydrological laws. Another example of a conceptual model presented by Flügel is HRU's (hydrological response units) concept describing a system through GIS-analysis and reflecting different dominant subsystems (atmosphere, vegetation, soil, groundwater and river) of the basins hydrological cycle (Flügel 1996). Additionally, we mention the physical-based CATFLOW model of (Maurer 1997; Zehe, Maurer, Ihringer, & Plate 2001) and REW's (representative elementary watersheds) model of (Reggiani, Sivapalan, & Hassanizadeh 1998) based on global balance laws for mass, momentum, energy and entropy and formulated for representative hydrological control volumes. The authors discretized a watershed into a series of discrete spatial units (REW's). Moreover, the concept classifies each REW into five sub-regions in the terms of field observations, geometry and hydrodynamic regime. Nowadays, (Wienhöfer & Zehe 2014) propose a hydrological predicting model for a forested hillslope based on a concept of representative elementary volume (REV) that reflects an averaged sum of the representative spatial pore-space structure. Another recent model suggesting by (Zehe et al. 2014) is CAOS (Catchment As Organized Systems) model, which reinterprets the HRU concept of (Flügel 1996) from the thermodynamic perspective to link spatial organisation and functioning at the intermediate catchment scale. The CAOS model classifies a catchment in a given geological setting into a hierarchy of elementary functional units (EFU's) at the field scale, lateral topological units (LTU's) at the hillslope scale and hydro-geomorphic units (HGU's)

at the sub-catchment scale. Following (Zehe et al. 2014), we can understand an EFU as a set of control volumes/landscape elements which react statistical homogeneous controlling the radiation balance, the Bowen ratio, evapotranspiration and root water uptake, and upward flows of capillary water in the soil matrix. In contrast to EFU's, LTU's control runoff formation during rainfall-driven conditions, whereas HGU's regulate the hydrogeological and geomorphic setting of sub-catchments (Zehe, et al. 2014). After identifying these functional units in a catchment, the CAOS authors can characterize class members of the different unit types in more detail. The CAOS team (Zehe, et al. 2014) believes that the definition of these functional units is consistent with HRU concept as well as with the REW concept of (Reggiani, Sivapalan and Hassanizadeh 1998). Finally, to conclude our discussion on the West landscape school, we mention an example of a geophysical landscape classification identifying the geophysical signatures based on resistivity data and lithology-stratigraphy (Mele, Bersezio, & Giudici 2012; Mele, Bersezio, Giudici, Gavalli, & Zaja 2013).

* * *

Moreover, if we compare the Russian landscape school with the West landscape school, we can see that both schools have any similar techniques and concepts to describe the landscape system. Both schools consider the hierarchical principle to describe the landscape as a system. In contrast to the Russian school, the West school does not give a clear classification of the landscape, for example in terms of taxon or facie illustrating by concrete nature examples. If we combine the Russian landscape classification based on the concept "gravitational paradigm" with the mathematical-physical basis describing by (Reggiani, Sivapalan and Hassanizadeh 1998) as REW concept or by (Zehe, et al. 2014) as CAOS model, we can obtain a good starting concept to describe the landscape in the efficient way.

Therefore, taking into account the different concepts of the landscape classification, we will apply the hierarchical principle for the design of the system-oriented geophysical approach, in order to develop a dialogue between geophysics, hydrology and landscape science.

1.3 Ground geophysical application for hillslope characterization

The application of the ground geophysics techniques in hydrology is important to understand the relevant hydrological processes running in the subsurface (Robinson, et al. 2008). Today, there are many studies, which use different geophysical techniques for the understanding of the flow processes. (Robinson, et al., 2008) lists some examples of such studies. The most famous applied geophysical technique in hydrology is the resistivity survey or direct current (DC) because of simple application and it predicates directly from electrical resistivity water conductive zones in the subsurface (Telford, Geldart and Sheriff 1990). To detect the ground water level and the interface between the weathered layer and the bedrock, the refraction seismic (RS) is mostly helpful (Telford, Geldart and Sheriff 1990). The next two subchapter introduce several case studies applying the geo-electrical, refraction seismic techniques and the combined interpretation of both methods.

1.3.1 The application of geo-electric

Many hydrological scientific studies (for examples, Graeff et al., 2009; Koch, Wenninger, Uhlenbrook, & Bonell, 2009; Hübner, Heller, Günther, & Kleber, 2015) apply resistivity method to characterize hillslopes in a catchment. Thereby, the most applicable resistivity survey is electrical resistivity tomography or ERT (Kirsch, 2006) because it provides a detailed spatial 2D-section of subsurface. We start with the case study of (Pánek, Hradecký, & Silhán, 2008), which characterized slope deformations on the four ERT profiles. The next example for the hillslope characterization is illustrated by (Koch, Wenninger, Uhlenbrook, & Bonell, 2009) where the 111 ERT-transects were measured parallel and perpendicular to the hillslope in the Black Forest Mountains (Germany) and interpreted in the context of process hydrological understanding. Another case study from Schaefertal catchment combined top-down thinking, field work and process modelling (Graeff, et al., 2009), and subdivides the catchment into 15 representative hillslopes whereas ERT-measurements were conducted only at one representative hillslope and could not detect bedrock interface. The case study of (Travelletti, Sailhac, Malet, Grandjean, & Ponton, 2011) used time-lapse electrical resistivity tomography in clay-shale slope to study landslide. Moreover, the recent example for hillslope characterization provided by (Hübner, Heller, Günther, & Kleber, 2015) conducted ERT measurements on the 7 transects parallel and perpendicular to the hillslope in order to map the spatial heterogeneities of periglacial cover beds and monitor long-term soil moisture dynamics. In contrast to ERT, Vertical electrical sounding or VES survey is more applicable for aquifer characterization (several recent examples presented by Mele, Bersezio, Giudici, Gavalli, & Zaja, 2013; Niwas & Celik, 2012) than for hillslope characterization. We also mention an example from Greece presenting by (Atzemoglou & Tsourlos, 2012), which constructed 2D sections from 1D VES measurements in the Sarantaporon basin. Besides, we refer some examples of combining ERT with VES: the first case study presents the investigation for landslide characterization (Godio & Bottino, 2001), whereas the second example demonstrates identification, mapping and monitoring of different saline domains in a coastal plain region (Zarroca, Bach, Linares, & Pellicer, 2011). However, our case study using the combined interpretation of ERT and VES bridges a gap in the poor application of these techniques for hillslope characterization, especial to show advantages and limitations of each method.

1.3.2 The application of refraction seismic

Several hydrological studies used the refraction seismic to predict the groundwater level, the bottom boundary of weathered layer, to characterize the shallow critical zone in the catchment and to investigate hillslope characterising by the earth mass moving (landslides). We mention some interesting studies used refraction seismic for the hydrological and geomorphological tasks. The study of (Glade, Stark and Dikau 2005) analysed the regionally characteristics of landslides using refraction seismic survey. The other case study of (Clarke and Burbank 2010) applied the refraction seismic method for the interpretation of the differences in the fractured bedrock. The case study of (Befus, Sheehan, et al. 2011)

1 Introduction

measured many refraction seismic profile lines parallel as well as cross to the hillslope to characterize the shallow structures of the critical zone from the surface to the bedrock in two eroded catchments. The study of (Rumpf, Böniger and Tronicke 2012) characterized a creeping hillslope in the Austrian Alp at six refraction seismic profiles using layer-based inversion strategy to develop refraction seismic velocity model from first arrival times.

1.3.3 The combined application of resistivity and refraction seismic surveys

Due to the ambiguity in the data interpretation, the use of joint interpretation of geophysical data is popular in the hydrological exploration, especial for the investigation of the slope stability, the landslides, the critical zone, the permafrost zones and the aquifer properties. Such interpretation allows a more precise understanding of geophysical data and models. We will introduce several studies applied the multiple geophysical methods (especial, refraction seismic and resistivity survey) to characterize the hillslope subsurface structures. We start with the early case study of (McCann and Forster 1990) using seismic and electrical resistivity surveys for the investigation of the landslides. The other early case study described by (Caris and Van Asch 1991) illustrated an example of the geophysical, geotechnical and hydrological investigations for the studying of a small landslide in the French Alp. Moreover, the case study investigating large landslides in Austria using the combination of refraction seismic, geo-electric and electro-magnetic techniques has been shown by (Mauritsch, et al. 2000). The other case study illustrated by (Hack 2000) combines multiple geophysical techniques to study the slope stability. Furthermore, the case study of (van Overmeeren 2001) combines refraction seismic with vertical electrical soundings to characterize the aquifers and salinity of the water in the coastal plain of Wadi Surdud in Yemen. This case study interprets the refraction seismic data using the Hagedoorn's plus-minus method. The additional research example investigated hillslope subsurface structures in the Swiss Alp using the combination of refraction seismic, resistivity survey and ground penetration radar, we can see by (Otto and Sass 2006). The master thesis of (Befus 2008) combines refraction seismic with electrical resistivity tomography to investigate the shallow subsurface of the critical zone from the surface to the bedrock in three small catchment. Additionally, the case study of (Leopold, et al. 2011) characterizes the subsurface structures of rock glaciers using refraction seismic, electrical resistivity tomography and ground penetration radar. The other case study investigates groundwater flow paths using multiple geophysical methods such as refraction seismic, electrical resistivity tomography and ground penetration radar (McClymont, et al. 2011). We also refer the other interesting case study illustrated by (Coulouma, et al. 2012), which predicts the bedrock along the Mediterranean hillslope using combined interpretation of seismic (Refraction seismic, the Spectral Analysis of the Surface Waves) and electrical (ERT) methods. Finally, we introduce a recent interesting example of (Francés, et al. 2014) developing a multi-technique methodology to design a hydrological conceptual model in hard rock aquifers. The authors combined the remote sensing with such geophysical methods as ground-

penetration radar, electrical resistivity tomography, frequency domain electromagnetic and magnetic-resonance sounding as well as borehole and slug test data.

* * *

Summarized the literature review introduced in this subchapter, many geophysical studies characterizing the hillslope provided quite expensive investigations measuring multi profile lines to obtain the wanted subsurface models. Such factors as a high resolved data density, the geometry of geophysical sensors, measurement conditions, logistic of equipment and measurement errors increase significantly the time effort in the field as well as in data processing. Following (Hennig 2006), the total measurement time increases proportional the financially effort. Additionally, we have to carry out all geophysical measurements in the limited frame time because the flow processes in a catchment depend on the time. However, we need an efficient geophysical approach to characterize the subsurface structures in the catchment.

1.4 Research objectives and structure of this monograph

Based on the literature review, we will define the aim of this research study. The research question of this study is how can we investigate subsurface structures in a catchment effective and cost-efficient using multiple geophysical methods and assuming a catchment as a hierarchical system? At the same time, we would like to develop a dialogue between geophysicists, hydrologists and other scientists (Robinson, et al. 2008) because the catchment is the complex, coupled system, which needs multi-disciplinary knowledge to understand all interacted complex processes.

To find an optimum between the effort, the advantages and the limitations of geophysical methods assuming the catchment as organised systems, we developed a system-oriented geophysical approach applying the combined interpretation of the electrical resistivity and refraction seismic techniques. To develop this approach, we hypothesised:

- (1) Subordination in the landscape structure between weak elements and powerful elements due to the gravity force and the interaction of the geo-factors;
- (2) Hillslope as fundamental landscape units requires the characterization of the typical class members;
- (3) Hillslope has to be representative and typical for an investigated catchment;
- (4) Hillslope has to be homogeneous (lateral invariable, horizontal stratified);
- (5) The geological knowledge are known;
- (6) Coupling between electrical and seismic parameters.

The key objectives of this research work is to provide detailed information on hillslope subsurface structures with minimal effort in the field taking the ambiguity in the data interpretation into the account. Based on the obtained geophysical models, we want to develop a hydrogeological conceptual model of the hillslope system, which represents hydro-stratigraphic units and system boundaries (Anderson and Woessner 1992). Moreover, the suggested approach can be helpful to select

1 Introduction

and to prove the idea on homogeneous representative hillslopes, especial for areas, which did not investigate, or poor investigated, or characterized by the problematic environmental conditions (as forested areas). In addition, the approach should distinguish functional hydrological units with respect to the physical rules as well as to the definition of CAOS model (Zehe, et al. 2014). Finally, the obtained geophysical structural subsurface models have to improve the conceptual understanding of the subsurface hydrology by the integration of the geophysical models into hydrological modelling.

Until now, we organised this scientific monograph into seven chapters.

The first chapter introduced the readers in the research objective of this thesis and provided the outline of the fundamental literature relevant to the landscape organisation and the hillslope characterisation using geophysical techniques such as resistivity survey, refraction seismic and their combination.

The chapter 2 contributes an outline of the landscape complexity for its description as well as the research philosophy for a multi-disciplinary project including the landscape classification in terms of taxon according to the Nikolaev's classification. The chapter concludes by the discussing the catchment characterization from geophysical perspectives.

The chapter 3 describes the location and hydrogeological background of two catchments, where we performed intensive fieldwork to characterise a hillslope as representative landscape subunit.

The chapter 4 describes the methodology of the system-oriented geophysical approach, which applies the combination of electrical resistivity and refraction seismic techniques. The chapter introduces the measuring layout of the approach and the principle of each technique as well as experimental composition. We also discussed the advantages and limitations of the individual as well as joint interpretation and how can we improve geophysical models using the different interpretation techniques. The chapter concludes by the discussing the application of the three-dimensional image of the investigated hillslope, in order to prove the suitability of the system-oriented geophysical approach.

The chapter 5 describes and interprets the obtained geophysical hillslope models at each study site and discusses the advantages and limitations of each methods. We consider the geophysical hillslope models individual as well as combined. We also discuss how we can distinguish geophysical functional units, which can control the hydrological processes with respect to the CAOS model (Zehe, et al. 2014). The chapter concludes by the discussing the imaging of the three-dimensional hillslope subsurface model, which verifies the correctness of the applied approach.

The chapter 6 discusses the obtained geophysical hillslope models in the light of hydrogeological conditions, in order to integrate these models into hydrological modelling for the improving the understanding of the conceptual hydrological models and to develop a dialogues between geophysicists and hydrologists. The chapter also demonstrates why the conceptual hydrogeological model is necessary, and what the model needs to assume, in order to represent a meaningful conceptual model. Besides, we discuss the advantages of the system-oriented geophysical approach for each study site. The chapter

1 Introduction

concludes by the presenting and the description of the conceptual hydrogeological models developed for each representative hillslope.

The chapter 7 presents the conclusion of this scientific work.

This monograph was prepared in the framework of the multi-disciplinary CAOS project – Catchment As Organised Systems¹ supported by the National Research Fund of Luxembourg - FNR - and the National Research Fund of Germany - DFG (FOR 1598, ZE 533/9 - 1). Helmholtz Impulse and Networking Fund through Helmholtz Interdisciplinary Graduate School (HIGRADE) for Environmental Research also kindly supported this work (Bissinger & Kolditz, 2008).

¹ www.caos-project.de

2 Research philosophy of the landscape system and the research

“... *It is a question of discipline ...*” - from

“The Little Prince” of Antoine de Saint Exupéry

2.1 State of the art and understanding landscape as complex system

Landscape is a complex but organised system (Basu, et al. 2010; Blöschl, Thybo and Savenije 2015), which consists of the different geo-elements reflecting the state and behaviour. To understand this system, we have to know how the nature system works, what key units define this system, and what processes act in the system. The Figure 2-1 illustrates the conceptual model for understanding the landscape as an open interactive system in the terms of a triangle and landscape evolution cycles. The triangle peaks represent the terms of state, functioning and developing, whereas the landscape itself takes a central place in the triangle. In order to illustrate the landscape dynamic, we linked all three terms together starting from the position of “state” and moving clockwise. The intervals between two terms represent a functional role in the landscape dynamic in terms of act, results and change. With the respect to the time scale, we can differ the two groups of processes characterizing the past and the present, which define the state, the type and the behaviour of a landscape in the given event intervals (Mamaj 2013). It is important to recognize that “time” in the landscape evolution and measurement is characterized by the event duration and the interval between them. We also can consider the present only as instant between the past and the future. Therefore, to understand the processes and the landscape characteristics in the present and to predict them in the future, we can use data registered the landscape state and behaviour in the past. Moreover, the processes occurred in the past create a primary landscape, whereas the current processes change the original landscape system through the action and the interaction between different morphological landscape units as well as atmosphere, hydrosphere and lithosphere. The current processes develop the primary landscape to the secondary landscape, which we can consider as the primary landscape for the next landscape cycle. The differences between different cycles imply the landscape dynamic. Therefore, the triangle concept illustrates the complexity of the landscape structure and dynamic in the simple way. Now, the question is *how we can describe and predicate the landscape system using suitable concepts and paradigms based on the triangle conceptual model.*

The properties and processes of the landscape system characterize the state and quality of the nature system. However, we can describe the landscape system in terms of its states resulted over time. The number of the states depends on the sets of the processes as well as on the landscape level. This relation is based on the numerous field works studied the landscapes of Siberia, European Russia, Georgia and Ukraine in the 60s – 80s of the 20th century (Mamaj 2013). The number of the states increases with the increased sets of the processes and the higher landscape level. For example, a small and simple facie belongs to the lower landscape level (see the Table 1-1) characterizing by minimal set of the processes. Consequently, the minimal number of states characterizes the facie. Moreover, the

2 Research philosophy of the landscape system and the research

landscape studies conducted in the 60s – 80s of 20th century investigated and interpreted only the several processes separately at the facie level. They did not interpret the processes as a set at the landscape level (Mamaj 2013). If we look back on the West landscape concepts, we also will see many study cases (see the chapter 1.2 and several examples introduced by (Castillo, Castelli and Entekhabi 2015)) investigated several processes and interpreted it at small scale. Nevertheless, (Reggiani, Sivapalan and Hassanizadeh 1998) and (Zehe, et al. 2014) suggested the REW concept and CAOS model, respectively, based on the thermodynamic approach and interpreted the landscape system at the intermediate scale (REW concept at the watershed scale, and CAOS model at the sub-catchment scale). Besides, (Ehret, et al. 2014) examined the potential paradigms and theories, which could improve the understanding the complex hydrological systems under change based on the fundamental literature. The Table 2-1 summarizes the several perspective on catchments under change described by (Ehret, et al. 2014). The best way to understand and to predict the catchment dynamic under the change is the combination of these perspectives in the sequence of historical exploration and interpretation, which implies the causal explanation of processes. The theory of dynamical systems helps to recognize the system structure in terms of states over time, whereas the principle of hierarchy, co-evolution and similarity consider the landscape system at various scales and across many components assuming non-random behaviour of the system. The knowledge of thermodynamic support the system understanding from physical perspective and optimisation technique. Therefore, the introduced fundamental literature shows that it exists the fundamental theoretical background from different viewpoints for the description and the predication of the state of the nature system. Nevertheless, it exists still a gap in the practical application how the sets of processes operate in the complete landscape jointly, and why the several different catchments can be similar.

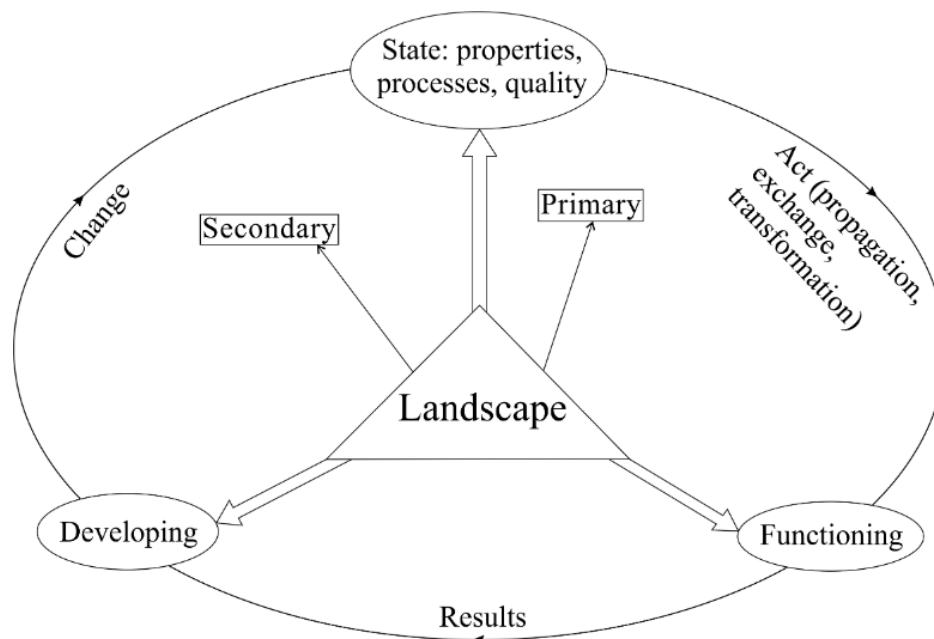


Figure 2-1: Conceptual diagram representing the landscape as an open interactive system

Table 2-1: Perspectives on catchments under change described by (Ehret, et al. 2014)

Viewpoints	Main principles	Outcome research and science application
Catchments as complex dynamic system	The theory of dynamical systems based on the degrees of freedom and the nature of dynamic to identify the system structure (border, components, and state variables), the laws controlling the dynamic, in order to evaluate system state over time and to predict it.	(Forrester 1968); weather prediction, ecology, hydrology, geomorphology and coupled human-ecological systems
Catchments as self-organising systems	The system is a hierarchy: developed from micro-scale to macro-scale; the dependence of the unit value / state on the state / value of another; comparable with Darwin's evolution concept	(Ashby 1962); hydrology, soil science
Catchments as co-evolving systems	Darwinian approach: Detailed analysis of the signatures and functional patterns in the individual catchments; comparative analysis of many catchments based on the functional similarity; funding of generalizable mechanisms of the landscape change, in order to parameterize hydrological models	(Ghiselin 1969) geomorphology, pedology and ecology
Catchment similarity	To find similarities and their organizing principles by estimating the distance between two catchments using suitable metric space, in order to estimate the future behaviour of the catchment under changed boundary conditions and to understand the potential impacts of environmental change	(Budyko 1974), (Wagener, et al. 2007) Hydrology
Catchments as open dissipative systems far from equilibrium	The application from thermodynamic perspective based on the second law of thermodynamics: the gradient and fluxes describe a form of energy	(E. Zehe, U. Ehret, et al. 2013), (Kleidon and Renner 2013a)
Catchments as sources and flow paths of information	Based on the information theory (Shannon entropy), to analyse and optimize the way information feeds into predication	(Shannon 1948) cryptography, communication engineering and signal processing

To start describing the states of the landscape system, we have to know what forces and processes act and change the landscape state? We can differ two groups of forces, which influence the state of the earth landscapes. On the one hand, the cosmic forces can change the landscape state due to the Earth moving around the Sun and the interaction between these objects. On the other hand, the terrestrial forces triggered by the Earth form, rotation, axis inclination, circulation of air / water mass and tectonic processes form and develop the landscape structure considerable. Moreover, the landscape state depends on the location, time, geomorphological forms, sedimentary depositions as well as the distribution of the warm and moisture, and plant cover. The other force, which we have to refer, is the human factor, which can change the landscape state and structure significant positive as well as negative.

The next questions that we have to answer are how we can describe the landscape states, and what fundamental physical units can describe the landscape states from the original state to the current state, in order to predict it in the future. The classical equations of the mass and energy conservation are too general to describe the nature landscape because they characterize each component in any fluvial system and cannot describe the surface form of the landscape (Leopold and Langbein 1962). The equations must explain the particle tracks or the relation between neighbour parts in time. (Leopold and Langbein 1962) applied the second law of thermodynamics to describe the energy distributions and their relation to changes of landforms in space and time. Later, (Reggiani, Sivapalan and Hassanizadeh 1998) and (Zehe, et al. 2014) interpreted the catchment system from thermodynamics perspectives in the terms of entropy and fluxes. The recent example of (Castillo, Castelli and Entekhabi 2015) examined the hydrologic complexity measured the distance of a given distribution of soil moisture from a Dirac delta and uniform distribution based on the Shannon entropy information concept and discretization-invariant dimensionless index. However, the use of the entropy (H) is a good idea, to describe the nature system because it is a fundamental thermodynamic value describing the physical state of the system

$$\Delta H = \frac{\Delta Q_{rev}}{T} \quad [J/K] \quad (2-1)$$

as well as the uncertainty measure:

$$H = -k_B \sum p_i \ln p_i \quad [J/K] \quad (2-2)$$

where Q_{rev} is the reversible transfer of the heat [J/K] into the system, T is the absolute temperature of the system measured in Kelvin [K], $k_B \approx 1.3806488(13) \cdot 10^{-23}$ [J/K] is the Boltzmann constant and p_i is the probability of the system in the i -microstate. The sum over all probabilities describes all possible microstate of the system. The equation (2-2) known as Shannon entropy or an information bit implies the rate information and quantifies the uncertainty of measure (Shannon 1948). For example, the most uncertain situation occurs by the maximum entropy when all probabilities are equal (Shannon 1948). This is the case of the isolated system implying the thermodynamic equilibrium. Moreover, the entropy describing by the equation (2-1) characterizes an isolated system in classical thermodynamic equilibrium characterizing by uniform values of pressure, density and temperature over time and implies the change (Δ) in entropies of two different equilibrium states (H_1 and H_2). Therefore, entropy describes the degree of order-disorder in the system in terms of probability or improbability of the observed states. In addition, the physical chemistry formulates the entropy in the abstract form as *“the ratio of the probability of a*

given physical state to the probability of all other possible alternative states” (Leopold and Langbein 1962).

We know that a nature landscape system represents an open dissipative thermodynamic system because it exchanges the mass, energy and entropy with the neighbour systems (Zehe, et al. 2014). The open thermodynamic systems also imply the dissipation of the free energy and produce entropy because of irreversible change in the system caused by the dissipative losses of the soil hydraulic conductivity and the drag forces in the porous medium (E. Zehe, U. Ehret, et al. 2013). Moreover, the entropy production in the nature systems is dominant by the evapotranspiration due to the large energy conversions and the large specific heat of vaporization (E. Zehe, U. Ehret, et al. 2013).

To link the different landscape states and components based on the entropy concept, we need to develop the landscape model, which can identify, evaluate and validate systems components implying the landscape change in space and time. The landscape model must provide a monitoring program describing important aspects of the ecosystems, management effective strategies and the used framework. The main difficulty of the landscape research is to embrace the complete field investigations at the whole landscape scale due to personal costs, logistic of the equipment and the financial costs. We would like to suggest the rational program for the landscape exploration. This landscape model for the case “catchment” aims to integrate all relevant data, improve deeper understanding of the catchment system and should predict all relevant processes and phenomena. The Table 2-2 summarizes the research program to study a catchment as open thermodynamic system in terms of representative landscape units and their dynamic states. Moreover, we assume that a landscape system includes various alternative states (H_i where $i = 0, 1, 2, 3, \dots, n$) with individual probabilities and the sets of the physical parameters and processes (Leopold, et al. 2011), which represent the episodes of the landscape life. Therefore, we can define the sequence of history matrixes: from the initial state H_0 to the i -microstate H_i where we define a “state” by some measurable properties representing the initial static values and the changed values. We also believe a catchment system is an open system consisting of water and debris / sediments (Leopold and Langbein 1962). Then, we can specify the most probable distributions of the energy in the system because the different forms of energy exist in the catchment system. Precipitation brings the potential energy in the system due to elevation differences and gravity force. The kinetic energy exists in the system in terms of the flowing water. Other form of energy is the thermal energy, which is responsible for the temperature of the landscape system. The change in the thermal energy results to the heat transfer done without work. Additionally, some energy is being lost due to convection, conduction and radiation (Leopold and Langbein 1962). With the respect to the gravity potential, the energy in the catchment takes different level in the sequence of landscape evolution shown a longitudinal profile and moving downhill toward a stream channel. However, the nature system represents the dynamic equilibrium state with the increased entropy. (Leopold and Langbein 1962) characterize the dynamic equilibrium state as rate of internal entropy generation that implies the energy gradient between two points. Additionally, the rate of internal entropy generation equals the rate of the outflow of the entropy

2 Research philosophy of the landscape system and the research

characterizing by the dissipation of the energy as heat. Each system can reach a stationary state. If an open system implies the minimal rate of the entropy production per volume unit done by the minimal work, the stationary state characterizes the open system (Leopold and Langbein 1962). We can characterize such stationary open system as stable. There is the equivalence between the principle of the least work and maximum entropy (Leopold and Langbein 1962).

The nature itself tends to the minimum work. One example from optics known Fermat's principle is the principle of least time implied that a ray takes a path between two points in the least time. Moreover, the equivalence between the principle of the least work and maximum entropy is useful in the

Table 2-2: The suggested research program to develop landscape model for the case "catchment"

Steps	Parameters	Description
Conceptualization	The functional principle	The action and the interaction between all entities in the catchment; data integration; deeper understanding and predication of the processes and phenomena
	The landscape units	Hillslopes, stream channel, wetlands, plateaus
	Processes	Transpiration, evaporation, latent heat flux, soil heat flux, surface and subsurface flow, infiltration, root water uptake, photosynthesis
Formalization	State variable	Temperature (air, water, soil), precipitation, surface and subsurface topography, groundwater level, vegetation cover, LAI, soil moisture, subsurface physical parameters (resistivity, seismic velocity)
	Assumptions and Criteria	An open thermodynamic system with consistent distribution of physical values; Complexity, functional homogeneity, thresholds and dominance (Basu, et al. 2010)
Implementation	Field observations	Visual
	Field measurements	Installation of measuring equipment
	Data processing	Analysis and interpretation jointly
Parameterization	Collected data	Definition of states in space and time, assigning to measuring variables
Verification	Modelling and simulation of alternative scenarios	
Sensitivity / Uncertainty analysis	The importance of each input parameter in terms of its impact on the results	
Model analysis and validation		

statics, and it means, “*the distribution of stresses is most probable, and the total strain energy in the several members is minimum*” (Leopold and Langbein 1962). If we transform this principle on the catchment system, we will find similarity in the statics. The set of the physical processes and properties includes many variables (several example see in the Table 2-2), which characterize various states. Many variables can be indeterminate. However, the catchment system can regulate many possibilities of indeterminate variables to find wanted hydrological conditions for maximum probability by minimum work ($s_1 + s_2 + s_3 + \dots + s_n = \text{minimum}$).

So, the energy distribution in the catchment tends to the maximum probabilities by minimum work and the equal rate of entropy gain in each interval of length along a selected unit. Hence, (Leopold and Langbein 1962) describes the statement for the river system in the following way

$$\frac{dH}{dt} \frac{1}{Q} = \frac{dh}{dx} \frac{1}{h} \propto \log p \quad (2-3)$$

The left site of the equation (2-3) represents entropy per unit of mass volume rate (discharge), whereas the right site implies the loss of potential per unit of distance (dx) and base level (h). The extent dh/dx represents the rate of energy lost for a given state, whereas the amount h symbolizes the range of choice of the rate of energy lost at any level. The probability p denotes the proportion of the total elevation lost. However, we can consider the catchment system in terms of selected length units characterizing by a loss of potential and a given probability (p_i). The joint probability of all units is greatest when all unit probabilities are equal and constant. Consequently, the sequence of several unit intervals follows to a uniform increase of entropy in each unit length, whereas the ratio between a known state to the number of the alternative states implies the rate of energy loss at any point related to the elevation above the base level. Hence, the selected length units represent the members of the landscape system. According to the rule of the least work, we can phrase that the total energy in the several landscape members or units has to be minimum, and the distribution of the various landscape states can be most probable. Therefore, the choice of the appropriate length unit corresponds to one of a hillslope, a point to which we refer in the next section where we will discuss about the landscape classification in terms of units as a taxon, and a hillslope as representative landscape unit, which permits the catchment characterization in an efficient manner.

2.2 Hillslope as a functional unit to understand processes in catchment

In the catchment, the unit under the consideration is a unit of length along a hillslope profile. So, why is a hillslope? The hillslope is a fundamental landscape unit (Bachmair, Weiler and Troch 2012; Hübner, et al. 2015), which represents a complex coupled geomorphic system where many processes (hydrological, meteorological, geochemical and biological) are active and interact with each other (Basu, et al. 2010). Such factors as uniform geological base, homogeneous relief, climate (the balance of warm and moisture), character and intensity of surface water and groundwater, the typical set of soil type, typical pattern of vegetation create the form of the hillslope as well as the whole catchment. There is also the direct connection between the hillslope and the stream. The interaction between all elements lead to

2 Research philosophy of the landscape system and the research

the hierarchy (see the chapter 2.1). In the chapter 1.1, we showed the landscape classification after the Solncev's concept where we can subdivide the landscape into three level: landscape, landscape subunit, facie (see the Table 1-1). The Solncev's successor, (Nikolaev 2006), classified the landscape using the structural genetic principle based on the taxon landscape hierarchy shown in Table 2-3, which represents some examples of these taxon units. A taxon joints all landscape elements with similar properties and characteristics in the groups and class, which assume the functional of the landscape system, developing and the estimation of the behaviour of several landscape units and subunits. The functional of the landscape structure is associated with the landscape developing as the change of the nature events according to the physical laws (see the Figure 2-1). However, the principle of the landscape classification described by (N. Solncev 1948), (B. Solncev 1981) and (Nikolaev 2006) can be used for the catchment characterisation in order to link different disciplines. Landscape hierarchy also can identify the processes at different scales and develop the rules to translate information across the scales.

Table 2-3: Landscape classification according to the Nikolaev's concept (Nikolaev 2006)

Taxon	Allocation principle	Example
Section	The interaction type in the landscape structure	Aquatic and terrestrial environment
System	Energetic base of the landscape, belt-zonal difference because of climatic zones	Polar area, tropical area
Subsystem	Climatic differences between climatic zones	Moderate continental, oceanic clime
Class	Morphological structures of the higher order, type of nature zonal pattern	Plains, highlands
Subclass	Landscape hierarchy subdivision at the plains and highlands	Low-lying, high-lying
Group	Type of river regime, moisture degree	Hydromorphic soil, eluvial soil
Type	Soil, biological, climatic characteristic based on the soil type and the plant formation class	Forest steppe, steppe, grassland
Subtype	Soil, biological, climatic characteristic based on the soil subtype and the plant formation	Grassland forested, forest-grassland
Form	Genetic relief type	Plane plains, archaic-
Sub-form	Genetic type of near surface substratum	Loess-loamy
Kind	Similarity of dominant landscape subunits	Plane wavy archaic-alluvial plains

Therefore, the hillslope is a universal unit that can provide the description of all processes in a catchment in the efficient manner, because it couples subsurface and land surface processes. (Rihani,

2 Research philosophy of the landscape system and the research

Maxwell and Chow 2010) investigated the role of terrain and heterogeneous subsurface based on the interactions between groundwater dynamics and land surface energy fluxes. The authors developed the Common Land Model, which examines various effects such as effects of subsurface formations, effects of terrain and formation thickness, effects of terrain slope, effects of subsurface properties, effects of land cover, and effects of atmospheric conditions. Hence, to understand the processes at the hillslope scale, it is necessary to consider an interdisciplinary data set (McDonnell, et al. 2007). The Figure 2-2 illustrates the flow chart for multidisciplinary investigation in the catchment. To reach successful multidisciplinary investigation, at the beginning we have to select a hillslope with respect to such parameters as geomorphology, soil properties, density and type of vegetation, uniform climatic and hydraulic conditions, which essentially influence the flow processes. However, the need of the diagnostic selection tool is necessary to provide a link between physics of the subsurface flow processes, hillslope geometry, and hydraulic properties.

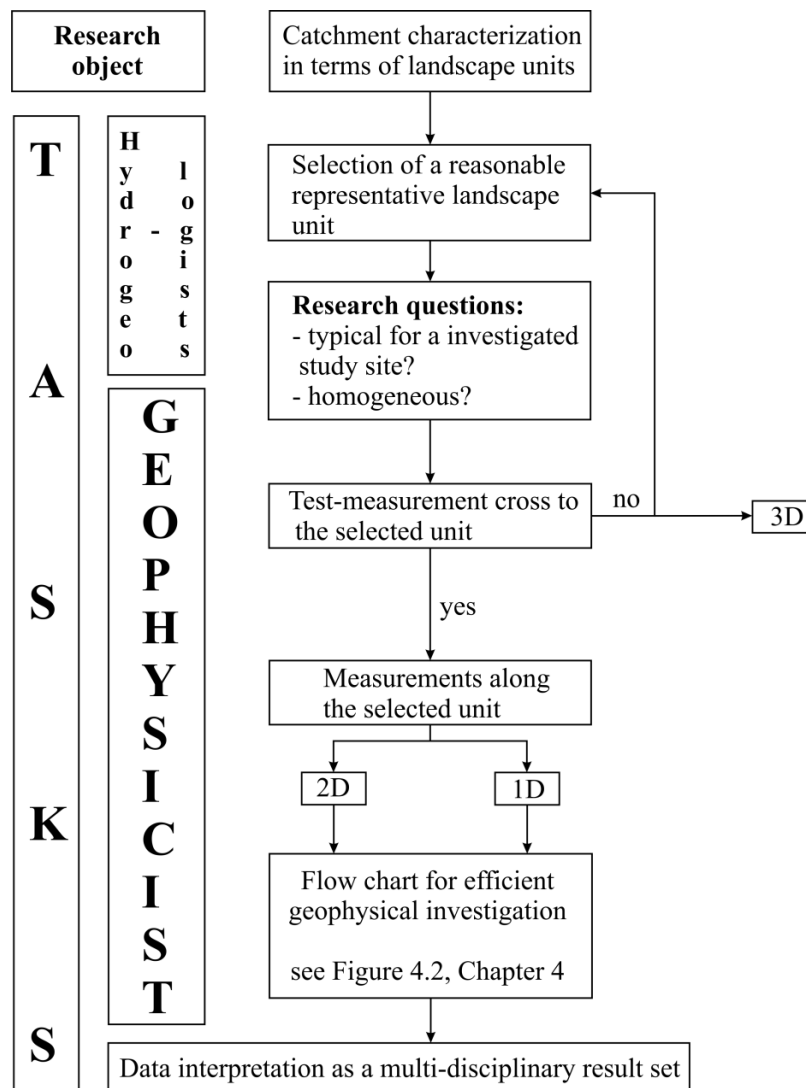


Figure 2-2: Flow chart for multidisciplinary catchment characterization in terms of landscape units

In order to develop the diagnostic selection tool, it is necessary to consider such criteria as complexity, functional homogeneity, thresholds and dominance. (Basu, et al. 2010) described these terms in the details. Interaction of different geo-factors as well as interconnected subsystems and processes characterizing by various states describe the complexity of the system. From hydrological perspective (Basu, et al. 2010), functional homogeneity associates with the similarity of hydrological responses, whereas structural heterogeneity link to the spatial patterns of specific landscape attributes (soil and land use). Hence, in order to define functional heterogeneity, we must respect the specific hydrological response (hydrographs) and the spatial scale of observation (Basu, et al. 2010). The next criterion “thresholds” play an essential role in the hydrological response for a given rainfall event. It controls the partitioning of the rainfall, the change of soil water storage and the loss of water from landscape system. Due to the different flow paths of water (overland flow, fast subsurface flow and groundwater flow), it exists the different runoff mechanisms that characterize hydrological regime in terms of a single, dominant and persistent flow pathway.

So far, the selected hillslope with one set of dimensions should be as a reference hillslope, which we can transfer to other hillslopes with similar dimensions. In order to compare different reference of hillslopes with each other and to describe the their characteristic subsurface flow response, one similarity parameter is sufficient. This parameter called as the hillslope Péclet number (Pe) depends only on the geometric characteristics of the hillslope and requires the diffusion and advection terms (Berne, Uijlenhoet, & Troch 2005). The ratio of the characteristic diffusive timescale (τ_K) and the characteristic advective timescale (τ_U) defines the dimensionless hillslope Péclet number (Pe) (Lyon and Troch 2007):

$$\tau_U = \frac{Lf}{2k(\sin\alpha - a_c p D \cos\alpha)} \quad (2-4)$$

$$\tau_K = \left(\frac{Lf}{2k}\right) \left(\frac{L}{2pD}\right) \left(\frac{1}{\cos\alpha}\right) \quad (2-5)$$

$$Pe = \left(\frac{L}{2pD}\right) \tan\alpha - \left(\frac{a_c L}{2}\right) \quad (2-6)$$

where f is the drainable porosity, L is the hillslope length, k is the hydraulic conductivity, α is the hillslope angle, pD is the averaged saturated depth, D is the soil depth, p is a linearization parameter in the range from 0 to 1, and a_c is the hillslope convergence rate. Advection and diffusion interpret only the water transport due to the total head gradient (Berne, Uijlenhoet and Troch 2005). The dimensionless hillslope Péclet number implies the hydrological similarity between hillslopes with respect to their characteristics response function and predicts subsurface flow response dynamics. The use of the characteristic diffusive term needs for the normalization of time dimension due to the infinite approach by $Pe = 0$ (Berne, Uijlenhoet and Troch 2005). Moreover, the similarity index Pe is always positive because of the positive advective term by the positive geometric constraint $\sin\alpha > a_c p D$ (Berne, Uijlenhoet and Troch 2005). Besides, the decrease of the similarity index implies the increased role of the diffusion. Moreover, in order to provide the similarity analysis in the term of the hillslope number Pe , it needs to make numerous simple assumptions. Shallow soils, impermeable bedrock characterizing by the constant slope angle, streamlines parallel to the bedrock, the absence of the overland flow, negligible storage in the unsaturated

zone, uniform hydraulic parameters, zero head boundary conditions near outlet and no-flow boundary at divides require the similarity analysis of the hillslope number Pe (Lyon and Troch 2007). The nature does not provide any hillslopes that meet all these assumptions. The most difficulty and uncertainty, to estimate the similarity index, remains for the assumption of uniform hydraulic parameters due to the heterogeneous nature of the subsurface (Lyon and Troch 2007). Nevertheless, the contribution of the hillslope Péclet number permits to separate the effects of the hillslope properties, boundary and initial conditions, and implies the importance of advection and diffusion, in order to estimate normalized and dimensionless response functions for each hillslope in the simple way. This similarity index does not depend on the scale. Therefore, it is necessary to provide the future tests of the similarity hillslope index Pe for capturing complex hillslope geometries in different climatic regions (Lyon and Troch 2007). Such analysis can prove the effects of the spatial heterogeneity on the similarity index Pe . Hence, it can solve the famous upscaling problem in the hydrology (Lyon and Troch 2007).

However, the knowledge on the soil depth and saturated depth as well as hydrological parameters require the similarity analysis. The knowledge on the subsurface can deliver geophysics. An efficient investigation from geophysical perspective is a point to which we refer in the next section where we will discuss what efficient geophysical investigation needs, in order to provide detailed results on the subsurface.

2.3 Catchment investigation from geophysical perspectives

Geophysical techniques provide a good opportunity to explore the complex subsurface structure at various surface scale, in order to develop a hydrogeological conceptual model (Binley, et al. 2015). Besides, geophysical measurements suffer from large time consume. Every geophysicist who is employing in applied geophysics knows how expensive can be geophysical investigation. The effort of the geophysical investigation depends on the environmental conditions of the investigated area, equipment logistic, and on the choice of suitable measurement scale and resolution. However, this research work focuses on the developing of a system-oriented geophysical approach, which can investigate the subsurface structures of the catchment in the efficient routine with the respect to the hydrological functions.

In order to minimise the time effort in the geophysical investigation, we have to consider a catchment in terms of representative functional hillslopes. It is also impossible to cover all representative hillslopes in the catchment. However, we should answer one question asking: “*How representative is the selected hillslope in the investigated catchment?*” From geophysical perspective, we associate the representative hillslope with subsequent questions: (1) “*is the hillslope typical for the investigated catchment in terms of hydrogeological and climatic conditions?*” and (2) “*how homogeneous is the hillslope?*” Geophysicists associate the hillslope homogeneity with the horizontal stratified and lateral invariable subsurface. In contrast to geophysical association of homogeneity, the hydrologists (Basu, et al. 2010) associate functional homogeneity with the similarity of hydrological responses. Moreover, the

high spatial variability of water table response reflected by trench flow characterizes a representative hillslope from hydrological perspective (Bachmair and Weiler 2013). Hence, the spatial variability depends on topography and wetness (Woods, Sivapalan and Robinson 1997). According to (Woods, Sivapalan and Robinson 1997), many studies confirm that the downslope characterizes the increase of the subsurface flow per unit catchment. Furthermore, the increase in the subsurface flow per unit area links to the topographic convergence. Besides, the change of the spatial variability due to catchment wetness is observable at the timescale from days to months and longer by the recharge measurements (Woods, Sivapalan and Robinson 1997). The interpretation of the wetness is relatively complex, to describe the total wetness in the catchment (Woods, Sivapalan and Robinson 1997). The increase of the storm runoff generated at all points in the catchment tends to wetter soil moisture conditions (Woods, Sivapalan and Robinson 1997). In addition, the hillslope indicates a strong dependence on the weather conditions confirmed by the case study of (Bachmair and Weiler 2013). Therefore, the use of the electrical resistivity tomography can help to localize the saturation zones before the installation of long-term monitoring network (Bachmair and Weiler 2013).

To conclude the problem of the *hillslope selection as representative functional response units*, we summarize the following *key words* such as *uniform stratified subsurface, topography, wetness, the specific hydrological response (hydrographs), and the spatial scale of the observation*, which should help to identify a hillslope as representative functional unit in the catchment and link geophysics and hydrology. In our opinion, the last key word “the spatial observation scale” is most important to connect geophysics and hydrology and to translate the estimated geophysical parameters into hydrological parameters. The Table 2-4 illustrates the link between geophysics and hydrology using the fundamental relations. Geophysics can measure at the various scales from the small plot-scale to the large catchment-scale. The effort of the geophysical exploration depends on the measured scale. It increases with the large landscape level. Moreover, the translation from the geophysical measurements into the wanted hydrological properties that provides hydro-geophysical relations as Archie’s equation, Gassmann’s equation (Telford, Geldart and Sheriff 1990) also suffers from the limitations of measurement scale and resolution. Such translation is an important hydrological interpretation of geophysical data and needs profoundly knowledge. The Table 2-4 demonstrates several famous geophysical and hydrological relations, which connect geophysical data with hydrological parameters. *The joint terms* that can connect geophysical (Gassmann’s equation, Biot’s theorie and Archie’s equation) and hydrological (the Darcy’s law) relations are *porosity and fluid saturation*. Seismic relations imply more complex transformation into the hydrological parameters than the geo-electrical relationship. Hence, the Gassmann’s equation are easier for the practical transformation than the Biot’s theory. Gassmann’s equation estimates the elastic bulk moduli of the mineral grain from the elastic bulk moduli of fluid, dry rock and saturated rock frame, and porosity. The elastic moduli depend on the seismic velocity and the density. Hence, the most difficulty by the Archie’s equation is the estimation of the resistivity of the water. Nevertheless, there are many studies, which tried to transform geophysical data into hydrological parameters (Binley, et al.

2 Research philosophy of the landscape system and the research

Table 2-4: Link between Geophysics and Hydrology focused on geo-electrical and seismic surveys

Item	Geophysics	Hydrology
Variables	Electrical properties (resistivity, conductivity), elastic properties (seismic velocity, slowness)	Porosity, permeability, water content, hydraulic conductivity
Spatial observation scale	Field plot - hillslope - catchment	
Observed static data	1D-, 2D-, 3D-distribution of the subsurface in terms of electrical and elastic properties	
Data observed temporal changes in the states	Time-lapse observations in terms of resistivity; micro-seismic monitoring	Precipitation, evaporation, discharge measurements, hydraulic head, dissolved matter
Relations	<p><u>Gassmann's equation (low frequency):</u></p> $K_S = K_D + \frac{K_0(1 - K_d/K_0)^2}{1 - \phi - K_d/K_0 + \phi K_0/K_f},$ <p>where K_0, K_f, K_D, and K_S are the bulk moduli of the mineral grain, fluid, dry rock and saturated rock frame, respectively; ϕ is porosity;</p> <p><u>Biot's theory (high frequencies):</u> see (Biot 1956-1; Biot 1956-2);</p> <p><u>Archie's equation</u> expressed in resistivity:</p> $\rho_w = \rho_{aq} \frac{\phi^m}{a},$ <p>where ρ_w is resistivity of the water, ρ_{aq} is resistivity of the saturated aquifer, a and m are material empirical factors, and ϕ is porosity (Vouillamoz, et al. 2007)</p>	<p>Darcy's law:</p> $Q = AK \frac{(h_1 + z_1) - (h_2 + z_2)}{L},$ <p>where Q is the volume flow rate, A is the rate of porous media normal to the flow, K is hydraulic conductivity, h is the pressure head, z is elevation, and L is the length of the flow path (Brown 2002)</p>
Description to the relations	<p><u>Gassmann's equation</u> estimates the fluid-saturation effect on bulk modulus that depend on seismic velocity (Han and Batzle 2004);</p> <p><u>Biot's theory</u> describes the propagation of acoustical wave in porous elastic solid containing a compressible viscous fluid (Biot 1956-1; Biot 1956-2);</p> <p><u>Archie equation</u> describes the relation between electrical conductivity / resistivity of sedimentary rock, its porosity and fluid saturation</p>	The Darcy law describes the flow of fluid through a porous medium

2015). Furthermore, the geophysical applications in hydrology focuses more on the structural characterization using static data. Besides, the geophysical monitoring in terms of the time-lapse observations and micro-seismic monitoring takes a central place in the hydrological exploration due to the temporal change of the hydrological processes in the states (Binley, et al. 2015). It also is possible to combine several techniques in the various configurations, in order to optimize the sensitivity, to understand the nature and ambiguity of measured data and to improve the subsurface images. It exists many studies providing geophysical exploration at the local scale. The largest interests of hydrology is the mapping subsurface patterns over large areas (Binley, et al. 2015). However, the need of an efficient geophysical investigation is necessary, to understand, predict and manage shallow subsurface systems characterizing by complex and multi-scale interactions at the large catchment scale (Binley, et al. 2015).

After the definition of the representability and the homogeneity from geophysical and hydrological perspectives, we can start the geophysical exploration, in order to select the potential functional hillslope units for future intensive long-term investigations. To recognize the representative, homogeneous hillslopes in the catchment structure from geophysical perspective assuming all hydrological criteria, we recommend performing a test-measurement cross to a selected hillslope unit. We call this test-measurement as a pre-investigation which can be done by the electrical resistivity tomography (ERT) or ground penetration radar (GPR) because these geophysical techniques involve a rapid visualisation of the subsurface directly in the field. In the case “representability and homogeneity”, we can perform the system-oriented geophysical approach, which we will explain and discuss in the chapter 4. In the case of the hillslope untypically and heterogeneity, we have to re-select the hillslope because (Bachmair and Weiler 2013) do not consider such hillslopes with the high spatial variability as homogeneous responding functional units. On other hand, the performing of the expensive three-dimensional measurements is necessary.

Finally, the interpreted geophysical models can be analysed with the results obtained from other disciplines, in order to improve the conceptual understanding the role of the subsurface in determining the hillslope functionality in the catchment.

3 Study sites

To illustrate the suitability of the suggested approach, we conducted measurements in two catchments. The first catchment called the Weierbach catchment takes a place in the hydrological observatory Attert Basin (Martinez-Carreras et al. 2010) that lies in the mid-western part of the Grand Duchy of Luxembourg (Figure 3-1) and is an intensive research site of the Centre de Recherche Public – Gabriel Lippmann² as well as CAOS³ project. The second catchment called the Schaefertal catchment is an intensive research site of TERENO⁴ (Martini, et al., 2014) in the Central Germany and belongs to the Elbe Basin (Figure 3-3). Besides, the Pleistocene periglacial slope deposits (PPSDs) characterize both catchments. The presence of the PPSDs plays an important role in the ecosystem functioning, especially for the formation of soil type, the distribution of soil, the flow paths, and reflecting ecological and climates conditions of landscape in the past (Semmel & Terhorst 2010; Juilleret, Iffly, Pfister, & Hissler 2011). According to the concept of the periglacial cover beds (Semmel & Terhorst 2010), we can describe the PPSDs in Europa in terms of three stratigraphic units:

- (1) the basal periglacial layer (BPL) lies on the top of the bedrock and consists of periglacial debris and debris of bedrock oriented usually parallel to the slope;
- (2) the intermediate or middle periglacial layer (IPL) is generally located on the top of BPL and occurred in dell accumulated with loess, or also can be absent;
- (3) the upper periglacial layer (UPL) reflects the depth of the former active layer, and contains loess and rock fragments oriented usually parallel to the slope.

Hence, the selected catchments differ in topography, hydrological conditions, land use and basic geological formation. Therefore, it makes an interesting contrast to apply the system-oriented geophysical approach, in order to receive an impression how good can the approach work for hillslope characterization in diverse environmental conditions taking advantages and limitations of geophysical techniques into account.

3.1 Weierbach catchment

The Attert Basin (Figure 3-1) lies in the contact zone between the schistous Ardennes massif (Oesling) and the sedimentary Paris Basin (Gutland). We can characterize the Attert Basin by homogeneous and mixed geological setting from schist to marl, sandstone and limestone, different land use and semi-oceanic climate (Zehe, et al. 2014).

The Weierbach catchment takes a place in the north-west part of the Attert Basin, in the Oesling part (Figure 3-1) that represents the Luxembourg part of the Rhenish Massif (Juilleret, Iffly, Pfister, & Hissler 2011). We describe the climate by high precipitation (ca. 800 mm/a), particularly in late summer

² www.lippmann.lu

³ www.caos-project.de

⁴ www.tereno.net/

3 Study sites

(Martinez-Carreras et al. 2010). The hydrological regime is pluvial oceanic with low flows from July to September, and with high flows from December to February (Martinez-Carreras et al. 2010). The dominant runoff mechanisms is the lateral subsurface flow at the contact zone between soil and underlying bedrock due to permeable forested soil (Fenicia et al. 2014).

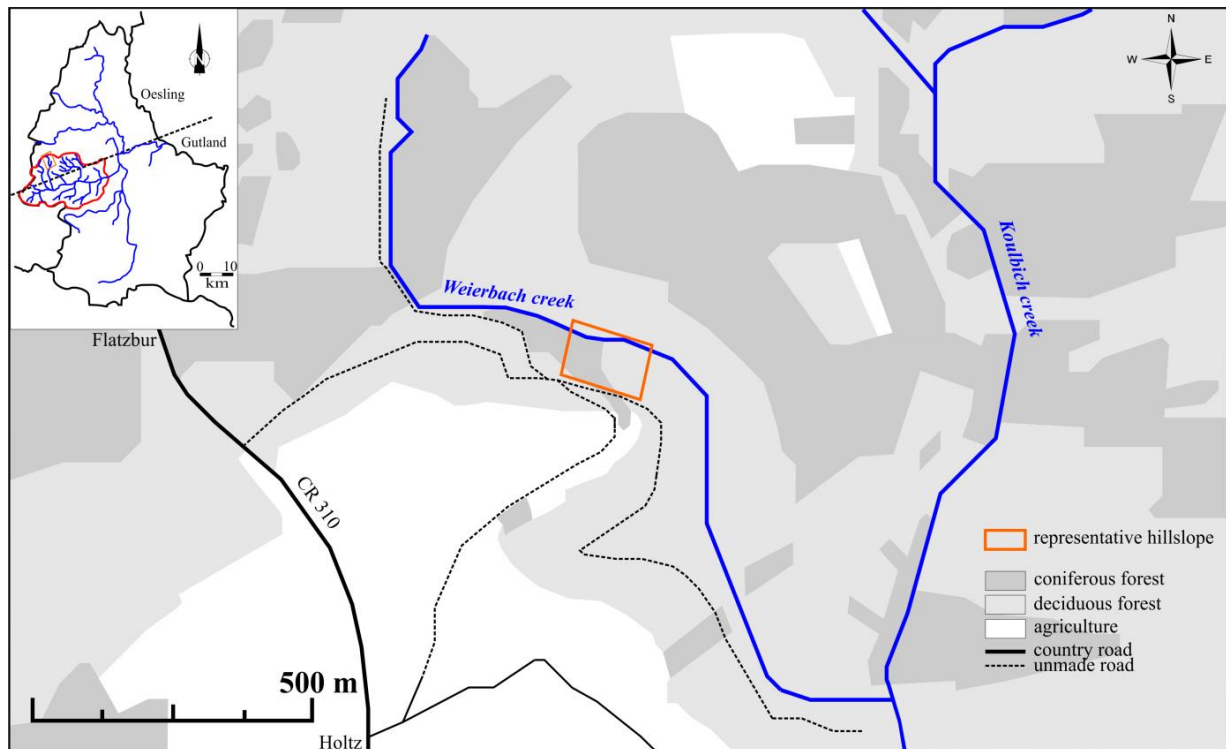


Figure 3-1: Location of a representative hillslope (the orange line) at the Weierbach catchment study site in the hydrological observatory Attert Basin (the red line in the north-west graph), the mid-western part of Grand Duchy of Luxembourg

The Weierbach catchment is the first order catchment and covers an area of 0.7 km² (Martinez-Carreras, et al., 2010). We describe the catchment form as a deep V-shaped valley caused by uplifting processes (Juilleret, Iffly, Pfister, & Hissler 2011). The valley slopes are mainly forested (ca. 84%) with coniferous and deciduous, whereas the plateau surface represents agriculture landscape (ca. 13%). Grassland (3%) covers only the valley bottom. The Devonian schist presents the lithological base of this study site, which differs in two parts: the fractured schist underlain by the compact schist. On the top of the bedrock exists the Pleistocene periglacial slope deposits (PPSDs) reported by (Juilleret, Iffly, Pfister, & Hissler 2011 and Wrede, et al., 2014). The forested soil surficial horizon covers the PPSDs. According to the concept of PPSDs in Luxembourg describing by (Juilleret, Iffly, Pfister, & Hissler 2011), the PPSDs recognize only the Upper layer and the Basal layer. The intermediate layer is absent. (Wrede, et al., 2014) reports that this PPSDs may store significant amounts of water. Moreover, the authors believe that the soils are homogeneous, and classify into Distric Cambisol. The thickness of soil from the surface to the saprock is ca. (79 ± 17) cm characterising by loamy soils with lower bulk density (0.96 ± 0.14)

3 Study sites

g/cm³ (Wrede, et al. 2014). The significant macro-porosity causing by the tree roots and scattered schist stones characterize this loamy soil (Wrede, et al. 2014). Silt texture, root networks reaching to the saprock and higher water infiltration rate (2832 ± 936 cm/d) cause the fast drainage in the upper soil and require the preferential subsurface flow (Wrede, et al. 2014).

The north exposed representative hillslope (Figure 3-1) takes a place at the forested valley slope with moderate inclination of ca. 12° characterized by the strong variability of the micro-topography. The Figure 3-2 illustrates the digital elevation model of the investigated representative hillslope. The hillslope length is ca. 110 m. The investigated hillslope wide range is ca. 80 m. The height difference between the upslope and the downslope is ca. 30 m. The coniferous forest (mainly spruce) covers the West site of the hillslope, whereas the deciduous forest (dominant beech) characterizes the east site of the hillslope.

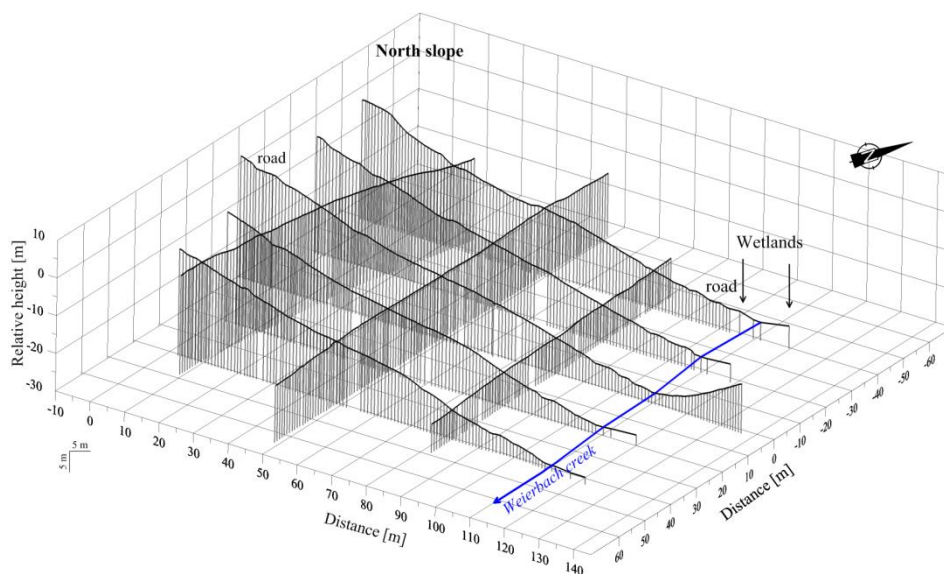


Figure 3-2: Digital elevation model of the representative hillslope at the Weierbach catchment study site

Moreover, the Weierbach creek flows directly at the outcropped bedrock presenting by Devonian schist. Hydrological and meteorological measurement stations with soil moisture sensors have been installed on the investigated hillslope in the frame work of CAOS (Catchment As Organized System) project since January 2012 and conduct the intensive investigations (Zehe, et al., 2014).

3.2 Schaefertal catchment

The Schaefertal catchment takes a place in the Lower Harz Mountains, Central Germany (Graeff, et al., 2009), ca. 150 km southwest of Berlin. The Figure 3-3 shows the location of the catchment and a representative hillslope. We characterize the climate of Harz by regular precipitation from Atlantic throughout the year. The most precipitation occurs at west exposed Upper Harz (1600 mm). In contrast to it, the East Lower Harz receives ca. 600 mm of precipitation per annum (Kistner 2007). The variations in evapotranspiration and snowmelt events in winter cause the seasonal change in discharge (Ollesch,

3 Study sites

Kistner, Meissner, & Lindenschmidt, 2006). Additionally, the mining industry in the vicinity caused the change of a local groundwater level, which influences the runoff mechanisms of the Schaeferfetal catchment (Kistner, 2007; Graeff, et al., 2009). Due to the change of the groundwater level the Schaeferbach creek can dry out during the low rainfall period from July until autumn (Ollesch, Kistner, Meissner, & Lindenschmidt, 2006; Kistner 2007). Moreover, the most important factors of runoff generation are initial soil moisture and occurrence of soil frost in combination with snowmelt or rain-on-snow events (Ollesch, Kistner, Meissner, & Lindenschmidt, 2006). However, the dominant runoff mechanism is surface flow, which causes higher erosion rates in winter (Ollesch, Sukhanovski, Kistner, Rode, & Meissner, 2005).

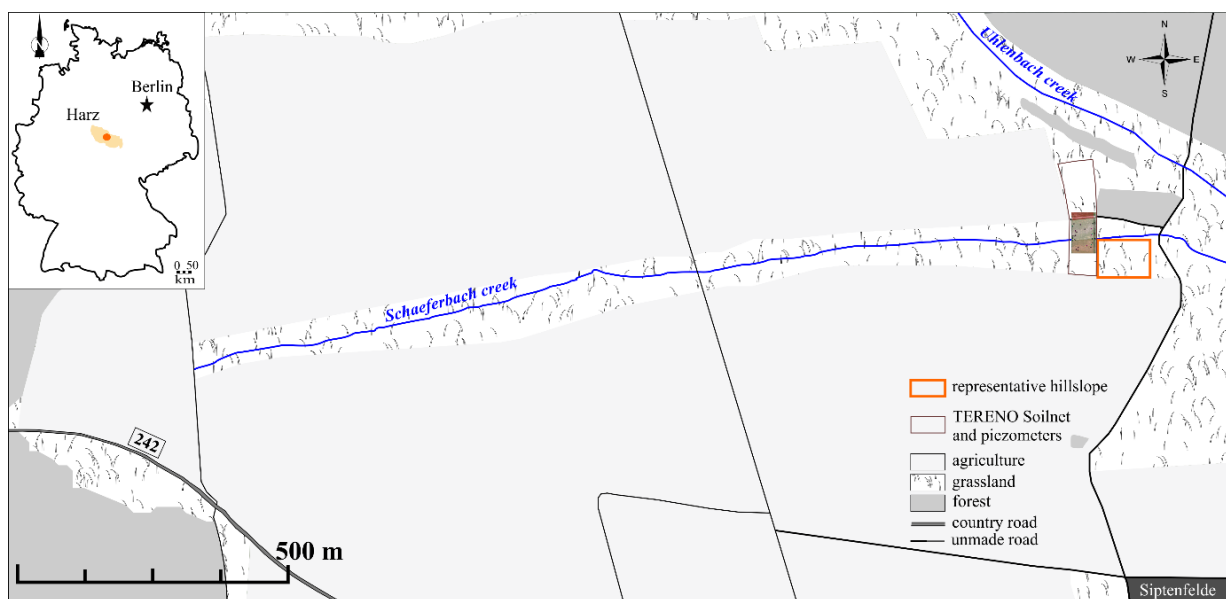


Figure 3-3 Location of a representative hillslope (the orange line) at the Schaeferfetal catchment study site in the Lower Harz, the Central Germany (the north-west graph)

This low-mountain catchment with the Selke catchment covers an area of 1.44 km² and is the first order catchment in the form of a typical U-valley (Kistner 2007). The plateau surface and valley slope represent mainly agriculture landscape (ca 80%), whereas the grassland covers the valley bottom (ca. 16%). The small areas (ca. 3%) in the west part of catchment represent the forested landscape (Kistner 2007). Moreover, following (Altermann 1989) and (Becker & McDonnell 1998), the Devonian greywacke and schist of the so-called Tanner zone characterize the lithological base of the investigated catchment differing in two parts: the fissured upper bedrock underlain by the compact bedrock. On the top of the bedrock exists the Pleistocene periglacial slope deposits (PPSDs) reported by (Altermann 1989) and (Becker and McDonnell 1998). The soil surficial horizon covers the PPSDs. The structure of PPSDs depends on the relief form (Kistner 2007). The typical European PPSDs structure described by (Semmel & Terhorst 2010) in terms of three layer units (UPL, IPL and BPL) characterizes the plateaus, whereas the slope structure consists of two layers (UPL and BPL). The intermediate layer can be absent

3 Study sites

(Altermann 1989). The less permeable fine soil with rock waste and fragments by mountain loam describes the upper periglacial layer. The Luvisols covered mainly the south-facing slope and Cambisols shielded mostly the north-facing slope are the dominant soil type in the catchment (Ollesch, et al. 2006).

The north exposed representative hillslope with slope inclination of ca. 7° is located in the valley bottom covered completely with pasture without agricultural practices at the intensively investigated TERENO hillslope area (Figure 3-3). Hybrid wireless sensor network (SoilNet) and geophysical methods such as electro-magnetic induction (EMI) and gamma ray spectrometry monitored TERENO hillslope area from September 2012 to November 2013, to study temporal and spatial soil-moisture dynamic with high temporal resolution (Martini, et al., 2014). The authors identified four soil-topographic units (STUs) with respect to relevance of hydrological processes, soil morphological characteristics and topographic position. Moreover, the soil moisture dynamic indicates two states: the wet state and the dry state (Martini, et al., 2014). The wet state presents in the winter period and at the beginning of the spring with stable soil water content required by strong rainfall events, snow melting (if snow coverage presents) and decreasing evapotranspiration, and by the dominance of the overland flow. Besides, the valley bottom are more water saturated than back slope areas (Martini, et al., 2014). The dry state begins after the end of intensively precipitation and characterized by the increasing evapotranspiration due to plant activity, solar radiation and high air temperature, and by dominance of vertical water flow without the lateral connection between different areas of the slope (Martini, et al., 2014).

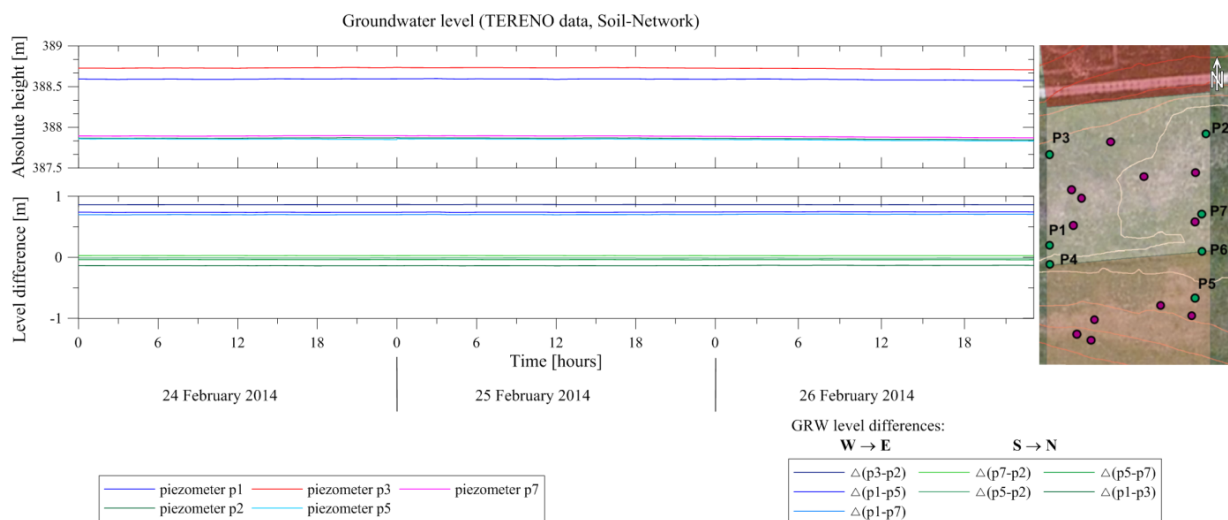


Figure 3-4: Groundwater level (in absolute height) at the TERENO Soil-Network hillslope at the Schaefertal catchment study site

Furthermore, to monitor the ground water level at the north-facing TERENO hillslope in the wetlands, the TERENO staff installed a network of seven water level loggers illustrated on the map in the Figure 3-4. The loggers organize two transect along the hillslope three loggers at the west site and four loggers at the east site. The distance between transects is ca. 100 m. We used water level data of

3 Study sites

five loggers. The logger data⁵ observed from 24th February 2014 to 26th February 2014 and shown in the left graph of the Figure 3-4 demonstrate the ground water level in the absolute height (the upper graph) and the ground water level difference between two loggers (the below graph). The ground water level is higher at the west site investigated hillslope. The difference between the water level logger transects is ca. 0.8 m. Therefore, the direction of ground water flow is from the west to the east, and we can assume that the rate of the ground water change from the west to the east is ca. 0.8 m at 100 m distance. This rate is only valid for this hillslope part.

The investigated representative hillslope is remote ca. 200 m from the SoilNet and the ground water level network hillslope. The Figure 3-5 illustrates the digital elevation model of the investigated representative hillslope. The hillslope length is ca. 96 m. The investigated hillslope wide range is ca. 80 m. The height difference between the upslope and the downslope is ca. 10 m. We characterize the hillslope topography as relatively invariable. We can classify the hillslope into two parts: slope and wetlands separating by the visual jump observed in the field as well as in aerial imaging (see in the Appendix E the Figure E - 1). The water level in the Schaeferbach creek was high during the fieldwork that happened in end of February. The wetlands were more water saturated than back slope area.

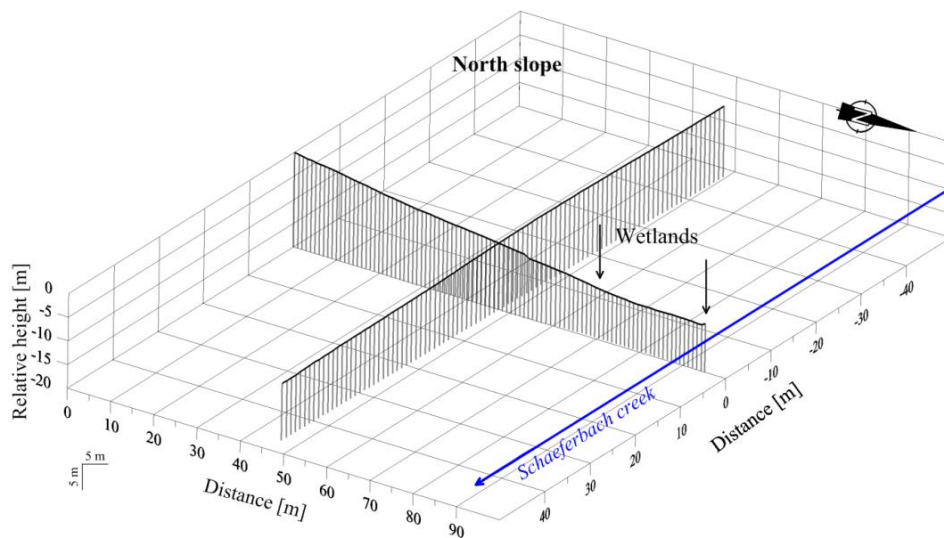


Figure 3-5: Digital elevation model of the representative hillslope at the Schaeferfetal catchment study site

⁵ See the chapter Contribution

4 Methodology

In order to characterize a representative hillslope as a functional unit with respect to hydrological function in a catchment, we will apply two geophysical surveys that provide the content on the hydrogeological situation from the ground surface to the deeper subsurface structures based on physical and geometrical parameters. There are electrical resistivity techniques and refraction seismic survey. On the one hand, we will investigate the hillslope in terms of electrical properties illustrated the contrast between saturated and no saturated media. On the other hand, we will obtain the knowledge on the subsurface structure in the light of elastically properties linked directly to geotechnical parameters. Such combined investigation has to offer a detailed outlook on the subsurface structure of the investigated representative hillslope. In this chapter, we therefore will introduce the theoretical background of applied geophysical techniques and describe experimental composition at investigated study sites.

We can subdivide the working process into three parts: (1) definition of measuring design, (2) data collection in the field and (3) data processing in the office. Following, we will introduce each processing step.

In order to improve the quality in the geophysical data interpretation and to decrease the costs in the field as well as in the office, we find reasonable to conduct geophysical investigations at one profile along the representative hillslope. In this case, we assume that the investigated hillslope is typical for investigated study site and homogeneous. These two points have to discuss together with hydrogeologists. To understand hydrological processes at the hillslope scale, we have to know why this hillslope is typical for the investigated catchment and how homogeneous. If we will know clear that it is typical, representative and homogeneous, we can provide the detailed investigation only at single profile.

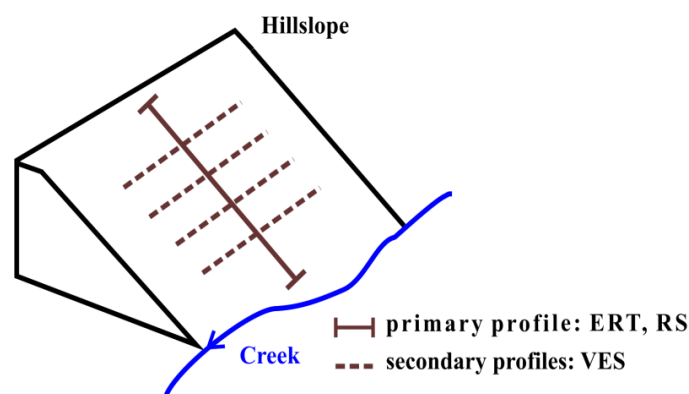


Figure 4-1: Measuring layout to combine geo-electrical and refraction seismic techniques for the characterization of a representative hillslope

The Figure 4-1 shows the measuring design at the representative hillslope where we will conduct sounding and profiling measurements. The idea is that profiling measurements are along the hillslope called as the primary profile, whereas the sounding spreads are perpendicular to the hillslope profile

4 Methodology

named as secondary profiles. The analysis of profiling will inform on the distribution of electrical and seismic parameters in the subsurface along the hillslope. The examination of soundings provides contents of the presence of the two-dimensional structures at each site from the hillslope profile.

The geophysical literature provides several scientific studies using measured layout illustrated in the Figure 4-1 and recommends it as efficiently (Gyulai & Ormos, 1999). The authors describe boundary surfaces and physical parameters using vertical electrical sounding (VES) data collected separately in a set of arrays along the profile with perpendicular oriented VES spreads. The other example presenting by (Nardis, Cardarelli and Dobroka 2005) interprets separately VES data measured in a set of array perpendicular to the profile and refraction seismic (RS) data measured along the profile, in order to provide the joint inversion of coupling electrical and seismic models. Both literature examples assume the slight lateral change in the layer thickness and resistivity, and reference other literature examples applied the suggested measuring layout. The use of the local 1D-approximation by the application of the function based on the priori information (known geological setting) reduce the equivalence in the data interpretation (Gyulai and Ormos 1999). In contrast to these scientific works, we therefore propose to interpret the joint geophysical data set in terms of VES, RS and electrical resistivity tomography (ERT) qualitative.

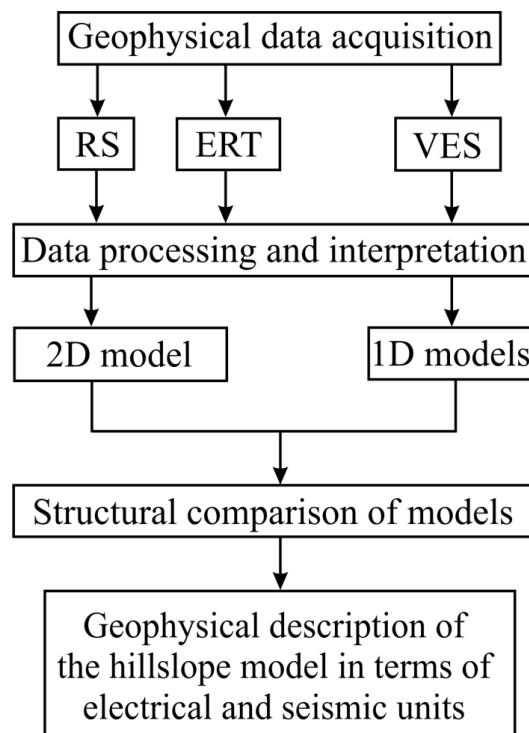


Figure 4-2: Flow chart for geophysical investigation of a representative hillslope in a catchment in an effective manner

After we established the measuring layout, we can introduce the main steps of the geophysical exploration at the single hillslope profile. We illustrate the working steps in the Figure 4-2. At the

beginning, we will process and interpret the collected geophysical data (resistivity and seismic data) individual in terms of one-dimensional models as well as two-dimensional models in order to analyse the advantages of each technique. The one-dimensional models predicate the distribution of physical parameters as a function with the exact depth interpreting quantitative, whereas the two-dimensional model describe detailed lateral distribution of the subsurface parameters explaining qualitative or semi-quantitative. Then, we will compare the single obtained subsurface models with each other in the light of physical and geometrical parameters. The combined geophysical interpretation will provide the description of the investigated hillslope in terms of electrical and seismic units. This joint analysis also will consider the ambiguity in the data interpretation. Finally, we will discuss the interpreted resistivity and seismic subsurface models in the light of hydrological conditions.

Well, let us introduce the principle of resistivity and seismic techniques as well as the experimental composition of each method at the selected hillslope.

4.1 Geo-electrical survey

The application of geo-electrical technique as part of hydrogeological investigation, we explain by identification of electrical homogeneous and heterogeneous patterns of the subsurface structures at the hillslope scale because the subsurface structure can control subsurface flow processes (Freeze R. , 1972; Shahedi, 2008). We therefore can recognise these electrical patterns by resistivity variations in the subsurface causing through porosity, fracture, texture, water content, temperature and concentration of ions (Telford, Geldart, & Sheriff, 1990). As expressed by (Koch, Wenninger, Uhlenbrook, & Bonell, 2009), the adoption of resistivity method along hillslope profile provides spatial electrical patterns of the subsurface structures and can identify subsurface flow paths. To obtain a detailed subsurface image of the hillslope in terms of 3D, many scientific studies such as Koch, Wenninger, Uhlenbrook, & Bonell, 2009; Hübner, Heller, Günther, & Kleber, 2014 conducted quite expensive measurements with many profile lines along the hillslope as well as perpendicular to the hillslope. The main principle of geo-electrical investigation is to describe the subsurface in terms of resistivity and thickness values. Using four-electrode system, a pair electrode known current electrodes create an electrical field in subsurface by the sending of current (I_{AB}) where two other electrodes measure a potential difference or voltage (V_{MN}). The following function known as the Ohm's law describes the relation between measured resistivity or apparent resistivity (ρ_a), measured voltage (V_{MN}) and current (I_{AB})

$$\rho_a = k \frac{V_{MN}}{I_{AB}} \quad [\Omega\text{m}] \quad (4-1)$$

with the geometric factor $k = 2\pi \left(\frac{1}{AM} - \frac{1}{AN} + \frac{1}{BN} - \frac{1}{BM} \right)^{-1} \quad [1/\text{m}]. \quad (4-2)$

This factor describes the geometric configuration of four-electrode system. There are many electrode configurations. Their application depends on the investigation aim and wanted predicated depth.

The inversion from the measured resistivity data set into section of true resistivity happens by using forward modelling based on mathematical algorithms. Such inversion suffer from ambiguity in the

data interpretation. Moreover, the image of inverted resistivity data subjects to non-uniqueness (Hoffmann & Dietrich, 2004) caused by finite number of electrodes and comprises measurements of limited precision (Friedel, 2003). However, the interpretation of geo-electrical data without considering ambiguity can lead to misinterpretation (Hoffmann & Dietrich, 2004).

In order to investigate the resistivity distribution in the subsurface, to address the ambiguity in the interpretation of geo-electrical data and to provide an efficient survey tool for hydrological research, we suggest applying two geo-electrical techniques along the representative hillslope in terms of profiling and perpendicular to this hillslope within the meaning of sounding only at a single profile. We illustrated the measuring design in the Figure 4-1. The vertical electrical soundings (VES) perpendicular to the hillslope predicate the resistivity distribution as a function of the depth and interpret the measuring data quantitative, whereas the profiling by using electrical resistivity tomography (ERT) performs the qualitative or semi-quantitative data interpretation.

The suggested geo-electrical approach for the hillslope characterization can become an efficient survey for the hillslope subsurface characterization in hydrological science. However, according to the measuring layout in the Figure 4-1, we carried out ERT and VES surveys at a single profile along the hillslope in February 2014 in the Schaefertal catchment and in April 2014 in the Weierbach catchment. The measured resistivity data will provide 2D-images of subsurface structures of the investigated hillslope. The Table 4-1 summarizes the applied geo-electrical field parameters at each study site. In the below following subchapters, we will introduce the background of VES and ERT and explain the choice of applied field parameters.

4.1.1 Vertical electrical soundings

The sounding technique uses a symmetrical electrode configuration with the closely, fixed potential electrodes (MN) to the array centre and the stepwise increased current electrodes (AB) outwards. Such configuration provides a good signal-to-noise ratio in the depth. The sounding survey assumes constant resistivity, horizontal homogeneous layering and good vertical contacts (Telford, Geldart, & Sheriff 1990; Pous, Queralt, & Chavez, 1996; Kirsch, 2006).

We therefore performed VES measurements perpendicular to the hillslope profile with respect to the measuring layout illustrated in the Figure 4-1. We measured with the classical Schlumberger (SC) array by stepwise increase the current electrode distance ($AB/2 = 2, 3, 5, 7, 10, 15, 20, 30, 40$ m) and keeping the potential electrode distance ($MN/2 = 1$ m) constant using the 4point-light-hp-Lippmann⁶ device (Germany). We summarize the VES field parameters for each study site in the Table 4-1.

We know that it is better to start a measurement at small electrode distances (from 0.5 m for $AB/2$ and 0.10 m for $MN/2$) for the gathering of soil surficial horizons. In this study, we decided to start our measurements at the relatively large electrode distance ($AB/2 = 2$ m and $MN/2 = 1$ m) because we

⁶ http://www.l-gm.de/de/de_resistivity.html

4 Methodology

want to provide a rather fast geo-electrical survey for hydrological investigation. This investigation aims to image contrasting interfaces by constant homogeneous resistivity values at the geological scale and to identify electrical homogeneous units. We also know that the soil surficial horizon can be heterogeneous

Table 4-1: The acquisition field parameters of geo-electrical investigations at two study sites (explanation see in the chapters 4.1.1 and 4.1.2)

Study site	Field parameters	VES	ERT
Weierbach catchment (forest)	Profile length in m	100	143
	Electrode spacing in m	AB/2: min = 2; max = 40 MN/2 = 1	1 AB _{min} = 3, AB _{max} = 33
	Electrode number	4	144
	Electrode array	SC & HSC	SC
	Field staff	3 men	
	Time effort in the field:		
- preparation	5 minutes	1 hour	
- execution	30 minutes per a point	1.5 hour	
- completion	5 minutes	1 hour	
Schaeferal catchment (grassland)	Profile length in m	95	95
	Electrode spacing in m	AB/2: min = 2; max = 40 MN/2 = 1	1 AB _{min} = 3, AB _{max} = 45
	Electrode number	4	96
	Electrode array	SC & HSC	SC
	Field staff	3 men	
	Time effort in the field:	Per one VES point:	
- preparation	5 minutes	40 minutes	
- execution	25 minutes per a point	1 hour	
- completion	5 minutes	40 minutes	

at local spots along a hillslope, especial in the forest. Therefore, the gathering of soil surficial horizon needs more detailed investigation and can be conducted for designated electrical homogeneous patterns in the future. The other point that we had to decide is the required length of the current electrode spread because the maximal penetration depth depends on the length of the maximal electrode spread. There is a rule of thumb for the estimation of wanted investigated depth (ID) for the case of the Schlumberger array: $AB \sim 5 \cdot ID$ (Kirsch 2006). The penetration depth also depends on the geology and terrain

4 Methodology

conditions. On the other hand, the large electrode spread can take more time and can be impractical in the forested terrain. Hence, we can predicate for our approach the investigated depth by ca. 16 m by the maximal electrode spread (AB) of 80 m. We find that the penetration depth of ca. 16 m is quite enough for the hydrological prospection to characterize the hillslope and to detect possible subsurface flows.

Moreover, to obtain the hillslope 2D resistivity model, we achieved the VES measurements from the upslope to the downslope with the distance between sounding location of 5 m. We therefore collected 21 VES-measurements in the Weierbach catchment and 20 VES-measurements in the Schaeferal catchment. Additionally, to prove the lateral horizontal layering over the width of the hillslope, we modified the classical VES survey to Half-Schlumberger (HSC) array or pol-dipole array by keeping one current electrode at an infinite distance approx. 250 – 300 m on the hillslope plateau. Here, we should accent that the location of the removal electrode at a relatively short distance can affect significant on the measurement and misinterpret data (Yadav, Singh, & Strivastava, 1997; Robain, et al., 1999). We also took into account the two relations characterising homogeneous horizontal subsurface and are useful for the data analysis of HSC technique

$$\rho_a^{AMNB} = \frac{\rho_a^{AMN} + \rho_a^{BMN}}{2} \quad [\Omega\text{m}] \quad (4-3)$$

$$\rho_a^{AMN} \approx \rho_a^{BMN} \approx \rho_a^{AMNB} \quad [\Omega\text{m}] \quad (4-4)$$

The relations (4-3) and (4-4) mean that (1) the apparent resistivity of the full Schlumberger array is equal to the arithmetic average of Half-Schlumberger array values; and (2) all three apparent resistivity values must be approximately equal in the homogeneous medium (Telford, Geldart, & Sheriff, 1990).

At the beginning the data processing, we assessed the quality of measured data. The lower level of the standard deviation error (STD) characterizes the measured data: in the range of 1 - 6% for the Weierbach data sets and 1 - 2.5% for the Schaeferal data sets. The lower level of STD for each measurement we could reach by the controlling of phase and by increasing/decreasing of the injected current during the field measurement.

We plotted the collected VES data in a diagram with logarithmic axes in the terms of so-called sounding curves: apparent resistivity versus current electrode spacing (AB/2), separately for each VES location. These sounding curves illustrate the behaviour of the measured electrical field in the subsurface. Then, we evaluated the sounding curves of Schlumberger and Half-Schlumberger arrays in order to prove the assumption on horizontal layering and to reveal the validity of relation (4-4). We note that the discrepancy between Schlumberger and Half-Schlumberger sounding curves indicates the presence of the lateral variability over the width of the hillslope. In the case of the lateral variability, the assumptions on the stratified homogeneous subsurface are not valid more, and we cannot invert measured resistivity data into a depth model and should interpret these data careful because of the data misinterpretation.

After data evaluation, we selected VES data accepting the relation (4-4) and processed these data using conventional inversion technique of 1D forward modelling. The most forwards modelling programs match iterative measured and modelled data based on the root-mean-square deviation (RMSD).

4 Methodology

Such inversion offers the one-dimensional subsurface model with exact predicated depths. To interpret sounding curves, we have to look their behaviour because the change of the sounding curves indicates the change of the apparent resistivity. We therefore can formulate the main steps of the interpretation of measured resistivity data. In the first step, we define a starting model with appropriate layer number, resistivity and thickness values. The knowledge on geology of the investigated area, the behaviour of the sounding curves (the extreme values) establish the number of layers. Moreover, we can classify the character of the sounding curves with the respect to the statement describing by (Telford, Geldart and Sheriff 1990). As soon as the starting model is prepared, we can start the inversion of measured data. The iterative matching of calculated and measured data, we did using the software Interpex IX1D⁷. To control the quality of the data interpretation and to win the best fitting between calculated and measured data, we also can change the starting model and repeat inversion many times. Finally, we found the correct solution if the measured and calculated data are consistent with each other and the model reflects the geological setting of the investigated study site.

For now, we discuss the data fitting for each case study. The most inversion models of the Schaeferal catchment are well fitted with the RMSD-range from 0.96 to 2.58%. In contrast to it, the fitting of 1D models of the Weierbach catchment ranges RMSD from 1.03% to 8.22%. Besides, we remark that several VES measured data, which do not accept the relation (4-4), we also inverted into the depth models. As starting model for these data, we used already obtained 1D-models of the valid VES data.

Moreover, we assembled all obtained 1D depth models and corrected these models with topography, in order to construct the two-dimensional hillslope subsurface model. For it, we considered following steps:

- (1) Definition of the resistivity consistent stratigraphic units along the hillslope profile characterizing the hillslope subsurface according to VES models and the geological structure;
- (2) Correlation of the resistivity consistent interface between VES locations along the hillslope profile in order to bound the subsurface areas with approximately constant and equal electrical resistivity;
- (3) Definition of layer depths and calculation of their confidence interval. We associated the depth confidence interval with variability of resistivity and depth caused by equivalence in the interpretation of resistivity data.

Final analysis of the interpreted VES hillslope subsurface model distinguishes the homogeneous and heterogeneous hillslope areas called in this study as elementary functional units (EFU's), and splits the vertical underground structure in consistent electrical stratigraphic units (ESU's) with exact predicated depths.

⁷ <http://www.interpex.com/ix1d/ix1d.htm>

4.1.2 Electrical resistivity tomography

In this subchapter, we introduce the background of electrical resistivity tomography (ERT) and the experimental setup of ERT at each investigated area. ERT also utilizes the symmetrical four-electrode system, which moves array laterally along the geo-electrical profile by fixed electrode spacing and measures apparent electrical resistivity as a function of a pseudo-depth. This profiling measurement provides a two-dimensional section of lateral variations in electrical resistivity. In contrast to VES, ERT does not inform on the vertical distribution of electrical resistivity and interprets the data only qualitative.

We conducted ERT measurements on the profile along the investigated hillslope from upslope to downslope with respect to measuring layout shown in the Figure 4-1. We used for this survey the RESECS⁸ multi-electrode device (GeoServe, Germany) and united the ERT field parameters for each study site in the Table 4-1. At the beginning of the ERT measurements, we have to consider the two important points. The first point is the use of an appropriate electrode spacing. Geology and topography of the study site, investigation aim and economic costs influence the suitable choice of electrode spacing. We know that the penetration depth depends on the spacing between the two active current electrodes and the profile length. There is a rule of thumb for estimation of the investigated depth (ID). It ranges from $AB/6$ to $AB/4$ (Kirsch 2006). The interest of our study is to explore the shallow structures, which are relevant for hydrological processes, in the efficient manner with minimal effort. The use of small electrode spacing images near surface structures but it needs more time for preparation and measuring. In contrast to it, the use of large electrode spacing is efficient but it loses the information on the near subsurface structures. We therefore think that the optimal electrode spacing of one meter is quite efficient to explore shallow subsurface structures controlling hydrological processes. Consequently, we can estimate the predicated investigated depth (ID) for fixed electrode spacing of 1 m using the rule of thumb. We summarized the predicated investigated depths for different current electrode spacing (AB) in Table 4-2. Hence, we expect the maximal investigated depth for our measurements by ca. 10 m.

Table 4-2: Estimation of the investigated depth (ID) according to the rule of the thumb (Kirsch 2006)

AB [m]	ID [m]
1.5	0.25 – 0.38
3	0.5 – 0.75
33	5.5 – 8.25
45	7.5 – 11.25

Other important point is a choice of array electrode. In order to find a suitable electrode array for investigated study sites characterizing with different environment conditions, we measured with

⁸ <http://www.geoserve.de>

4 Methodology

different electrode arrays such as Wenner-Alpha (WN), Schlumberger (SC), Dipole-Dipole (DD), Pol-Dipole (PD) and Pol-Pol (PP) with variable configuration parameters. These arrays are characterized by different signal-to-noise ratios, vertical and lateral resolution, sensitivity of electrode configurations, and the noise contamination levels (Dahlin & Zhou, 2004). The accurate choice of the electrode array reflects the time effort in the field and the quality of subsurface image, which should offer ideally the maximum anomaly information, reasonable data coverage and a high signal-to-noise ratio (Dahlin & Zhou, 2004). WN is mostly popular applying electrode array due to lower sensitivity to the noise in the subsurface compared to the other arrays. Nevertheless, the spatial resolution of WN with the increased depth is poorer, whereas SC, PD and DD can resolve better (Dahlin & Zhou, 2004). On the other hand, SC can cause more edge effects (Dahlin & Zhou, 2004). Moreover, DD indicates high anomaly effects and can resolve better the location of vertical and dipping structures but can produce at the same time lower signal-to-noise ratios and cannot exactly detect the depth (Dahlin & Zhou, 2004). The other limitation factor of DD is that this array is more sensitive to the electrode spacing errors and 3D subsurface features (Dahlin & Zhou, 2004). PD and PP also demonstrate well anomaly effects and lower signal-to-noise ratios but cannot produce well spatial resolution (Dahlin & Zhou, 2004). The another limitation factor of PD and PP is the use of remote electrodes that limits the measurement only on one site and confuses data quality checks because of the higher noise level at the remote electrodes (Dahlin & Zhou, 2004). However, following (Dahlin & Zhou, 2004) the recommended electrode arrays for multichannel-recording configurations are PD, DD and SC. Finally, aiming to produce a high-resolution subsurface model of the investigated hillslope, we decided to use the Schlumberger array because this array indicates lesser limitation factors and can be more applicable for steeper slopes without effects caused by 3D subsurface features than DD and PD. Besides, we denote that ERT measured data present a 2D pseudo-section in terms of apparent resistivity versus electrode separation along the profile.

Moreover, we can reach a realistic geophysical subsurface model by understanding of the nature of the measured data (Meju 1995). The quality of inversion images also depends on the model and the noise level (Szalai, Koppán, Szokoli, & Szarka, 2013). We however started the interpretation of measurement data with the evaluation of data quality. The data quality in each study case is characterized by the relatively lower STD error in the shallow subsurface (by ca. 6 % for the Weierbach catchment and by ca. 8 % for the Schaeferfirtal catchment) with the increased STD error in the depth (between 10 and 30 %). Besides, we denote that the apparent resistivity data of the Weierbach catchment demonstrate extremely strong resistivity contrast in the subsurface in contrast to the Schaeferfirtal catchment.

In order to provide a high-resolution depth model with the true electrical resistivity values, we inverted the measured data. The inversion of ERT data is happened using standard iterative procedure starting with an initial model from the first data part (Muiuane & Pedersen 1999) and repeating many times in order to find an optimal final model with an appropriate fitting between measured and calculated pseudo-sections with respect to root-mean-square deviation (RMSD) and noise. Additionally, we have to remark that the main problem of ERT data inversion is the model quality in respect to its RMSD

(Muiuane & Pedersen 1999). Another problem is the appropriate error criterion or the best fitting between measured and calculated forwards models (Muiuane & Pedersen 1999). Moreover, measurement error increases the ambiguity of inversion models and decreases the matching of calculated and measured models (Hoffmann & Dietrich, 2004). Besides, the model misfit can increase with the iteration number, especially where the resistivity contrast extremely high (Olayinka & Yaramanci, 2000).

So far, we computed down the ERT resistivity model to a maximum depth of 10 m in each study case using the software DC2DInvRes⁹ of (Günther, 2004) based on the sensitivity analysis. Before the starting of the inversion, we discretized the starting model. We have to respect that the time of inversion increases with a fine discretization. However, we discretized the starting model into 15 layers with a linear horizontal increment (Δx) of 1 m, and a logarithmic vertical increment (Δz) from 0.3 m to 1.8 m. The fitting of calculated and measured data indicates the moderate RMSD: by 7.75 % for the hillslope model of the Schaeferal catchment, and by 9.58 % for the hillslope model of the Weierbach catchment. Moreover, the inversion model of the Weierbach catchment describes an anti-ideal behaviour with strong resistivity contrast and the increased RMS-misfit with respect to the classification of behaviour of the model RMS-misfit (Olayinka & Yaramanci, 2000), whereas the Schaeferal inversion model shows a behaviour with lower resistivity contrast and relatively small RMS-misfit.

The final ERT inversion model describes the lateral distribution in electrical resistivity. We can compare this model with the resulting VES subsurface model.

4.1.3 VES versus ERT, and versus Combination

After detailed description of applied geo-electrical techniques, we summarized the advantages and limitations of both techniques in the Table 4-3. This subchapter also shows how we can reconstruct a realistic resistivity subsurface model of the investigated hillslope taking the advantages of both geo-electrical techniques into account. We know that geo-electrical models suffer from the ambiguity in the interpretation. To solve the equivalence problem in data interpretation, we can combine both geo-electrical techniques and interpret the results together with geological information. Such interpretation eliminates mistakes and provides an accurate geo-model of the subsurface.

So far, the comparative analysis ERT with VES surveys indicates that data acquisition in case of VES is easier and faster in contrast to ERT. The logistic of VES equipment is also easier and more practical in the regions with difficult environment conditions (especial at a steep slope, with dense vegetation cover) because the use of only four electrodes instead of multi-electrode system make easy to bring it into terrains with hard environment settings. On the other hand, to conduct ERT measurements it is needed maximal two persons for the preparation and the completion and long time for one measurement in contrast to VES, whereas it needs three persons and conducts three measurements (SC and HSC in both directions) at the same time on one VES location. Moreover, the depth in the VES case

⁹ <http://resistivity.net/>

4 Methodology

can be resolved better and deeper because of the geometrical factor ($AB \gg MN$) and larger current electrode spacing than in the ERT case because the penetration depth of ERT depends strongly on the electrode configuration, electrode spacing, and the length of a geo-electrical line. Furthermore, both surveys can provide modified measurements with remote electrodes (the case of PD, PP arrays), but the data interpretation in the ERT case is more confused because of one-sided measurement (see subchapter 3.2, (Dahlin & Zhou, 2004)) in compared to VES. The VES measurements with the remote electrode can easily prove the correctness of homogeneous stratified subsurface. Furthermore, the both surveys suffer from non-uniqueness (Hoffmann & Dietrich, 2004), but the problem of ambiguity in ERT interpretation is presented stronger than in VES, whereas 1D interpretation with equivalence models is clearer.

Table 4-3: Comparison of ERT and VES techniques (explanation see in the chapters 4.1.1 and 4.1.2)

Method	Advantage	Limitation
ERT	<ul style="list-style-type: none"> → automatic measurement → lateral resolution → low personnel costs (1-2 men) 	<ul style="list-style-type: none"> → equipment is heavyweight, especial electrode cable → high time costs in the field for preparation, execution of measurements and completion → ambiguity of models (Hoffmann & Dietrich, 2004)
VES	<ul style="list-style-type: none"> → equipment is lightweight and not expensive! → vertical resolution → deep penetration depth compared to ERT → information on lateral heterogeneities (Half-Schlumberger) → clear equivalent models 	<ul style="list-style-type: none"> → non-uniqueness → manual measurements → high personnel costs (3 men) → manual processing of data

We therefore compared the resulting ERT and VES models in terms of investigation depths and resistivity change. In order to qualify how similar are the obtained subsurface models, we considered the following criteria. The first and main criterion is the exact detectability of an anomaly, which addresses the correctness of location and resistivity (Szalai, Koppán, Szokoli, & Szarka, 2013). Other points are resolution of an inversion model and uncertainty in the depth detection, and specific geometry. Then, in order to demonstrate, how well both models are matching, we overlay these models transparent.

We interpreted the resulting resistivity hillslope models in the light of data quality, differences in resistivity and thickness distribution and the hydrogeological functions. From the analysis of Half-Schlumberger data, we classified the geo-electrical subsurface models into homogeneous lateral subsurface hillslope areas. We called these areas as elementary functional units (EFU's). We also can distinguish in the vertical structure of the hillslope the resistivity consistent stratigraphic divisions called as the electric-stratigraphic units (ESU's).

4.2 Refraction seismic

The application of the refraction seismic in the framework of hydrogeological exploration, we motivate to determine the structural and lithological setting of the investigated hillslope subsurface structures and to predict the basement of the Pleistocene periglacial slope deposits or the interface of bedrock in terms of seismic velocity.

4.2.1 *The theoretical background of refraction seismic (RS)*

The seismic investigation focuses on the analysis and the interpretation of the propagation of elastic waves (Telford, Geldart und Sheriff 1990) in the subsurface triggered by different sources (sledgehammer, vibration and explosion) at the ground surface. In seismic we identify two types of elastic waves. The first type is the body wave, and the second type is surface wave. In this research work, we will consider body wave. Body wave differ in longitudinal or compressional or P-wave¹⁰, and shear or transverse or S-wave (Telford, Geldart und Sheriff 1990). Moreover, the triggered body wave takes different paths in the subsurface (see Figure 4-3). One part of this wave propagates from the source along the ground surface direct to receivers and is characterised by lower seismic velocity values (V_1). This seismic wave, we know as a direct wave. The other part of the triggered seismic body wave transmits inside of the subsurface, where it reflects or breaks under an appropriated angel. If the seismic wave breaks abrupt at the contrasting interface under the critical angel

$$\sin \theta_c = \frac{\sin \theta_1}{\sin(\theta_2=90^\circ)} = \frac{V_1}{V_2}, \quad (4-5)$$

it travels along this interface in the below medium with higher seismic velocity values (V_2) than the overlaying layer, and radiate its energy back to the ground surface. Such broken wave has the name a refracted wave or head wave, or Mintrop wave. Receivers (black triangles in the Figure 4-3) called as geophones and placed usually at the ground surface record the first arrivals of the direct wave and the head wave in a digital signal that can be analysed. The direct wave, we observe at the short distance by first geophones (Figure 4-3). The head wave, we can distinguish at the given critical distance shown in the Figure 4-3 (Telford, Geldart und Sheriff 1990):

¹⁰ In this study, we focuses on the analysis and the interpretation of the longitudinal wave or P-wave.

$$x_c = 2z \tan\theta_c = 2z \left\{ \left(\frac{V_2}{V_1} \right)^2 - 1 \right\}^{-1/2} \quad (4-6)$$

where z is the depth. The equation (4-6) demonstrates that the critical distance decreases by the increased velocity ratio. We also can see that the refraction occurs at the distance by doubly depth to the refractor

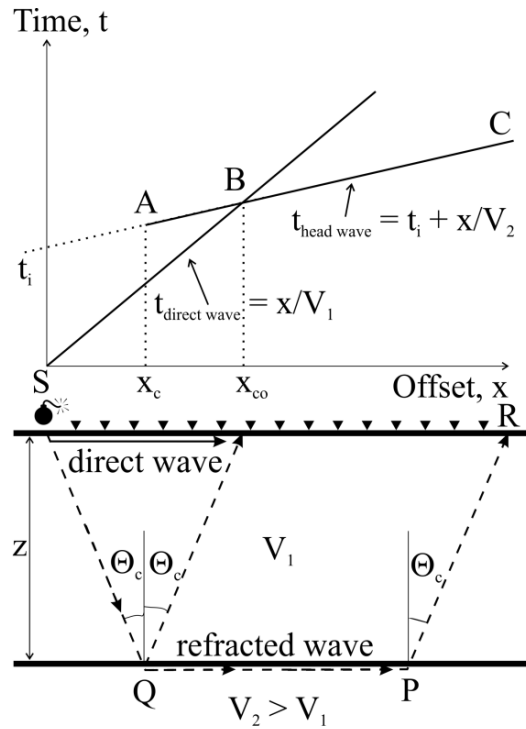


Figure 4-3¹¹: Refraction ray paths and travel time curves modified from (Telford, Geldart und Sheriff 1990)

(Telford, Geldart und Sheriff 1990). Note that the refracted wave cannot exist at the offsets less than critical distance. The refracted wave overtakes the direct wave at the distance larger than the critical distance. This overtake distance we known as the crossover distance and can calculate using the following equation:

$$x_{co} = \frac{2z}{\sqrt{\frac{V_2 - V_1}{V_2 + V_1}}} \quad (4-7)$$

The objective of RS is to find structural parameters (the thickness or the depths) and velocities of the subsurface from recorded first arrival times presenting in a travel time diagram. Division of the horizontal distance (x) and the seismic velocity of the upper layer represents the travel time of the directed wave:

$$t_{direct\ wave} = \frac{x}{V_1} \quad (4-8)$$

¹¹ I created this figure by myself based on the Figure 4.31 Relation between reflection and refraction raypaths and travelttime curves in the chapter 4.3.3 Geometry of Refraction Paths from (Telford, Geldart und Sheriff 1990).

4 Methodology

The travel time of the refracted wave (SQPR, see Figure 4-3) can be calculated (Telford, Geldart und Sheriff 1990) as

$$t_{head\ wave} = 2\frac{SQ}{V_1} + \frac{QP}{V_2} = \frac{2z\cos\theta_c}{V_1} + \frac{x}{V_2} = t_i + \frac{x}{V_2} = t_i + px \quad (4-9)$$

$$p = constant = \frac{\sin\theta_i}{V_1} = \frac{1}{V_2} \quad \text{if } \theta_2 = 90^\circ \quad (4-10)$$

Therefore, from linear equation (4-9) we can find the seismic velocity of the head wave by determination from the slopes of the time-distance curve in terms of the slowness or ray path parameter (p) as reciprocal (see equation (4-10)). If we project the refracted slope line back to the time axis (Figure 4-3), we find the intercept time t_i of the refracted wave. From velocity, intercept time and calculated critical angle (equation 4-5) we can calculate the thickness or the depth of the contrasting interface:

$$z = \frac{V_1 \cdot t_i}{2 \cos\theta_c} \quad (4-11)$$

We therefore can obtain the wanted thickness (or depth) of the refractor, using two methods via the crossover distance (equation (4-7)) as well as intercept time (equation (4-9)). Nevertheless, the intercept time method determinates the depth more precise than relation between the velocities and the crossover distance because we can determinate the intercept time from linear relation (4-9) better than the crossover distance.

Due to the complex mathematical description of the propagated elastic wave in the rock based on the elasticity concepts (Telford, Geldart und Sheriff 1990), the seismic technique assumes many conditions that show the validity of seismic technique and the quality in seismic interpretation. In following, we list the making assumptions in the refraction seismic:

- (1) Homogeneous isotropic horizontally stratified medium with consequent lithological change;
- (2) Ray parameter or slowness p is constant along all rays (incident, refracted and reflected);
- (3) Description of seismic wave front through straight rays;
- (4) Boundary conditions (the normal and tangential components of stress and displacements) have to be continuous;
- (5) The seismic velocity depends on the elastic constants (bulk modulus and shear modulus), the density, porosity, and granular structure of the rock, and increases with the increasing depth because of the increased pressure and density with the depth;
- (6) The change in first arrival time caused by the refractor dip can influence the quantity in seismic interpretation drastically. The utilised equations for the calculation of the refractor dip assume small dip (less than 10°), and has limited value in the practice, especial for a case with more than two refracting interfaces;
- (7) The zone of low velocity layer (LVL) or the weathered zone in the near ground surface space is characterised by lower velocity values, rapid change in velocity, high absorption of seismic energy and high impedance contrast at the base of LVL. This zone can content of gas as well as water. Because of high absorption of seismic energy, recorded travel time

date in the LVL are characterised by lowly quality and it requires locating the shot below the zone of LVL (Telford, Geldart und Sheriff 1990);

- (8) RS determines the ray paths and travel time, but it does not analyse the amplitudes of reflected and transmitted waves;
- (9) Results of RS also like geo-electric results suffer from ambiguity because of complex environmental conditions of an investigated study site (a steep hillslope, lateral velocity change, elastic anisotropy).

The other important point that we have to consider is the quality of seismic data. The quality of seismic interpretation depends strongly on the quality of recorded data. The quality of recorded seismic data depends on the environmental conditions of an investigated area and on the applied acquisition techniques. If we record a wanted seismic event, we denote it as “signal”. Unwanted events we represent as “noise”, which differ in coherent noise and incoherent noise. If we observe unwelcome events at a few traces and can predict it, we characterize as coherent noise (seismic events from near-surface structures, caused by vehicular traffic and farm transport, multiples). Unpredictable seismic events called as incoherent noise (wind shaking, reflexion from roots of trees, distant earthquakes, and a person walking near a geophone), we characterize by spatially random. The incoherent noise we can consider as coherent noise by placing of geophones at a small spacing (Telford, Geldart und Sheriff 1990). To improve the quality of recorded seismic data (the appropriated signal-to-noise ratio or S/N), we have to take coherence, travel direction, and repeatability into account (Telford, Geldart und Sheriff 1990). There are some techniques to improve the signal-to-noise ratio (S/N) and to reduce the coherent noise. The S/N can be estimated as the square root of the sum of n coherent in-phase signals $S/N = \sqrt{n}$. The coherent noise we can greatly reduce by the close geophone spacing. We also can decrease the noise level by the summing (stacking) together tracers of several shots in subsequent processing at different time or different places or both (Telford, Geldart und Sheriff 1990). There are different techniques of stacking: vertical stacking, common-midpoint stacking, uphole stacking and many other complicated stacking. The fundamental literature (Telford, Geldart and Sheriff 1990) therefore recommends applying the stacking techniques in difficult areas.

4.2.2 *Experimental composition*

The experimental section of the refraction seismic investigation, we subdivided into three working packages: data acquisition in the field, data processing of the collected data and the interpretation of the processed data using different interpretation techniques.

Data acquisition, we performed at two study sites (see the chapter 3) along the hillslope profile according to the measuring layout shown in the Figure 4-1 where we also conducted resistivity measurements (see the subchapter 4.1). The applied seismic acquisition field parameters, we summarized in the Table 4-4. Before beginning a RS survey, we formulated a seismic measuring design. For it, we

4 Methodology

had to answer several questions: (1) how many active channels should register for the covering of the refractions, and (2) how large geophone spacing and shoot point distance have to be.

Table 4-4: The acquisition field parameters of refraction seismic at two study sites

Field parameters	Weierbach catchment (forest)	Schaeftal catchment (grassland)
Length of profile in m	95	95
Geophone spacing in m	1	1
Source point distance in m	5	5
Number of active channels	96	48
Recording instrumentation	Geometrics ES-3000, Geode, Seismic-Module Control System MGOS	
Number of active geodes	4	2
Natural frequency of geophones	14 Hz	
Type of geophone	P-wave, vertical	
Source type	Metal hammer 5 kg	Plastic hammer 5 kg
Sampling rate in msec	0.25	0.25
Recording time in msec	125	125
Filter	Without filter	Low-pass filter 10 Hz
Number of stacks at a shot position	3	1
Data format	SEG2	SEGY
Number of assistants	3	
Total number of shoots:	26	20
Inside of geophone spread	20	20
Outside of geophone spread	6	-

To predict the whole path of refractions in the underground, it is better to use a long linear profile with many geophone groups. At the same time, the use of over long profile is not practical to record all geophone groups and leads to communication and logistic problems, especial for forested hillslopes. It is sometimes recommendable to spread the profile in segments. We also know that the length of refraction seismic profile can depend on wanted penetration depth and environmental conditions. In our study, we therefore applied two schemas of seismic measuring layout, in order to exam which schema is more suitable for an efficient investigation. The first schema records along the whole hillslope with all 96 active channels, and the second schema spread the hillslope profile in two segments and registers with 48 active channels. Note to reach a consistent coverage of recorded data along the profile by using of

4 Methodology

small active spreads, we have to overlay both segments measuring in roll-along technique. Moreover, we decided for the relative close geophone spacing of one meter. The choice of this spacing we find as optimal to register direct wave as well as refractions because the using of the larger geophone spacing can lead to the missing of the direct wave in the seismogram. On the other hand, we know that the use of the closest geophone spacing is not appropriately for refraction data because of low frequency and longer travel paths of the head wave. Furthermore, to reconstruct continued refractors along the whole hillslope, we performed the series of reversed refraction profiles starting at the top hillslope and moving to the foot slope in a constant source point distance of five meter. Note we completed the shooting refraction profiles inside of geophone spread as well as outside of geophone spread. The shooting outside of geophone spread offers only the information about refracted waves.

After we formulated the seismic measuring design, we placed the geophones at regular, equidistant spacing of one meter along the hillslope profile with a length of 95 m. In the Weierbach catchment, we applied the first schema with 96 active channels for registration of seismic wave, whereas in the Schaeferfetal catchment, we spread the refraction seismic profile in two segments and registered the seismic wave with 48 active channels. The splitting of hillslope refraction profile in the Schaeferfetal, we argue that surface topography in the middle part of the hillslope profile make evident a jump causing probably by presence of a two-dimensional geological-geomorphological feature. The feature we can identify in a satellite image (see Appendix the Figure E - 1). This jump in topography separates the hillslope into two part: the upslope and the foot slope with wetlands. We also have to note that we did not do the overlay of these two segments. This mistake we will take into account in the data interpretation. Anymore, we recorded all seismograms using Geometrics¹² ES-3000 with Geodes and Seismic-Module Control for Multi-Geodes Operation System (MGOS). We triggered the seismic wave with a hammer at ground surface in terms of P-waves recorded by vertical geophones with natural frequency of 14 Hz. To the point of data quality, we mention that we had stack the traces (especial at the forested study site - Weierbach catchment) for the elimination of incoherent noise causing mostly by the wind shaking and the reflexion from roots of trees. In case study of Schaeferfetal, we did not stack the traces, but we applied the low-pass filter of 10 Hz. Thus, we filtered the lowest frequented noise.

We therefore collected refraction seismic data at each study site: 26 shooting refraction profile in the Weierbach and 20 shooting refraction profile in the Schaeferfetal. We thereby have to note that we could not shoot outside of the geophone spreading in the Schaeferfetal because of an agriculture field at the upper part of hillslope slope and the Schaeferbach creek at the bottom of the hillslope. In the below following passages, we will describe the steps of data processing and applied interpretation techniques.

Due to the elevation correction of refraction seismic data, we also measured the hillslope surface topography with the Leica-Tacheometer of type TPS1200+ in a local Cartesian coordinate system with the fixed zero-point at the top of the hillslope profile. The zero-point is the position of the first geophone.

¹² <http://www.geometrics.com/>

*The flow chart of data processing called in this study from collected data to travel time diagram*¹³ contains following steps:

- (1) Data reduction includes the correction of the measured refraction data for elevation and weathering variations. This step is crucial because this correction respect the influence of hillslope topography and near surface zone. The negligence of this correction can provide the misinterpretation of the seismic velocity model. The elimination of the effects of near weathering layer we can do using the so-called static correction. This correction assumes that (1) the shot points and the geophones have to be at the planar interface; (2) the material below this interface is homogeneous and does not content the material of LVL; and (3) the medium between the surface elevation and the planar homogeneous medium is characterised by velocity changes. The static correction (Δt) is computed as the sum of the source correction (Δt_s) and the receiver correction (Δt_r). To estimate the static correction, we need to know the surface topography, the source depth (shot-hole depth) and information about the near surface layer (Al-Sadi 1980). One way to win the information about LVL, is results obtained from Plus-Minus methods (the explanation see below in the passage *From travel time to the structural subsurface model*).
- (2) Seismogram analysis and identification of the first arrivals: From recorded digital signals and elevation corrected data, we analysed the seismograms for each shots and defined the first arrivals of seismic wave. Before beginning the identification of first arrivals of the P-wave, we filtered the data to remove the noise that we could not eliminate by stacking in the field. After filtering, we analysed the first arrivals of the seismic events. To recognise the first arrivals of the direct wave and the refracted wave in a seismogram, it is necessary to consider such factors as (1) coherence, (2) amplitude standout, (3) character, and (4) dip and normal moveout (Telford, Geldart und Sheriff 1990). We found the similarity in appearance of signal from trace to trace for each shot, and identified the shape of the envelope and the amplitude standout from trace to trace. We also diagnosed the systematic difference in the trace-to-trace travel time of an event.
- (3) Travel time analysis and definition of slope velocities: We examined the data in terms of the first arrivals in a travel time diagram in order to define seismic velocities of P-waves. Recognition and identification of the direct wave and the refracted wave in the travel time diagram based on the slopes of time-distance curve. We also proofed that (a) the reciprocal time is the same for reversed profiles; (b) the intercept time for profile shot in different directions at the same shot point is equal; and (c) travel time curves of series shooting profiles

¹³ We processed and analysed the collected refraction seismic field data at each study site using software REFLEXW Version 6.0.9 (Sandmeier 1998-2009) from <http://www.sandmeier-geo.de>

have to be parallel. From travel time analysis, we also can recognize the refractor dip by different apparent velocity and different intercept time.

We note that the main problem of RS is to recognize the different head waves. We should decide: when did the several refractors occur; how many refractors can we identify; how strong is the effect of the earth surface topography and the near surface layer.

From travel time to the structural subsurface model

The main task of RS is to reconstruct the path of seismic wave and to develop a structural subsurface model with the physical properties of the lithology and the predicated depths of the contrasting interfaces in the underground. However, we used different interpretation techniques of refraction seismic. The use of different interpretation techniques can avoid the misinterpretation of the refraction seismic data, and can control correctness of obtained results. The fundamental literature (Telford, Geldart und Sheriff 1990) refers that there are three classical options to interpret refraction seismic data: (1) the application of equation (4-6), (4-7), (4-9) and (4-11); (2) Delay-time method; and (3) Wave front reconstruction method. There also are other useful interpretation techniques for the subsurface reconstruction, for example (4) refraction seismic tomography and (5) ray tracing modelling.

The use of equations (4-7), (4-9) and (4-11) assumes that refractor is planar and it does not consider the topography of the refractor. This technique is successful for the case for two-layer model, but it can fail for multi-layers because it solves the deeper refractors by locating the shot point and geophones at the first refractor.

The delay-time technique introduced by Gardner in 1939 is quite famous in the interpretation of refracted data (Telford, Geldart und Sheriff 1990). Nowadays, there are many interpretation schemes using delay time such as Barry's method and Wyrobek's methods (Telford, Geldart und Sheriff 1990). The delay-time technique assumes that (1) refraction travel time has to correct for elevation and weathering, and (2) the predicted depth from source / receiver to the refractor is a perpendicular projection (Telford, Geldart und Sheriff 1990). We therefore can determine the delay time as

$$\delta = \delta_s + \delta_r \approx t_g - \frac{x}{v_2}, \quad (4-12)$$

where δ_s and δ_r are called as the delay time at the shot point and the geophone, and t_g is the observed refraction time at the geophone. This technique offers the relief of the refractor and the certain errors, but it does not consider the velocity variation in the near surface zone (NSZ).

In this study, we will interpret refraction seismic data using wave front reconstruction technique (plus-minus method), refraction seismic tomography and ray tracing modelling. In the next passages, we will introduce and describe the principle of these techniques.

The wave front reconstruction technique provides an elegant method (Telford, Geldart und Sheriff 1990) to map the refractors using two wave front systems from symmetrical shot points: forward and reversed. Thornburgh applied the technique of the wave front reconstruction in 1930 (Militzer und Weber 1987). (Hagedoorn, 1959) mentioned that the attractive Thornburg's technique was not famous

4 Methodology

during the long time. In 1946, the Russians developed and published (Riznichenko 1946) the same method in more complete form than Thornburgh (Hagedoorn 1959). The concept of the wave front reconstruction considers the wave motion in a three dimensional space and bases on the Huygens's principle. The advantage of this concept is that it requires only the knowledge about seismic velocity in the subsurface, and not the refractor. The refractor we can draw from observed travel time at the geophones as tangent of envelope of the intersecting wave fronts for the equal time interval. Using this principle, we can consider the multi-layer system. Nowadays, there are many interpretation techniques based on the wave front methods. In the next passage, we will describe one of the classical interpretation techniques published by (Hagedoorn 1959) known as the plus-minus method.

Plus-Minus method (PMM) can reconstruct the refractor with irregular topography and gather the lateral velocity variation in a simple and rapid manner. This technique can investigate the subsurface structure of LVL in order to apply the obtained result for the static correction in reflexion seismic. This technique also admits the controlling of data quality and the optimisation of the shot configuration (van Overmeeren 2001). The principle of PMM developed by (Hagedoorn 1959) shown in the Figure 4-4. Two symmetrical shot points (A and B) placing far enough from each other draw a diamond pattern of wave fronts at regular time intervals. The horizontal diagonals of diamonds shape an envelope where

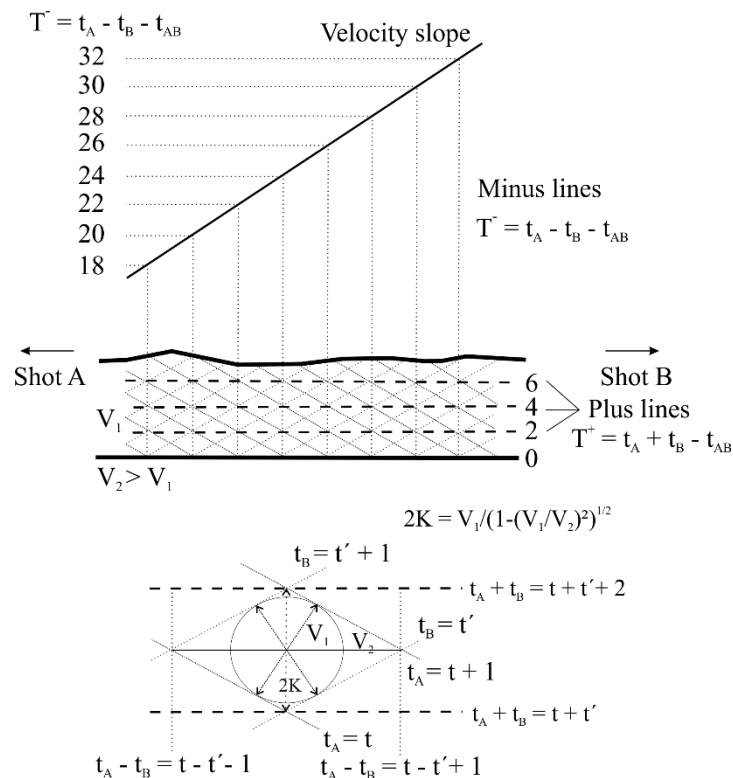


Figure 4-4: The principle of the "Plus-Minus" method developed by (Hagedoorn 1959)

4 Methodology

the sum of travel time from both shot point is equal. These lines describe Plus-lines, which determine location of the refractor in the subsurface. The following equation (4-13) calculates the time plus values (T^+)

$$T^+ = t_A + t_B - t_{AB} \quad (4-13)$$

where t_A and t_B are the observed travel time at the geophones from the shot point A and from the shot point B, respectively, and t_{AB} is the total travel time from the shot point A to the shot point B. These Plus-values also represent intercept times of the refractors when we project the time-distance slope from the refractor back to the shot point.

The vertical diagonals of diamonds represent the difference between the travel times from the shot points A and B. This difference must be constant because of increased equal travel time interval of overlapped wave fronts. Hagedoorn titled these time difference lines as Minus-lines and calculated the time minus values (T^-) in the following way

$$T^- = t_A - t_B - t_{AB}. \quad (4-14)$$

These vertical lines characterise the constant velocity from surface to the refractor. The upper graph in the Figure 4-4 shows the slope of plotted time units versus distance. This slope describes the measured velocity of the wanted refractor.

PMM therefore assumes that (1) the parallel plus lines to the refractor; (2) the minus lines do not converge or diverge; (3) constant velocity values and (4) the range of detected refractor bounded by the two crossover (x_{co}) points of symmetrical spreads. PMM interpretation finally results the exact depth of refractor.

Plus-minus technique can calculate from first arrivals the location of refractor using conventional software such as Microsoft Office Excel, MATLAB. For example, (van Overmeeren 2001) demonstrates the plus-minus program developing in MATLAB to investigate an aquifer in Yemen.

Our case study will illustrate the determination of refractor with plus-minus technique using software Microsoft Office Excel installing on each laptop or PC with relatively lower costs and needing simple knowledge of programming. The processing steps based on the processing of (van Overmeeren 2001) include the interpretation of single symmetrical spreads and integration of these spreads into the investigated hillslope profile. We therefore subdivided the RS data interpretation processing into following steps:

- a) Selection of single symmetrical spreads from collected RS data and preparation into a single matrix, which we plotted in a travel time-distance diagram;
- b) Definition of velocity slope segments in terms of direct wave and refracted wave, and calculation of velocity values;
- c) Determination of the total travel time between the two symmetrical shot points;
- d) Calculation of plus and minus times values using the equations (4-13) and (4-14);
- e) Definition of the refractor velocity from the minus time values based on the time difference-distance slope;

- f) Calculation of the refractor depth from plus times (the intercept times) values and the measured velocity values of the overlying layer and underlying layer with equation (4-11);
- g) The visual demonstration of the resulting interpretation.

The obtained interpretation results using Plus-Minus technique, we future will compare with interpretation results obtained by seismic tomography and ray tracing. We can integrate PMM subsurface model as starting model by FD ray tracing modelling or for the static correction in order to reprocess the field data. Due to the study aim to suggest an efficient and fast technique, we will not reprocess the data in the terms of static corrected data. In our study case, we will compare different RS interpretation techniques and decide what kind of technique is more efficient for the hillslope characterization.

After introduction of Plus-Minus technique, we will describe the principle of seismic tomography and ray tracing modelling as well as applied software.

Refraction seismic tomography (RST) is quite a popular interpretation technique by geophysicists as well as by no geophysicists for interpretation of refraction seismic data in many scientific studies (Hausmann, et al. 2013) because of easy application and it does not require the advantage knowledge for the deeper understanding of seismic principle.

The principle of seismic tomography is that the first arrivals of series of refraction seismic spreads will inverted to the two-dimensional section. Today, there are various refraction seismic inversion programs to invert refraction seismic data. The principle of mostly seismic tomography programs is to solve forward problem based on the tomographic algorithms. These programs adapt iterative and automatically synthetic travel time data to real data to obtain the two-dimensional section describing the seismic velocity field in the subsurface, but it does not predict exact refractor depths. Nevertheless, we applied refraction seismic tomography in the data processing in order to receive the first information about the distribution of seismic velocity field in the subsurface.

In our study case, we processed measured RS data with Ra/TT2dTomo¹⁴ software (Günther, Bentley and Hirsch 2006). This inversion program calculates the subsurface model using the algorithm of Shortest Path (Dijkstra 1959) and unstructured triangle meshes and can integrate surface topography. The algorithm also can provide robust modelling. After loading of travel time data in the program, we specified a starting model with respect to geometry (model discretization) and velocity values. Then, it calculates theoretical travel time and compares with real data to find an appropriate subsurface model. The process is iterative repeated by model changing, and it is breaks if a good matching of theoretical and real travel time data fulfil the stop criterions. The final inversion model describes the distribution of seismic velocity in the underground. At the same time, we can consider the inversion results in terms of the ray parameter. The image in view of the ray parameter can provide precise information about contrasting interface because of the uniformity of the ray parameter and its abrupt change at contrasting interfaces.

¹⁴ <http://www.resistivity.net>

The ray tracing modelling is other technique to interpret seismic data. This technique simulates the travel time of propagated seismic wave based on the wave front inversion and finite-difference (FD) approximation of the Eikonal equation (Weber, Rumpker and Gajewski 2007)

$$|\nabla T(\vec{r})| = \frac{1}{\beta(\vec{r})} \quad (4-15)$$

where $T(\vec{r})$ is the Eiconal or travel time from source to the point, and $\beta(\vec{r})$ is medium velocity depending on the position vector \vec{r} at the point with the coordinates (x, y, z) . The Eiconal equation means that a wave front propagates perpendicular to themselves with local velocity (Weber, Rumpker and Gajewski 2007).

We performed the ray tracing modelling using software REFLEXW¹⁵ Version 6.0.9 (Sandmeier 1998-2009). With respect to the software introduction given by (Sandmeier 1998-2009), we executed iterative developing of subsurface model trough assign and combine of travel time based on the wave front inversion and FD-approximation of the Eiconal equation. We subdivided the modelling process into the following steps:

- a) Loading of first arrivals from spread series with respect to forward and reverse spread because wave front inversion requires the application of symmetrical wave fronts;
- b) Assign of measured travel time to layers;
- c) Travel time combine for the upper layer and deeper layers. In this step, we also included the surface topography by processing of the upper layer. Therefore, the obtained inversion subsurface model considers the effect of surface topography;
- d) The application of the wave front inversion for each assigned layer individually based on a linear regression for all forward and reverse spreads (Sandmeier 1998-2009). We note that the difference of the total travel time between forward and reverse spreads must be small.

This developed subsurface model based on the wave front inversion, we used as a starting model for the ray tracing modelling. The principle of the ray tracing modelling is to compare calculated travel time data to the measured data. We executed iterative and manual changes of model parameters (geometry of refractors and velocity values) and repeated the ray tracing process many times until we found a wanted subsurface model reflecting measured travel time and matching calculated and real data.

Finally, to control the results of applied interpretation techniques, we used **vertical seismic profiling (VSP)** at several shot positions based on CMP¹⁶ (1D) velocity analysis. We realized VSP technique using software REFLEXW¹⁷ Version 6.0.9 (Sandmeier 1998-2009). CMP analysis results a one-dimensional velocity-depth profile trough iterative velocity adaption.

As a final point, we will compare and discuss results obtained from different RS interpretation techniques in the light of refractor depths and velocity values.

¹⁵ <http://www.sandmeier-geo.de>

¹⁶ CMP is meaning common midpoint

¹⁷ <http://www.sandmeier-geo.de>

4.3 Geo-electric versus refraction seismic, and versus Combination

After the individual representation of resistivity and refraction seismic techniques, we will interpret jointly resulting geo-electrical and refraction seismic subsurface models. We also will discuss the advantages and limitations of each technique. On the one hand, geo-electrical models provide the information on the saturated subsurface zones, whereas refraction seismic links directly to geotechnical parameters (Cardarelli, Cercato and Donno 2014). On the other hand, we know that the geophysical interpretation of geo-electrical data as well as seismic data suffer from ambiguity. The joint interpretation of resistivity and seismic techniques therefore can complement our understanding about the nature of geophysical data interpretation in order to improve the geo-image of the investigated area. The Table 4-5 summarizes the advantages of each technique. The one-dimensional geo-electrical modelling predicts exact the depths of contrasted electrical boundaries, whereas the two-dimensional geo-electrical tomography images only the patterns of saturated and dry subsurface zones. The application of RS is useful to predict the weathered bedrock interface and link to the geotechnical parameters.

The discussion questions in this chapter is how we can understand the geophysical models obtained from resistivity and seismic data sets using 1D- and 2D-techniques, in order to estimate the structural similarity between resistivity and seismic velocity models. Hence, to interpret the geo-models jointly, we make the assumptions that there are the coupling between geo-electrical and seismic models and the slight lateral change of petro-physical parameters.

Table 4-5: Summarization of applied geophysical methods

Method	Effectiveness	Interpretation technique
VES	The exact depth predication of contrasted electrical interfaces	Four-electrode system to develop the 1D-models
ERT	The illustration of the patterns of saturated and dry subsurface zones	Multi-switch system for the imaging of the 2D-section
RS	The predication of the weathered bed rock boundary and linking to the geotechnical parameters	Seismic tomography, wave front reconstruction using PMM and ray tracing to illustrate the 2D-section

Nowadays, it does not exist a universal relation between electrical resistivity and seismic velocity values (Bedrosian, et al. 2007). One way to couple electrical and seismic models is to perform the joint inversion based on the mathematical algorithms using the common boundaries between the neighbouring layers obtained through the VES local 1D-approximation (Nardis, Cardarelli and Dobroka 2005). Other example described by (Bedrosian, et al. 2007) provide a quantitative, statistical approach based on the magneto-telluric seismic models to link electrical and seismic parameters. Many

geophysical investigations also implement qualitative correlation between electrical and elastically properties based on the joint interpretation of resistivity and seismic data.

This research study focuses on the qualitative interpretation of resistivity and seismic velocity models through the structural comparison between geophysical models. The best and fast way to compare qualitative the individual models with each other is a transparent overlay of models, in order to localize seismic and electrical patterns to respect with the geological-lithological knowledge. Moreover, the more precise comparison is through the subordination of the exact layer boundaries of seismic and electrical interfaces with the uniform petro-physical values. The seismic and electrical tomography offers the qualitative comparison by the funding of the localized similar patterns. Whereas the structural boundaries obtained from the one-dimensional analyse and wave front reconstruction provide a better compiling of the models. We will join both techniques, in order to develop a realistic hydro-geophysical conceptual model, which has to be representative for the investigated catchment.

4.4 Joint three-dimensional interpretation of the investigated hillslope

The three-dimensional geophysical interpretation of measured geophysical data provides the visualisation of the investigated area in terms of 3D and the understanding of the relevant hydrological processes. The construction of a detailed three-dimensional image involves the large effort in the field as well as during the data processing (Hoyer , et al. 2015). Many scientific studies conduct many profile measurements along and cross to the investigated area. We introduced the several examples of these studies in the chapter 1.3.

We motivate to create a three-dimensional section using two profiles with minimal effort, in order to prove the suitability of the suggested system-oriented approach. One profile is along the investigated study site, whereas the second profile is cross to the first profile. We believe that such design can provide enough information on the subsurface structure to understand the relevant hydrological processes.

To create the three-dimensional hillslope subsurface model, we considered the following three steps:

- (1) Structural comparison of geo-models of two profiles. The first profile along the hillslope, and the second profile is cross to the hillslope;
- (2) Proving of the correctness of the stratified subsurface of the investigated hillslope using VES data along the hillslope profile and ERT data cross to the hillslope profile;
- (3) The creation of the 3D-hillslope subsurface model in terms of seismic velocity units using Golden software Grapher.

Therefore, the obtained three-dimensional subsurface model has to demonstrate the validity and the correctness of the developed system-oriented geophysical approach.

5 Results and discussions

This chapter will present the results at the two study sites (the Weierbach and Schaefertal catchments) and discuss in the light of the successful of the suggested system-oriented geophysical approach. At the beginning, we will show the geo-models obtained individual and independent from each other using the different interpretation techniques. Then, we will compare the geophysical models in order to demonstrate the similarities and discrepancies between VES-, ERT- and RF-models. To conclude this chapter, we will show the three-dimensional subsurface model for each study case.

5.1 Geo-electrical investigation

5.1.1 Application in the Weierbach catchment

We begin to demonstrate and to discuss the result of ERT survey shown in the Figure 5-3 in the upper diagram. Also included are slope topography, geographic direction, slope exposition and the geomorphologic features (the Weierbach creek, wetlands, and forested road) that can help to interpret the inversion model. We calculated the ERT model to the maximum depth of 10 m. The ERT images recognizes three lateral continuous electrical resistivity patterns. The thin upper layer with relatively high resistivity values in the range of 1000 - 1900 Ωm reaches the depth of ca. one meter and continues almost whole slope. We can observe that this layer is absent in the bottom slope and the wetlands contenting of lower resistivity values (300 - 1000 Ωm). The relatively high resistivity upper layer, we can associate with the loamy soil, whereas the low resistivity in the bottom slope and the wetlands we can associate with the conductive-outcropped fractured bedrock. Beneath the middle layer with the high resistivity values (more than 3000 Ωm) occurs the whole slope and reaches the depth of ca. five meter. The middle part of this layer in the depth of ca. 2.5 m demonstrates an extremal significant resistivity variability (more than 5000 Ωm). We can assume that this high resistant layer associating also with loamy soils indicates a good possibility for the drainage system causing by the tree root networks and scattered schist stones. Moreover, if we follow this high resistant layer in the direction of the downslope and the wetlands, we will observe that this layer does not exist here because this profile part demonstrates the low resistivity values ranging from 300 Ωm to 1000 Ωm . As in the case of the upper layer, we associate this hillslope part with the conductive-outcropped fractured bedrock. The low resistivity layer (300 - 400 Ωm) exists below the high resistant layer. This layer outcrops in the foot slope and wetlands. Maybe, we can subordinate this low resistant unit with the fractured bedrock. Moreover, if we observe the subsurface area framing between the two isolines from 1000 Ωm to 375 Ωm , we can mark this subsurface part as a transition zone associating with the possible subsurface flow path.

As we can see, the ERT image represents only the several patterns of the localized conducted areas without precise boundaries. Therefore, the main difficulty in the interpretation of the ERT results is that ERT model cannot detect the precise depth interface between layers. We can only determine by the bounding of significant resistivity areas using the contour lines or isolines. Therefore, we cannot

5 Results and discussions

determine precise the interface between the upper layer and the middle layer because it is resolved unclear. In contrast to it, the interface between the high resistant middle layer and the low resistant down layer, we determined by the isoline of $1000 \Omega\text{m}$ in the depth of 4 - 5 m or with respect to topography (the relative height) from -5 m to -25 m.

At that point, let us demonstrate and discuss the results of the VES survey shown in the Figure 5-3 in the below diagram. Before we start describing the VES image, we will demonstrate and analyse the VES measured and inverted data. The analysing of the sounding curves with respect to the sounding curves classification presented by (Telford, Geldart, & Sheriff, 1990) informs us that the most sounding curves indicate the type K (for example the Figure 5-1, the left graph) and Q (for example the Figure 5-2, the left graph). Furthermore, we proved the correctness on homogeneous stratified subsurface. The left

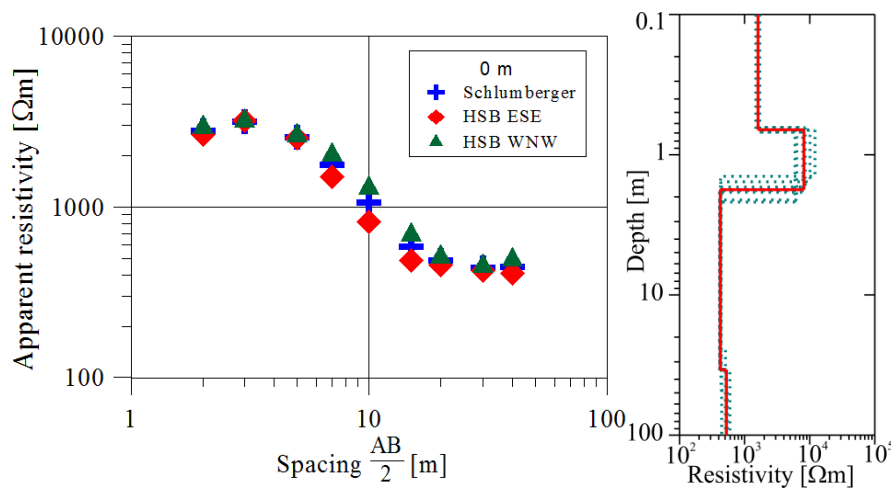


Figure 5-1: The case study of the Weierbach catchment: Sounding curves of Schlumberger and Half-Schlumberger measurements (the left diagram) at the ERT profile 0 meter presenting an example for lateral homogeneity perpendicular to the ERT profile, and their inversion result with equivalent models (the right graph)

graph in the Figure 5-1 representing one example for the lateral homogeneous medium confirms the agreement of the equation (4-4). The 16 from 21 VES profile points describe the hillslope profile as the homogeneous stratified subsurface. In contrast to it, the five VES profile points in the middle slope (between 65 and 85 profile meter) does not agree the equation (4-4) and indicate the shallow heterogeneity in the hillslope subsurface structure representing the presence of the two-dimensional features. The left graph in the Figure 5-2 illustrates an example for lateral shallow heterogeneous medium. Actually, we cannot invert these measured VES data to a 1D-depth model because it can lead to the misinterpretation of the obtained VES model (Hoffmann and Dietrich 2004).

After analysing the sounding curves and the proof of the correctness the equation (4-4), we inverted the valid sounding curves to the 1D-depth models with quite good fitting shown in the Appendix A - 1. The right graph in the Figure 5-1 shows an example of 1D-inversion results with equivalent models.

5 Results and discussions

The obtained 1D-models content of the four layers because we can identify in the behaviour of the sounding curves four parts (decreasing-increasing-decreasing-increasing). We want to stress that the presence of the deepest layer is not sharp due to the poor contrast in the depth. Nevertheless, we believe that the deepest layer exists in the underground because the apparent resistivity values increase gradually at the large current electrode spacing. Besides, we have to note that we also inverted the invalid measured VES data taking as a starting model from the inversion of the VES valid models into account. The middle graph on the right site in the Figure 5-2 illustrates an example of 1D-inversion results for invalid VES data with equivalent models. The Table in the Appendix A - 1 as well as the lower graph of the Figure 5-3 also demonstrates the homogeneous marked as bold letters or lines and heterogeneous hillslope areas.

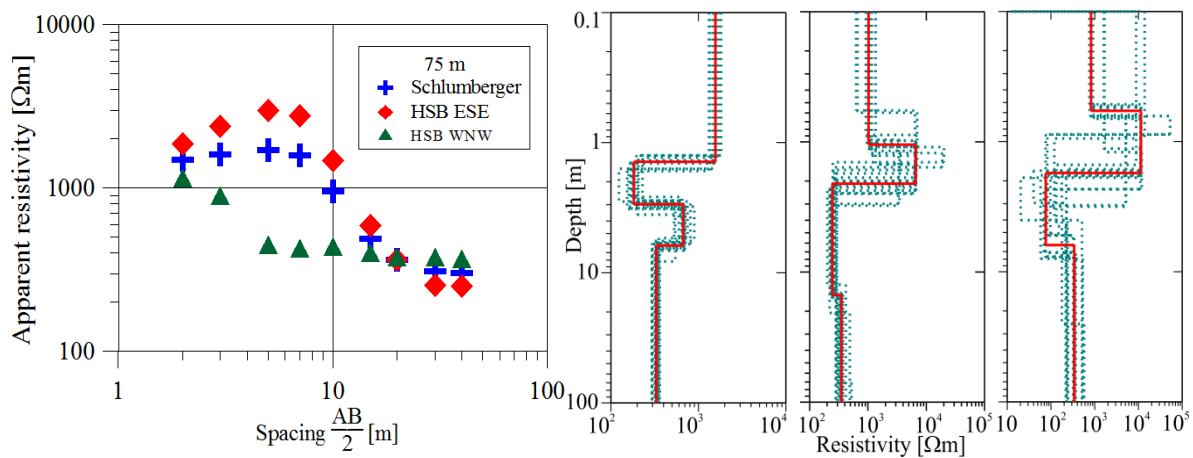


Figure 5-2: The case study of the Weierbach catchment: Sounding curves of Schlumberger and Half-Schlumberger measurements (the left diagram) at the ERT profile 75 meter indicating significant shallow heterogeneity perpendicular to the ERT profile, and their inversion results with equivalent models (three graphs at the right site). The central graph of the inversion results presents Schlumberger measurement, whereas the left graph from the central graph is HSB for WNW-site, and the right graph from the central graph is HSB for ESE-site

As soon as we prepared the 1D-depth models from measured data, we collected all models joint and constructed the VES hillslope model shown in the Figure 5-3 in the below diagram. In order better to interpret the constructed VES model, the figure also contents of slope topography, geographic direction, slope exposition, the geomorphologic features (the creek channel, wetlands), layer boundaries with confidence interval of $\pm 95\%$, and the localized homogeneous hillslope areas drawn with the bold lines. In contrast to the ERT model, the VES hillslope model demonstrates a deeper 2D-section, which reaches the averaged depth of ca. 18.5 m. The predicated depth describing in the chapter 4.1.1 according to the rule of thumb (Kirsch 2006) is 16 m for the current electrode spacing $AB = 80$ m. Moreover, the two-dimensional VES-image recognizes four lateral continuous electrical subsurface units. The relative high resistant upper layer with the averaged resistivity values of $1730 \Omega\text{m}$ reaches

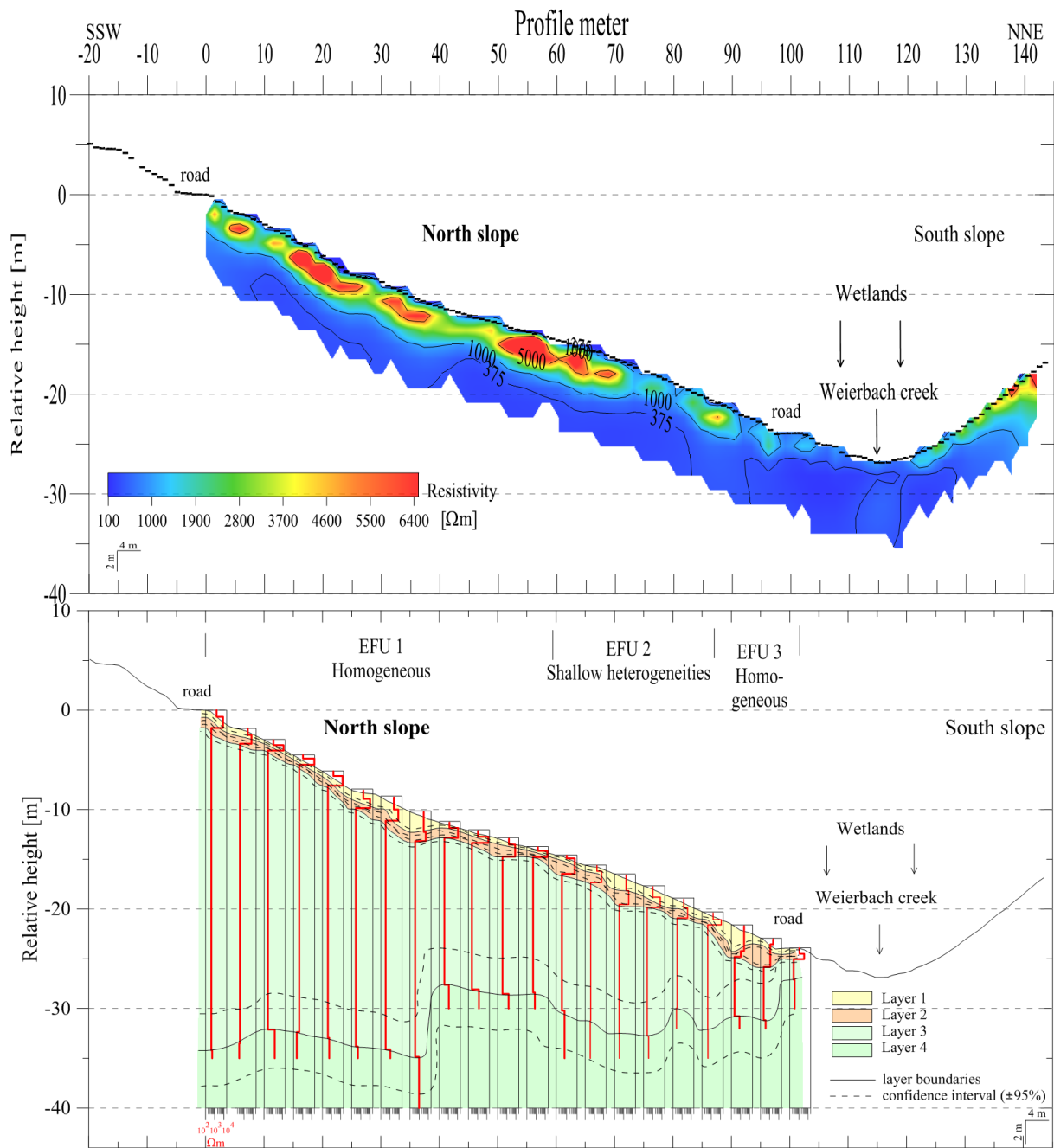


Figure 5-3: The case study of the Weierbach catchment: Geo-electrical investigation using ERT slope profile (the upper diagram) perpendicular to the Weierbach creek, and VES-spreading (the below diagram) parallel oriented to the creek. The VES results for locations with lateral homogeneity perpendicular to the ERT profile are drawn with bold line

a depth of approx. 0.8 m along whole hillslope, after which the resistivity values increase rapidly. The high resistivity values of ca. 8940 Ωm characterize the second layer along upslope and middle slope, which reaches a depth of ca. 1.7 – 1.8 m, after which the resistivity values decrease rapidly (330 Ωm). The intermediate resistivity values of 2020 Ωm characterize the second layer along the bottom slope. We can associate the high resistant layer with well subsurface drainage. The underlying low resistivity layer

5 Results and discussions

(330 Ωm) range a depth of 18.7 – 18.8 m, after which the resistivity values increase gradually. We can associate the low resistivity layer with the fractured bedrock, whereas the deeper layer with gradual increased resistivity values subordinates into the compact bedrock. The high resistant bedrock (850 Ω) characterize the upslope and middle slope, whereas the slightly increased resistivity values of ca. 350 Ωm characterize the bedrock in the bottom slope.

As we can see, the VES image delivers the deeper insights of the underground and predicates precise the contrasting interfaces in contrast to the ERT image. Besides, we can estimate and illustrate the uncertainty in the depth detection and in the determination of the resistivity values through the equivalent models. We determinate the confidence interval where the resistivity vales can be approximately constant. Moreover, the examining the measured resistivity VES data categorizes the investigated hillslope into the significant hillslope areas differing in the two homogeneous areas and one heterogeneous area. We called these significant hillslope areas as the elementary functional units (EFU's) and marked with the number (EFU 1, EFU 2 and EFU 3) in the below diagram in the Figure 5-3. We believe that these hillslope areas can significant control the character of the subsurface flow. EFU 1 and EFU 3 represent the homogeneous hillslope areas, whereas EFU 2 identified the impact of the varied shallow subsurface on the down slope at the profile meter from 65 m to 85 m. EFU 1 characterizes the upslope and the middle slope at the profile meter from 0 m to 65 m. The foot slope in the range of the profile meter from 85 m to 100 m represents the homogeneous EFU 3. We also marked the significant hillslope areas in Table presenting in the Appendix A - 1.

Moreover, in order to compile the distinguished EFUs with the identified layer units, we plotted resistivity and thickness values for each layer in terms of EFU's as a box-whisker diagram illustrated in the Figure 5-4. This diagram illustrates clearly the resistivity contrast between high resistant upper layers (the first and second layers) and low resistant bottom layers (the third and fourth layers). The upper layer of the EFU 1 and EFU 2 demonstrates significant higher resistivity values and a strong contrast between the first and second layer compared to the EFU 3, which implies intermediate resistivity values and a poor contrast between these layers. Moreover, if we consider the deeper low resistant layers we can see that the EFU 2 does not indicate the significant resistivity contrast between the third and fourth layer, whereas the EFU 1 and EFU 3 reflect the resistivity contrast between these layers, especial the EFU 1. Furthermore, we can observe the variability in the layer thickness in terms of EFU's. The little thickness values of ca. 0.8 - 1.5 m characterize the high resistivity upper layers for all EFU's. The low resistivity layers for EFU 1 and EFU 2 imply the massive stratum (ca. 18 m) in contrast to the EFU 3 indicating the relatively little thickness values of ca. 3.5 m. The total investigated thickness reflecting the boundary of the bedrock takes the different places in the depth. The deeper bedrock location characterizes the EFU 1 (in the depth of ca. 30 m) and EFU 2 (in the depth of 18 m), whereas the bedrock of EFU 3 reaches the depth of ca. 4.5 m.

Until now, we can see the good correlation between the interpreted resistivity layers and the significant hillslope areas (EFU's). However, we classified the interpreted resistivity layers more detailed

5 Results and discussions

into the so-called electro-stratigraphic units (ESUs) with respect to the resistivity distribution and variability in each stratum. We demonstrated this classification in the Figure 5-5 und in the Table 5-1. The classification assumes that a stratigraphic unit implies a uniform resistivity distribution and reflects the geological-geomorphological background. The Figure 5-5 illustrates four ESUs (ESU 1, ESU 2, ESU 3 and ESU 4). The ESU 1 and ESU 3 represent the first and the third layer, respectively, and imply the

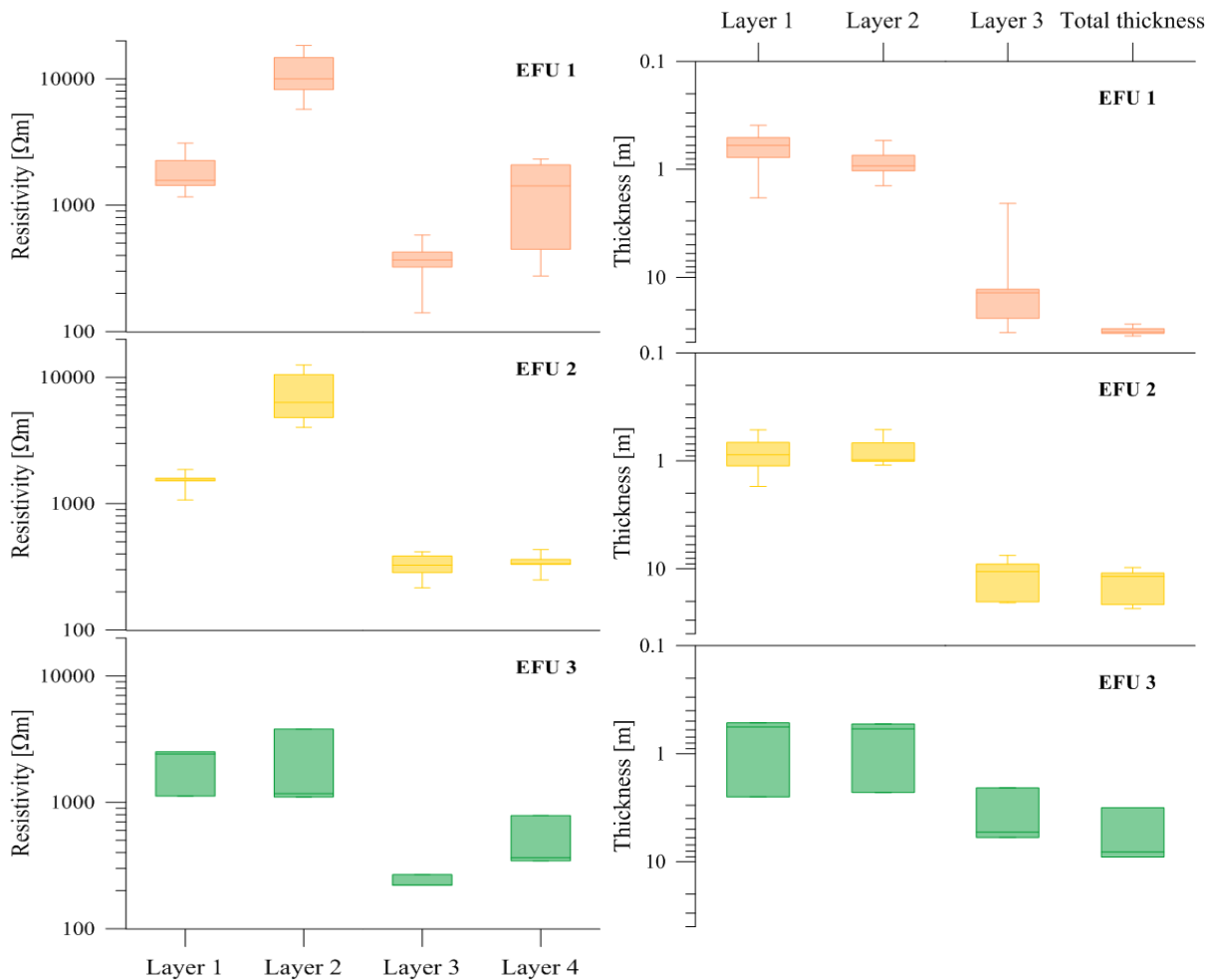


Figure 5-4: The case study of the Weierbach catchment: Box-whisker plots of resistivity (the left diagrams) and thickness (the right diagrams) distribution downhill as well as over the width of the hillslope in terms of EFU's

uniform resistivity distribution without significantly discrepancies inside of these layers. In contrast to it, the ESU 2 and ESU 4 recognise two patterns inside of each layer. We subordinated these patterns the in subunits (ESU 2a and ESU 2b; ESU 4a and ESU 4b). The high resistivity values characterize ESU 2a (more than 5000 Ωm) and ESU 4a (ca. 1000 Ωm) along the upslope and middle slope, whereas ESU 2b and ESU 4b characterize the below slope and imply the relatively lower resistivity values of ca. 2000 Ωm for ESU 2b and ca. 500 Ωm for ESU 4b. The Table 5-1 describes the electro-stratigraphic units with the respect to the obtained results and the lithological knowledge. How we can see from the Table 5-1 that the ESU 2 represents the good drainage stratum. We believe that the tree root networks and the

5 Results and discussions

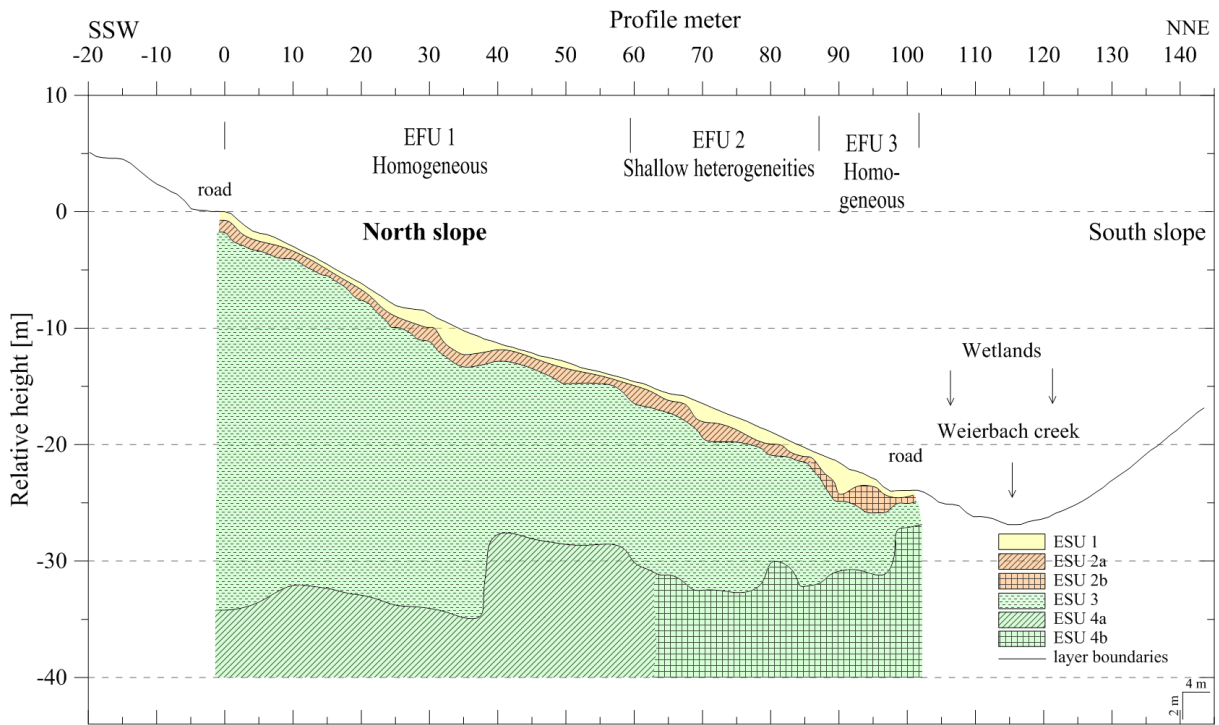


Figure 5-5: The case study of the Weierbach catchment: Interpretation of VES results in terms of ESU's

Table 5-1: The case study of the Weierbach catchment: The interpreted ESU's

ESU	Electrical resistivity , Ωm	Unit description	Depth, m
ESU 1	ca. 1730 ± 620	Uniform resistivity distribution; Loamy soils	
ESU 2a	ca. 8940 ± 4500	Loamy soils with scattered schist stones and the massive tree root networks	ca. -0.83 ± 0.5
ESU 2b	ca. 2020 ± 1530	Loamy soils with scattered schist stones and the little tree root networks	
ESU 3	ca. 330 ± 74	Uniform resistivity distribution; Fractured bedrock	ca. -1.81 ± 0.6
ESU 4a	ca. 855 ± 440	Compact or less fractured bedrock	ca. -18.71 ± 8.4
ESU 4b	ca. 403 ± 162	Fractured bedrock	

scattered schist stones as well as the slope topography require the resistivity differences between the two subunits (ESU 2a and ESU 2b). In contrast to ESU 2, the ESU 3 represents a reservoir for the water store. Moreover, we associate the bedrock subunits with the geologic-geomorphological developing of the hillslope and the study site.

5 Results and discussions

Finally, to demonstrate how similar the ERT and VES hillslope models, we compared both models through the transparent overlay. We can compare only the first and the second layers, because the ERT image does not deliver the deeper insights. The Figure 5-6 demonstrates a good matching of both models. The interface of the first layer indicates approximately the same depths in each case, whereas the discrepancy of the second layer between two models is ca. 0.7 m. Such discrepancy in the depth detection, we can associate with the resistivity change in the model developing.

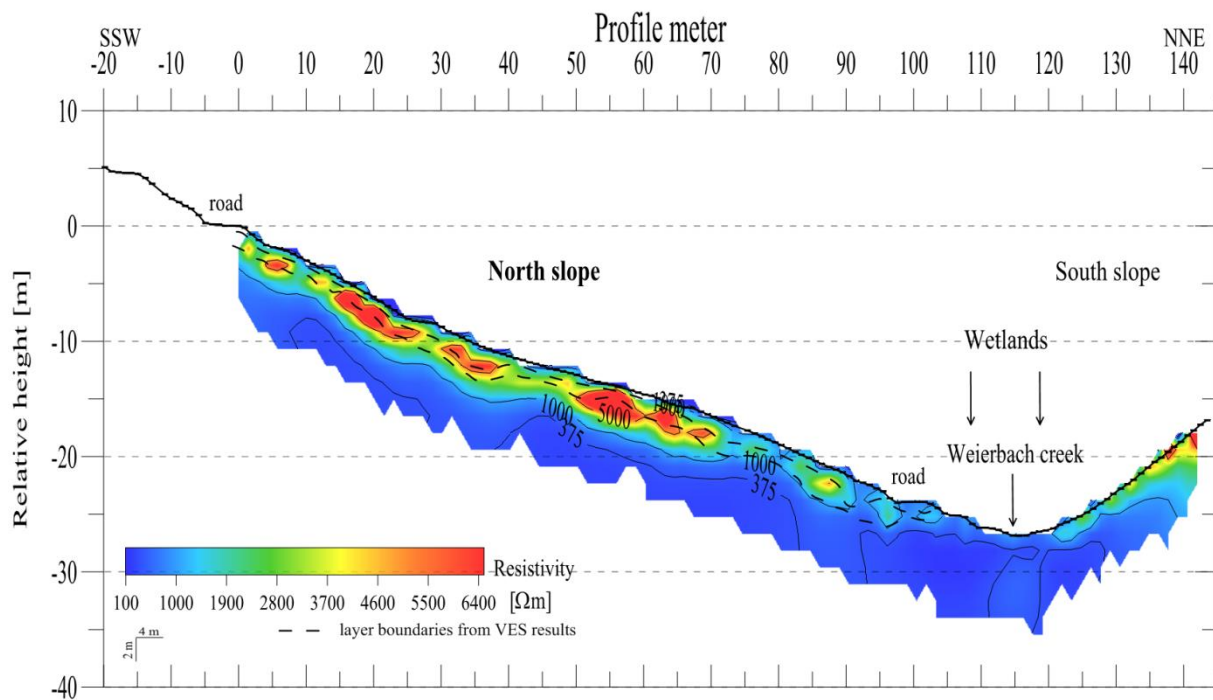


Figure 5-6: The case study of the Weierbach catchment: Comparison of ERT and VES results of the first and second interfaces

5.1.2 Application in the Schaeferfartl catchment

Here we start presenting and discussing the result of ERT survey illustrated in the Figure 5-9 in the upper diagram. In order better to understand the inverted ERT model, we also included slope topography, geographic direction, slope exposition and the geomorphologic features (the Schaeferbach creek, wetlands). We calculated the ERT hillslope model to the maximum depth of 10 m. The ERT image implies the two lateral continuous electrical resistivity layers. The upper layer with relatively high resistivity values in the range of 250 - 350 Ωm continues almost whole slope and reaches the depth of 4.5 meter at the upslope and 2 meter at the down slope. We can observe that this layer is absent in the wetlands containing of lower resistivity values (less than 150 Ωm). Moreover, the significant high resistant (450 - 600 Ωm) small features characterize the first 1.5 meters of the upper layer. The relatively high resistivity upper layer, we can associate with the fine loamy soil, whereas the significant high resistivity anomalies we can associate with the rock waste and fragments of mountain loam. The low

5 Results and discussions

resistivity layer (less than 150 Ωm) exists below the high resistant layer. This layer outcrops in the wetlands. Maybe, we can subordinate this low resistant unit with the well water saturated fissured upper bedrock. Moreover, the wetlands imply a well-conducted homogeneous zone (less than 150 Ωm) and does not indicate the structure. Furthermore, if we observe the subsurface area framing between the two isolines from 250 Ωm to 150 Ωm , we can mark this subsurface part as a transition zone associating with the possible subsurface flow path or a connection zone between the hillslope fissured upper bedrock and the wetlands.

The ERT image of the Schaeftal hillslope also delivers the spatial patterns of localized resistivity areas without precise boundaries. As in the case of the Weierbach hillslope, we predicted the interface between the high resistant upper layer and the low resistant bottom layer by the resistivity isoline of 250 Ωm , which continues in the depth from 4.5 m to 2 m or with respect to topography (the relative height) from -5 m to -10 m.

Up to now, we will demonstrate and discuss the results of the VES survey shown in the Figure 5-9 in the below diagram. As in the case of the Weierbach hillslope, we will begin with the analysis of the measured and inverted data. The analysing of the sounding curves with respect to the sounding curves classification presented by (Telford, Geldart, & Sheriff, 1990) informs us that the most sounding curves

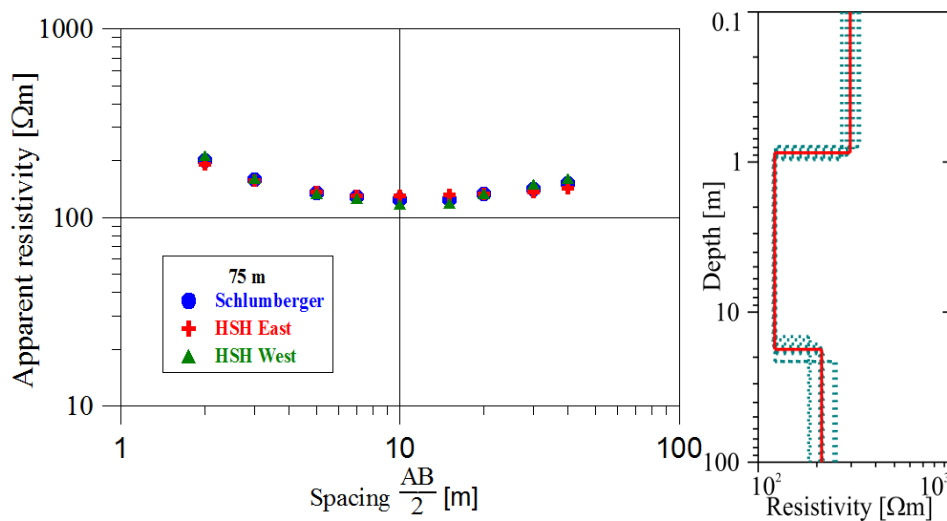


Figure 5-7: The case study of the Schaeftal catchment: Sounding curves of Schlumberger and Half-Schlumberger measurements (the left diagram) at the ERT profile 75 meter presenting an example for lateral homogeneity perpendicular to the ERT profile, and their inversion result with equivalent models (the right graph)

measured at the upslope indicate the type Q (for example the Figure 5-8, the left graph). Whereas the type H describes the most sounding curves of the down slope and wetlands (for example the Figure 5-7, the left graph). Additionally, the sounding curves of middle slope (between 45 and 55 profile meters) draw the type K. Furthermore, we proved the correctness on homogeneous stratified subsurface. The left

5 Results and discussions

graph in the Figure 5-7 representing one example for the lateral homogeneous medium confirms the agreement of the equation (4-4). The six from 20 VES profile points describe the hillslope profile mostly in the well-saturated wetlands as the homogeneous stratified subsurface. In contrast to it, the 14 VES profile points at the slope (between 0 and 65 profile meter) does not agree the equation (4-4) and indicate the shallow heterogeneity in the hillslope subsurface structure representing the presence of the two-dimensional features. The left graph in the Figure 5-8 illustrates an example for lateral shallow heterogeneous medium with the minor discrepancies of sounding curves (ca. 60 Ωm) at the small electrode distance. Actually, we cannot invert these measured VES data to a 1D-depth model because it can lead to the misinterpretation of the obtained VES model (Hoffmann and Dietrich 2004). Nevertheless, we will invert these data because of the slight discrepancies (ca. 60 Ωm).

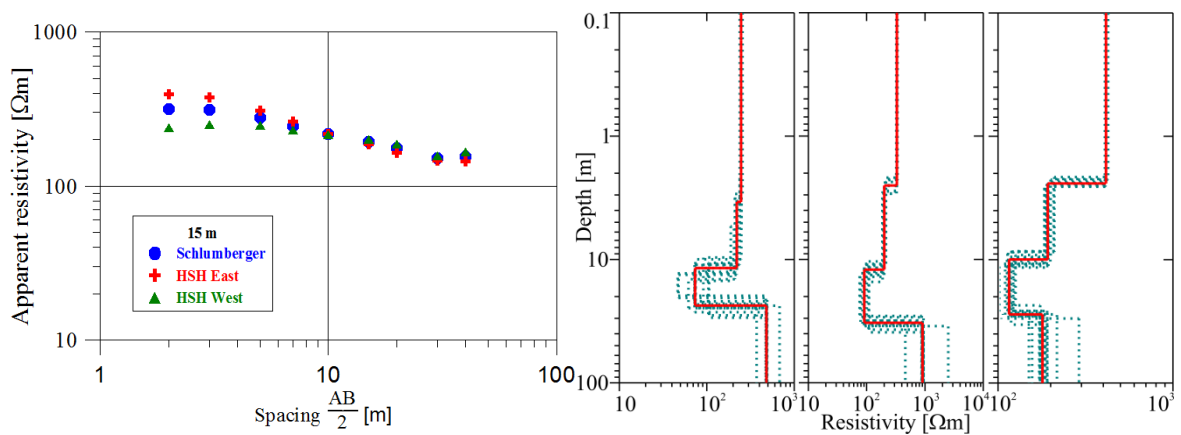


Figure 5-8: The case study of the Schaeferfirtal catchment: Sounding curves of Schlumberger and Half-Schlumberger measurements (the left diagram) at the ERT profile 15 meter illustrating a light shallow heterogeneity perpendicular to the ERT profile, and their inversion results with equivalent models (three graphs at the right site). The central graph of the inversion results presents Schlumberger measurement, whereas the left graph from the central graph is HSB for West-site, and the right graph from the central graph is HSB for East-site

After analysing the sounding curves and the proof of the correctness the equation (4-4), we inverted the valid sounding curves to the 1D-depth models with quite good fitting shown in the Appendix A - 2. The right graph in the Figure 5-7 shows an example of 1D-inversion results with equivalent models. The obtained 1D-models content of the different number of the layers. The layer number depend on the behaviour of the sounding curves. We can observe that the behaviour of the sounding curves is connected with the position of the hillslope profile. The hillslope himself imply the four- and three-layer model, whereas the two-layer model characterizes the wetlands. The Table in the Appendix A - 2 illustrates the layer number along the hillslope profile. We want to stress that the presence of the deepest layer is not sharp due to the poor contrast in the depth. Nevertheless, we believe that the deepest layer exists in the underground because the apparent resistivity values increase gradually at the large current electrode

5 Results and discussions

spacing. Besides, we have to note that we also inverted the invalid measured VES data because we believe that the discrepancies of sounding curves (ca. 60 Ωm) are too small and we can consider the measured data as nearly homogeneous data sets. The middle graph on the right site in the Figure 5-8 illustrates an example of 1D-inversion results for invalid VES data with equivalent models. The Table in the Appendix A - 2 as well as the lower graph of the Figure 5-9 also demonstrates the homogeneous marked as bold letters or lines and heterogeneous hillslope areas.

After we prepared the 1D-depth models from measured data, we collected all models joint and constructed the VES hillslope model shown in the Figure 5-9 in the below diagram. In order better to understand the VES hillslope model, we also included in the graph slope topography, geographic direction, slope exposition, the geomorphologic features (the Schaeferbach creek, wetlands), layer boundaries with confidence interval of $\pm 95\%$, and the localized homogeneous hillslope area drawn with bold lines). In contrast to the ERT model, the VES hillslope model demonstrates a deeper 2D-section, which reaches the averaged depth of ca. 23 m. The predicated depth describing in the chapter 4.1.1 according to the rule of thumb (Kirsch 2006) is 16 m for the current electrode spacing $AB = 80$ m. Moreover, the two-dimensional VES-image splits the profile in two part. The first part (the hillslope himself) recognizes the four and three lateral continuous electrical subsurface units. Whereas, the other part (the wetlands) imply the two lateral continuous electrical subsurface units. The relatively high resistant upper layer with the averaged resistivity values of 460 Ωm has a form of a wedge and reaches a depth from 3 m to 0.2 m decreasing in the downslope direction, after which the resistivity values decrease gradually. The relatively low resistivity values of ca. 300 Ωm characterize the second layer, which continues almost the whole slope in the form of a wedge with the variable depths decreasing in the downslope direction and ranging from 15 m (at upslope) to 1 m (at down slope) and is absent in the wetlands. The underlying low resistivity layer (130 Ωm) range an averaged depth of 30 m, after which the resistivity values increase gradually (ca. 270 Ωm). We can associate the low resistivity layer with the fissured bedrock, whereas we subordinate the deeper layer with gradual increased resistivity values into the fresh bedrock.

As we can see, the VES image delivers the deeper insights of the underground and predicates precise the contrasting interfaces in contrast to the ERT image, but the determination of depth was a bit difficult in contrast to the Weierbach hillslope because of the a diffuse contrast of medium parameters. Besides, we can estimate and illustrate the uncertainty in the depth detection and in the determination of the resistivity values through the equivalent models. We determinate the confidence interval where the resistivity vales can be approximately constant. Moreover, the examining the measured resistivity VES data categorizes the investigated hillslope into the significant hillslope areas differing in one homogeneous area and one heterogeneous area. We called these significant hillslope areas as the elementary functional units (EFU's) and marked with the number (EFU 1 and EFU 2) in the below diagram in the Figure 5-9. We believe that these hillslope areas can significant control the character of the subsurface flow. EFU 2 represents the homogeneous hillslope area at the profile meter from 65 m to

5 Results and discussions

95 m and connects directly to the Schaeferal creek, whereas EFU 1 identified the impact of the varied shallow subsurface at the profile meter from 0 m to 65 m (e.g. rock fragments). We also marked the significant hillslope areas in Table presenting in the Appendix A - 2.

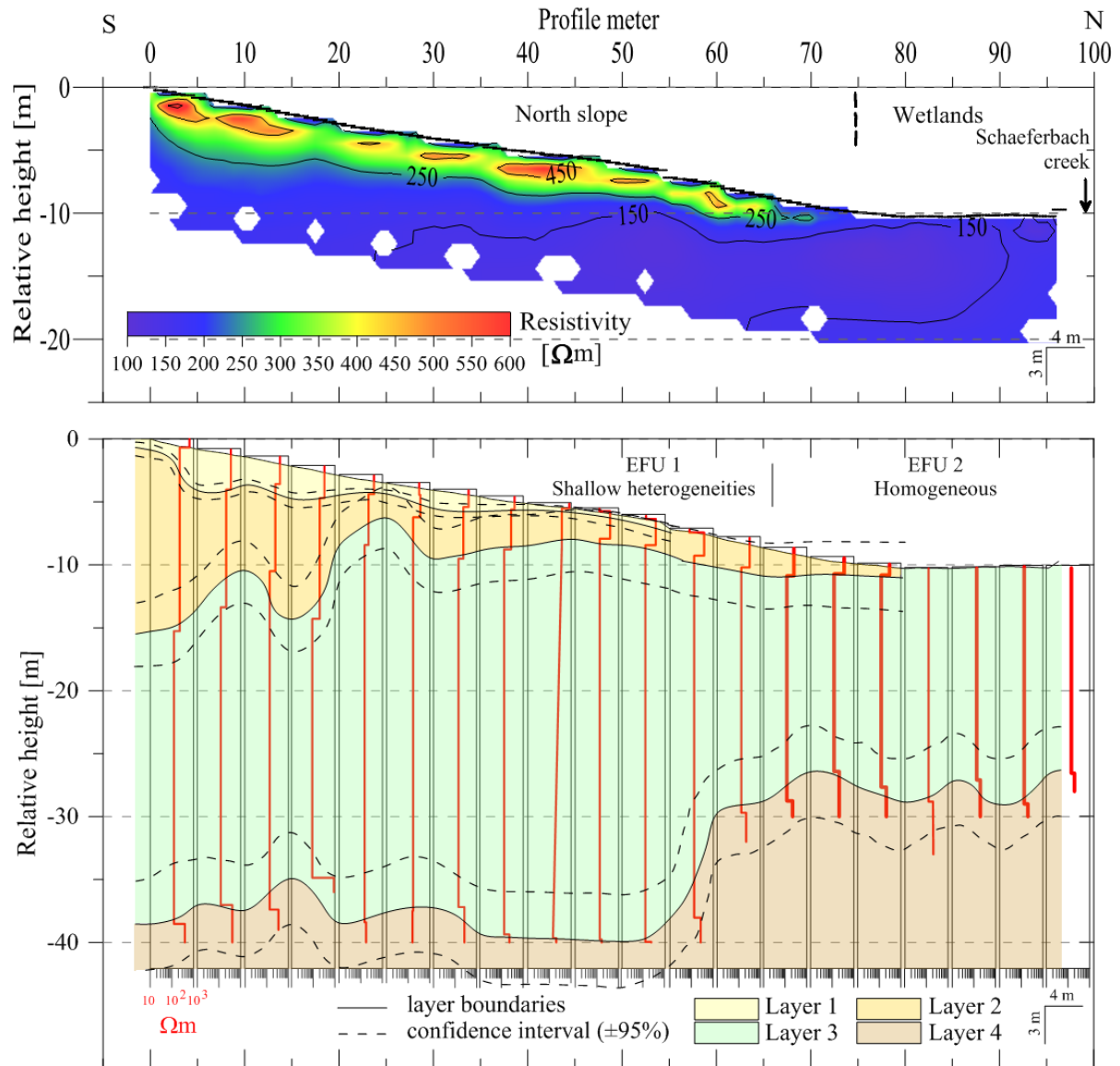


Figure 5-9: The case study of the Schaeferal catchment: Resistivity results of ERT slope profile (the upper diagram) perpendicular to the Schaeferbach creek, and VES-spreading (the below diagram) parallel oriented to the creek. The VES results for locations with lateral homogeneity perpendicular to the ERT profile are drawn with bold line

Moreover, in order to compile the distinguished EFUs with the identified layer units, we plotted resistivity and thickness values for each layer in terms of EFU's as a box-whisker diagram illustrated in the Figure 5-10. This diagram illustrates clearly the resistivity contrast between high resistant upper layers (the first and second layers) and low resistant bottom layers (the third and fourth layers). The Figure 5-10 also demonstrates the absence of the high resistivity upper layer in the space of the uniform

5 Results and discussions

EFU 2. The upper layer of the EFU 1 and EFU 2 demonstrates intermediate high resistivity values of ca. 300 Ωm . How can we see that the covered first upper layer of EFU 1 demonstrates a strong variability of the resistivity values from 100 Ωm to 900 Ωm . The low resistivity layer with the values of ca. 130 Ωm represents a relatively uniform layer for both EFU's. The deepest high resistivity layer indicates the averages resistivity values of ca. 270 Ωm for all EFU's, but EFU 1 is more resistivity variable ranging from 200 Ωm to 900 Ωm than EFU 2 representing relatively uniform stratus with the resistivity values of ca. 200 Ωm . In generally, we can observe the diffuse contrast of the investigated hillslope. Furthermore, we can observe the variability in the layer thickness in terms of these two EFU's. The little thickness values of ca. 1.0 - 4.5 m characterize the high resistivity upper layers for all EFU's. The low resistivity layers of EFU 1 imply the massive stratum (ca. 26 m) in contrast to the EFU 2 indicating the relatively little thickness values of ca. 20 m. The total investigated thickness reflecting the boundary of the bedrock takes the different places in the depth. The deeper bedrock location characterizes the EFU 1 (in the depth of ca. 30 m), whereas the bedrock of EFU 2 reaches the depth of ca. 20 m.

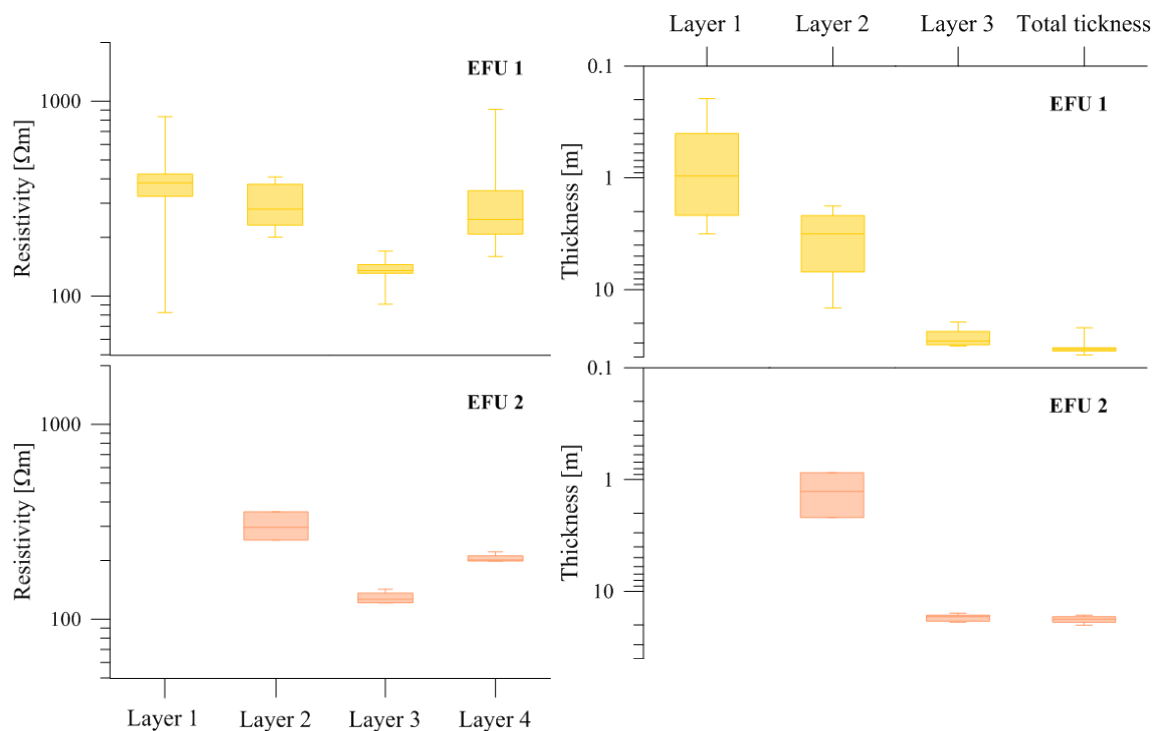


Figure 5-10: The case study of the Schaeferthal catchment: Box-whisker plots of resistivity (the left diagrams) and thickness (the right diagrams) distribution downhill as well as over the width of the hillslope in terms of EFU's

Up to now, we can see the good correlation between the interpreted resistivity layers and the significant hillslope areas (EFU's). However, we classified the interpreted resistivity layers more detailed into the so-called electro-stratigraphic units (ESUs) with respect to the resistivity distribution and variability in each stratum. We demonstrated this classification in the Figure 5-11 und in the Table 5-2.

5 Results and discussions

The classification assumes that a stratigraphic unit implies a uniform resistivity distribution and reflects the geological-geomorphological background.

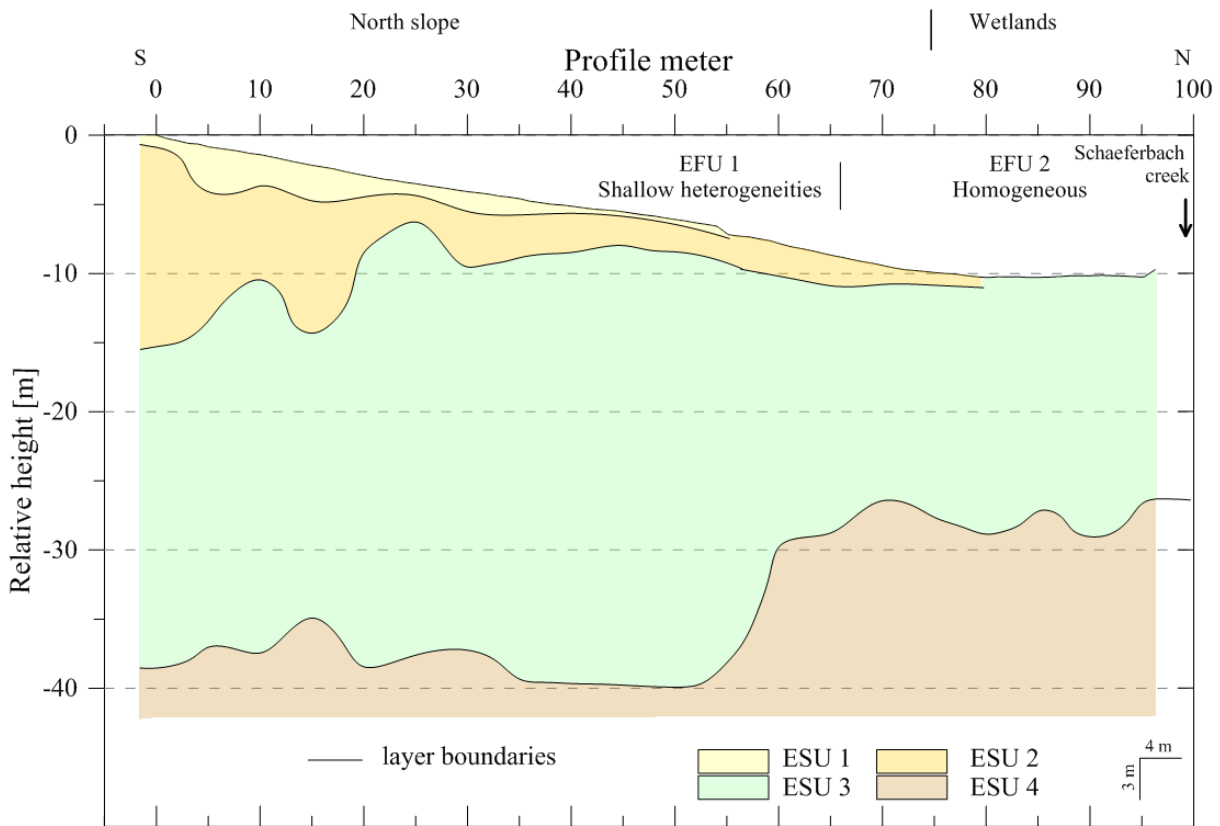


Figure 5-11: The case study of the Schaeferfalter catchment: Interpretation of VES results in terms of ESU's

Table 5-2: The case study of the Schaeferfalter catchment: The interpreted ESU's

ESU	Electrical resistivity, Ωm	Unit description	Depth, m
ESU 1	ca. 460 ± 201	Variable resistivity distribution;	
ESU 2	ca. 300 ± 72	Fine soil with rock waste, fragments of mountain loam; good drainage	ca. -1.19 ± 0.9
ESU 3	ca. 130 ± 15	Fissured upper bedrock (greywacke)	ca. -5.23 ± 4.5
ESU 4	ca. 270 ± 165	Fresh bedrock (greywacke)	ca. -30.67 ± 7.1

The Figure 5-11 illustrates four ESUs (ESU 1, ESU 2, ESU 3 and ESU 4) implying the uniform resistivity distribution without significantly discrepancies inside of these layers. The Table 5-2 describes the electro-stratigraphic units with the respect to the obtained results and the lithological knowledge. How we can see from the Table 5-2 the ESU 1 and ESU 2 can represent the drainage stratum. In contrast to it, the ESU 3 can represent a reservoir for the water store. Moreover, the EFUs and ESUs are in good agreement with each other. The shallow heterogeneous high resistant upper layers of EFU 1 reflect the

presence of irregular distributed 2D features of the periglacial substance (e.g. rock fragments), whereas the relatively homogeneous layers of EFU 2 mirrors the consistent saturated subsurface.

Finally, to demonstrate how similar obtained ERT and VES hillslope models are, we compared both models through the transparent overlay. We can compare only the first and the second layers, because the ERT image does not deliver the deeper insights. The Figure 5-12 demonstrates considerably discrepancies between two models. The interface of first layer indicates the depth discrepancy of 1 m - 1.5 m, whereas the discrepancy of second layer between two models is ca. 4.7 – 12 m, but the fitting of both models at the down slope is quite close to each other. Such discrepancy in the depth detection, we can associate with the diffuse contrast of medium parameters in the Schaeferfalter and the assumption on the uniform stratified subsurface, especially for the upslope.

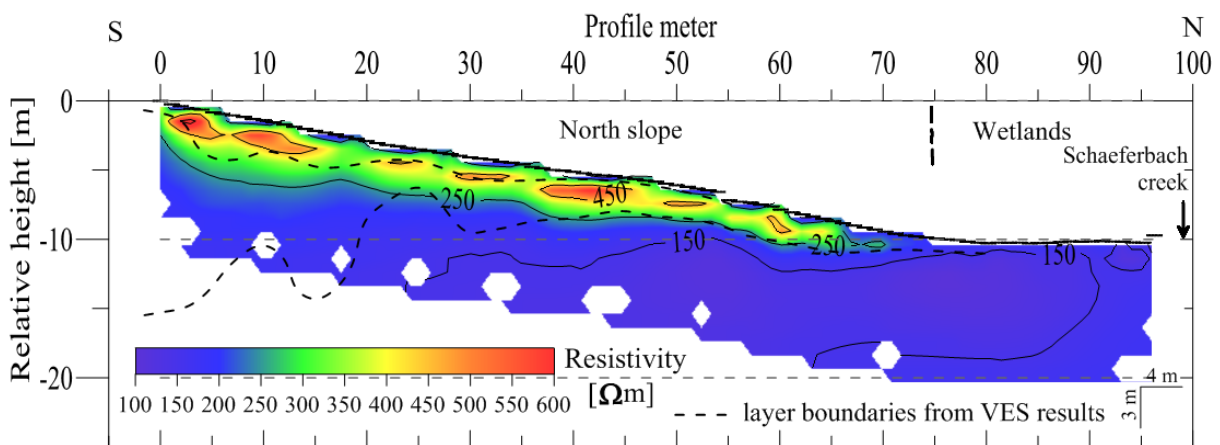


Figure 5-12: The case study of the Schaeferfalter catchment: Comparison of ERT and VES results of the first and second interfaces

5.2 Refraction seismic investigation

5.2.1 Application in the Weierbach catchment

Here we will present and discuss the refraction seismic models obtained at the study site the Weierbach catchment using the different seismic interpretation techniques such as Plus-Minus method, seismic tomography, ray tracing FD modelling and vertical seismic profiling. Before we demonstrate the obtained results, we will introduce the reader to the data quality. In order better to identify the first arrivals, we had to filter several seismograms. We observed one phenomena that the seismograms shooting from the top to down are less noisy than the seismograms shooting from the down to the top, especially for the last 24 traces. We demonstrated the unfiltered seismograms for the shot position 0 meter (the upper diagram) and 95 meter (the middle diagram) in the Appendix B in the Figure B - 1. The upper diagram of the Figure B - 1 illustrates a relatively clear seismogram, whereas the middle diagram of this Figure demonstrates noisy traces of the last 24 traces. To eliminate the unwanted noise, we applied the

5 Results and discussions

band-pass filter with the lower cut-off of 10 Hz and the upper cut-off of 75 Hz. The bottom diagram of the Figure B - 1 illustrates the filtered seismograms.

As soon as we corrected the collected data in the elevation and filtered to remove the unwanted noise, we identified the first arrivals of the P-wave and plotted it in the travel time diagram, in order to analyse and to develop the structural subsurface model of the investigated hillslope.

Plus-Minus Method

We plotted the two pair of selected symmetrical wave fronts (WF's) in the travel time diagram illustrated in the Figure 5-13a. One pair interprets the shot position at -5 m and 100 m, whereas other pair analyses the shot positions at 0 m and 95 m. The travel time diagram recognises the first arrivals of the direct wave and the first refractor. We believe that we can consider the subsurface model of the investigated hillslope as the two-layer model. Moreover, we interpret the variability in the travel time as the effect of the surface topography. Other effect causing by the surface topography is the delay between the wave fronts at the shot position -5 m and 0 m. Then, we calculated the time plus values and time minus values using the equations (4-13) and (4-14) with the total travel time of 45 ms. The diagrams (b) and (c) of the Figure 5-13 illustrate the calculated time plus and minus values, respectively. The time plus values or the intercept times reflect the location of the refractor, whereas the time minus values reveal the seismic velocity of the second layer (1513 m/s for shots 0 m and 95 m; 1715 m/s for shots -5 m and 100 m). The intercept times imply the relatively homogeneous distribution indicating a nearby horizontal layering with a slightly topography refractor. To develop structural subsurface models, we considered the three models summarized in the Table 5-3. The seismic veloci-

Table 5-3: The case study of the Weierbach catchment: Ray parameters and seismic velocities to develop subsurface models using PMM

Subsurface model	Ray parameter, ms/m		Seismic velocity, m/s	
	WF: -5 m and 100 m	WF: 0 m and 95m	WF: -5 m and 100m	WF: 0 m and 95 m
Model A	DW: 2.73 HW: 0,5698	DW: 2.73 HW: 0.6607	DW: 366.55 HW: 1755	DW: 366.55 HW: 1513
Model B	DW: 1.92 HW: 0.29	DW: 1.92 HW: 0.3042	DW: 520 HW: 3449	DW: 520 HW:3290
Model C	DW: 1.56 HW: 0.33		DW: 638 HW: 3028	

ties obtained from the time minus values characterize the Model A, whereas the Model B uses the seismic velocities calculated from the slope of the time-distance curve (3290 m/s for shots 0 m and 95 m; 3449 m/s for shots -5 m and 100 m). Moreover, the Model A applies the seismic velocity for the direct wave obtained from the slope of the time-distance curve (366.55 m/s) for the shot position 95 m, whereas the Model B uses the seismic velocity obtained for the shot position 0 m (520 m/s). Furthermore, we

5 Results and discussions

considered the third Model C with the seismic velocities (638 m/s and 3028 m/s) obtained by the ray tracing interpretation, in order to compare the structural subsurface model with each other. Then, we calculated the refractor depth for the considered models shown in the Table 5-3

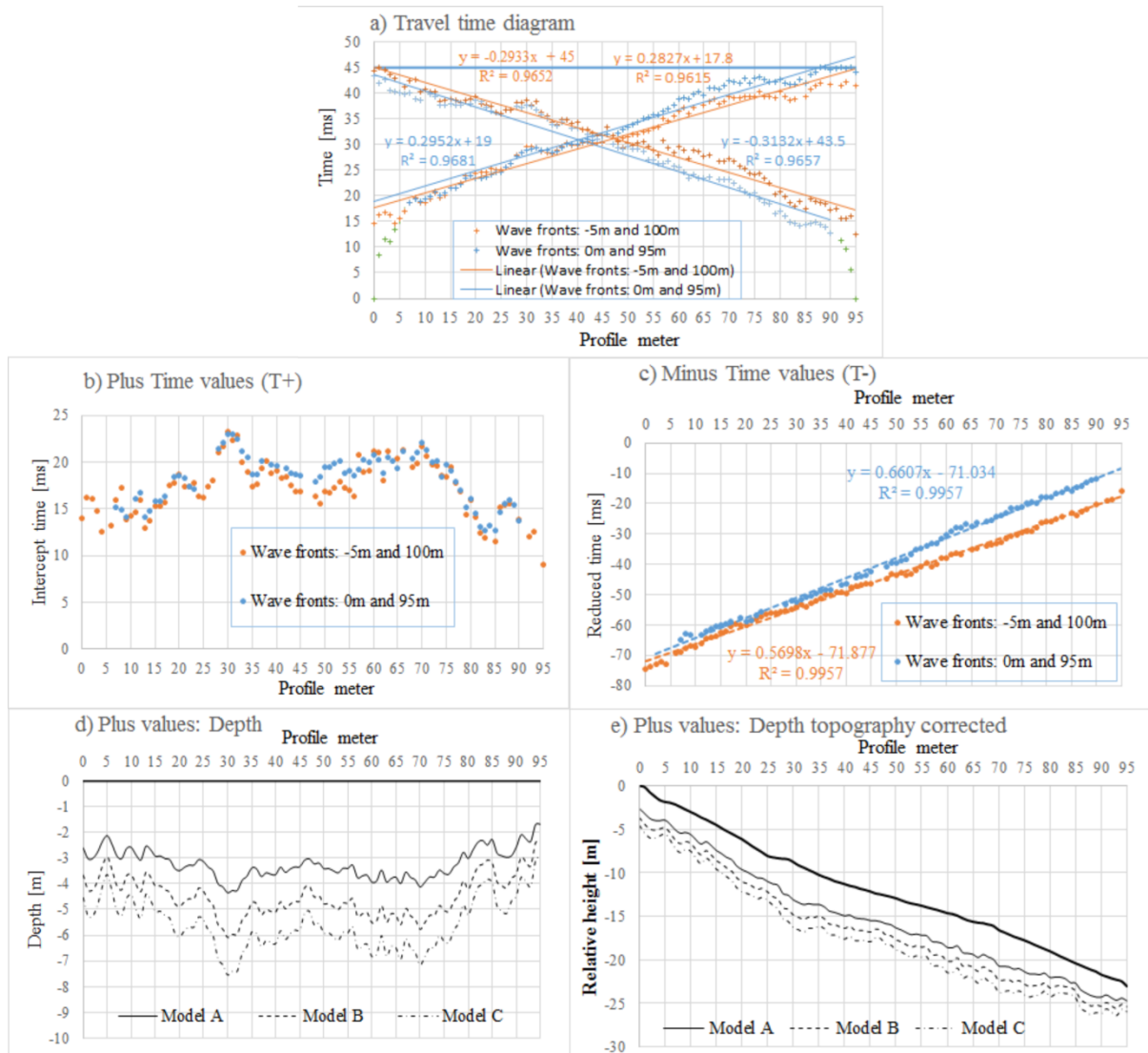


Figure 5-13: The case study of the Weierbach catchment: Refraction seismic travel-time data interpretation using Plus-Minus technique of two symmetrical wave fronts. (a) the travel time diagram with slowness slopes; (b) the diagram of calculated Plus-time values; (c) the diagram of calculated Minus-time values with seismic velocity slope. Structural subsurface models for assumed seismic velocity models (d) without topography and (e) with topography

without the surface topography and with the surface topography using the calculated time plus values and the equation (4-11). The Figure 5-13 visualizes the subsurface models without the surface topography (d) and with the surface topography (e). The different RS subsurface models reflect the different refractors in the underground. The difference between model A and model C is ca. 2.36 m. We describe the zone between these two models as a transition zone including the periglacial debris and

debris of bedrock. The shallow layer with the seismic velocity of 366.55 m/s and the averaged depths of ca. 3.23 m represents the loamy soils, whereas the deepest refractor (Model C) with the seismic velocity of 3028 m/s and the averaged depths of 5.59 m characterizes the boundary of the fractured bedrock (schist).

Refraction seismic tomography

The Figure 5-14 demonstrates the inversion results obtained from the refraction seismic tomography. The inverted seismic subsurface model characterizes a good matching of the theoretical and real travel time by the 0.9% rms. The RS tomography image illustrated in the upper diagram of the Figure 5-14 describes the seismic velocity field in the subsurface without the exact predication of the refractor depth. The below diagram of the Figure 5-14 demonstrates the distribution of the seismic ray parameter

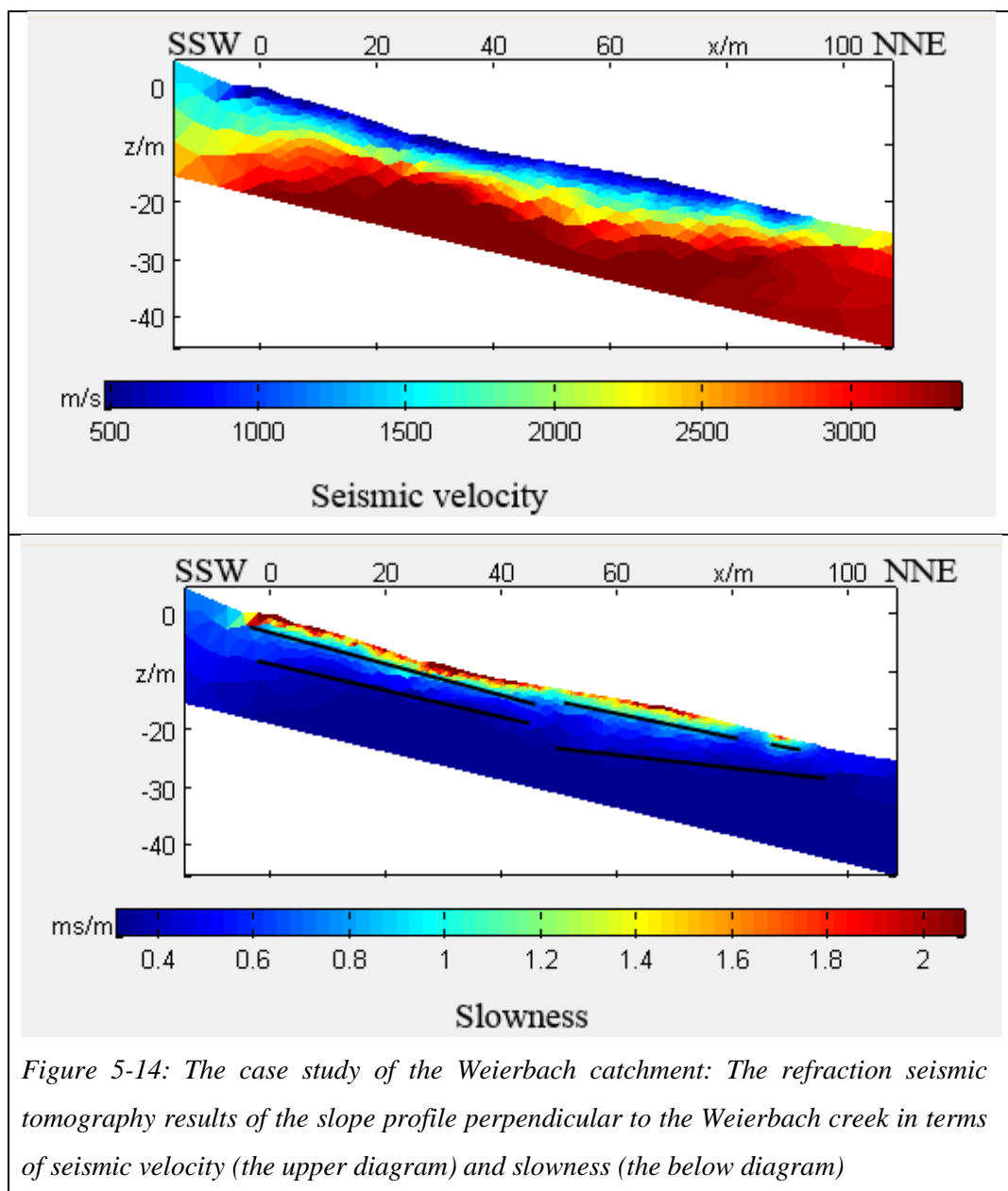


Figure 5-14: The case study of the Weierbach catchment: The refraction seismic tomography results of the slope profile perpendicular to the Weierbach creek in terms of seismic velocity (the upper diagram) and slowness (the below diagram)

in the subsurface. The use of the ray parameter can help to recognize the refractors because of the uniformity of ray parameter and its abrupt change at the contrasting interfaces. The seismic velocity image recognizes the two seismic velocity fields. The shallow seismic velocity field with values of ca. 600 - 700 m/s reaches the depth of ca. 3 - 4 m. The refracting layer with the seismic velocity values of ca. 2800 m/s follows the depth boundary at the 6 - 7 m. The diffuse transition zone demonstrating the seismic velocity values of 1500 - 2500 m/s exists between the shallow layer and the refractor. Moreover, the ray parameter image tells us clear that the subsurface reveals the two contrasting stratum: the shallow layer and the deeper layer. The boundary between these two layers reaches the depth of ca. 3 - 4 m with the slowness values of 0.6 ms/m (or 1600 m/s). We can recognize the structures in the depth, but it is not sharp for the refraction seismic. Therefore, if we compare the RS tomography model with the models obtained from PMM (especial, the Model A), we can see several similarity (the refractor velocity of 1500 - 1600 m/s and nearby the same depth) of both models. Furthermore, we can apply the obtained information from the previous seismic interpretation techniques as a starting model for the ray tracing FD modelling.

Ray tracing FD modelling

To develop a seismic subsurface model based on the wave front inversion and the ray tracing FD modelling, we considered the two cases. One case develops a seismic subsurface model using the two pairs of the symmetrical wave fronts. Other case applies all shot seismic spreading along the investigated hillslope to create a seismic subsurface model. Moreover, the seismic model obtained from the first case, we integrated as a starting model for the second case. We executed iterative and manual changes of model parameters (geometry of refractors and velocity values) and repeated the ray tracing process many times until we found a wanted subsurface model reflecting measured travel time and matching calculated and real data.

The Figure 5-15 illustrates the results of the ray tracing FD modelling for the first case where we considered the two pairs of symmetrical wave fronts. One pair of WF analyses the profile shot positions at 0 m and 50 m, and other WF pair characterizes the profile shot positions at 50 m and 95 m. After the visual analysing of these WF's, we can observe a relatively short critical distance (less than 5 m) indicating on the increased the velocity ratio (the equation (4-6)) and a good contrast. From the knowledge of the previously seismic results obtained by PMM and seismic tomography, we created as a starting model contenting of the two layers, and processed the ray tracing modelling by manual change of the model parameters (the refractor geometry). The upper diagram of the Figure 5-15 illustrates the matching between the theoretical and measured travel time as well as the calculated ray paths in the underground. The bellow diagram of the Figure 5-15 demonstrates the final subsurface model as well as the travel time diagram of the considered symmetrical wave fronts. How we can see from the results, the relatively variable seismic velocity values ranging from 209 m/s to 587 m/s characterize the shallow upper layer. Whereas the refracting layer implies the nearby uniform velocity value of 3010 m/s. We can observe a good matching of the theoretical and real travel time of the head wave. The ray paths of the

5 Results and discussions

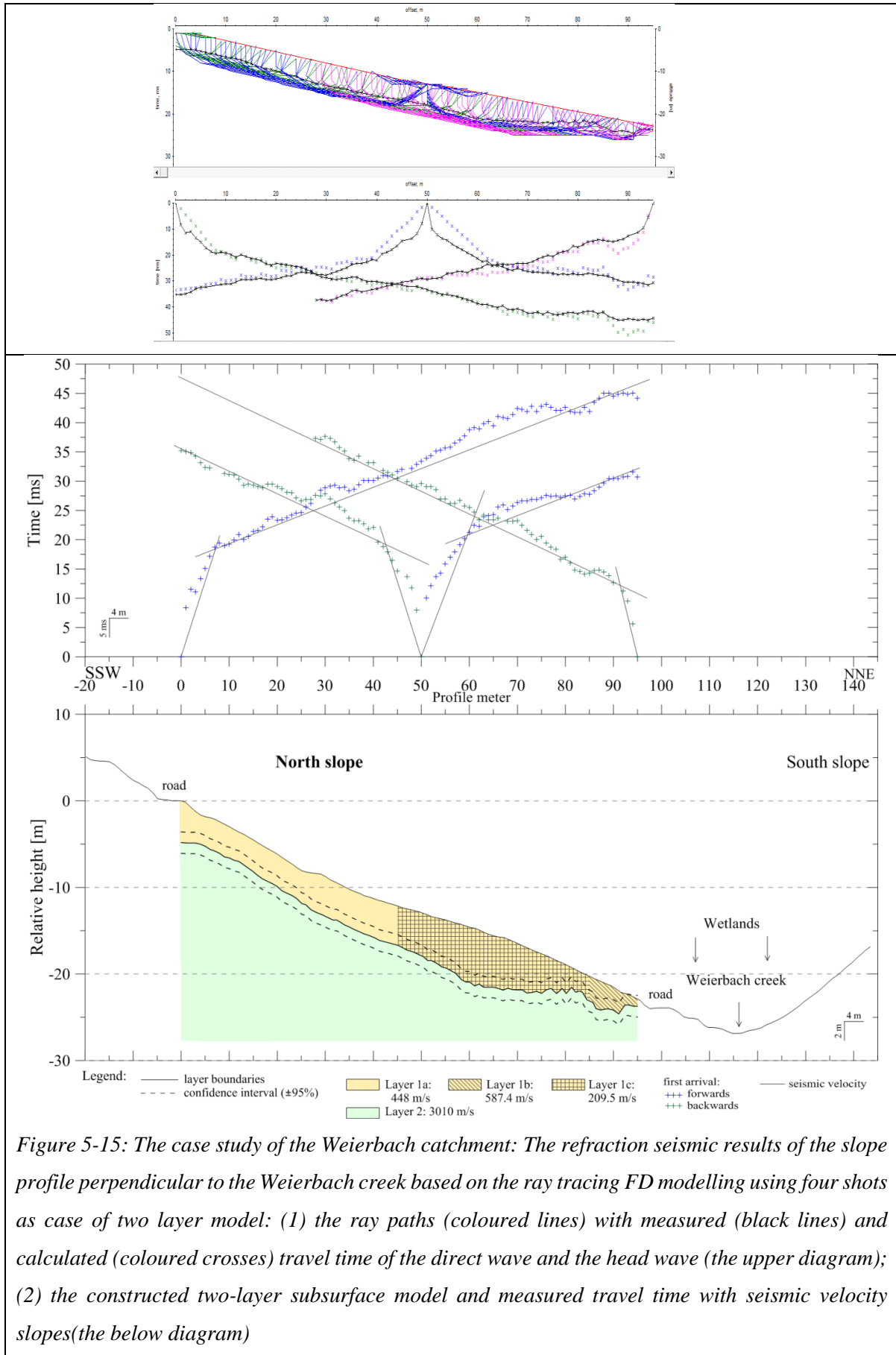


Figure 5-15: The case study of the Weierbach catchment: The refraction seismic results of the slope profile perpendicular to the Weierbach creek based on the ray tracing FD modelling using four shots as case of two layer model: (1) the ray paths (coloured lines) with measured (black lines) and calculated (coloured crosses) travel time of the direct wave and the head wave (the upper diagram); (2) the constructed two-layer subsurface model and measured travel time with seismic velocity slopes (the below diagram)

5 Results and discussions

WF's illustrate quite the consistent image in the underground. We believe that the surface topography as well as the scattered material of the PPSD's cause the variable seismic velocity field in the upper shallow layer. The subsurface model reveals the nearby horizontal layering with the minor variety of the refractor topography in the below part of the investigated hillslope. The refractor reaches the depth of ca. 4.24 m. Therefore, we will integrate the obtained seismic structural subsurface model for the future ray tracing modelling using all shots recorded along the whole hillslope, in order to develop a final seismic structural model.

The Figure 5-16 illustrates the results of the ray tracing FD modelling for the second case where we considered all symmetrical wave fronts including the near shots as well as the far shots. Using the obtained subsurface model illustrated in the below diagram in the Figure 5-15 as a starting model, we created the final subsurface model changing the refractor geometry and the seismic velocity values, in order to find the best matching between the calculated and real travel time. The upper diagram of the Figure 5-16 illustrates the good matching between the theoretical and measured travel time as well as the calculated ray paths in the underground. The below diagram of the Figure 5-16 demonstrates the final subsurface model as well as the travel time diagram of all first arrivals. To develop the final seismic subsurface model, we decided for the constant seismic velocity of 638 m/s for the shallow upper layer, in order to eliminate the velocity variations causing by the surface topography and the scattered material of the PPSD's. We also changed the seismic velocity of the refracted layer characterising this layer by the velocity value of 3028 m/s. Therefore, we reached the good matching of the theoretical and real travel time for the refracted wave, but we had to ignore the travel time fitting for the direct wave due to the strong velocity variability and the irregular surface topography. The ray paths of the symmetrical wave fronts illustrate quite the consistent image in the underground. The obtained seismic structural subsurface model describes the relatively horizontal layering with the stepped refractor topography. We believe that the debris of the fractured schist could create such refractor form. The refractor reaches the depth of ca. 4.92 m. We also calculated and drawn (broken line in the below diagram of the Figure 5-16) the depth uncertainty amounting ca ± 2.3 m.

Furthermore, the Table 5-4 summarizes the results obtained with the ray tracing FD modelling for both cases. Both cases imply nearby the same refractor depth and refractor velocity values, but they differ in the refractor topography and the seismic velocity of the shallow upper layer. We will compare the final subsurface model of the ray tracing modelling with the other seismic models obtained with the Plus-Minus method and the refraction seismic tomography.

Up to now, we will compare quantitative the seismic structural subsurface models obtained with the Plus-Minus method (Model C) and the ray tracing FD modelling. The Figure 5-17 illustrates the comparison of both models. The difference between these models is ca. 0.95 m. The models differ in the refractor topography.

5 Results and discussions

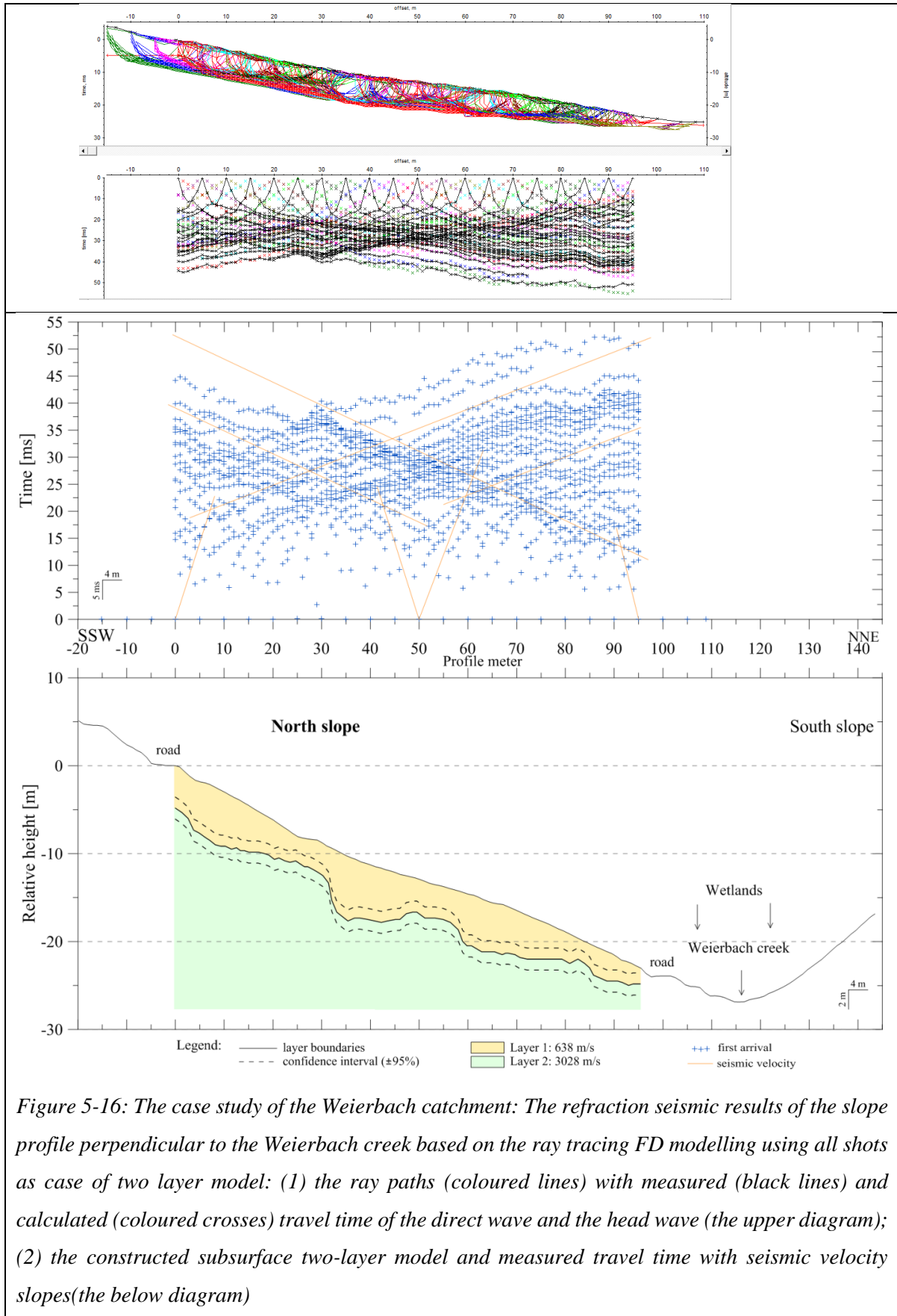


Table 5-4: The case study of the Weierbach catchment: Seismic subsurface parameters obtained with the ray tracing FD modelling for both cases

Layer Number	Seismic velocity [m/s]		Depth [m]	
	Model with four shots	Model with all shots	Model with four shots	Model with all shots
Layer 1a	ca. 448 ± 15	ca. 638 ± 246	ca. -4.24 ± 1.19	ca. -4.92 ± 2.3
Layer 1b	ca. 587.4 ± 37			
Layer 1c	ca. 209.5 ± 22			
Layer 2	ca. 3010.5 ± 30	ca. 3028 ± 735		

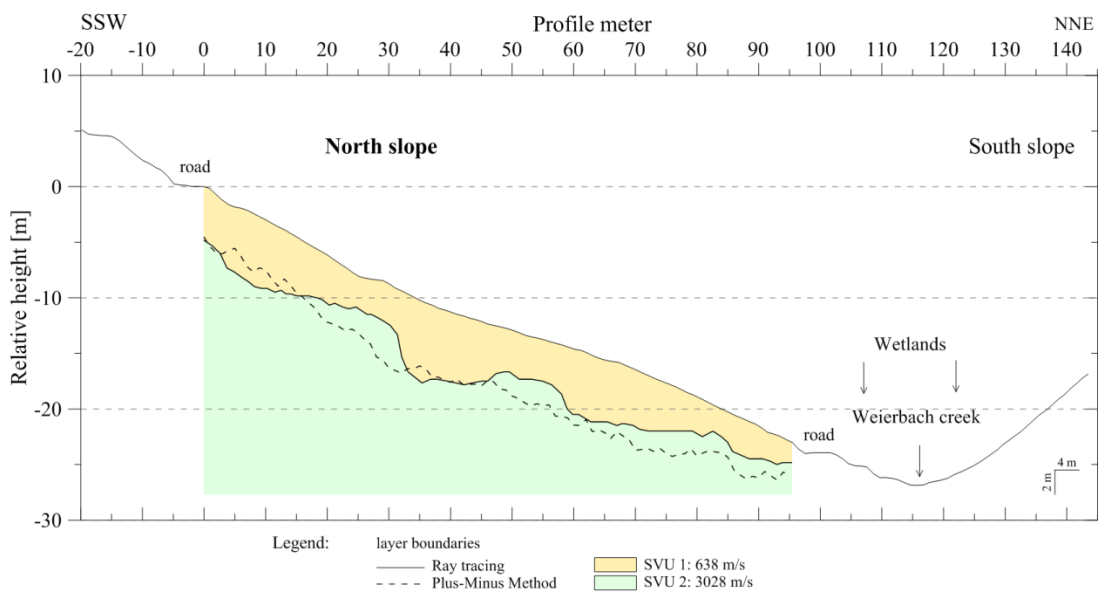


Figure 5-17: The case study of the Weierbach catchment: The hillslope refraction seismic subsurface model in terms of SVU's compares results obtained with ray tracing and plus-minus methods

Finally, to control the results of the applied seismic interpretation techniques, we realized **vertical seismic profiling (VSP)** at several shot positions (0 m, 50 m and 95 m) based on the CMP analysis and resulted one-dimensional velocity-depth profiles through iterative velocity adaptations. The Figure C - 1 in the Appendix illustrates the VSP models as the two layer models at the profile shot positions 0 m (the upper diagram), 50 m (the middle diagram) and 95 m (the below diagram). All VSP models imply approximately the same seismic velocity values of 450 m/s for the upper layer and 3100 m/s for the refracted layer. The VSP models indicate the slightly variations in the refractor depth ranging from ca. 2.5 m (for the profile meter 95) to ca. 3.8 m (for the profile meter 0). The surface topography and the scattered material of the PPSD's can cause these variations in the depth.

All resulted refraction seismic subsurface models complement well one another. Therefore, we can discuss the seismic models in the light of the hydrogeological conditions as well as for the joint interpretation with geo-electrical subsurface models.

5.2.2 *Application in the Schaeferfirtal catchment*

At this point, we will describe and discuss the refraction seismic models obtained at the study site the Schaeferfirtal catchment using the different seismic interpretation techniques such as Plus-Minus method, seismic tomography, ray tracing FD modelling and vertical seismic profiling. At the beginning, we will introduce the reader to the data quality. In order better to identify the first arrivals, we had to filter several seismograms. We observed the same phenomena with the noisy traces by the shooting from the down to the top as in the Weierbach catchment. We demonstrated the unfiltered seismograms for the shot position 1 meter (the upper diagram) and 96 meter (the middle diagram) in the Appendix B in the Figure B - 2. The upper diagram of the Figure B - 2 illustrates a relatively clear seismogram, whereas the middle diagram of this Figure demonstrates noisy traces of the last six traces. To eliminate the unwanted noise, we applied the band-pass filter with the lower cut-off of 15 Hz and the upper cut-off of 120 Hz. The bottom diagram of the Figure B - 2 illustrates the filtered seismograms.

As soon as we corrected the collected data in the elevation and filtered to remove the unwanted noise, we identified the first arrivals of the P-wave and plotted it in the travel time diagram, in order to analyse and to develop the structural subsurface model of the investigated hillslope.

Plus-Minus method

We plotted the two pair of selected symmetrical wave fronts (WF's) in the travel time diagram illustrated in the Figure 5-18a. One pair interprets the shot position at 1 m and 48 m, whereas other pair analyses the shot positions at 49 m and 96 m. The travel time diagram recognises the first arrivals of the direct wave and the first refractor. We believe that we can consider the subsurface model of the investigated hillslope as the two-layer model. Moreover, we observe that the upper and middle hillslope profile recognizes the lower seismic velocity values (the steeper time-distance slope) than the below hillslope and the wetlands characterizing by the increased seismic velocities. We also observe the relatively large critical distance (ca. 10 m) implying the decreased velocity ratio and a poor medium contrast. After recognizing the refractor time-distance slope, we calculated the time plus values and time minus values using the equations (4-13) and (4-14) with the total travel time of 53.5 ms (for the upper and the middle hillslope profile) and 44 ms (for the below hillslope and the wetlands). The diagrams (b) and (c) of the Figure 5-18 illustrate the calculated time plus and minus values, respectively. The time plus values or the intercept times reflect the location of the refractor, whereas the time minus values reveal the seismic velocity of the second layer (603 m/s for shots 1 m and 48 m; 818 m/s for shots 49 m and 96 m). The intercept times imply the relatively homogeneous distribution indicating a nearby horizontal layering with a slightly topography refractor at the shot distance. To develop structural subsurface models, we considered the two models summarized in the Table 5-5. The seismic velocities

5 Results and discussions

obtained from the time minus values characterize the Model A, whereas the Model B uses the averaged seismic velocities calculated from the slope of the time-distance curve (1299 m/s for shots 1 m and 48 m; 1741 m/s for shots 49 m and 96 m). Moreover, the Model A applies the seismic velocity for the direct

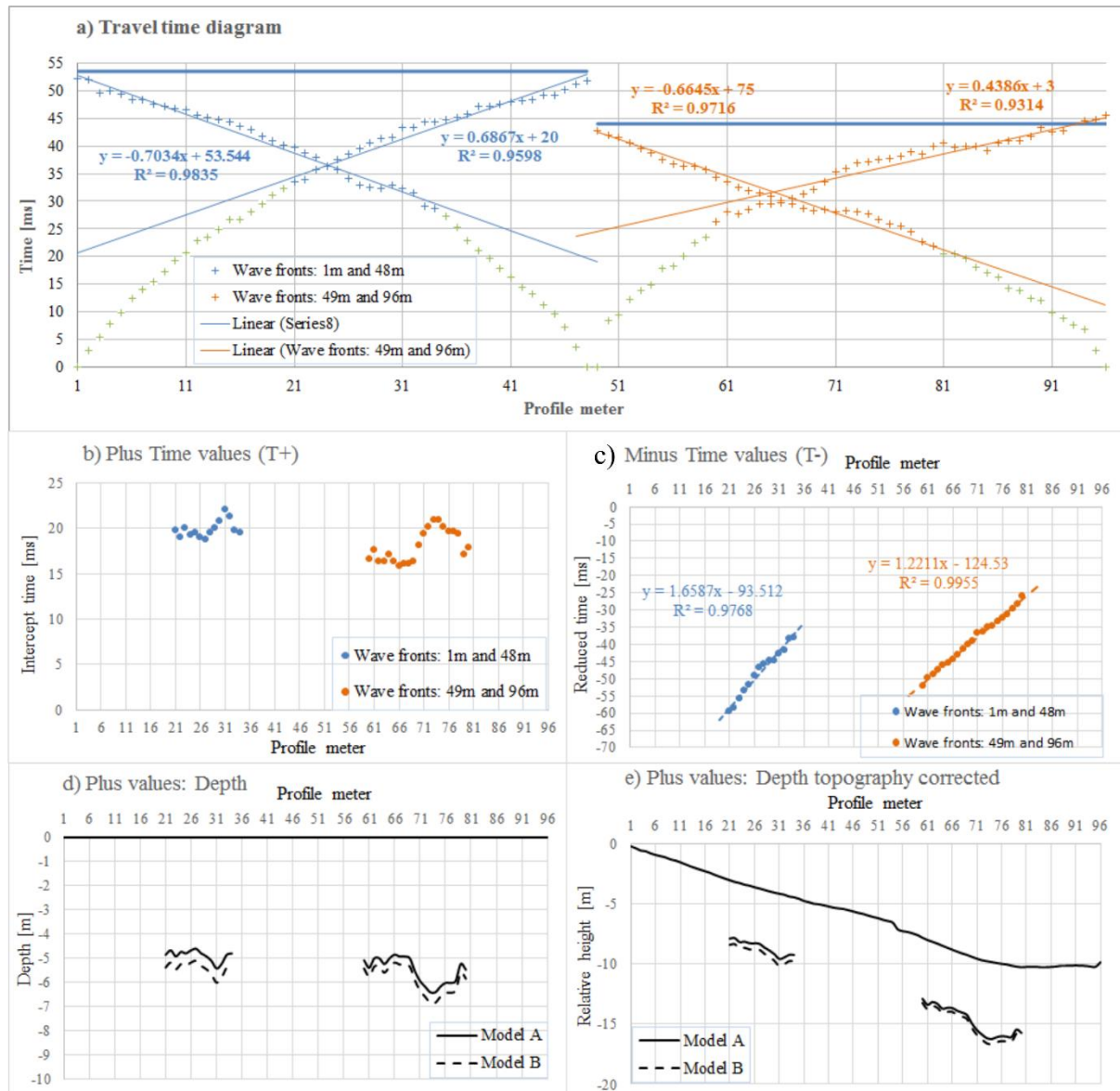


Figure 5-18: The case study of the Schaeferal catchment: Refraction seismic travel time data interpretation using Plus-Minus technique of two symmetrical wave fronts. (a) the travel time diagram with slowness slopes; (b) the diagram of calculated Plus-time values; (c) the diagram of calculated Minus-time values with seismic velocity slope. The structural subsurface models for assumed seismic velocity models (d) without topography and (e) with topography

wave obtained from the slope of the time-distance curve (380 m/s and 611 m/s). The Model B uses the seismic velocity values of the upper layer of 500 m/s and 611 m/s. Then, we calculated the refractor depth for the considered models shown in the Table 5-5 without the surface topography and with the

5 Results and discussions

surface topography using the calculated time plus values and the equation (4-11). The Figure 5-18 visualizes the subsurface models without the surface topography (d) and with the surface topography (e). Unfortunately, we could not describe the whole refractor due to the short analysed travel time. The refractor reaches the depth of ca. 5 - 6 m at the profile meter 21 - 36 m and 61 - 81 m. Both subsurface models characterize proximate the horizontal layering with the slightly topography refractor. The different RS subsurface models reflect the different refractors in the underground. The difference between model A and model B is ca. 0.5 m.

Table 5-5: The case study of the Schaeferfetal catchment: Ray parameters and seismic velocities to develop subsurface models using PMM

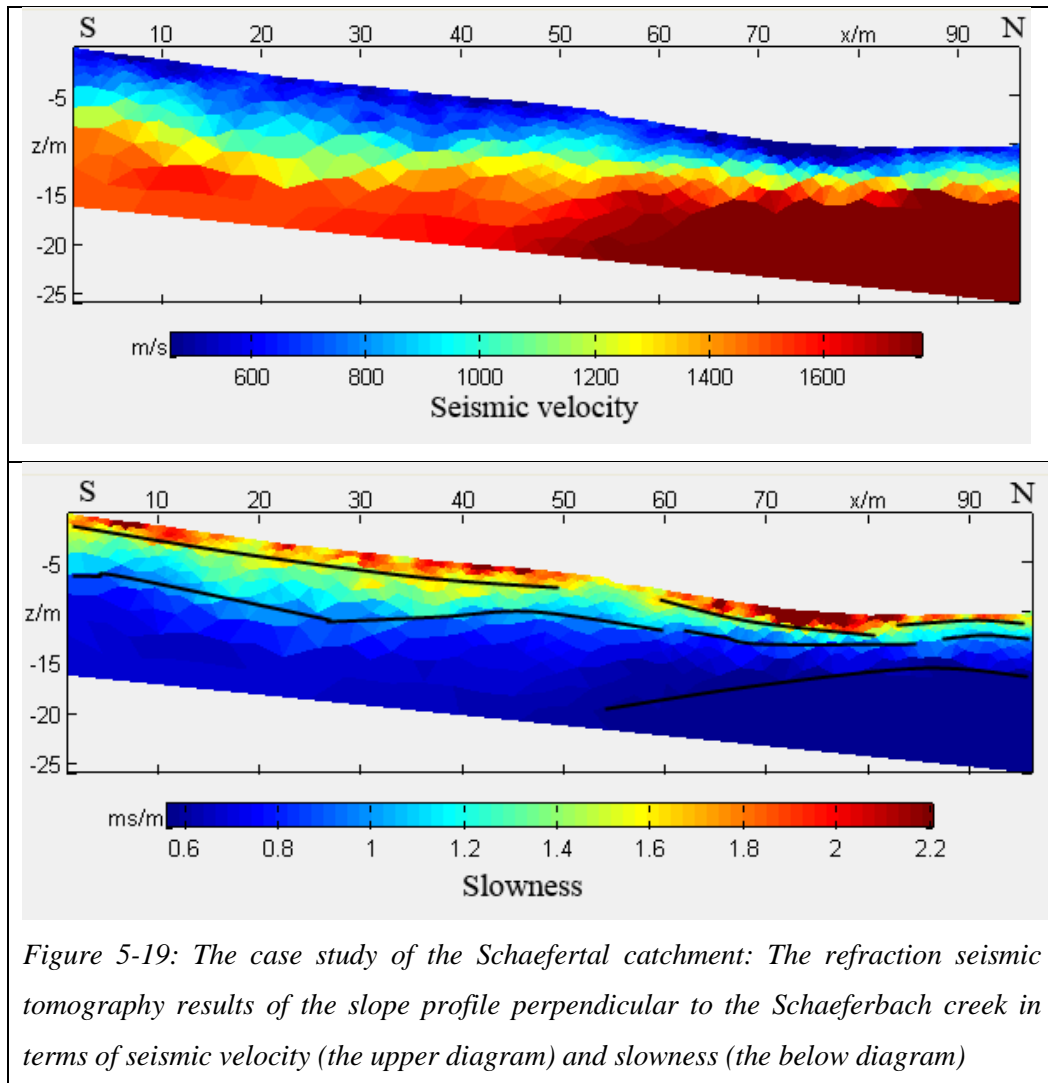
Subsurface model	Ray parameter, ms/m		Seismic velocity, m/s	
	WF: 1 m and 48 m	WF: 49 m and 96m	WF: 1 m and 48 m	WF: 49 m and 96 m
Model A	DW: 2.63	DW: 1.64	DW: 380	DW: 611
	HW: 1.66	HW: 1.22	HW: 603	HW: 818
Model B	DW: 1.99	DW: 1.64	DW: 500	DW: 611
	HW: 0.78	HW: 0.57	HW: 1299	HW: 1741

Refraction seismic tomography

The Figure 5-19 demonstrates the inversion results obtained from the refraction seismic tomography. The inverted seismic subsurface model characterizes a good matching of the theoretical and real travel time by the 0.83% rms. The RS tomography image illustrated in the upper diagram of the Figure 5-19 describes the seismic velocity field in the subsurface without the exact predication of the refractor depth. The below diagram of the Figure 5-19 demonstrates the distribution of the seismic ray parameter in the subsurface. The use of the ray parameter can help to recognize the refractors because of the uniformity of ray parameter and its abrupt change at the contrasting interfaces. The seismic velocity image recognizes the two seismic velocity fields along the hillslope profile. The shallow seismic velocity field with values of ca. 600 - 800 m/s reaches the depth from 5 m to 2 m decreasing in the creek direction. The refracting layer with the seismic velocity values of ca. 1500 m/s follows the depth boundary at the 8 m between profile meters 1 - 55 m. In the below part of the profile, we observe the increased velocity values of ca. 1700 m/s reaching the depth of ca. 3 - 4 m. The diffuse transition zone demonstrating the seismic velocity values of 1000 - 1300 m/s exists between the shallow layer and the refractor at the profile distance 1 - 60 m. Moreover, the ray parameter image tells us clear that the subsurface reveals the two contrasting stratums: the shallow layer and the deeper layer. The shallow upper layers reaches the depth of ca. 1 m with the slowness values of 2 ms/m (or 500 m/s). The deeper refractor with the slowness values of 0.8 ms/s (or 1250 m/s) reaches the depth from 6 m to 3 m decreasing in the Schaeferbach creek direction. In the wetlands, we can recognize the deepest refractor with the slowness values of 0.6 ms/s (or 1670 m/s) reaching the depth of ca. 5 m. We have to note that the refraction seismic tomography

5 Results and discussions

illustrates the diffuse contrast in the depth and a thin shallow contrasting layer. The diffuse contrast and the thin layer make more difficult to interpret the refraction seismic data due to the physical-mathematical validity of this technique.



Ray tracing FD modelling

From the previous interpretation techniques, we know that the relatively poor medium contrast and thin layering characterize the investigated hillslope. It makes more difficult to recognize a representative refractor. Moreover, from the travel time, we can observe the scenario of so-called hidden layer (see the travel time diagram in the Figure 5-20). In generally, we can recognize a two-layer model for the whole profile. Nevertheless, if we exam the upper profile part, we can recognize the structure of the three-layer model only for this profile part. Therefore, we decided to consider two scenarios, to develop a seismic subsurface model based on the wave front inversion and the ray tracing FD modelling. The first scenario develops a two-layer subsurface model, whereas the second scenario consider the model with a three-layer for the upper and middle hillslope. Both scenarios develops subsurface models

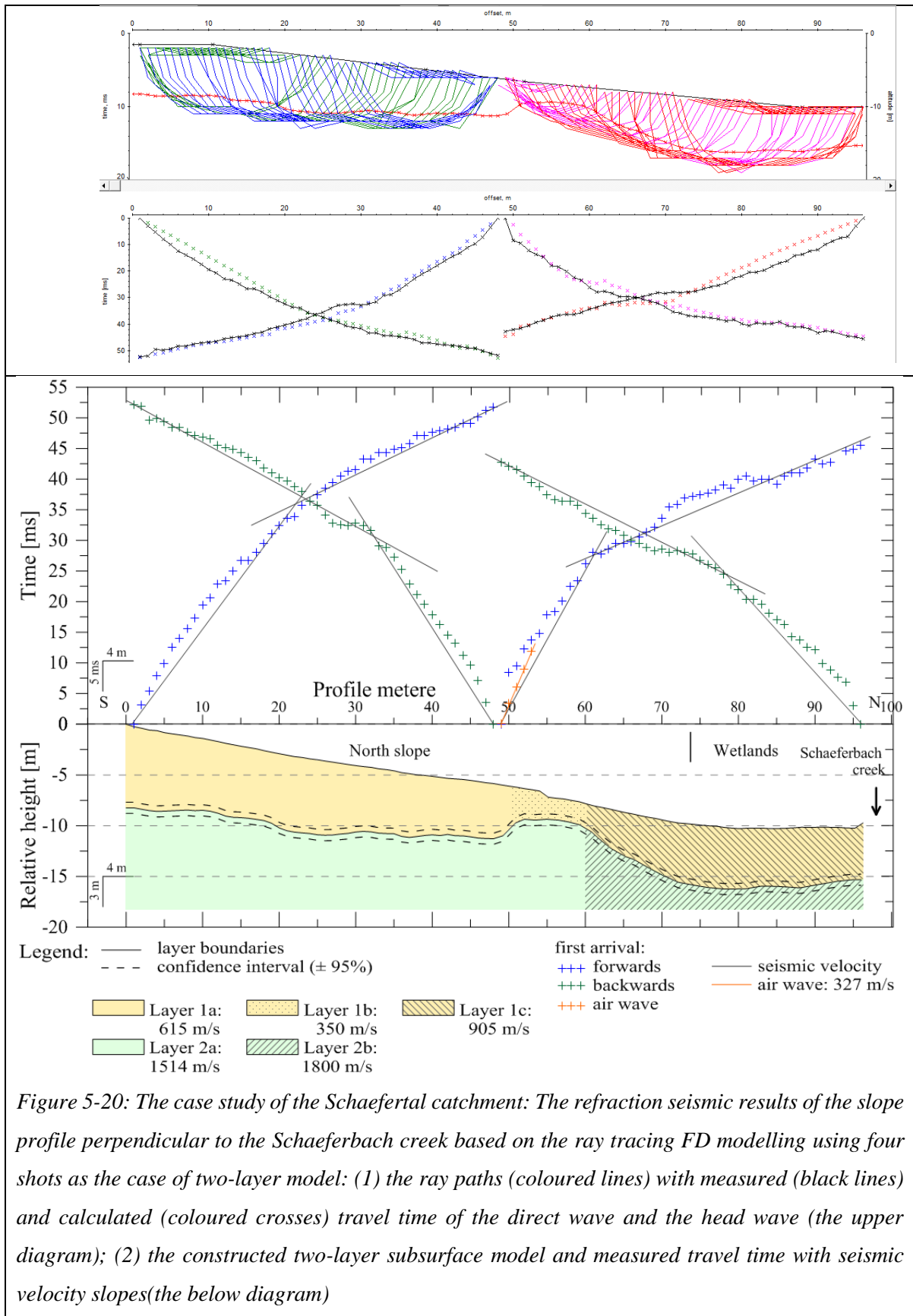


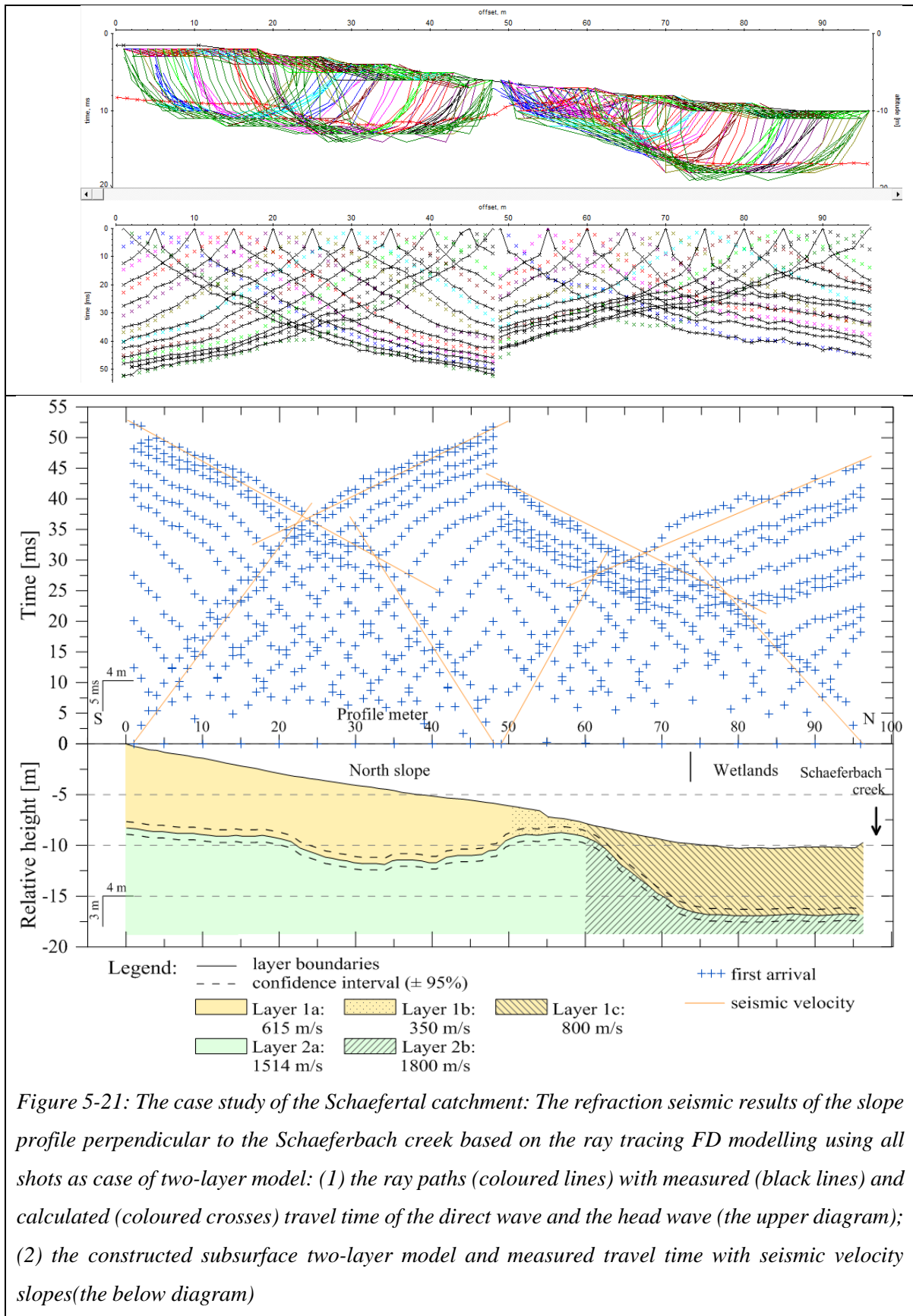
Figure 5-20: The case study of the Schaeferfartl catchment: The refraction seismic results of the slope profile perpendicular to the Schaeferbach creek based on the ray tracing FD modelling using four shots as the case of two-layer model: (1) the ray paths (coloured lines) with measured (black lines) and calculated (coloured crosses) travel time of the direct wave and the head wave (the upper diagram); (2) the constructed two-layer subsurface model and measured travel time with seismic velocity slopes (the below diagram)

5 Results and discussions

using the two pairs of the symmetrical wave fronts as well as all shot seismic spreading along the investigated hillslope. Moreover, the seismic model obtained from the several shots, we integrated as a starting model for the modelling with all shots. We executed iterative and manual changes of model parameters (geometry of refractors and velocity values) and repeated the ray tracing process many times until we found a wanted subsurface model reflecting measured travel time and matching calculated and real data.

Well, let us start considering the first scenario presenting **the two-layer subsurface model**. The Figure 5-20 illustrates the results of the ray tracing FD modelling for the case using the two pairs of symmetrical wave fronts. One pair of WF's analyses the profile shot positions at 1 m and 48 m, and other WF pair characterizes the profile shot positions at 49 m and 96 m. After the visual analysing of these WF's, we can observe a relatively large critical distance (ca. 10 m) indicating on the decreased the velocity ratio (the equation (4-6)). Moreover, we have to note that it makes difficult to recognize the identification of the first arrivals between direct seismic wave and airwave for the first traces due to the close recording. The below diagram of the Figure 5-20 illustrates the identified airwave (ca. 327 m/s) in the travel time diagram. The upper diagram of the Figure 5-20 illustrates the matching between the theoretical and measured travel time as well as the calculated ray paths in the underground. The bellow diagram of the Figure 5-20 demonstrates the final subsurface model as well as the travel time diagram of the considered symmetrical wave fronts. How we can see from the results, the relatively variable seismic velocity values ranging from 615 m/s to 905 m/s characterize the shallow upper layer. The refracting layer also implies the variable velocity value from 1514 m/s (the upper and middle slope) to 1800 m/s (the below slope and wetlands). We can observe a nearby good matching of the theoretical and real travel time of the head wave. The ray paths of the WF's illustrate quite the consistent image in the underground. The subsurface model reveals the nearby horizontal layering with the jump in the middle part of the profile. The refractor depth varies from ca. 8 m to 5 m decreasing in the creek direction. Therefore, we will integrate the obtained seismic structural subsurface model for the future ray tracing modelling using all shots recorded along the whole hillslope, in order to develop a final seismic structural model contenting of the two-layers.

The Figure 5-21 lustrates the results of the ray tracing FD modelling using all symmetrical wave fronts. Using the obtained subsurface model illustrated in the below diagram in the Figure 5-20 as a starting model, we created the final subsurface model changing the refractor geometry, in order to find the best matching between the calculated and real travel time. The upper diagram of the Figure 5-21 illustrates a quite good matching between the theoretical and measured travel time as well as the calculated ray paths in the underground. The bellow diagram of the Figure 5-21 demonstrates the final subsurface model as well as the travel time diagram of all first arrivals. The shallow upper layer describes a relatively variable seismic velocity field from 615 m/s (the upper and middle slope) to 800 m/s (the below slope and the wetlands). The increased velocity values ranging from 1514 m/s to 1800 m/s characterize the refracting layer. Therefore, we reached the good matching of the theoretical and real travel time for the refracted



5 Results and discussions

wave, but we had to ignore the travel time fitting for the direct wave due to the strong velocity variability. The ray paths of the symmetrical wave fronts illustrate quite the consistent image in the underground. The obtained seismic structural subsurface model describes the relatively horizontal layering with the jump in the middle part of the profile. The refractor depth of ca. varies from ca. 8 m to 5 m decreasing in the creek direction. We also calculated and drawn (broken line in the below diagram of the Figure 5-21) the depth uncertainty amounting ca ± 3.2 m. Furthermore, the Table 5-6 summarizes the results obtained with the ray tracing FD modelling for the scenario of the two-layer model using the two pairs of the symmetrical wave fronts as well as all shot seismic spreading along the investigated hillslope. Both cases imply nearby the same refractor depth and refractor velocity values.

Table 5-6: The case study of the Schaeferthal catchment: Seismic subsurface parameters obtained with the ray tracing FD modelling for the scenario of the two-layer model

Layer Number	Seismic velocity [m/s]		Depth, m	
	Model with four shots	Model with all shots	Model with four shots	Model with all shots
Layer 1a	ca. 615 \pm 18		ca. -5.94 \pm 1.5	ca. -5.51 \pm 3.2
Layer 1b	ca. 350 \pm 15			
Layer 1c	ca. 905 \pm 25	ca. 800 \pm 20		
Layer 2a	ca. 1514 \pm 30			
Layer 2b	ca. 1800 \pm 30			

Until now, we will present the second scenario presenting **the three-layer subsurface model** for the upper and middle hillslope. The Figure 5-22 illustrates the results of the ray tracing FD modelling for the case using the pair of symmetrical wave fronts locating at the profile shot positions of 1 m and 48 m. After the visual analysing of these WF's, we assigned the first arrivals for the direct wave and the two refractors, in order to conduct the wave inversion and the ray tracing FD modelling for the developing of the three-layer subsurface model. The upper diagram of the Figure 5-22 illustrates a good matching between the theoretical and measured travel time as well as the calculated ray paths in the underground. The ray paths of the WF's illustrate quite the consistent image in the underground. The bellow diagram of the Figure 5-22 demonstrates the final subsurface model as well as the travel time diagram of the considered symmetrical wave fronts. The subsurface model reveals the nearby horizontal layering. The upper layer with the lower velocity values of 409 m/s reaches the depth of ca. 1.8 m. The middle layer with the intermediate velocity values of 750 m/s reaches the depth of ca. 8 m underlying by the second refracting layer with velocity values of 1762 m/s. We can integrate the obtained seismic structural subsurface model for the future ray tracing modelling using all shots recorded along the upper hillslope, in order to develop a final seismic structural model contenting of the three-layers.

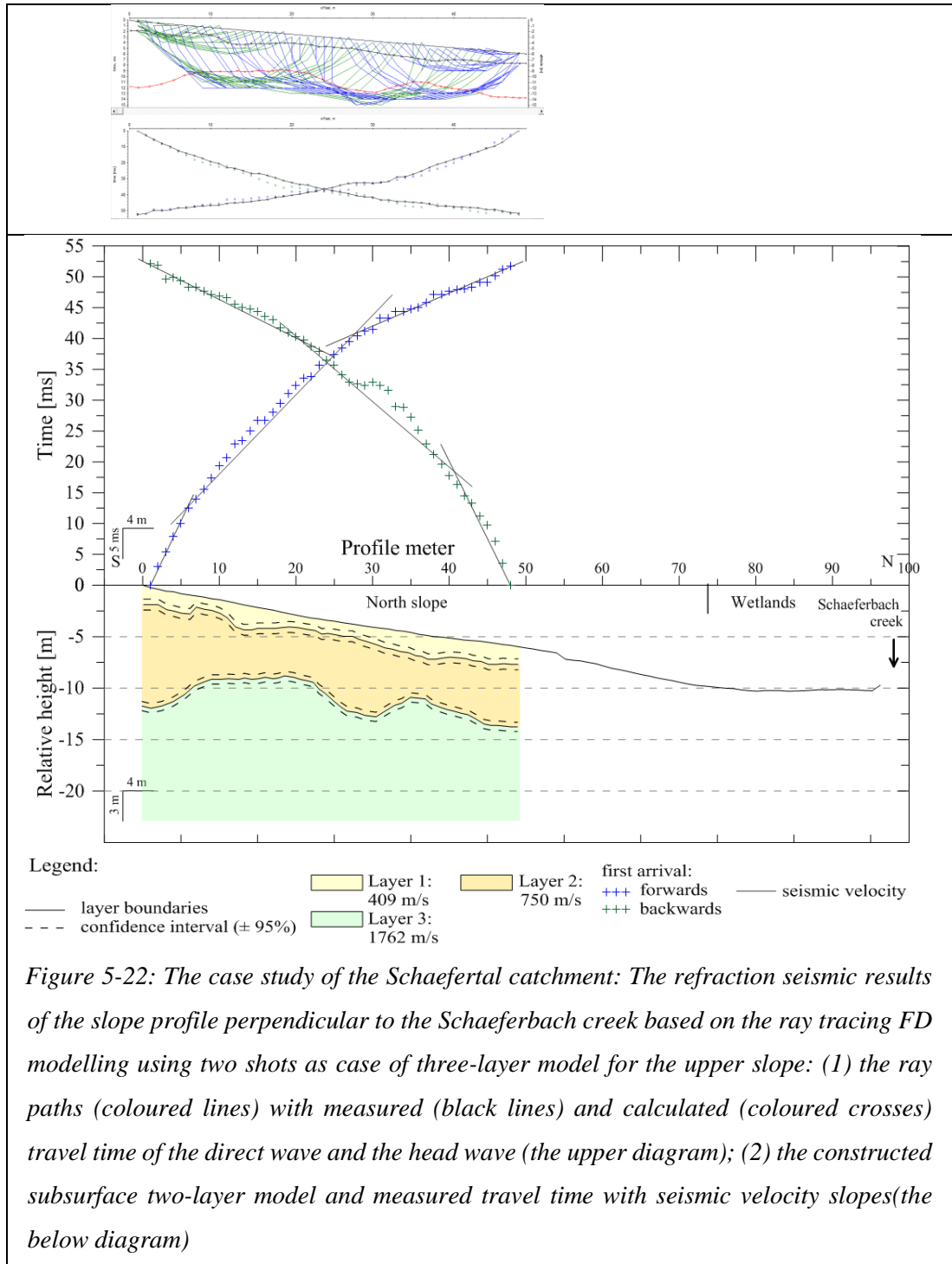
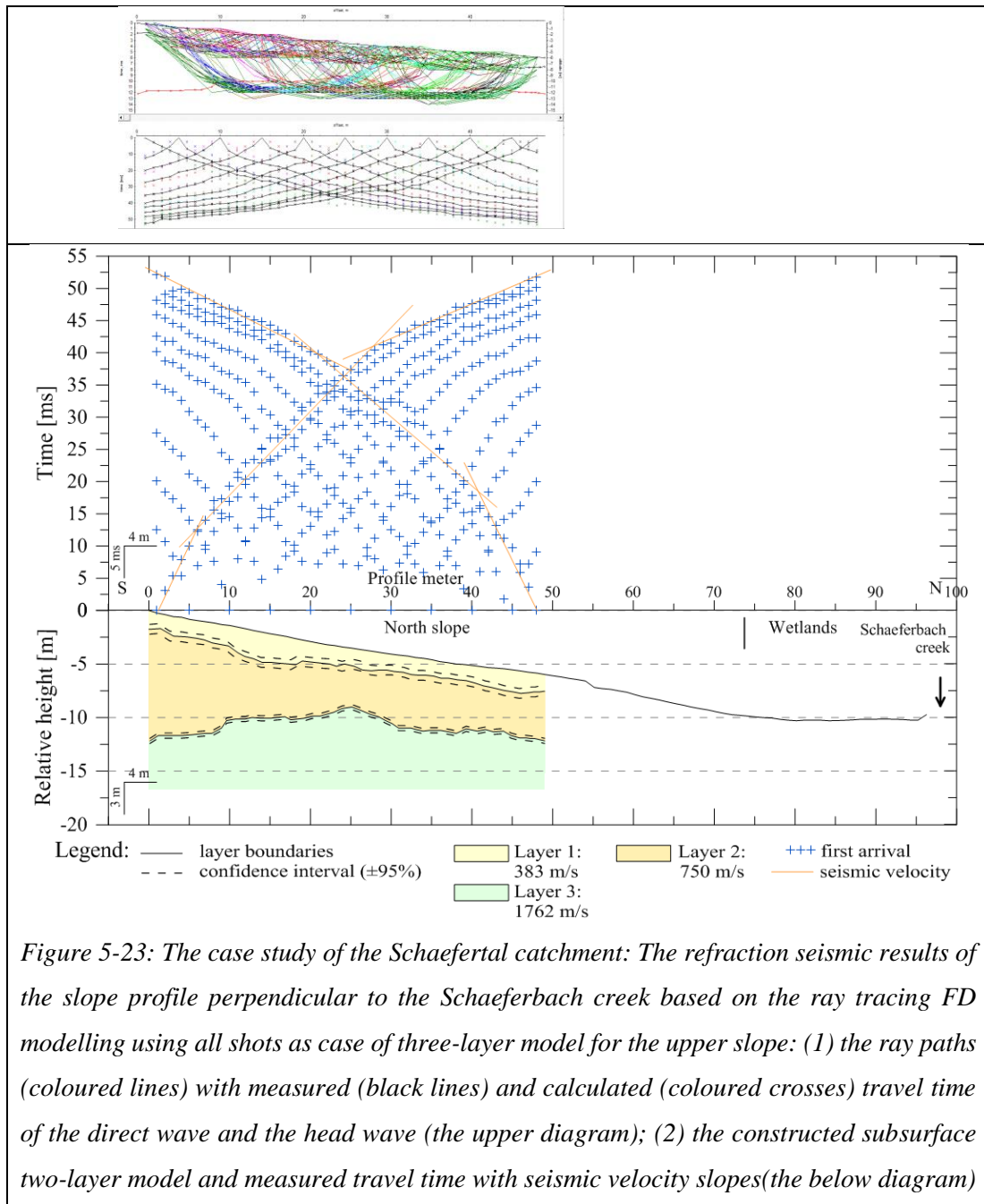


Figure 5-22: The case study of the Schaeferfartal catchment: The refraction seismic results of the slope profile perpendicular to the Schaeferbach creek based on the ray tracing FD modelling using two shots as case of three-layer model for the upper slope: (1) the ray paths (coloured lines) with measured (black lines) and calculated (coloured crosses) travel time of the direct wave and the head wave (the upper diagram); (2) the constructed subsurface two-layer model and measured travel time with seismic velocity slopes (the below diagram)

The Figure 5-23 illustrates the results of the ray tracing FD modelling using all symmetrical wave fronts. Using the obtained subsurface model illustrated in the below diagram in the Figure 5-22 as a starting model, we created the final subsurface model changing the refractor geometry, in order to find the best matching between the calculated and real travel time. The upper diagram of the Figure 5-23 illustrates a quite good matching between the theoretical and measured travel time as well as the calculated ray paths in the underground. The ray paths of the WF's illustrate quite the consistent image in the underground. The bellow diagram of the Figure 5-23 demonstrates the final subsurface model as



well as the travel time diagram of all first arrivals. The subsurface model reveals the nearby horizontal layering. The upper layer with the lower velocity values of 383 m/s reaches the depth of ca. 1.9 m. The middle layer with the intermediate velocity values of 750 m/s reaches the depth of ca. 7.5 m underlying by the second refracting layer with velocity values of 1762 m/s. We also calculated and drawn (broken line in the below diagram of the Figure 5-23) the depth uncertainty amounting ca ± 1.7 m. Furthermore, the Table 5-7 summarizes the results obtained with the ray tracing FD modelling for the scenario of the three-layer model using the one pair of the symmetrical wave fronts as well as all shot seismic spreading along the investigated hillslope. Both cases imply nearby the same refractor depth and refractor velocity values.

Table 5-7: The case study of the Schaefertal catchment: Seismic subsurface parameters obtained with the ray tracing FD modelling for the scenario of the three-layer model applied for the upper slope

Layer Number	Seismic velocity [m/s]		Depth, m	
	Model with two shots	Model with all shots	Model with two shots	Model with all shots
Layer 1	ca. 409 ± 16	ca. 383 ± 14	ca. -1.74 ± 0.4	ca. -1.95 ± 0.6
Layer 2	ca. 750 ± 23			
Layer 3	ca. 1762 ± 32		ca. -7.82 ± 1.3	ca. -7.55 ± 1.7

Up to now, we will compare qualitative the seismic two-layer model with the three-layer model. The upper and middle diagrams of the Figure 5-24 demonstrate the considered subsurface models. The below diagram of the Figure 5-24 illustrates the qualitative comparison of two models. The Table 5-8 summarizes these subsurface models. The difference of the deeper refractor between these models is ca. 2 m. The models also differ in the refractor topography. For the future application, we will take the two-layer subsurface model because it respects the whole hillslope profile.

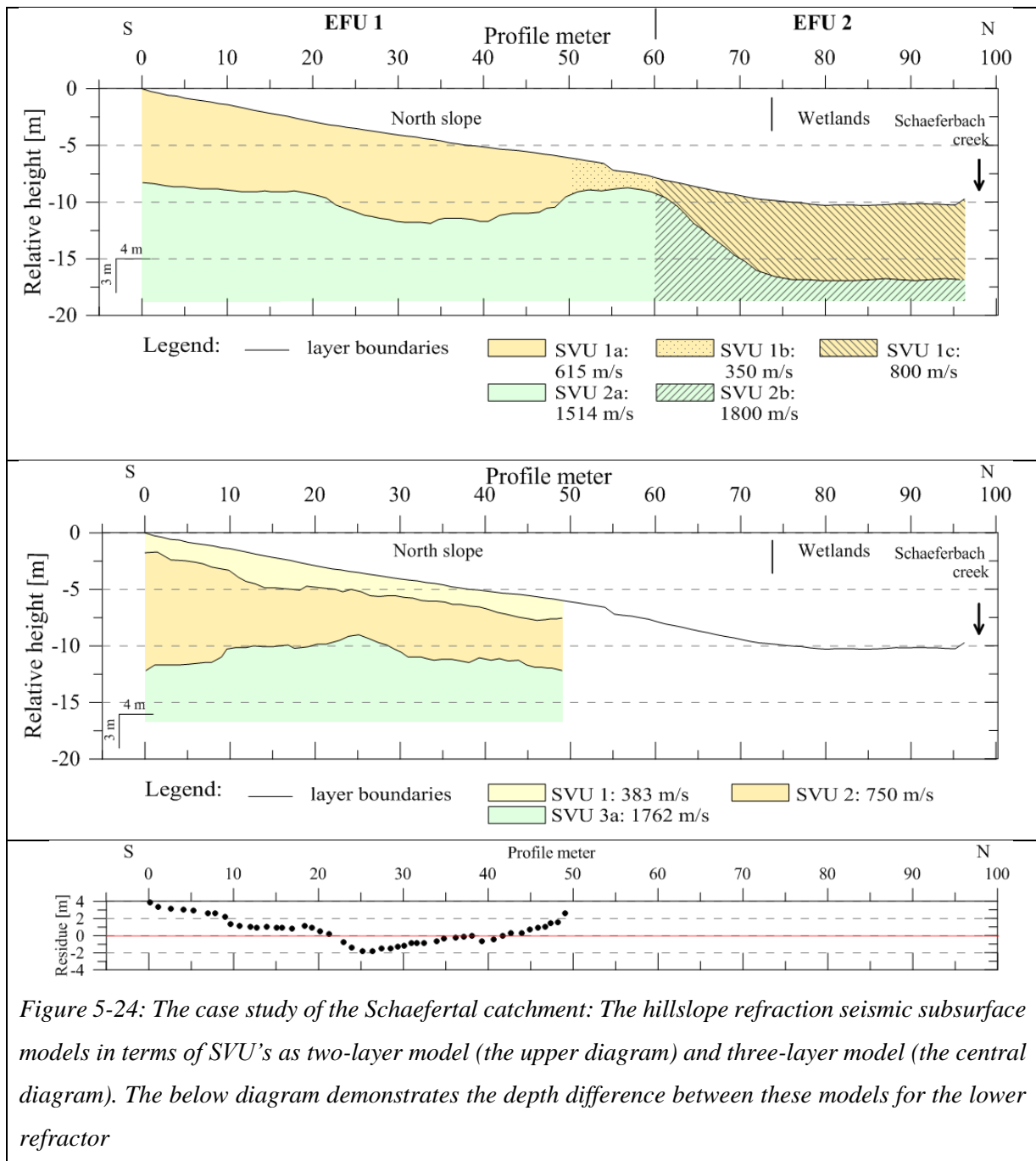
Table 5-8: The case study of the Schaefertal catchment: Comparison of seismic velocity values between two-layer model and three-layer model for the upper slope

Layer	Two layer model			Three layer model	
		Seismic velocity, m/s	Depth, m	Seismic velocity, m/s	Depth, m
Layer 1	a	ca. 615 ± 18	ca. -5.51 ± 3.2	ca. 383 ± 14	ca. -1.95 ± 0.6
Layer 2	b	ca. 350 ± 15		ca. 750 ± 23	
	c	ca. 800 ± 20			
Layer 3	a	ca. 1514 ± 30	ca. -5.51 ± 3.2	ca. 1762 ± 32	ca. -7.55 ± 1.7
	b	ca. 1800 ± 30			

Finally, to control the results of the applied seismic interpretation techniques, we realized **vertical seismic profiling (VSP)** at several shot positions (1 m, 48 m, 49 m and 96 m) based on the CMP analysis and resulted one-dimensional velocity-depth profiles through iterative velocity adaptations. The C - 2 in the Appendix illustrates the VSP models as the two layer models at the profile shot positions 1 m (the upper diagram), 48 m, 49 m (the middle diagrams) and 96 m (the below diagram). All VSP models locating on the upper and middle slope imply approximately the same seismic velocity values of 500 m/s for the upper layer and 1600 m/s for the refracted layer. Whereas VSP models analysed for the below

5 Results and discussions

profile and the wetlands indicate the increasing velocity values of 1800 m/s. The VSP models reaches the averaged depth of 6 m.



All refraction seismic subsurface models complement quite well one another. Therefore, we can discuss the seismic models in the light of the hydrogeological conditions as well as for the joint interpretation with geo-electrical subsurface models.

5.3 Geo-electric versus refraction seismic, and versus combination

How we can see the results of the individual interpretations describing in the chapter 5.4 illustrate quite good geophysical models of the investigated hillslopes. Now, we want to know how good the individual geo-models complement one other, in order to develop a conceptual hydro-geophysical model for the investigated hillslope of the Weierbach as well as Schaeferfirtal.

5.3.1 Application in the Weierbach catchment

The upper diagram of the Figure 5-25 illustrates the transparent comparison of electrical and seismic models. We compare the results of ERT, VES, ray tracing modelling and PMM. Here we do not consider the deepest layer unit interpreted by VES because ERT and RS do not imply this layer unit in the subsurface section. The resistivity of ERT and VES results correlate clear with each other. The rela-

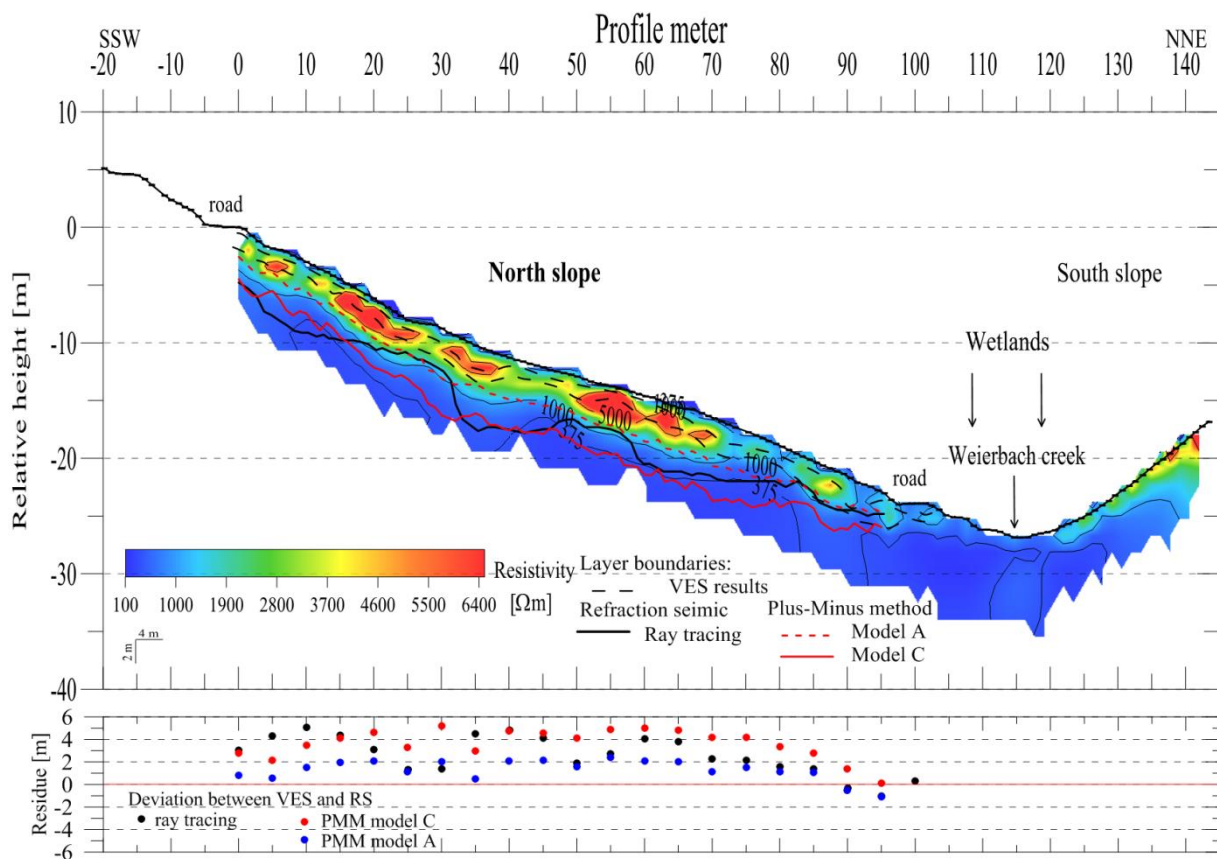


Figure 5-25: The case of the Weierbach catchment: The transparent comparison of layer interface between ERT, VES and RS (the upper diagram). The depth difference between VES and RS (the below diagram)

tively high resistant upper layer (ca. 1750 Ωm) reaches a depth of ca. 0.8 - 1 m along the hillslope underlying by the layer with the highest resistivity values (more than 5000 Ωm). The second interface of VES describing the highest resistivity values correlates well with the highest resistivity values of ERT.

5 Results and discussions

Moreover, if we observe the refractor characterising the Model A (366.55 m/s for the upper layer and 1755 m/s for the refracting layer), we will find that it describe the interface between the high resistant (more than 1900 Ωm) and low resistant (1000 Ωm) values. This refractor characterises nearby the form of the resistivity iso-line of 1000 Ωm . Besides, the refractor calculated with ray tracing and PMM as Model C (638 m/s for the upper layer and 3028 m/s for the refracting layer) describes well more or less the form of the resistivity iso-line of 375 Ωm . Furthermore, we can quantitative estimate the difference between RS and VES models. The below diagram of the Figure 5-25 demonstrates the difference between RS and VES models ranging from ca. 2 m to ca. 4 m. The difference between VES model and RS model A is relatively small by ca. 2 m in contrast to the deeper electrical (VES) and seismic (ray tracing and PMM model C) boundaries characterising by the difference of ca. 4 m. We assume the difference between electrical and seismic models as the geophysical uncertainty, which we can associate with a giving transition zone between different petro-physical layer units.

Up to now, a good agreement of resulting geo-models permits us to discuss in the light of the hydro-geological conditions. The Table 5-9 summarizes the electrical and seismic properties in terms of the representative layer units. We believe that the upper layers characterising by the low seismic velocity as well as high resistant values describe PPSDs. Electrical unit 1 and 2 characterize UPL and BPL, respectively. The below layer indicating the high seismic velocity values and low resistivity values, we can associate with the fractured bedrock representing the Devonian schist. Moreover, we associate the difference between electrical and seismic models with the transition zone from PPSDs to the fractured bedrock where may occur the preferential subsurface flow. The refractor calculated by the ray tracing and PMM (Model C) represents the top boundary of the upper fractured schist.

Table 5-9: The case study of the Weierbach catchment: Comparison of geophysical units

Unit	Sub-units	Electrical resistivity, Ωm	Depth, m	Seismic velocity, m/s	Depth, m	Geology
Unit 1	-	ca. 1730 \pm 620				PPSDs
Unit 2	a	ca. 8940 \pm 4500	ca. -0.83 \pm 0.5	ca. 638 \pm 46		
	b	ca. 2020 \pm 1530				
Unit 3	-	ca. 330 \pm 74	ca. -1.81 \pm 0.6	ca. 3028 \pm 35	ca. -4.92 \pm 2.3	Fractured bedrock
Unit 4	a	ca. 855 \pm 440	ca. -18.71 \pm 8.4			Compact bedrock
	b	ca. 403 \pm 162				

The Figure 5-26 complies three geophysical hillslope models together in terms of ERT (the upper diagram), VES (the middle diagram) and RS (the below diagram) subsurface models. How we can observe these diagrams, the VES subsurface model implies the deepest layer boundary characterising by the increased resistivity values (403 - 855 Ωm) in contrast to the previous layer. We can associate this

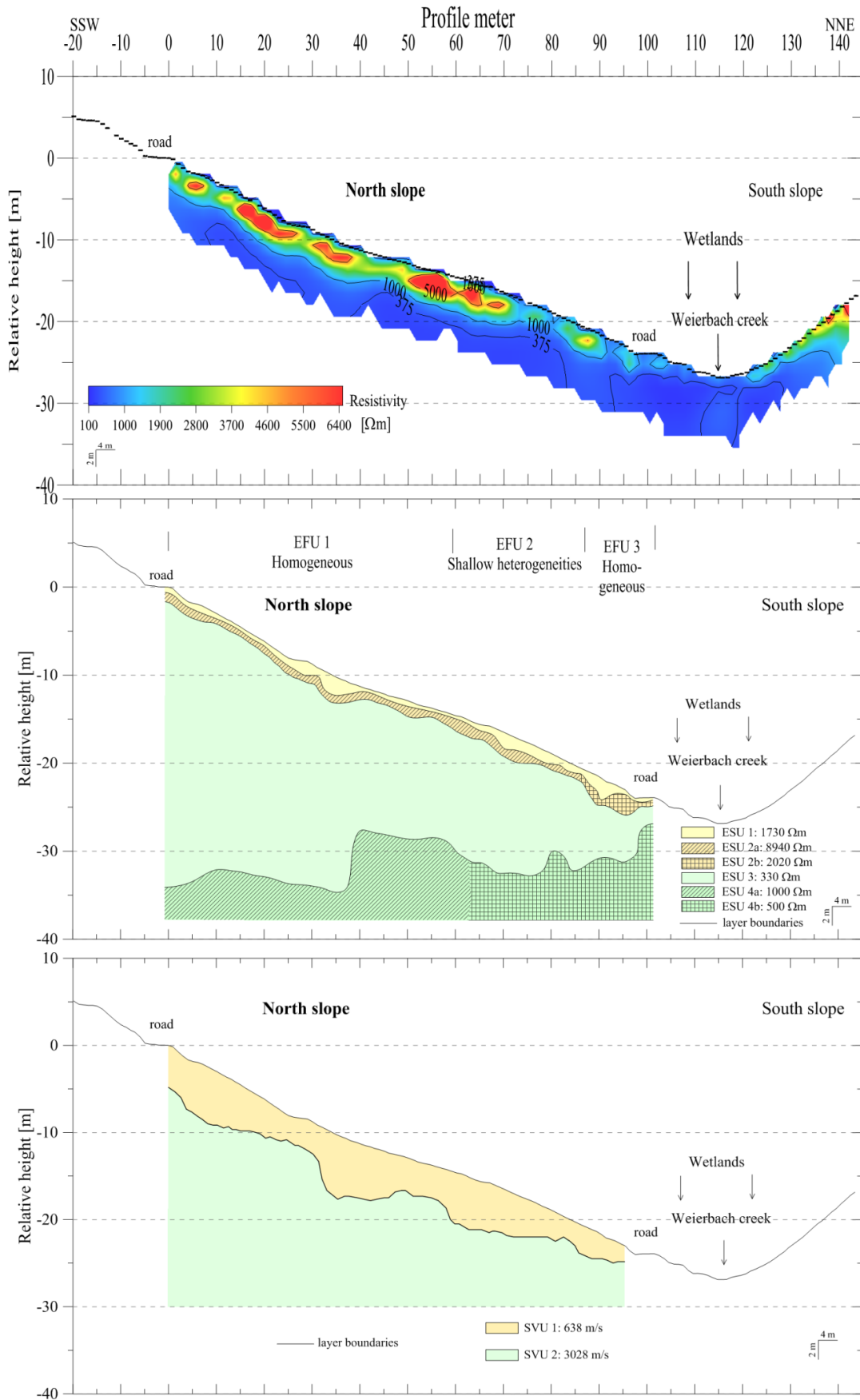


Figure 5-26: The case study of the Weierbach catchment: The hillslope subsurface models as joint geophysical interpretation in terms of ESU's, EFU's and SVU's

layer with the compact or fresh bedrock. ERT and RS could not resolve this deepest interface due to the poor medium contrast in the depth and the applied small profile line. Nevertheless, we believe that this interface exists in the underground because we predicated it using the VSP techniques. The Figure D - 1 in the Appendix illustrates the one-dimensional VSP models for the shot point locating at the profile meters of 0 m (the upper diagram) and 95 m (the below diagram). Both models predicate three layers. The upper layer with the seismic velocity values of ca. 490 m/s reaches the depth in the range from 2.5 m to 3.8 m. The below layer with seismic velocity values of ca. 3000 m/s predicates the deepest interface at the depth of ca. 16 -19 m implying the seismic velocity of ca. 4200 m/s.

Moreover, we could identified the significant hillslope areas (EFU's) only from geo-electrical data (especially, VES), which represent three EFU's along the investigated hillslope. Whereas the results of the refraction seismic, we can consider as relatively homogeneous stratum with the increased seismic velocities in the depth.

5.3.2 Application in the Schaeferfetal catchment

The upper diagram of the Figure 5-27 illustrates the transparent comparison of electrical and seismic models. We compare the results of ERT, VES and ray tracing modelling. Here we do not consider the deepest layer unit interpreted by VES because ERT and RS do not imply this layer unit in the subsurface section. We also cannot compare the results obtained with PMM because the refractor does not imply the length of the whole profile. Nevertheless, we discuss the scenarios of the two and three layer models. The resistivity of ERT and VES results correlate clear with each other. If we observe the upper high resistivity value layer (ca. 460 Ωm), we will find that it complements well the high resistivity patterns of ERT (450 - 550 Ωm). Moreover, the upper low velocity layer (383 m/s) predicated by the three-layer model describes nearby the interface form predicated by VES and ERT. Whereas the below layer describing the decreasing resistivity values (300 Ωm) and variable velocity values (600 - 800 m/s) does not match the bottom layer boundary. The below diagram of the Figure 5-27 demonstrates the difference between RS and VES models ranging from ca. 1 m to ca. 4 m. The difference between VES model and RS is relatively small by ca. 1 m for the case of the upper layer in contrast to the deeper electrical and seismic boundaries having the random difference of ca. 4 m. We think that the poor medium contrast and relatively strong water saturation cause the large differences and ambiguities between geo-models.

Nevertheless, we will try to interpret the obtained geo-models in the light of the hydro-geological conditions. The Table 5-10 summarizes the electrical and seismic properties in terms of the representative layer units. We believe that the upper layers characterising by the low seismic velocity as well as high resistant values describe PPSDs. Electrical unit 1 and 2 characterize UPL and BPL, respectively. The below layer indicating the high seismic velocity values (1500 - 1800 m/s) and low resistivity values (130 Ωm) we can associate with the fissured bedrock representing the Devonian greywacke. Moreover, we associate the relatively random difference between electrical and seismic models with the diffuse contrast between PPSDs and the fissured bedrock. We have to remember that we conducted the measurements in

5 Results and discussions

the end of February characterizing by the wet state. However, the increased groundwater level and subsurface flows can cause the homogeneous water saturation in the wetlands. We can associate the describing diffuse contrast with the possible path of the subsurface flow. It exists a good connection between the Schaeferbach creek and the hillslope through the relatively large wetlands.

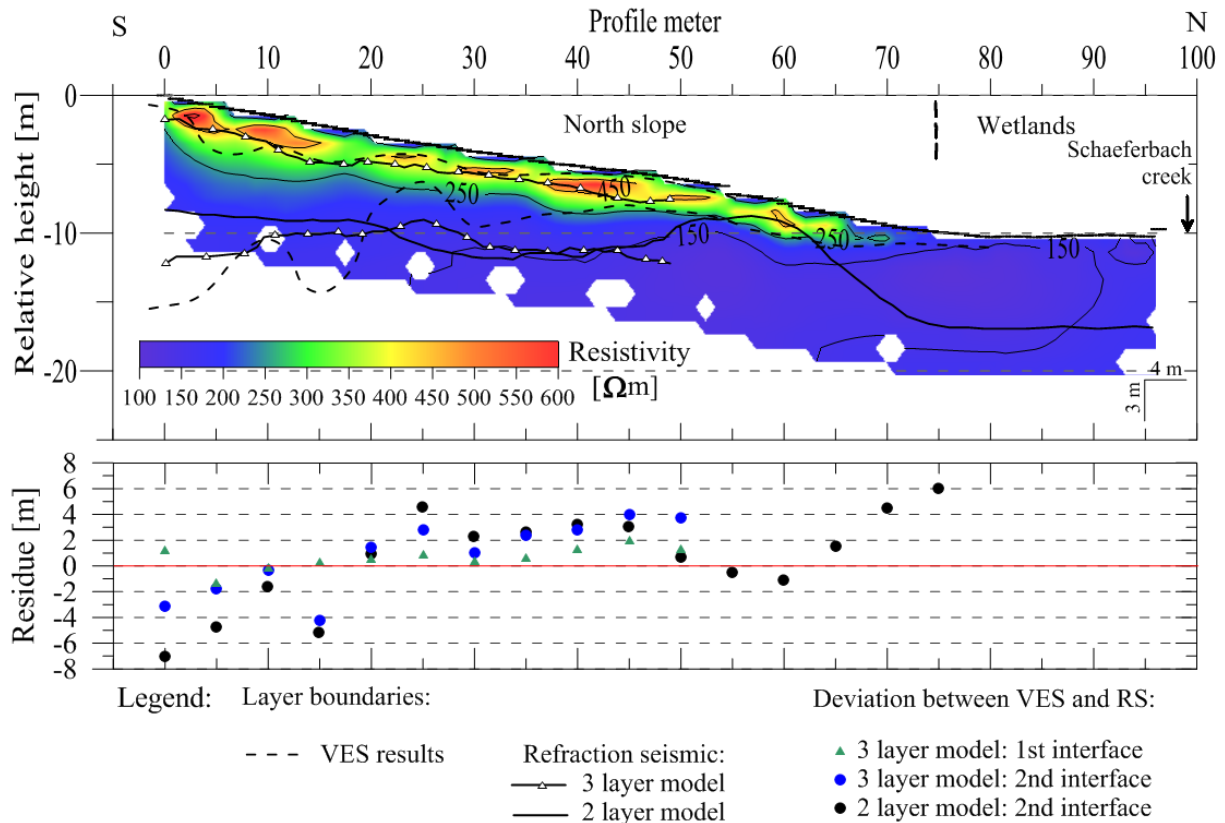


Figure 5-27: The case of the Schaeferfartl catchment: The transparent comparison of layer interface between ERT, VES and RS (the upper diagram). The depth difference between VES and RS (the below diagram)

Table 5-10: The case study of the Schaeferfartl catchment: Comparison of geophysical units

Unit	Sub-units	Electrical resistivity, Ωm	Depth, m	Seismic velocity, m/s	Depth, m	Geology
Unit 1	a	ca. 460 ± 201		ca. 615 ± 18		PPSDs
Unit 2	b	ca. 300 ± 72	ca. -1.19 ± 0.9	ca. 350 ± 15		
	c			ca. 800 ± 20		
Unit 3	a	ca. 130 ± 15	ca. -5.23 ± 4.5	ca. 1514 ± 30	ca. -5.51 ± 3.2	Fissured bedrock
	b			ca. 1800 ± 30		
Unit 4		ca. 270 ± 165	ca. -30.67 ± 7.1			Fresh bedrock

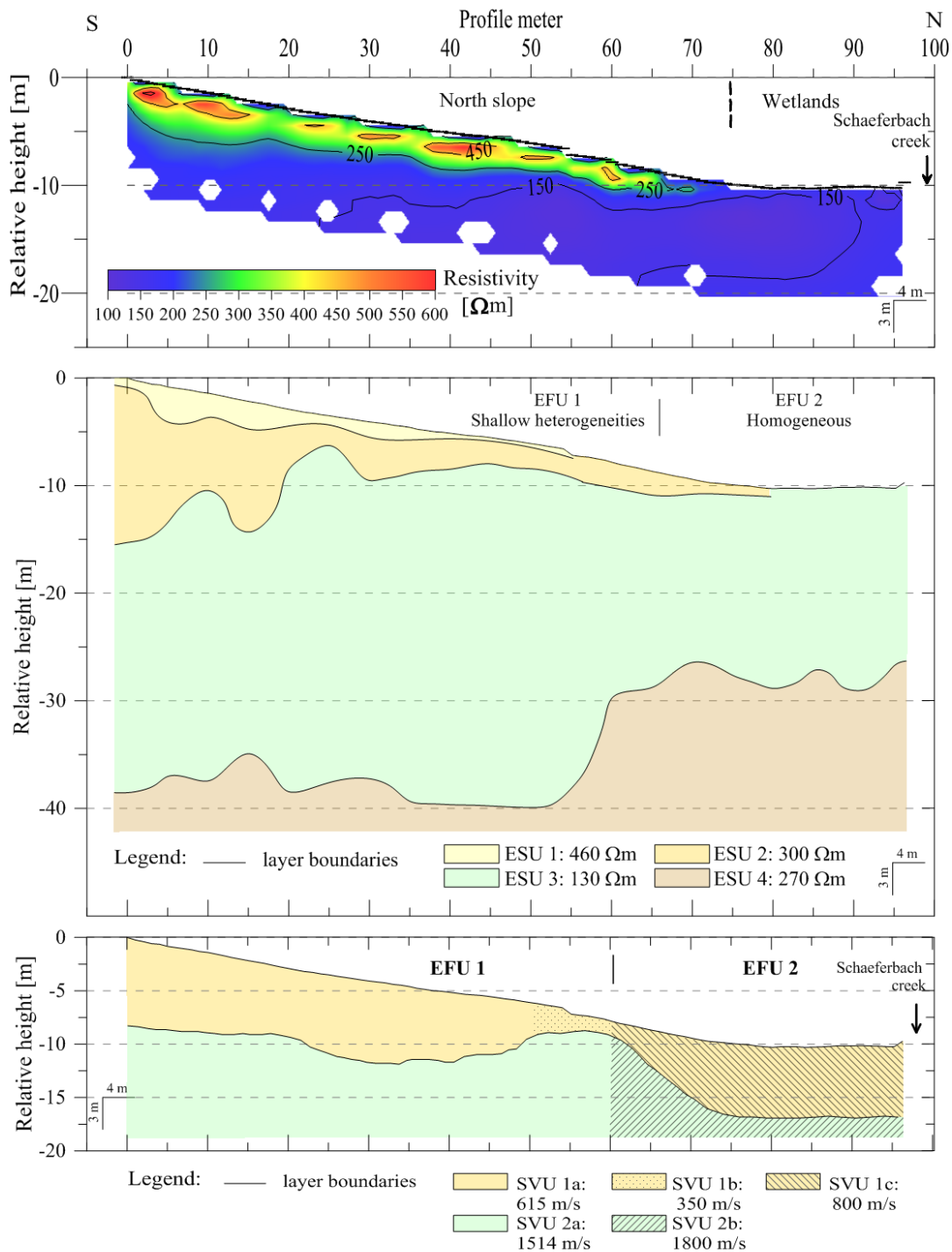


Figure 5-28: The case study of the Schaeferfalta catchment: The hillslope subsurface models as joint geophysical interpretation in terms of ESU's, EFU's and SVU's

The Figure 5-28 complies three geophysical hillslope models together in terms of ERT (the upper diagram), VES (the middle diagram) and RS (the below diagram) subsurface models. How we can observe these diagrams, the VES subsurface model implies the deepest layer boundary characterising by the increased resistivity values (270 Ωm) in contrast to the previous layer. We can associate this layer with the compact or fresh bedrock. ERT and RS could not resolve this deepest interface due to the poor

medium contrast in the depth, the applied small profile line and the strong water saturated below subsurface. Nevertheless, we believe that fresh bedrock locates in the relatively large depth. To prove this assumption, we have to conduct the future measurements during the dry state. Moreover, we want to prove the model structure representing the three-layers at the upper and middle slope profile, which we predicated in the Figure 5-24 as the three-layer model with relatively thin upper layer. For it, we used the VSP techniques. The Figure D - 2 in the Appendix illustrates the one-dimensional VSP models for the shot point locating at the profile meters of 1 m (the upper diagram) and 48 m (the below diagram). Both models predicate three layer. The upper layer with the seismic velocity values of ca. 375 m/s reaches the depth of ca. 1.5 m. The below layer with seismic velocity values of ca. 775 m/s predicates the next interface at the depth of ca. 8 m implying the seismic velocity of ca. 1750 m/s. However, these VSP models confirm the three-layer model resulting by the ray tracing modelling.

Moreover, we could identified the significant hillslope areas (EFU's) from geo-electrical data as well as from refraction seismic data. These EFU's complement well one other. The homogeneous EFU 2 with low resistivity values (130 Ωm) and relatively high velocity values (800 m/s) represents the wetlands and the below slope. Whereas the relatively heterogeneous EFU 2 with the higher resistivity values (350 - 450 Ωm) and low velocity values (615 m/s) represents the upper and middle slope.

5.4 Joint three-dimensional interpretation of the investigated hillslope

In this chapter, we will demonstrate the investigated hillslope at both study sites in the three-dimensional image, in order to prove the success of the system-oriented geophysical approach. We created the three-dimensional view using only two profiles. One profile characterize the hillslope parallel to the slope inclination, whereas the other profile is perpendicular to the first profile and separates the first profile approximately in the middle.

5.4.1 Application in the Weierbach catchment

The Figure 5-29 illustrates the combined geophysical model in terms of ERT-, VES- and RS-models of the profile parallel to the hillslope inclination. The detailed description to this profile subsurface model, we already presented in the chapters 5.1.1, 5.2.1 and 5.3.1 because this profile is the representative hillslope profile for the system-oriented geophysical approach according to the measuring design in the Figure 4-1 and plays the important role for the hydrological modelling. Therefore, we kindly refer the reader to the scheduled chapters for the detailed description. Moreover, to verify the hillslope homogeneity perpendicular to the slope inclination, we put the second geophysical profile across the first profile. The Figure 5-29 also shows the crossing point of the second profile locating at the 50-profile meter of the representative hillslope profile.

Up to now, let us demonstrate and interpret the results of the second geophysical profile. The Figure 5-30 shows the RS subsurface model for the second geophysical profile. We also marked the crossing point of the first profile locating at the 48-profile meter. We developed this RS model using the

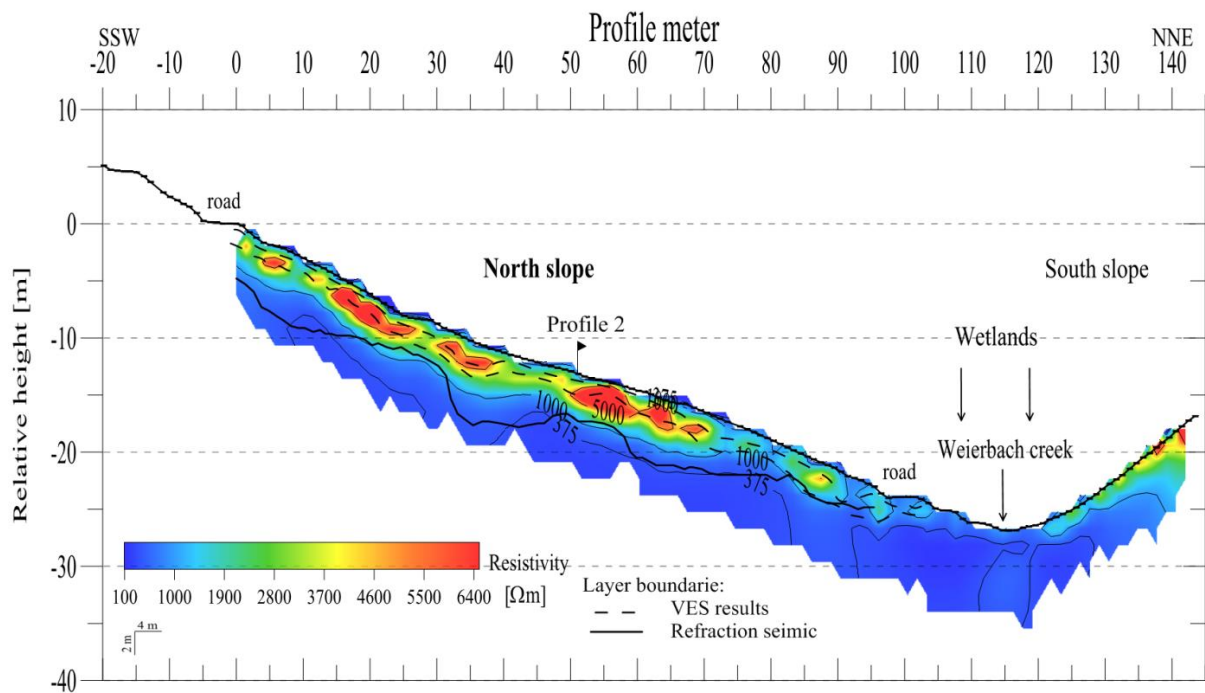


Figure 5-29: The case study of the Weierbach catchment: The transparent comparison of layer interfaces between ERT, VES and RS of the hillslope profile parallel to the slope inclination

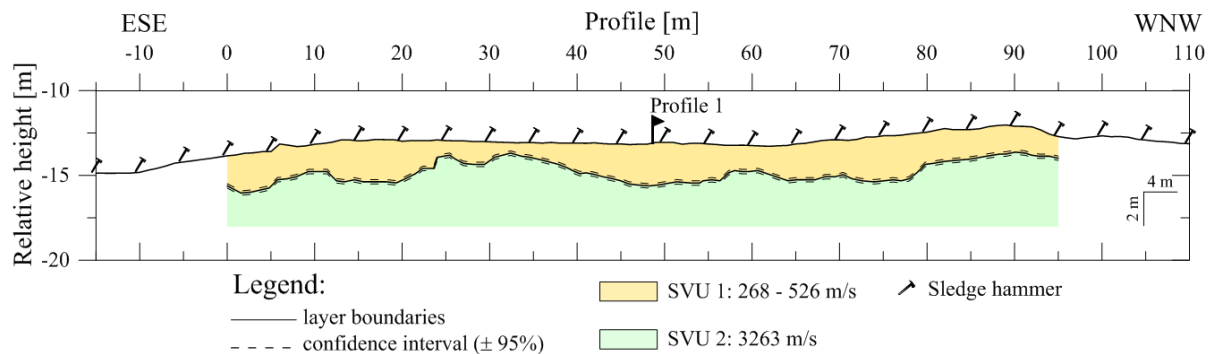


Figure 5-30: The case study of the Weierbach catchment: The refraction seismic model of the second geophysical profile perpendicular to the hillslope inclination in terms of SVU's

ray tracing FD modelling. The surface topography of this profile implies a slight inclination decreasing from WNW- to ESE-direction. The profile reveals a two-layer composition with high contrast and nearby horizontal layering. The relatively variable low seismic velocity values (268 - 526 m/s) characterize the upper layer, which reaches the depth of ca. 2.5 - 3 m. The below refracting layer implies the seismic velocity values of 3262 m/s. The slight variable topography characterizes the refracting interface causing probably through the orientation schist blocs. Moreover, we want to compare the RS subsurface model with resistivity models resulting from ERT and VES. The upper diagram of the Figure 5-31 illustrates the combined geophysical model in terms of ERT-, VES- and RS-models of the second geophysical

5 Results and discussions

profile. The two layers compose the two-dimensional ERT image. The high resistivity values ranging from 2800 Ωm to 5000 Ωm characterize the upper layer, which reaches a depth of ca. 3.5 m, after which the resistivity values decrease rapidly. The bottom layer implies the low resistivity values of ca. 375 Ωm . We can recognize the sharp contrast between high resistivity layer and low resistivity layer illustrating through the resistivity iso-line of the 1000 Ωm . If we compare visual this resistivity iso-line with the

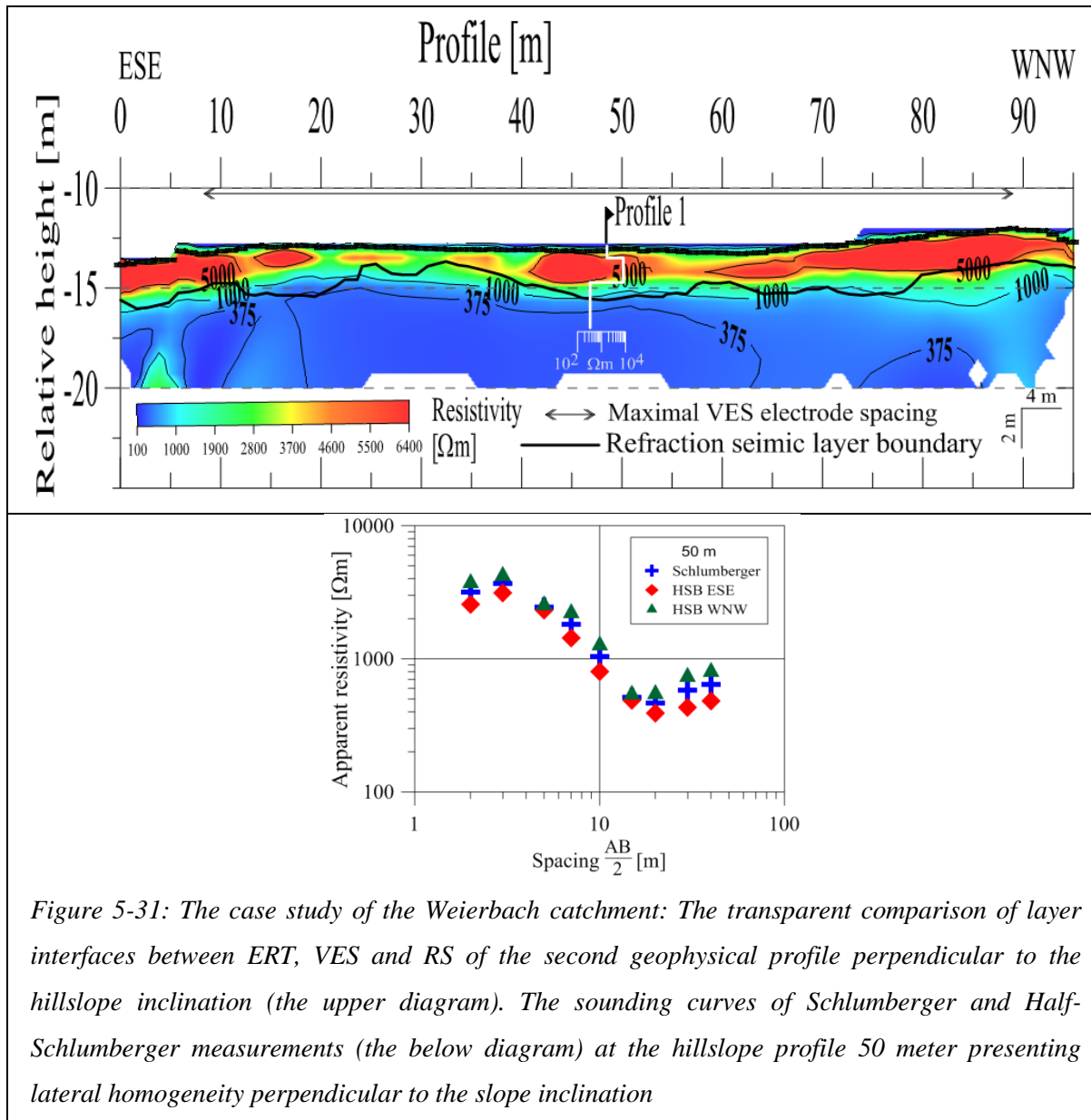


Figure 5-31: The case study of the Weierbach catchment: The transparent comparison of layer interfaces between ERT, VES and RS of the second geophysical profile perpendicular to the hillslope inclination (the upper diagram). The sounding curves of Schlumberger and Half-Schlumberger measurements (the below diagram) at the hillslope profile 50 meter presenting lateral homogeneity perpendicular to the slope inclination

seismic refractor (the black bold line), we will find that both boundaries correlate well with each other. The resistivity 1000 Ωm -iso-line describes nearby the same form as the refractor. Therefore, ERT subsurface model also describe the homogeneous and nearby horizontal layers. Furthermore, we want to analyse the result correctness through the VES measurements collecting at the 50-profile meter parallel to the hillslope inclination. The below diagram of the Figure 5-31 demonstrates the results of the VES measurements indicating the correctness of the equation (4-4) and the assumption on the homogeneous

5 Results and discussions

stratified subsurface. The inversion result of the VES measurement shown one-dimensional model (the white line) in the upper diagram of the Figure 5-31 confirms the results of ERT and RS. The one-dimensional model predicates nearby the same depth of the contrasting layer between the upper high resistivity layer (ca. 4000 Ωm) and the bottom low resistivity layer (ca. 350 Ωm). Moreover, the one-dimensional VES model identifies the thin relatively high resistivity layer (ca. 1500 Ωm), which reaches a depth of ca. 0.8 m.

Therefore, the cross profile proves well the success of the system-oriented geophysical approach at the study site Weierbach catchment. All results confirm that the investigated hillslope we can describe as homogeneous and representative hillslope for the considered catchment. However, we can create a three-dimensional subsurface model of the investigated hillslope. The Figure 5-32 demonstrates the three-dimensional subsurface model of the investigated north-facing hillslope in terms of seismic velocity units. The seismic velocity subsurface model indicates the slight anisotropy of the subsurface. The relatively increased velocity values represent the upper layer along the hillslope, whereas relatively decreased velocity values represent the upper layer perpendicular to the slope inclination. The anisotropy also characterizes the upper bedrock (the fractured schist). The increased seismic velocity values characterize the upper bedrock perpendicular to the slope inclination. The hillslope model also includes

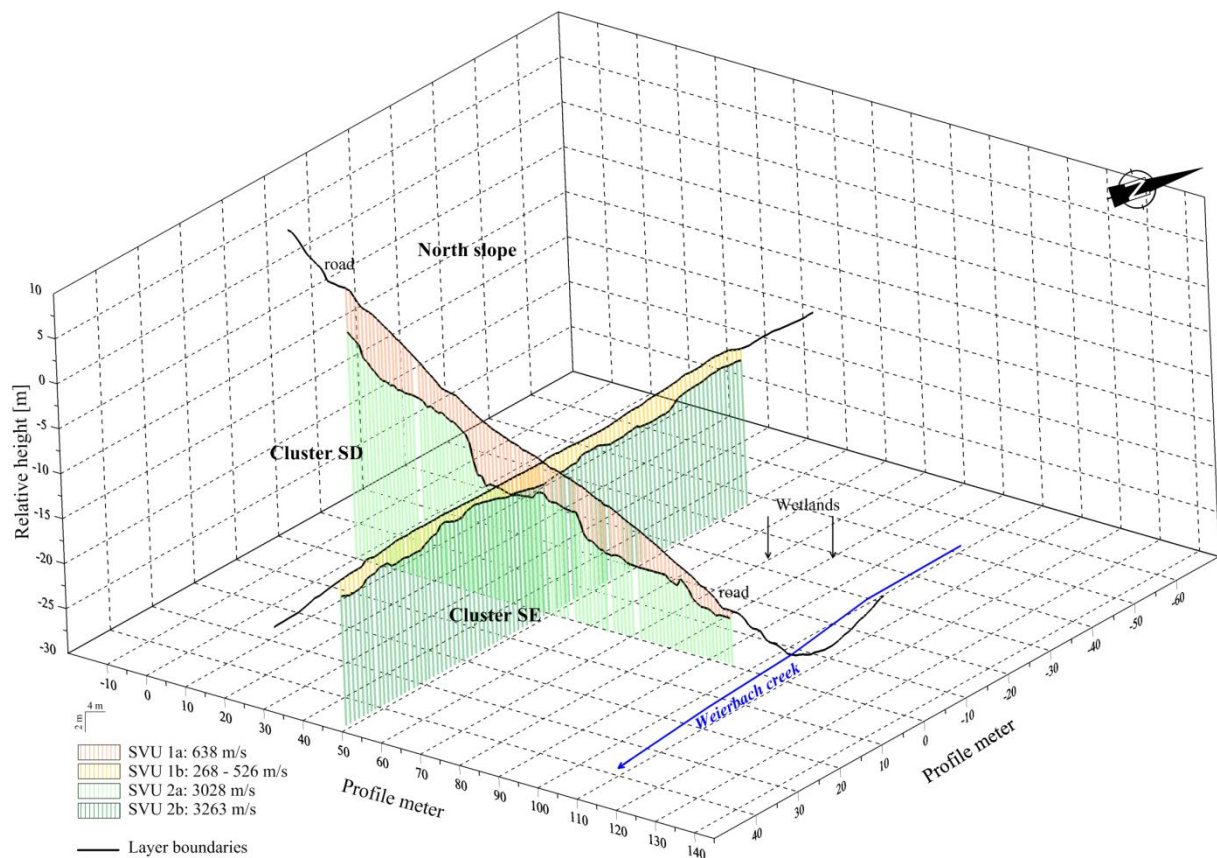


Figure 5-32: The case study of the Weierbach catchment presents the three-dimensional interpretation of the representative hillslope in terms of SVU's

the locations of the installed measurement cluster (marked as SD and SE) at the investigated hillslope.

5.4.2 Application in the Schaeferfetal catchment

The Figure 5-33 demonstrates the combined geophysical model in terms of ERT-, VES- and RS-models of the profile parallel to the hillslope inclination. The detailed description to this profile subsurface model, we already presented in the chapters 5.1.2, 5.2.2 and 5.3.2 because this profile is the representative hillslope profile for the system-oriented geophysical approach according to the measuring design in the Figure 4 1 and plays the important role for the hydrological modelling. Therefore, we kindly refer the reader to the scheduled chapters for the detailed description. Moreover, to verify the hillslope homogeneity perpendicular to the slope inclination, we put the second geophysical profile across the first profile. The Figure 5-33 also shows the crossing point of the second profile locating at the 48-profile meter of the representative hillslope profile.

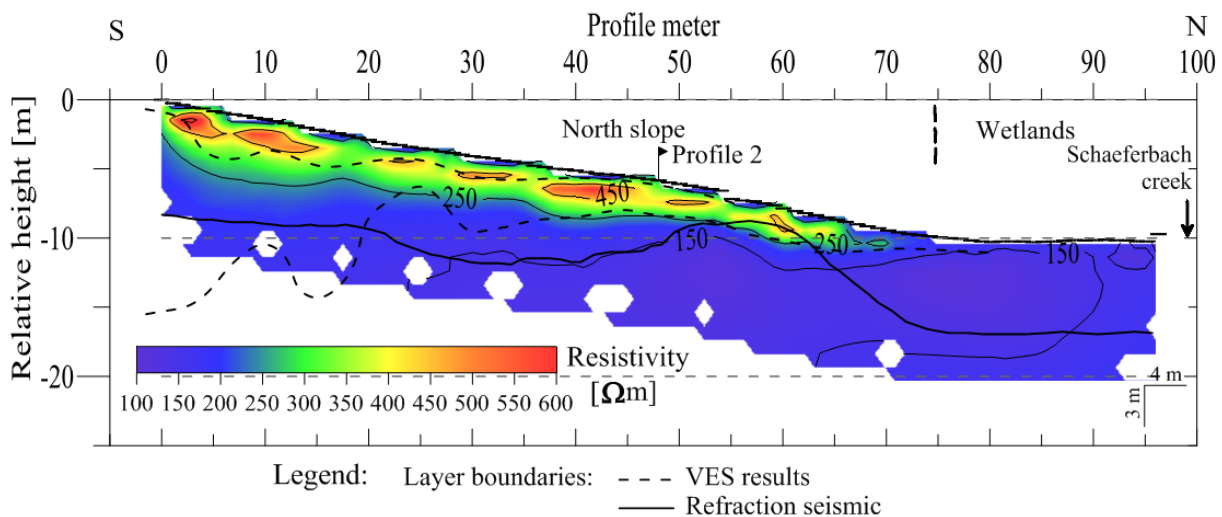


Figure 5-33: The case study of the Schaeferfetal catchment: The transparent comparison of layer interfaces between ERT, VES and RS of the hillslope profile parallel to the slope inclination

Up to now, we will demonstrate and interpret the results of the second geophysical profile. The Figure 5-34 shows the RS subsurface model for the second geophysical profile. We also marked the crossing point of the first profile locating at the 48-profile meter. We developed this RS model using the ray tracing FD modelling. The surface topography of this profile implies a slight inclination decreasing from the West to the East. The height difference between the west site and the east site is ca. 2.5 m. The profile reveals a two-layer composition with the relatively high contrast and nearby horizontal layering. The low seismic velocity values (270 m/s) characterize the upper layer, which reaches the depth of ca. 2.5 – 3.5 m. The below refracting layer implies the seismic velocity values of 1784 m/s. The slight variable topography characterizes the refracting layer. Moreover, we want to compare the RS subsurface model with resistivity models resulting from ERT and VES. The upper diagram of the Figure 5-35 illustrates the combined geophysical model in terms of ERT-, VES- and RS-models of the second

5 Results and discussions

geophysical profile. The two layers compose the two-dimensional ERT image. The high resistivity values ranging from 300 Ωm to 400 Ωm characterize the upper layer, which reaches a depth of ca. 3 m, after which the resistivity values decrease gradually. The several patterns of the upper layer imply the relatively high resistivity features (450- 550 Ωm) in the depth of ca. 1 - 2 m. Moreover, the low resistivity values ranging from 150 Ωm to 200 Ωm characterize the bottom layer. We can recognize the sharp

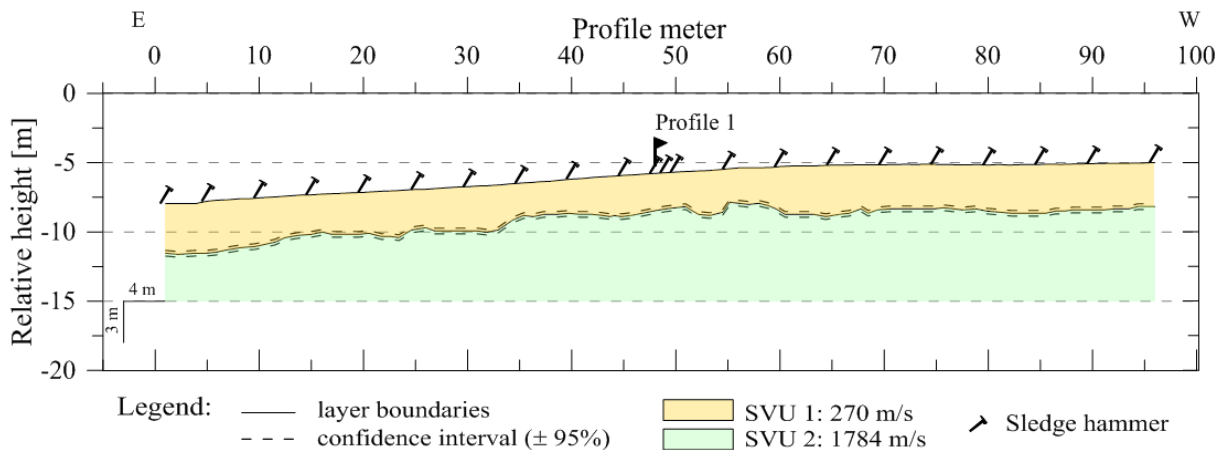


Figure 5-34: The case study of the Schaefertal catchment: The refraction seismic model of the second geophysical profile perpendicular to the hillslope inclination in terms of SVU's

contrast between high resistivity layer and low resistivity layer illustrating through the resistivity iso-line of ca. 250 Ωm . If we compare visual this resistivity iso-line with the seismic refractor (the black bold line), we will find that both boundaries correlate well with each other. The resistivity 250 Ωm iso-line reflects nearby the same form as the refractor. Therefore, ERT subsurface model also describe the homogeneous and nearby horizontal layers. We can associate the low resistivity bottom layer with the good conductive layer. The refractor and the resistivity iso-line of 250 Ωm represent the same inclination as the surface topography from the West to the East direction. We can associate this subsurface area with the possible subsurface flow from the West to the East. The date of the groundwater level presenting in the Figure 3-4 confirm the flow direction. We suspect that the subsurface flow occurs parallel to the slope inclination as well as perpendicular to the slope inclination during the wet state. The TERENO soil moisture hillslope has a giving connection with our investigated representative hillslope. This fact confirms the interaction between the neighbour landscape units.

Furthermore, we want to analyse the result correctness through the VES measurements collecting at the 50-profile meter parallel to the hillslope inclination. The below diagram of the Figure 5-35 demonstrates the results of the VES measurements indicating the small differences between sounding curves at the first 5 meter of electrode half spacing, but at the large electrode spacing it proves the correctness of the equation (4-4) and the assumption on the homogeneous stratified subsurface. Therefore, the small differences between sounding curves indicate the shallow heterogeneity at the depth from 0.8 m to 2 m, whereas the deeper layer seems to be as homogeneous. The inversion result of the

5 Results and discussions

VES measurement shown one-dimensional model (the white line) in the upper diagram of Figure 5-35 confirms the results of ERT and RS. The one-dimensional model predicates nearby the same depth of the contrasting layer between the upper high resistivity layer (ca. 350 Ωm) and the bottom low resistivity layer (ca. 130 Ωm). Moreover, the one-dimensional VES model identifies the thin relatively low resistivity layer (ca. 150 Ωm), which reaches a depth of ca. 0.5 m. However, the near surface heterogeneity of VES measurements confirm the resistivity variability of ERT measurements from the surface to the depth of ca. 0.8 - 2 m.

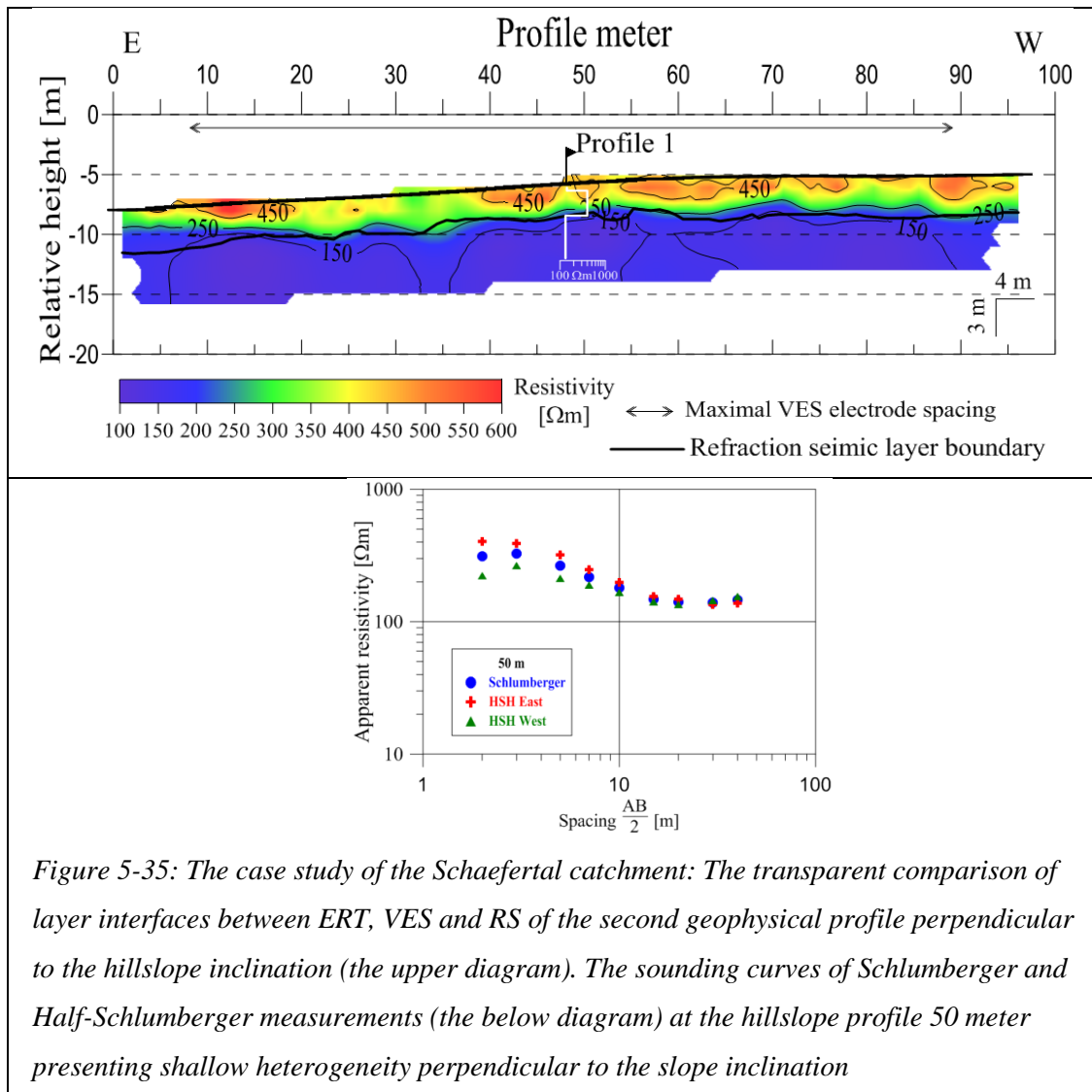


Figure 5-35: The case study of the Schaeferal catchment: The transparent comparison of layer interfaces between ERT, VES and RS of the second geophysical profile perpendicular to the hillslope inclination (the upper diagram). The sounding curves of Schlumberger and Half-Schlumberger measurements (the below diagram) at the hillslope profile 50 meter presenting shallow heterogeneity perpendicular to the slope inclination

Therefore, the cross profile proves well the success of the system-oriented geophysical approach at the study site Schaeferal catchment. All results confirm that the investigated hillslope we can describe as homogeneous and representative hillslope for the considered catchment. However, we can create a three-dimensional subsurface model of the investigated hillslope. The Figure 5-36 demonstrates the three-dimensional subsurface model of the investigated north-facing hillslope in terms of seismic velocity units. The seismic velocity subsurface model indicates the slight anisotropy of the subsurface in

5 Results and discussions

the upper layer. The relatively increased velocity values represent the upper layer along the hillslope, whereas relatively decreased velocity values represent the upper layer perpendicular to the slope inclination. The below layer with increased velocity values seems to be nearby isotropic.

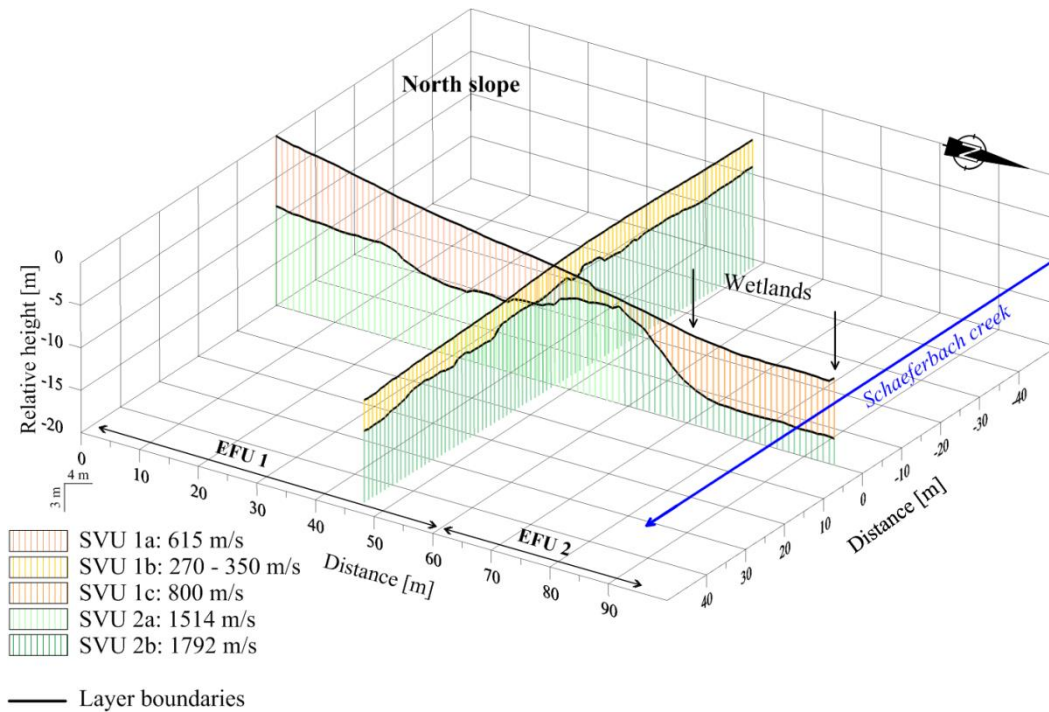


Figure 5-36: The case study of the Schaeferfartl catchment presents three-dimensional interpretation of the representative hillslope in terms of SVU's

* * *

To conclude this chapter, we note that the using of the different geophysical interpretation techniques requires the different opinions to develop a true geological subsurface model (Hoyer , et al. 2015). The differences of the different geophysical models provide a given degree of the real geological model. However, the combination of geophysical interpretation techniques requiring by the minimal geological background knowledge can provide a true geological situation of the investigated area. Moreover, the geophysical model ambiguity can help to understand the nature of geophysical data and to provide additional knowledge on the investigated area. Therefore, in order to obtain detailed knowledge, we have more to learn from the uncertainty!

6 Discussions of the design of the hydrogeological conceptual model

The good results presenting in the chapter 5 at the two-study site permit also to discuss the advantages of the suggested approach, in order to characterize a catchment as an organized system in terms of representative units, and to start a dialogue with hydrologists and other scientist dealing with catchment characterization. To develop this dialogue, we have to provide a conceptual hydro-geophysical model, which offers detailed knowledge, in order to improve our understanding of the subsurface processes at the hillslope scale. A conceptual model can help to calculate a numeric model. Due to the complex hydrogeological systems, the numeric model cannot characterize numerous aspects without the considering of the conceptual model.

Currently, it exists the various definition of conceptual models. A hydrogeological conceptual model usually describes a qualitative and pictorial conception of the groundwater systems consisting of the hydrogeological units, the system boundaries, inputs/outputs, and the description of the lithology and properties (Meyer and Gee 1999). Moreover, based on the priori information taking from literature, soil sampling or core drilling, a conceptual hydrogeological model must link field observations with theoretical model, in order to interpret the site observation and to predict quantitative the future conditions of the observed site (Meyer and Gee 1999). Besides, the hydrogeological conceptual model hypothesis the main components and the relation between these components, which characterize the observed study site. The conceptual model also can improve the preliminary theoretical model by input of obtained observed data. The conceptual hydrogeological model generally includes such zones as near-surface zone, unsaturated zone, saturated zone and the upper bedrock. However, in order to develop a meaningful hydrogeological conceptual model, it needs a good work together between experimenters and modellers. The joint observations of geologists, geophysicists and hydrologists result the expressive hydrogeological conceptual model.

So far, the proposed system-oriented geophysical approach investigates a catchment system in terms of representative landscape units, which link different landscape elements with each other. The fundamental landscape unit is a hillslope because it manages the water balance in the catchment and links different units such as plateau, slopes, riparian zone and stream channel with each other. The geophysical investigations are parallel to the slope inclination using only one profile (see the measuring design in the Figure 4-1 and the methodology description in the chapter 4), to collect the resistivity (ERT and VES) and refraction seismic data. Moreover, the geophysical uncertainty provide possibilities better to understand the nature of geophysical data. The geo-models of the investigated subsurface interpreted with different techniques construct the conceptual hydro-geological model based on the hydrogeological knowledge from previous literature sources.

To compile the developed geophysical subsurface models to the representative conceptual hydrogeological model, we defined the model functionality. This model should interpret the hillslope

system in terms of the hydro-stratigraphic units and system boundaries describing high and low hydraulic conductive zones. The starting point for the model construction is the collection of the geophysical model in terms of system boundaries and geophysical values (electrical resistivity and seismic velocity) obtained by resistivity and refraction seismic surveys. Besides, we made several assumptions. The model body should describe the two-dimensional profile with the exact measured surface topography including micro-topography. Moreover, the subsurface lithological parameters imply the homogeneous stratified subsurface, the fixed physical layer boundaries, the effective geophysical subsurface values, and the upper permeable bedrock underlying by impermeable bedrock. In addition, the uniform hydraulic parameters, the dominance of the subsurface flow, streamlines parallel to the permeable bedrock, and the connection between the hillslope and the creek should characterize the conceptual hydrogeological model. After making all assumptions, we considered the collected geophysical models and the available lithological knowledge from the previous studies of (Martinez-Carreras, et al. 2010, Juilleret, et al. 2011 for the Weierbach catchment; Altermann 1989, Martini, et al. 2014 for the Schaeftal catchment), in order to define the physical situation and the model design objective.

Therefore, based on the resulted geophysical subsurface models demonstrated in the chapter 5 and on the lithological-geological background introduced in the chapter 3, we created the conceptual hydrogeological models describing representative hillslope at the study site Weierbach and Schaeftal. The Figure 6-1 and the Table 6-1 describe the conceptual hydrogeological model for the study case of the Weierbach. Whereas the Figure 6-2 and the Table 6-2 characterize the conceptual hydrogeological model for the study case of the Schaeftal. The excellent results of the Weierbach permit to combine the resistivity models as well as the seismic models, in order to generate the conceptual hydrogeological model. In contrast to it, we interpreted the conceptual hydrogeological model of the Schaeftal based on the structure model obtained from VES data, because the seismic models imply many ambiguities in the data interpretation. Both models describe the lithological discontinuities of PPSD's and bedrock. The Figure 6-1 and Figure 6-2 reflect that the fresh bedrock locates in the large depth, where the medium contrast is significant poor. From this point, we believe that the bedrock influence on the subsurface flow is negligible. Nevertheless, the structure of PPSD's impacts on the hydrological processes significant. Many studies confirm this fact (Juilleret, et al. 2011). However, we delineated the PPSD's structure in terms of the upper periglacial layer (UPL) and the basal periglacial layer (BPL) in each study case. The upper periglacial layer implies relatively high resistivity values, lower seismic velocity values and less thickness (ca. 1 - 2 m). Whereas, the basal periglacial layer indicates decreased resistivity values and intermediate seismic velocity values. Moreover, in the case of the Weierbach, we identify the transition layer between UPL and bottom BPL with significant high resistivity values (more than 5000 Ωm). We called this zone as the upper BPL. We assume that this zone contents the periglacial debris filled by the air functioned as a dielectric. Besides, the UPL of the Schaeftal hillslope exists only at the upper and middle slope, and does not present in the wetlands, because the wetlands seem to be consistent water saturated during the wet state. The relevant subsurface flows occur in the relatively low resistant BPL on

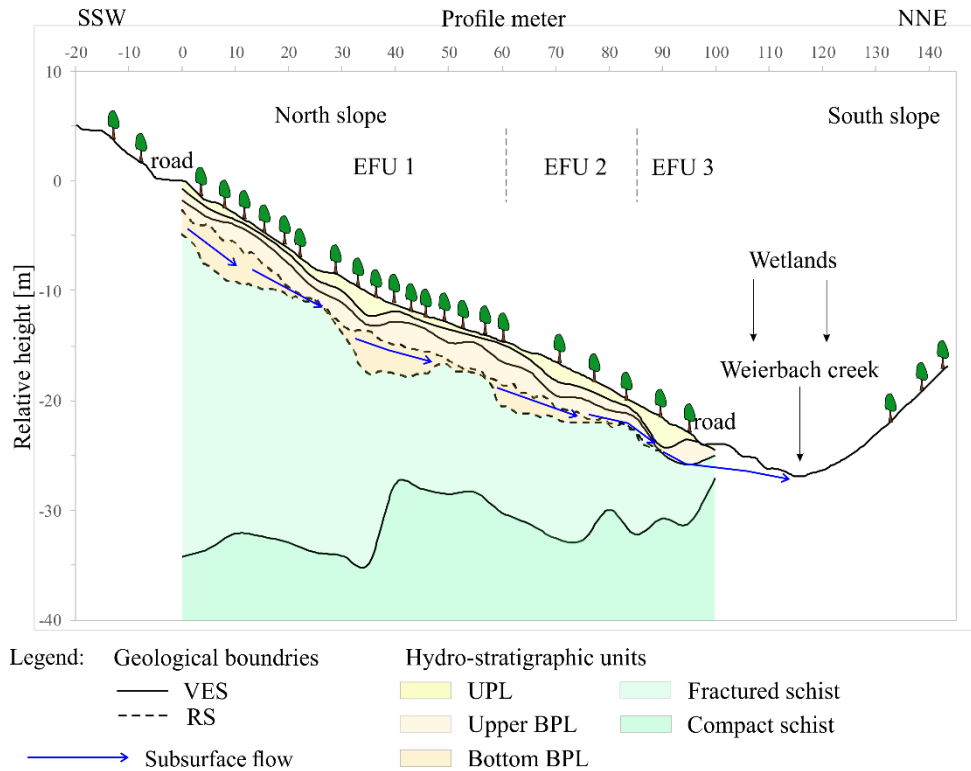


Figure 6-1: The conceptual hydro-geological model of the representative north-facing hillslope locating in the Weierbach catchment

Table 6-1: Description of the conceptual hydro-geological model for the case study the Weierbach catchment (see the Figure 6-1)

Hydro-stratigraphic unit	Description
Upper periglacial layer (UPL)	Relatively high resistivity values (ca. 1730 Ωm) and variable lower seismic velocity values (ca. 450 m/s). Loamy soils with many tree roots and fragments of schist stones. Good drainage zone.
Upper part of basal periglacial layer (Upper BPL)	Transition zone between UPL and bottom BPL characterised by extremal high resistivity values (more than 6000 Ωm) and intermediate seismic velocity values (638 m/s). Probably, it contents of periglacial debris as well as tree root network. Excellent drainage zone.
Bottom part of basal periglacial layer (Bottom BPL)	Transition zone between high resistant upper layer and low resistant (330 Ωm) below layer with intermediate seismic velocity values (638 m/s). Debris of the schist. Subsurface flows may occur.
Fractured schist	Low resistivity values (330 Ωm) and high seismic velocity values (3028 m/s). The upper bedrock may store significant amounts of water.
Compact schist	Increased resistivity values (500 – 1000 Ωm) and seismic velocity values (ca. 4000 m/s). The poor contrast in the depth.

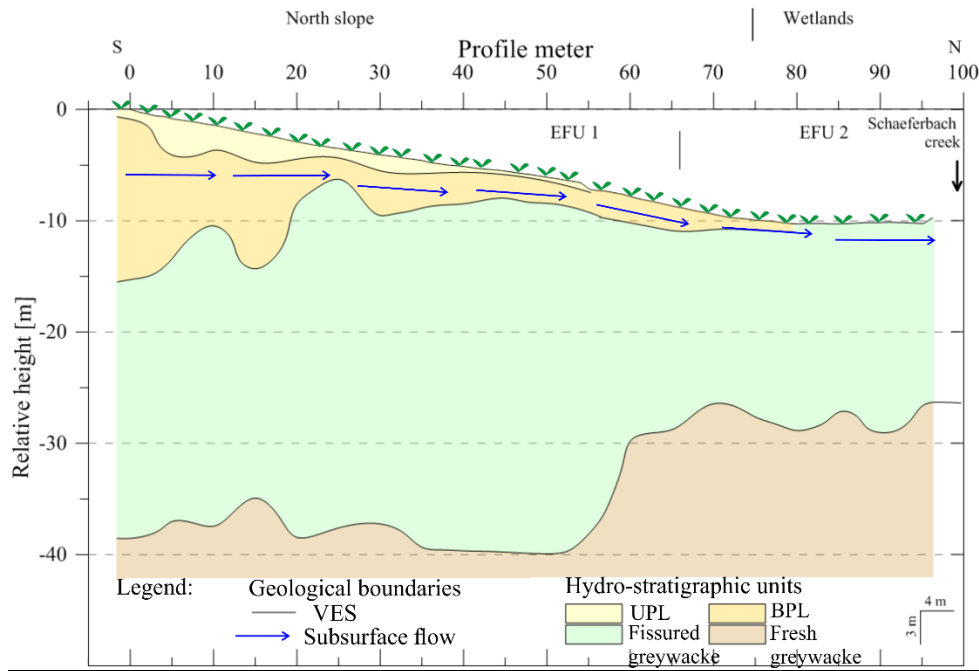


Figure 6-2: The conceptual hydro-geological model of the representative north-facing hillslope locating in the Schaeferfetal catchment for the wet state

Table 6-2: Description of the conceptual hydro-geological model for the case study the Schaeferfetal catchment (see the Figure 6-2)

Hydro-stratigraphic unit	Description
Upper periglacial layer (UPL)	High resistivity values (460 Ω m) and low seismic velocity values (383 m/s) characterize less permeable fine soil with rock waste and fragments by mountain loam. It also contents of the plant root network. A good drainage zone during the wet state.
Basal periglacial layer (BPL)	Decreased resistivity values (300 Ω m) and intermediate seismic velocity values (750 m/s). It contents of debris of the greywacke. Subsurface flows may occur.
Fissured greywacke	Low resistivity values (130 Ω m) and high seismic velocity values (from 1514 m/s to 1792 m7s) characterize the fissured bedrock. It can store significant amount of water.
Compact greywacke	Increased resistivity values (270 Ω m) characterize fresh bedrock. The deeper location of the fresh bedrock. The poor contrast in the depth.

the top of fractured bedrock. The fractured upper bedrock may store significant amount of water. Besides, the distinguished EFU's can represent the energetic levels in terms of states.

We also have to note that the conceptual hydrogeological model of the Weierbach hillslope can be representative for the whole year without considering of the seasonal changes, whereas the obtained Schaeferfetal model represents the conceptual hydrogeological model for the wet state. Therefore, to complete the geophysical interpretation at the Schaeferfetal hillslope, the additional measurements need to conduct during the dry state. Probably, we will obtain a clear structure of the near surface in the wetlands.

According to (Anderson and Woessner 1992), our developed conceptual models describe hydrostratigraphic units and system boundaries as well as subsurface flow. However, we believe that the developed hydrogeological models provide a detailed content from geophysical and geological perspectives, in order to test hydrological models for the making the various scenarios and for the prediction of hydrological processes. The models also can help to understand the behaviour of the hydrological systems. The conceptual hydrogeological models represent the results at the local-scale investigation performed at representative sites. Nevertheless, there is still a need the knowledge from other disciplines, especial hydrology (data of groundwater level), in order to demonstrate the groundwater level in the model and its correlation with saturated zone.

7 Conclusion

In conclusions, we summarize the points learning during the research in the multi-disciplinary project CAOS. At the first, such project assumes a good collaboration between different discipline partners. Then, to study the investigated area in the efficient manner and system-oriented, we recommend to consider the nature system as a set of the representative functional units assuming the interaction between the neighbour-units. Moreover, a hillslope represents a fundamental landscape element in the catchment structure. We can transfer the one set of dimensions from the representative hillslope to other hillslopes implying a similar set of dimensions using the similarity index or the hillslope Péclet number.

The catchment system is open thermodynamic system characterizing by many possibilities of indeterminate variables to find wanted hydrological conditions for maximum probability by minimum work. The entropy concept is a good approach to describe the catchment system in terms of states and representative functional units. Moreover, we can take into account other perspectives such as catchment as complex dynamic systems, self-organising systems, co-evolving systems and catchment similarity, which can help understand the catchment system under change.

To recognize the representative homogeneous hillslopes in the catchment and to link geophysics and hydrology, we defined the following key words such as uniform stratified subsurface, topography, wetness, the specific hydrological response (hydrographs), and the spatial scale of the observation from geophysical perspective assuming hydrological criteria (complexity, functional homogeneity, thresholds and dominance described by Basu, et al. 2010).

Before starting the installation of the hydrological and meteorological devices at the hillslope, we recommend to prove the selected hillslope for the homogeneity and the typical features using the cross test profiling and assuming the introduced key of the representatively and homogeneity. If the making assumptions are not valid, we have to re-select a reference hillslope or to conduct the three-dimensional measurements. According to (Bachmair and Weiler 2013), the hillslopes with the high spatial variability are not the homogeneous responding functional units. Besides, the system-oriented geophysical approach (SOGA) assumes the homogeneous, horizontal stratified subsurface and the coupling between the petro-physical parameters (in our case electrical and seismic).

Moreover, the approach designates lateral as well as vertical stratigraphic geophysical units in terms of EFU's, ESU's and SVU's. We believe that these units can control hydrological processes and represent energetic levels, which we can consider in a multi-disciplinary integrated analysis. Such analysis has to improve our understanding of the mechanisms of the complex processes in the subsurface. The approach is quite efficient for the forested investigated areas. Furthermore, an effective geophysical investigation on the hillslope scale, we can provide not only by expensive three-dimensional measurements, but also the use of the one- and two-dimensional measurements can explore in the details the hillslope as a representative landscape unit. However, the geophysical measurements according to

7 Conclusion

the measuring design shown in the Figure 4-1 at only single profile is quite efficient, in order to integrate the geophysical surveys into multi-disciplinary project.

Therefore, the aim of this work was to suggest an effective and cost-efficient approach for the investigation of subsurface structures in a catchment using ERT, VES and RS techniques as well as combined technique. On the other hand, to identify geophysical units that can control hydrological processes. The Table 7-1 summarizes the effectiveness of the applied geophysical techniques as well as the investigated depth. The resistivity and refraction seismic tomography illustrate the distribution patterns of the contrasting lithological units, whereas resistivity sounding and RS wave front reconstruction predict the boundaries of the hydro-stratigraphic units. Moreover, the Figure 7-1 demonstrates the cost-efficiency of the suggested approach. It compares the applied geophysical techniques (RS, ERT and VES) on the measure of horizontal and vertical survey scale achievable in 1 day by three-person field team for the complex accessible terrain at a single profile assuming the constant sensor spacing by 1m. This comparison demonstrates the range achievable during the field works from different geophysical methods at spatial scale as well as temporal sale, which is important to take into account for the choice of the appropriate technique (Binley, et al. 2015). ERT can cover larger profile length by relatively lower time effort, but cannot reach the large depth, in contrast to RS and VES. A bit large time effort by large depth penetration characterizes RS and VES, in contrast to ERT. VES survey can do three measurements at the same time characterizing the hillslope over the width compared to ERT. The penetration depth also depends on the subsurface conditions (medium contrast, especial for RS). To note, the Figure 7-1 demonstrates our subjective estimation of the effort based on the field experiences.

Table 7-1: The applied geophysical techniques to develop the system-oriented geophysical approach

Method	Effectiveness	Interpretation technique	Investigated depth
VES	The exact depth predication of contrasted electrical interfaces	Four-electrode system to develop the 1D-models	from 0.8 m to 16 m
ERT	The illustration of the patterns of saturated and dry subsurface zones	Multi-switch system for the imaging of the 2D-section	from 0.3 m to 10 m
RS	The predication of the weathered bed rock boundary and linking to the geotechnical parameters	Seismic tomography, wave front reconstruction using PMM and ray tracing to illustrate the 2D-section	10 -20 m, the strong dependence on contrast

7 Conclusion

We tested the suggested approach at the two study sites characterizing by Pleistocene periglacial slopes deposits and different environmental conditions such as land use, slope inclination. The investigations at the different hillslopes demonstrate that we can learn many facts from geophysical ambiguity, in order to develop a hydro-geological conceptual model based on the structural comparison of the geo-models and the differences in the interpretation techniques. The different geo-models reflect a given degree of the ambiguity. The combination of different geo-models can eliminate the model uncertainty and provide more or less realistic subsurface model. We identified for each representative hillslope the hydro-stratigraphic units and contrasting boundaries. We also could predicate the possible flow paths in the subsurface. The developed models are consistent with physical laws and lithological-geological background, and provide physical boundaries and values of the subsurface, in order to parametrize the hydrological models and to develop the hydrogeological conceptual model.

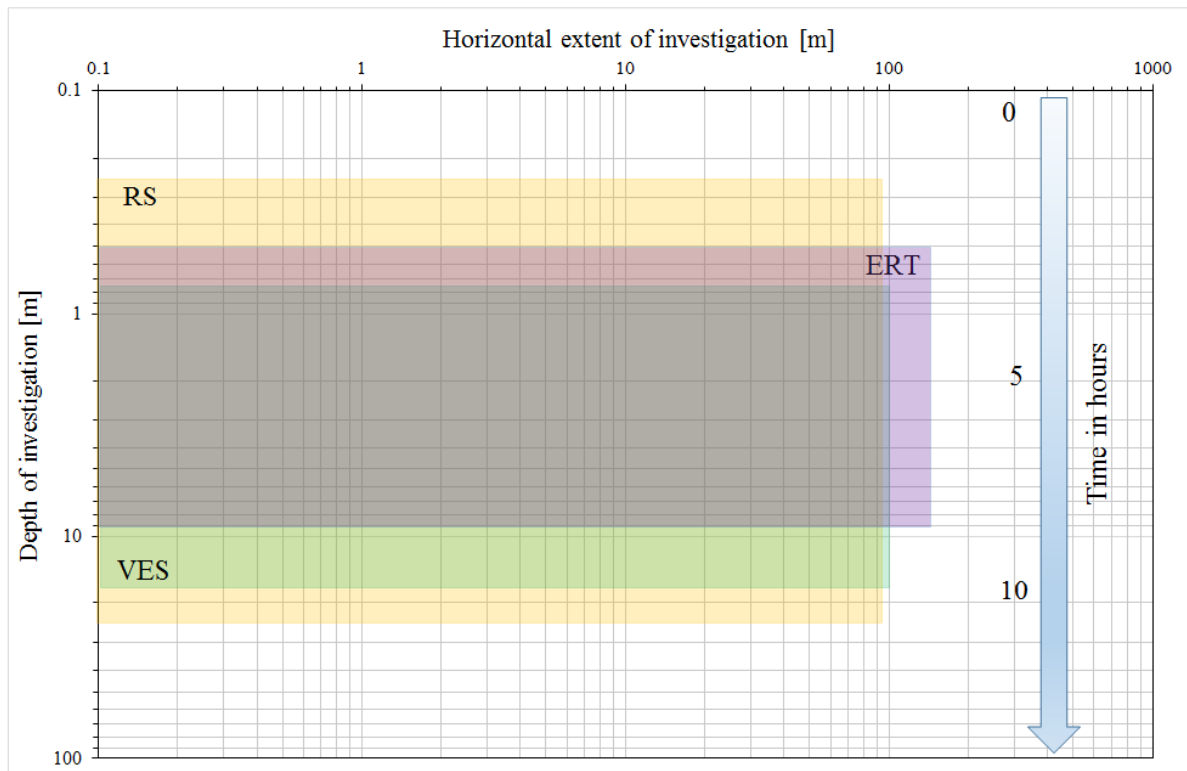


Figure 7-1: Comparison of horizontal and vertical survey scales achievable in 1 day by three-person field team for RS, ERT and VES demonstrates time effort in hours for the complex accessible terrain (like forest with changeable topography) using a single profile

Hence, the suggested approach systematises the catchment system in terms of representative landscape units and can provide a robust platform for understanding and modelling hydrological systems allowing flexible hypotheses and model testing. Our research shows that it is necessary to develop interdisciplinary and international programs, in order to describe complex nature systems. Besides, suggested results assume the importance of performing cost effective geophysical investigation, in order

7 Conclusion

to explore the nature systems at the large landscape scale. Hence, (Binley, et al. 2015) thinks that the use of landscape elements at the representative local sites can capture the landscape heterogeneity. Concluded, (Robinson, et al. 2008) and (Binley, et al. 2015) explain that geophysical investigation has a growing interest in hydrology now and in the future, in order to investigate subsurface patterns at the large-landscape scale and to monitor the processes connected with the temporal changes.

In the future, the system-oriented approach considered in this monograph will be improved and adapted for the studying the dune landscapes and structures locating along the seacoast boundary. The understanding of the dune landscape has the large importance due to the sensible character of such system, which suffer from nature actions as well as human activity.

Bibliography

- Al-Sadi, Hamid N. 1980. *Seismic Exploration: Technique and Processing*. Basel: Birkhäuser Verlag.
- Altermann, Manfred. 1989. *Pedologisch-hydrologische Kennzeichnung landwirtschaftlich genutzter Standorte des Unterharzes*. Leipzig: Abhandlung der Saechsischen Akademie der Wissenschaften zu Leipzig.
- Anderson, M.P., and W.W. Woessner. 1992. *Applied groundwater modelling: simulation of flow and advective transport*. San-Diego: Academic Press.
- Ashby, W.R. 1962. *Principles of the self-organising system, in Principles of Self-Organization: Transactions of the University of Illinois Symposium, edited by Von Foerster H. and Zopf Jr. G. W.* London, UK: Pergamon Press, 255-275.
- Atzemoglou, A., and P. Tsourlos. 2012. "2D interpretation of vertical electrical soundings: application to the Sarantaporon basin (Thessaly, Greece)." *Journal of Geophysics and Engineering* 9 50-59.
- Bachmair, S., M. Weiler, and A. Troch. 2012. "Intercomparing hillslope hydrological dynamics: Spatio-temporal variability and vegetation cover effects." *Water Resources Research, Vol. 48, W05537* 1-18.
- Bachmair, Sophie, and Markus Weiler. 2013. "Interactions and connectivity between runoff generation processes of different spatial scales." *Hydrological processes* 1-15.
- Barker, R. 1992. "A simple algorithm for electrical imaging of the subsurface." *First Break* 10 53-62.
- Basu, Nandita B., P.S. Rao, H. Winzeler, Sanjiv Kumar, Phillip Owens, and Venkatesh Merwade. 2010. "Parsimonious modelling of hydrologic responses in engineered watersheds: Structural heterogeneity versus functional homogeneity." *Water Resources Research, Vol. 46, W04501* 1-16.
- Becker, Alfred, and Jeffrey J. McDonnell. 1998. "Topographical and ecological controls of runoff generation and lateral flows in mountain catchments." *Hydrology, Water Resources and Ecology in Headwaters* 199-206.
- Bedrosian, P.A., N. Maercklin, U. Weckmann, Y. Bartov, T. Ryberg, and O. Ritter. 2007. "Lithology-derived structure classification from the joint interpretation of magnetotelluric and seismic models." *Geophysical Journal International, 170* 737 - 748.
- Befus, K.M. 2008. *Applied geophysical characterization of the shallow subsurface: Towards quantifying recent landscape evolution and current processes in the Boulder creek watershed, CO. Master thesis*. Colorado: University of Colorado, Department of Geological Sciences.
- Befus, K.M., A.F. Sheehan, M. Leopold, S.P. Anderson, and R.S. Anderson. 2011. "Seismic Constraints on Critical Zone Architecture, Boulder Creek Watershed, Front Range, Colorado." *Vadose Zone Journal, Vol. 10* 915-927.

Bibliography

- Berne, A., R. Uijlenhoet, and P.A. Troch. 2005. "Similarity analysis of subsurface flow response of hillslopes with complex geometry." *Water Resources Research*, Vol. 41, W09410, doi:10.1029/2004WR003629 1-10.
- Beven, Keith. 2004. "Robert E.Horton's perceptual model of infiltration processes." *Hydrological processes* 18 3447-3460.
- Beven, Keith, and Jim Freer. 2001. "A dynamic Topmodel." *Hydrological processes* 15 1993-2011.
- Binley, Andrew, Susan S. Hubbard, Johan A. Huisman, André Revil, David A. Robinson, Kamini Singha, and Lee D. Slater. 2015. "The emergence of hydrogeophysics for improved understanding of subsurface processes over multiple scales." *Water Resources Research, Special Section: The 50th Anniversary of Water Resources Research* 1-30.
- Biot, M.A. 1956-1. "Theory of Propagation of Elastic Waves in a Fluid-Saturated Porous Solid. I. Low-Frequency Range." *The Journal of the Acoustical Society of America*, Vol. 28, No. 2, March 168-178.
- Biot, M.A. 1956-2. "Theory of Propagation of Elastic Waves in a Fluid-Saturated Porous Solid. II. Higher Frequency Range." *The Journal of the Acoustical Society of America*, Vol. 28, No. 2, March 179-191.
- Bissinger, V., and O. Kolditz. 2008. "Helmholtz Interdisciplinary Graduate School for Environmental Research (HIGRADE)." 71-73.
- Blöschl, Günter, Hans Thybo, and HUbert Savenije. 2015. *A Voyage through scales. The Earth system in space and time*. Austria: Lammerhuber.
- Brown, G.O. 2002. "Henry Darcy and the making of a law." *Water Resources Research*, Vol. 38, No.7, 1106 1-12.
- Budyko, M.I. 1974. *Climate and Life*. New York: Academic.
- Cardarelli, E., M. Cercato, and G.De Donno. 2014. "Characterization of an earth-filled dam through the combined use of electrical resistivity tomography, P- and SH-wave seismic tomography and surface wave data." *Journal of Applied Geophysics* 106 87-95.
- Caris, J.P.T., and Th. W. J Van Asch. 1991. "Geophysical, geotechnical and hydrological investigations of small landslides in the French Alp." *Engineering Geology*, 31 249-276.
- Castillo, Aldrich, Fabio Castelli, and Dara Entekhabi. 2015. "An Entropy-Based Measure of Hydrologic Complexity and Its Applications." *Water Resources Research, Accepted Article*, doi: 10.1002/2014WR016035, April 1-38.
- Cherkashin, A.K. 2007. "Poly-system studying to develop the theoretical geography." *Geography and nature resources. In Russian* 27.37.
- Clarke, Brian A., and Douglas W. Burbank. 2010. "Bedrock fracturing, threshold hillslopes, and limits to the magnitude of bedrock landslides." *Earth and Planetary Science Letters* 297 577-586.

Bibliography

- Coulouma, G., K. Samyn, G. Grandjean, S. Follain, and P. Lagacherie. 2012. "Combining seismic and electric methods for predicting bedrock depth along a Mediterranean soil toposequence." *Geoderma* 170 39-47.
- Dahlin, Torleif, and Bing Zhou. 2004. "A numerical comparison of 2D resistivity imaging with 10 electrode arrays." *Geophysical Prospecting*, 52 379-398.
- Dijkstra, E.W. 1959. "A note on two problems in connexion with graphs." *Numerical Mathematics*, 1 269-271.
- Dooge, James C.I. 1986. "Looking for hydrologic laws." *Water resources research*, Vol. 22, Nr. 9 46-58.
- Ehret, U., H.V. Gupta, M. Sivapalan, S.V. Weijs, S.J. Schymanski, G. Blöschl, A.N. Gelfan, et al. 2014. "Advancing catchment hydrology to deal with predications under change." *Hydrology and Earth System Sciences*, 18 649-671.
- Fenicia, Fabrizio, Dmitri Kavetski, Hubert H.G. Savenije, Martin P. Clark, Gerrit Schoups, Laurent Pfister, and Jim Freer. 2014. "Catchment properties, function, and conceptual model representation: is there a correspondence?" *Hydrological processes*, 28 2451-2467.
- Flügel, Wolfgang-Albert. 1996. "Hydrological response units (HRU's) as modelling entities for hydrological river basin simulation and their methodological potential for modelling complex environmental processes systems. - Results from the Sieg catchment." *Die Erde*. 127 43-62.
- Forrester, Jay W. 1968. *Principles of Systems, 2nd Edn.* Portland, OR: Productivity Press, 391 pp.
- Francés, Alain P., Maciek W. Lubczynski, Jean Roy , Fernando A.M. Santos, and Mohammad R. Mohammadzadeh Ardecani. 2014. "Hydrogeophysics and remote sensing for the design of hydrogeological conceptual models in hard rocks - Sardón catchment (Spain)." *Journal of Applied Geophysics*, Volume 110, November 63-81.
- Freeze, R. Allan. 1972. „Role of Subsurface Flow in Generating Surface Runoff 2. Upstream Source Areas ." *Water resources research* 1272-1283.
- Freeze, R.A., and M.J. Kirckby. 1978. "Mathematical model of hillslope hydrology." *Hillslope hydrology*, chap. 6 177-225.
- Friedel, Sven. 2003. "Resolution, stability and efficiency of resistivity tomography estimated from a generalized inverse approach." *Geophysical Journal International*, 153 305-316.
- Ghiselin, M.T. 1969. *The Triumph of the Darwinian method.* New York, USA: Dover Publications.
- Glade, Thomas, Patrick Stark, and Richard Dikau. 2005. "Determination of potential landslide shear plane depth using seismic refraction - a case study in Rheinhessen, Germany." *Engineering Geological Environment* 64 151-158.
- Godio, A., and G. Bottino. 2001. "Electrical and electromagnetic investigation for landslide characterisation." *Physics and Chemistry of the Earth, Part C: Solar, Terrestrial & Planetary Science. Volume 26, Issue 9* 705-710.

Bibliography

- Graeff, Thomas, Erwin Zehe, Dominik Reusser, Erika Lück, Boris Schröder, Gerald Wenk, Hermann John, and Axel Bronstert. 2009. "Process identification through rejection of model structures in a mid-mountainous rural catchment: observations of rainfall-runoff response, geophysical conditions and model inter-comparison." *Hydrological processes* 23 702-718.
- Günther, T., L.R. Bentley, and M. Hirsch. 2006. *A new joint inversion algorithm applied to the interpretation of DC resistivity and refraction data*. Hannover: LIAG.
- Günther, Thomas. 2004. *Inversion methods and resolution analysis for the 2D/3D reconstruction of resistivity structures from DC-measurements.(PhD. Thesis)*. Freiberg, Germany: University of Mining and Technology.
- Gyulai, Ákos, and Tamás Ormos. 1999. "A new procedure for the interpretation of VES data: 1.5-D simultaneous inversion method." *Journal of Applied Geophysics* 41 1-17.
- Hack, Robert. 2000. "Geophysics for slope stability." *Surveys in Geophysics*, 21 423-448.
- Hagedoorn, J.G. 1959. "The plus-minus method of interpreting seismic refraction sections." *Geophysical Prospecting* 7 158-181.
- Han, De-hua, and Michael L. Batzle. 2004. "Gassmann's equation and fluid-saturation effects on seismic velocities." *Geophysics, Vol. 69, No.2, March-April* 398-405.
- Hausmann, Jörg, Hannes Steinel, Manuel Kreck, Ulrike Werban, Thomas Vienken, and Peter Dietrich. 2013. "Two-dimensional geomorphological characterization of a filled abandoned meander using geophysical methods and soil sampling." *Geomorphology* 201 335-343.
- Hennig, Thomas. 2006. *Objektorientierte Fokussierung in der Geoelektrik. Dissertation*. Clausthal: Technische Universität Clausthal, Fakultät für Energie- und Wirtschaftswissenschaften.
- Hoffmann, Ruth, und Peter Dietrich. 2004. „An approach to determine equivalent solutions to the geoelectrical 2D inversion problem.“ *Journal of Applied Geophysics* 79-91.
- Hoyer, A.-S., F. Jorgensen, N. Foged, X. He, and A.V. Christiansen. 2015. "Three-dimensional geological modelling of AEM resistivity data - A comparison of three methods." *Journal of Applied Geophysics* 115 65-78.
- Hübner, R., K. Heller, T. Günther, and A. Kleber. 2015. "Monitoring hillslope moisture dynamics with surface ERT for enhancing spatial significance of hydrometric point measurements." *Hydrology and Earth System Sciences*, 19 225-240.
- Isachenko, A.G. 1980. *Methods of applied landscape studies. In Russian*. Leningrad: 1980.
- Juilleret, Jérôme, Jean Francois Iffly, Laurent Pfister, and Christophe Hissler. 2011. "Remarkable Pleistocene periglacial slope deposits in Luxembourg (Oesling): pedological implication and geosite potential." *Société des naturalistes luxembourgeois a.s.b.l.* 112 125 - 130.
- Kalinski, Robert, William E. Kelly, and Istvan Bogardi. 1993. "Combined Use of Geoelectric Sounding and Profiling to Quantify Aquifer Protection Properties. ." *Ground Water. Vol 31, No. 4* 538-544.

Bibliography

- Kirsch, Reinhard. 2006. *Groundwater Geophysics. A Tool for Hydrology. Second Edition*. Berlin Heidelberg: Springer-Verlag.
- Kistner, Irina. 2007. *Anwendung des Modells ANIMO zur Simulation des gelösten Phosphors im Oberflächenabfluss auf der Feldskala und der Phosphorverfügbarkeit im Oberboden auf der Einzugsgebietsskala*. Halle: Helmholtz Zentrum fuer Umweltforschung - UFZ. ISSN 1860-0387.
- Kleidon, A., and M. Renner. 2013a. "Thermodynamic limits of hydrologic cycling within the Earth system: concepts, estimates and implications." *Hydrology and Earth System Sciences* 17 2873-2892.
- Koch, Kristof, Jochen Wenninger, Stefan Uhlenbrook, and Mike Bonell. 2009. "Joint interpretation of hydrological and geophysical data: Electrical resistivity tomography results from a process hydrological research site in the Black Forest Mountains, Germany." *Hydrological processes* 1501-1513.
- Kulasova, Alena, Keith J. Beven, Sarka D. Blazkova, Daniela Rezacova, and Juri Cajthaml. 2014. "Comparison of saturated areas mapping methods in the Jizera Mountains, Czech Republic." *Journal of hydrology and hydromechanics*, 62 160-168.
- Leopold, Luna B., and Walter B. Langbein. 1962. "The concept of the Entropy in Landscape Evolution." *Theoretical papers in the hydrologic geomorphic sciences. Geological survey professional paper 500-A A1-A20*.
- Leopold, M., M.W. Williams, N. Caine, J. Völkel, and D. Dethier. 2011. "Internal Structures of the Green Lake 5 Rock Glacier, Colorado Front Range, USA." *Permafrost and Periglacial Processes* pp.706.
- Lyon, S.W., and P.A. Troch. 2007. "Hillslope subsurface flow similarity: Real-world tests of the hillslope Peclet number." *Water Resources Research*, Vol. 43, W07450, doi:10.1029/2006WR005323 1-9.
- Mamaj, I.I. 2013. *Landscape library (Evolution of Solncev's ideas in the modern landscape studies)*. University of Moscow, Department of geography. In Russian. Moscow-Smolensk: Ojkumena.
- Martinez-Carreras, Nuria, Andreas Krein, Francesc Gallart, Jean-Francois Iffly, Laurent Pfister, Lucien Hoffmann, and Philip N. Owens. 2010. "Assessment of different colour parameters for discriminating potential suspended sediment sources and provenance: A multi-scale study in Luxembourg." *Geomorphology* 118 118-129.
- Martini, Edoardo, Ute Wollschläger, Simon Kögler, Thorsten Behrens, Peter Dietrich, Frido Reinstorf, Karsten Schmidt, Markus Weiler, Ulrike Werban, and Steffen Zacharias. 2014. "Spatial and temporal dynamics of hillslope-scale soil moisture patterns: Characteristic states and transition mechanisms. In review. Original Research Articles." *Vadoze Zone Journal* 1-54.
- Maurer, T. 1997. *Physikalisch begründete, zeitkontinuierliche Modellierung des Wassertransports in kleinen ländlichen Einzugsgebieten*. PhD. Karlsruhe, Germany: Fakultät für Bauingenieur- und Vermessungswesen, Universität Karlsruhe (TH).

Bibliography

- Mauritsch, Hermann J., Wolfgang Seiberl, Ranier Arndt, Alexander Römer, Klaus Schneiderbauer, and Gernot P. Sendlhofer. 2000. "Geophysical investigations of large landslides in the Carnic Region of southern Austria." *Engineering Geology* 56 373-388.
- McCann, D.M., and A. Forster. 1990. "Reconnaissance geophysical methods in landslide investigations." *Engineering geology*, 29 59-78.
- McClymont, Alastair F., James W. Roy, Masaki Hayashi, Laurence R. Bentley, Hansruedi Maurer, and Greg Langston. 2011. "Investigating groundwater flow paths within proglacial moraine using multiple geophysical methods." *Journal of Hydrology* 399 57-69.
- McDonnell, J.J., M. Sivapalan, K. Vaché, S. Dunn, G. Grant, R. Haggerty, C. Hinz, et al. 2007. "Moving beyond heterogeneity and process complexity: A new vision for watershed hydrology." *Water Resources Research*, Vol. 43, W07301 1-6.
- Meju, Max A. 1995. "Simple effective resistivity-depth transformation for infield or real-time data processing." *Computer & Geosciences Vol. 21, No. 8* 985 - 992.
- Mele, M., R. Bersezio, and M. Giudici. 2012. "Hydrogeophysical imaging of alluvial aquifers: electrostratigraphic units in the quaternary Po alluvial plain (Italy)." *International Journal of Earth Sciences (Geological Rundschau)* 2005-2025.
- Mele, M., R. Bersezio, M. Giudici, E. Gavalli, and A. Zaja. 2013. "Resistivity imaging of Pleistocene alluvial aquifers in a contractional tectonic setting: A case history from the Po plain (Northern Italy)." *Journal of applied geophysics* 93 114-126.
- Meyer, P.D., and G.W. Gee. 1999. *Information on Hydrologic Conceptual Models, Parameters, Uncertainty Analysis, and Data Sources for Dose Assessments at Decommissioning Sites*. Technical, Washington: U.S. Nuclear Regulatory Commission Office of Nuclear Regulatory Research .
- Militzer, H., und F. Weber. 1987. *Angewandte Geophysik, Seismik*. Wien, New-York, Berlin: Springer.
- Muiuane, E.A., and L.B. Pedersen. 1999. "Automatic 1D interpretation of DC resistivity sounding data." *Journal of Applied Geophysics* 42 35-45.
- Nardis, R. de, E. Cardarelli, and M. Dobroka. 2005. "Quasi-2D hybrid joint inversion of seismic and geo-electric data." *Geophysical Prospecting*, 53 705-716.
- Nikolaev, V.A. 2006. *Landscape study. Tutorial and practical application. In Russian*. Moscow, Russia: Faculty of Geography, Moscow University.
- Niwas, Sri, and Muhammed Celik. 2012. "Equation estimation of porosity and hydraulic conductivity of Ruhrtal aquifer in Germany using near surface geophysics." *Journal of Applied Geophysics* 84 77-85.
- Olayinka, Abel I., and Ugur Yaramanci. 2000. "Assessment of the reliability of 2D inversion of apparent resistivity data." *Geophysical Prospecting*, 48 293-316.

Bibliography

- Ollesch, G., Y. Sukhanovski, I. Kistner, M. Rode, and R. Meissner. 2005. "Characterization and modelling of the spatial heterogeneity of snowmelt erosion." *Earth Surface Processes and Landforms* 30 198-211.
- Ollesch, Gregor, Irina Kistner, Ralph Meissner, and Karl-Erich Lindenschmidt. 2006. "Modelling of snowmelt erosion and sediment yield in a small low-mountain catchment in Germany." *Catena* 68 161-176.
- Otto, J.C., and O. Sass. 2006. "Comparing geophysical methods for talus slope investigations in the Turtmann valley (Swiss Alp)." *Geomorphology* 76 257-272.
- Pánek, Tomáš, Jan Hradecký, and Karel Silhán. 2008. "Application of electrical resistivity tomography (ERT) in the study of various types of slope deformations in anisotropic bedrock: case studies from the flysch carpathians." *Studia Geomorphologica Carpatho-Balcanica. Vol. XLII* 57-73.
- Pous, Jaume, Pilar Queralt, and Rene Chavez. 1996. "Lateral and topographic effects in geoelectric sounding." *Journal of Applied Geophysics* 237-248.
- Preobrazhensky, V.S. 1966. *Landscape studies. In Russian*. Moscow: Nauka.
- Reggiani, P., and T.H.M. Rientjes. 2005. "Flux parameterization in the representative elementary watershed approach: Application to a natural basin." *Water resources research, Vol. 41, W04013, doi:10.1029/2004WR003693* 1-18.
- Reggiani, Paolo, Murugesu Sivapalan, and S. Majid Hassanizadeh. 1998. „A unifying framework for watershed thermodynamics: balance equations for mass, momentum, energy and entropy, and the second law of thermodynamics.“ *Advances in Water Resources, Vol. 22, Nr. 4* 367-398.
- Rihani, Jehan F., Reed M. Maxwell, and Fotini K. Chow. 2010. "Coupling groundwater and land surface processes: Idealized simulations to identify effects of terrain and subsurface heterogeneity on land surface energy fluxes." *Water Resources Research, Vol. 46, W12523* 1-14.
- Riznichenko, G.V. 1946. *Geometrical Seismology of Stratified Media*. Transactions of the Institute for Theoretical Geophysics II.
- Robain, Henri, Yves Albouy, Michel Dabas, Marc Descloitres, Christian Camerlynck, Pierre Mechler, and Alain Tabbagh. 1999. "The location of infinite electrodes in pole-pole electrical surveys: consequences for 2D imaging." *Journal of Applied Geophysics* 41 313-333.
- Robinson, D. A., A. Binley, N. Crook, F. D. Day-Lewis, T. P. A. Ferre, V. J. S. Grauch, R. Knight, et al. 2008. "Advancing process-based watershed hydrological research using near-surface geophysics: a vision for, and review of, electrical and magnetic geophysical methods." *Hydrological processes* 3604-3635.
- Rumpf, M., U. Böniger, and J. Tronicke. 2012. "Refraction seismic to investigate a creeping hillslope in the Austrian Alps." *Engineering Geology* 151 37-46.
- Sandmeier, K.J. 1998-2009. *REFLEXW 5.0 manual*. Karlsruhe: www.sandmeier-geo.de.
- Semmel, Arno, and Birgit Terhorst. 2010. "The concept of the Pleistocene periglacial cover beds in central Europe: A review." *Quaternary International*. 222 120 - 128.

Bibliography

- Shahedi, K. 2008. *Hillslope hydrological modelling: the role of bedrock geometry and hillslope-stream interaction. PhD thesis*. Wageningen, The Netherlands: Wageningen University.
- Shannon, C.E. 1948. "A mathematical theory of communication." *The Bell system technical journal*, Vol. 27, July, October 379-423, 623-656.
- Solncev, B.N. 1981. *Landscape organisation as system.(Problems, methodology and theory. In Russian*. Moskow: Mysl.
- Solncev, N.I. 1948. *The native-geographical landscape and its mainly principles. T1. In Russian*. Moscow: Geografiz.
- Szalai, S., A. Koppán, K. Szokoli, and L. Szarka. 2013. "Geoelectric imaging properties of traditional arrays and of the optimized Stummer configuration." *Near Surface Geophysics*, 11 51-62.
- Telford, W. M., L. P. Geldart, und R. E. Sheriff. 1990. *Applied Geophysics, second edition*. Cambridge: Cambridge Univ. Press.
- Travelletti, J., P. Sailhac, J.-P. Malet, G. Grandjean, and J. Ponton. 2011. "Hydrological response of weathered clay-shale slopes: water infiltration monitoring with time-lapse electrical resistivity tomography." *Hydrological Processes*. 1-14.
- van Overmeeren, R.A. 2001. "Hagedoorn's plus-minus method: the beauty of simplicity." *Geophysical Prospecting*, 49 687-696.
- Vouillamoz, J.M., B. Chatenoux, F. Mathieu, J.M. Baltassat, and A. Legchenko. 2007. "Efficiency of joint use of MRS and VES to characterize coastal aquifer in Myanmar." *Journal of Applied Geophysics* 61 142-154.
- Wagener, T., M. Sivapalan, P.A. Troch, and R. Woods. 2007. "Catchment classification and hydrologic similarity." *Geography Compass*, 1 901-931.
- Weber, Michael, Georg Rumpker, and Dirk Gajewski. 2007. *Theory of Elastic Wave. The manuscript is based on lecture given by Gerhard Müller on the theory of elastic waves at the universities of Karlsruhe and Frankfurt*. Potsdam, Frankfurt, Hamburg: Universities of Potsdam, Frankfurt and Hamburg.
- Wienhöfer, J., and Erwin Zehe. 2014. "Predicting subsurface streamflow response of a forested hillslope - the role of connected flow paths." *Hydrology and Earth System Sciences*, 18 121-138.
- Woods, Ross A., Murugesu Sivapalan, and Justin S. Robinson. 1997. "Modelling the spatial variability of subsurface runoff using a topographic index." *Water Resources Research*, Vol. 33, No.5, May 1061-1073.
- Wrede, Sebastian, Fabricio Fenicia, Núria Martínez-Carreras, Jérôme Juilleret, Christophe Hissler, Andreas Krein, Hubert H. G. Savenije, Stefan Uhlenbrook, Dmitri Kavetski, and Laurent Pfister. 2014. "Towards more systematic perceptual model development: a case study using 3 Luxembourgish catchments." *Hydrological processes* 1-20.
- Yadav, G.S., P.N. Singh, and K.M. Strivastava. 1997. "Fast method of resistivity sounding for shallow groundwater investigations." *Journal of Applied Geophysics* 45-52.

Bibliography

- Zarroca, Mario, Joan Bach, Rogelio Linares, and Xavier M. Pellicer. 2011. "Electrical methods (VES and ERT) for identifying, mapping and monitoring different saline domains in a coastal plain region (Alt Empordà, Northern Spain)." *Journal of Hydrology* 409 407-422.
- Zehe, E., U. Ehret, L. Pfister, T. Blume, B. Schröder, M. Westhoff, C. Jackisch, et al. 2014. „HESS Opinions: From response units to functional units: a thermodynamic reinterpretation of the HRU concept to link spatial organization and functioning of intermediate scale catchments.“ *Hydrology and Earth System Sciences (HESS)*, 18 4635-4655.
- Zehe, Erwin, T. Maurer, J. Ihringer, and E. Plate. 2001. "Modeling water flow and mass transport in a Loess catchment." *Physics and Chemistry of the Earth Part B-Hydrology Oceans and Atmosphere*. 26(7/8). 487-507.
- Zehe, Erwin, Uwe Ehret, Therese Blume, Axel Kleindon, U. Scherer, and M. Westhoff. 2013. "A thermodynamic approach to link self-organisation, preferential flow and rainfall-runoff behaviour." *Hydrology and Earth System Sciences*, 17 4297-4322.

Appendix A

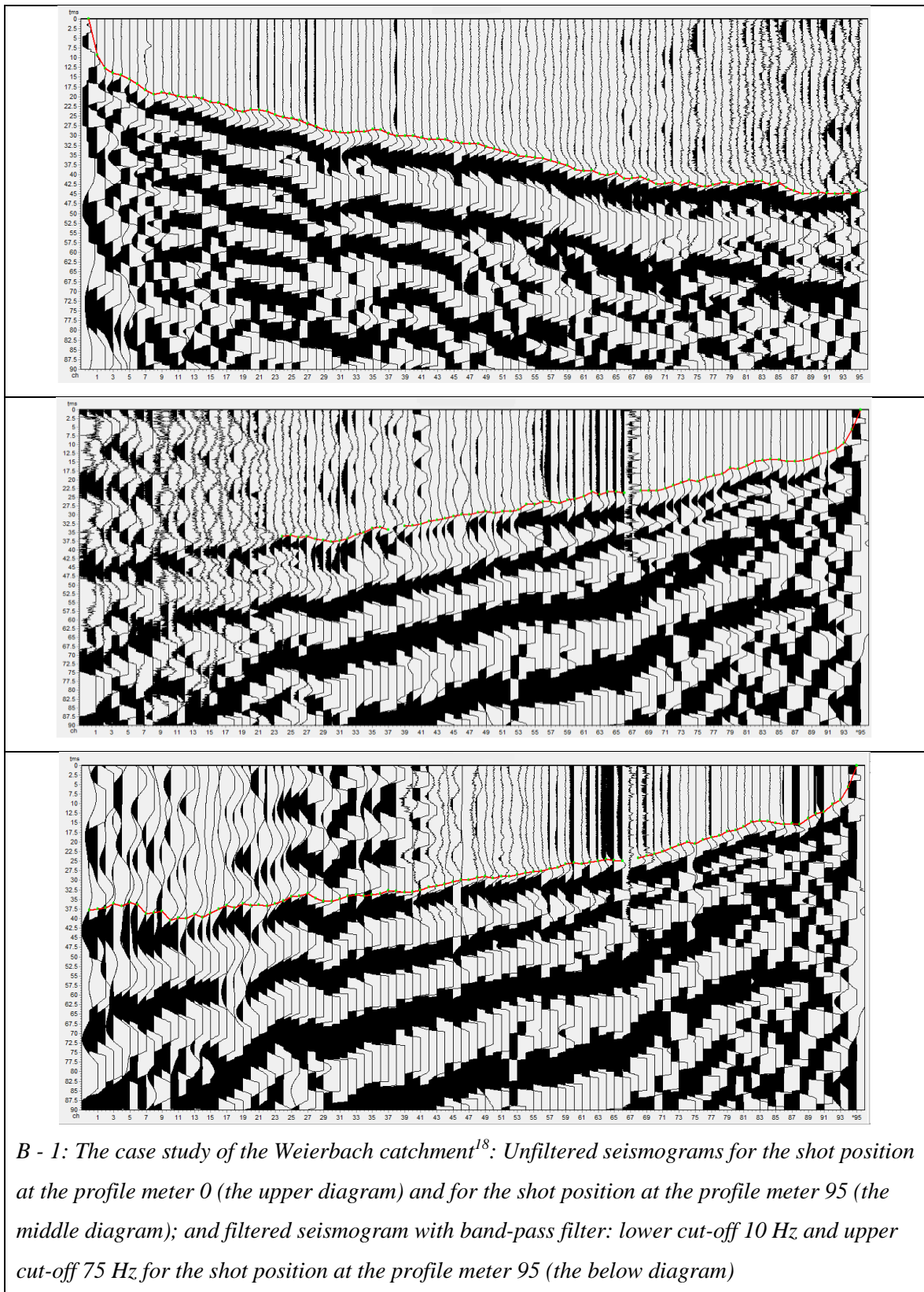
A - 1: The case study of the Weierbach catchment: RMS-fitting of the VES inversion

VES ID	Surface coordinates		Layer number	RMS [%]	Hillslope area unit
	X [m]	Z [m]			
VES_0	0	0	4	1.8	Homogeneous
VES_5	5	-1.846	4	3.03	
VES_10	10	-3.006	4	5.62	
VES_15	15	-4.504	4	6.38	
VES_20	20	-6.144	4	6.79	
VES_25	25	-8.07	4	3.86	
VES_30	30	-8.761	4	3.23	
VES_35	35	-10.245	4	1.03	
VES_40	40	-11.294	4	1.55	
VES_45	45	-12.137	4	3.91	
VES_50	50	-12.924	4	5.36	
VES_55	55	-13.777	4	4.18	
VES_60	60	-14.628	4	8.22	
VES_65	65	-15.623	4	3.74	Shallow heterogeneity
VES_70	70	-16.557	4	1.85	
VES_75	75	-17.745	4	4.67	
VES_80	80	-19.007	4	4.51	
VES_85	85	-20.391	4	6.62	
VES_90	90	-21.703	4	6.6	Homogeneous
VES_95	95	-23.029	4	7.89	
VES_100	100	-23.93	4	1.72	

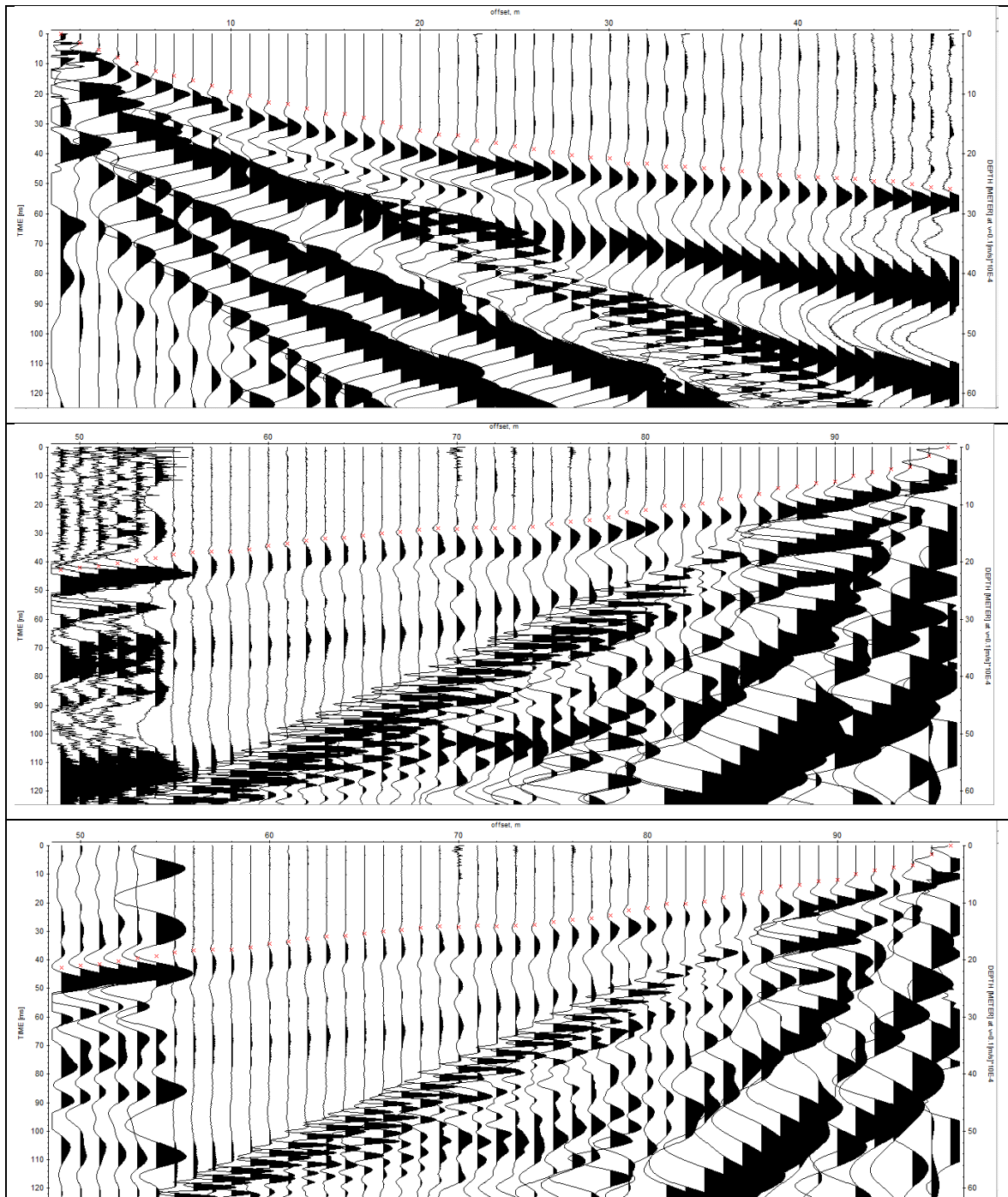
A - 2: The case study of the Schaefertal catchment: RMS-fitting of the VES inversion

VES ID	Surface coordinates		Layer number	RMS [%]	Hillslope area unit
	X [m]	Z [m]			
VES_0	0	0	4	1.84	Shallow heterogeneity
VES_5	5	-0.838	4	2.58	
VES_10	10	-1.407	4	1.76	
VES_15	15	-2.172	4	1.23	
VES_20	20	-2.911	4	1	
VES_25	25	-3.506	4	1.07	
VES_30	30	-4.083	4	1.75	
VES_35	35	-4.603	4	1.84	
VES_40	40	-5.132	4	1.13	
VES_45	45	-5.545	4	1.23	
VES_50	50	-6.1	4	1.72	
VES_55	55	-7.19	4	1.22	
VES_60	60	-7.851	3	1.43	
VES_65	65	-8.698	3	1.41	Homogeneous
VES_70	70	-9.45	3	1.77	
VES_75	75	-9.95	3	0.98	
VES_80	80	-10.293	2	2.74	
VES_85	85	-10.276	2	2.62	
VES_90	90	-10.15	2	3.27	
VES_95	95	-10.245	2	5.06	

Appendix B

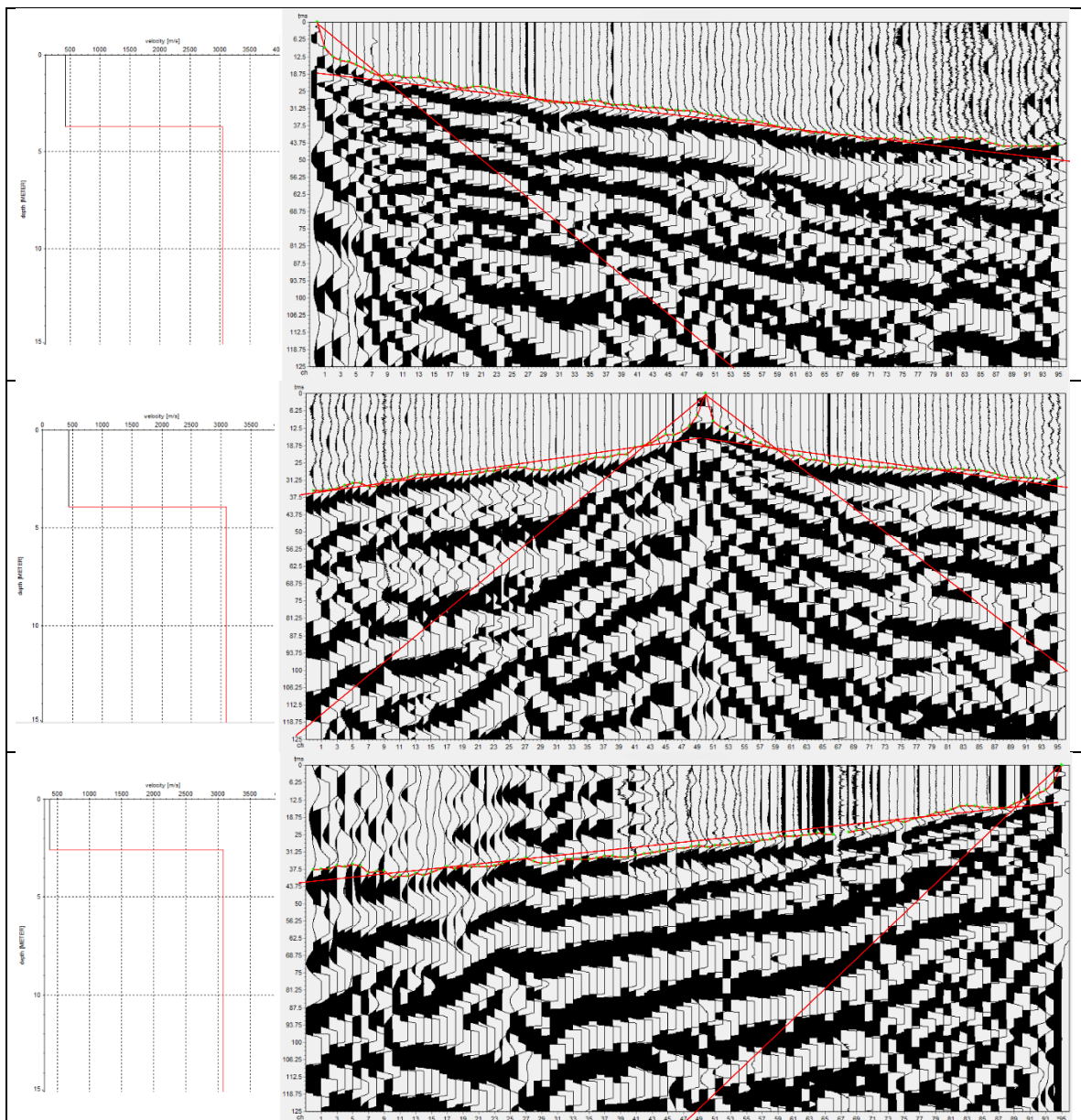


¹⁸ Seismograms for the Weierbach catchment were imaged in the program ZONDST2D (<http://zond-geo.ru>)



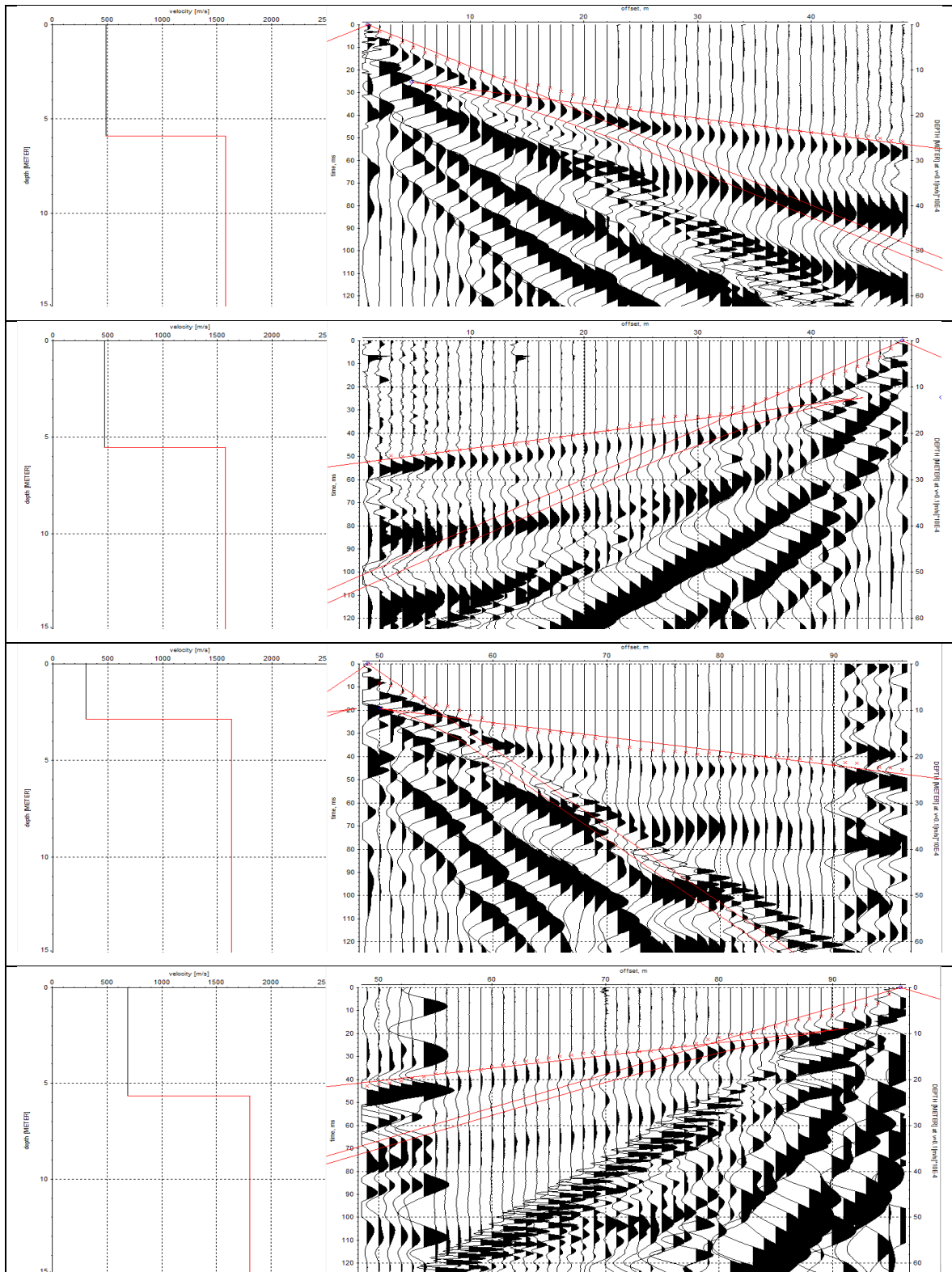
B - 2: The case study of the Schaefertal catchment: Unfiltered seismograms for the shot position at the profile meter 1 (the upper diagram) and for the shot position at the profile meter 96 (the middle diagram); and filtered seismogram with band-pass filter: lower cut-off 15 Hz and upper cut-off 120 Hz for the shot position at the profile meter 96 (the below diagram)

Appendix C



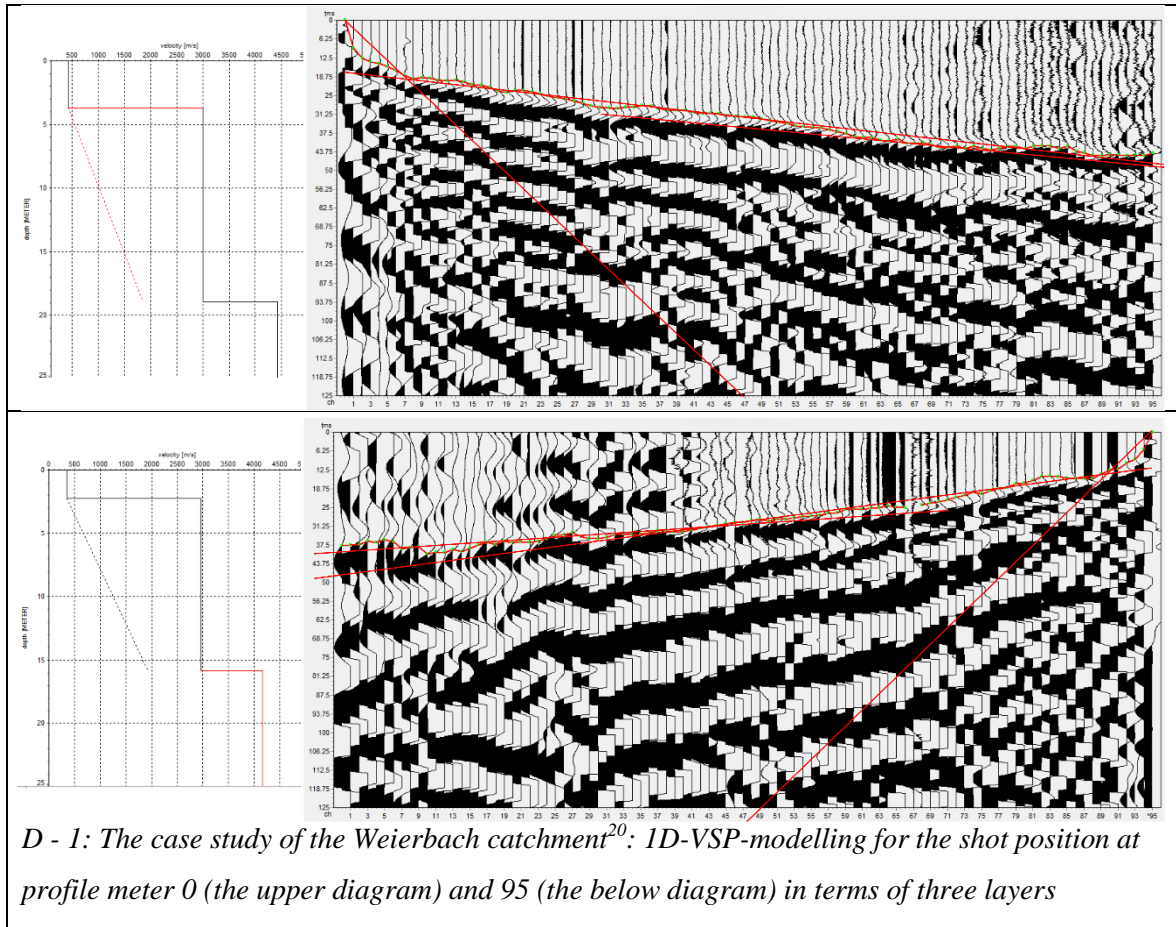
C - 1: The case study of the Weierbach catchment¹⁹: 1D-VSP-modelling for the shot position at profile meter 0 (the upper diagram), 50 (the middle diagram) and 95 (the below diagram) in terms of two layers

¹⁹ Seismograms for the Weierbach catchment were imaged in the program ZONDST2D (<http://zond-geo.ru>). 1D-VSP models were done in the program REFLEXW¹⁹ Version 6.0.9 (Sandmeier 1998-2009, <http://www.sandmeier-geo.de>)

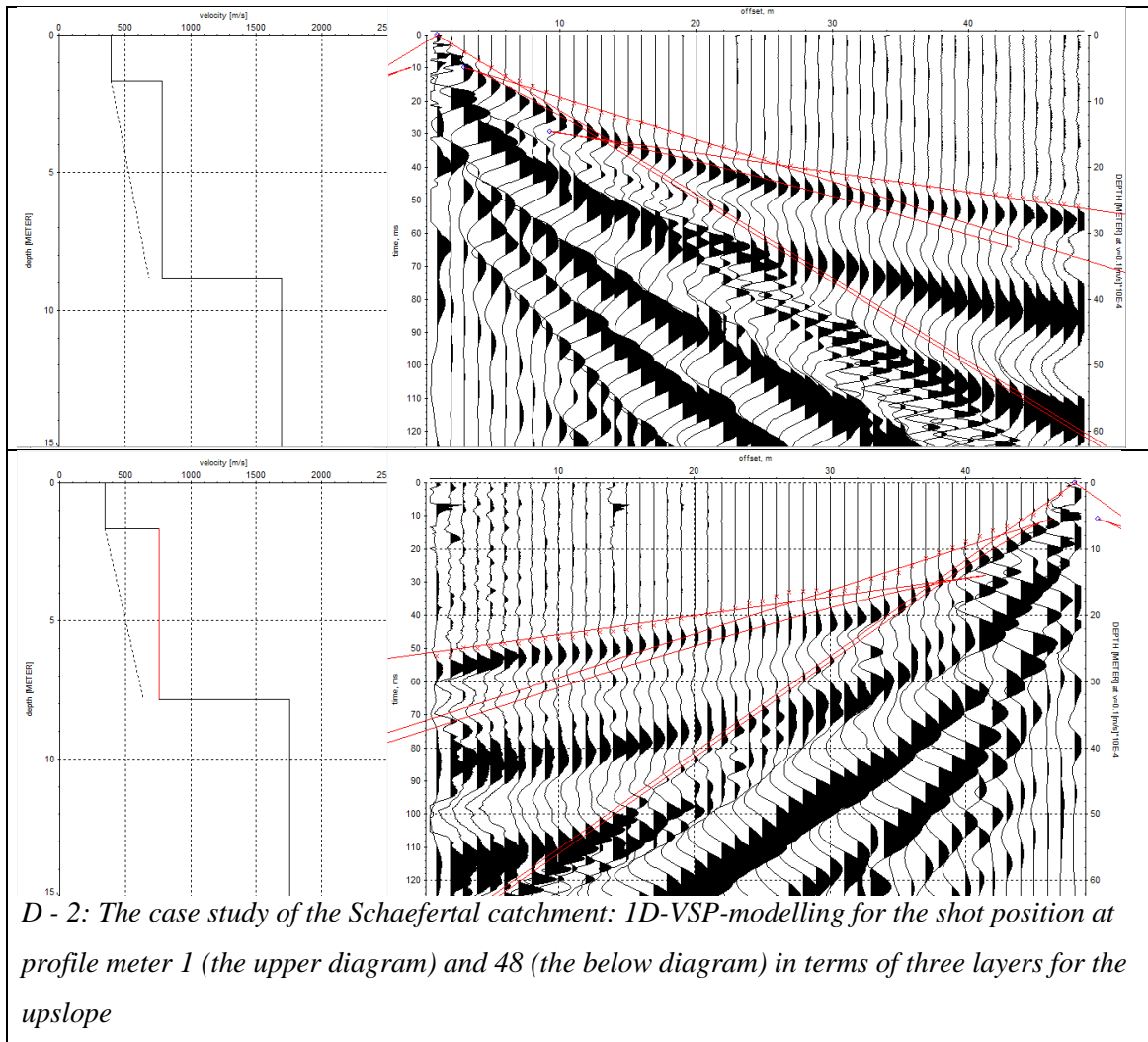


C - 2: The case study of the Schaeferal catchment: 1D-VSP-modelling for the shot position at profile meter 1 (the upper diagram), 48 and 49 (the middle diagrams), and 96 (the below diagram) in terms of two layers

Appendix D



²⁰ Seismograms for the Weierbach catchment were imaged in the program ZONDST2D (<http://zond-geo.ru>). 1D-VSP models were done in the program REFLEXW²⁰ Version 6.0.9 (Sandmeier 1998-2009, <http://www.sandmeier-geo.de>)



D - 2: The case study of the Schaeferfalta catchment: 1D-VSP-modelling for the shot position at profile meter 1 (the upper diagram) and 48 (the below diagram) in terms of three layers for the upslope

Appendix E



E - 1: The satellite image²¹ presents a possible geological-geomorphological 2D-feature at the Schaefertal study site

²¹ <http://www.bing.com/maps/>

Acknowledgments

This research monograph would not have been possible without the support of many people and funding sources. First of all I would like to thank my supervision committee Prof. Dr. Peter Dietrich and Prof. Dr. Erwin Appel for their support, patience, constructive critique and discussion. I especially want to thank Prof. Dr. Peter Dietrich for giving me the opportunity to join the multi-disciplinary CAOS²² project (Catchment As Organised Systems) and to become a member of his Department Monitoring and Exploration Technologies (MET) at the UFZ Leipzig.

This research was mainly supported by the National Research Fund of Luxembourg - FNR - and the National Research Fund of Germany - DFG (FOR 1598, ZE 533/9 - 1). Beyond this, Helmholtz Impulse and Networking Fund through Helmholtz Interdisciplinary Graduate School (HIGRADE) for Environmental Research kindly supported this work (Bissinger & Kolditz, 2008).

This field research would not have been a success without the help of many CAOS and MET colleagues. I especially would like to acknowledge the colleagues from the Centre de Recherche Public – Gabriel Lippmann: Dr. Laurent Pfister, Jean F. Iffly and Laurent Gourdol, and from the Helmholtz Centre for Environmental Research at UFZ Leipzig, MET: Dr. Ute Wollschläger for administrative supporting at the study site the Weierbach and Schaefertal catchment, respectively. Besides, I am also grateful to the Dr. Jörg Hausmann, Robert Nollau and Helko Kotas for the excellent supporting during the fieldwork. Moreover, many thanks go to the CAOS colleagues as well as PhD students for the kindly Mega field campaigns in Luxembourg, project meetings and workshops during the project phase of CAOS I. I also would like to thank MET colleagues as well as PhD students for friendship, general support and academic encouragement during the time at UFZ in Leipzig.

Additional, I acknowledge Tina Zeidler and Yulia Feskova for the abstract correction of language and stylistic in German and Russian, respectively.

Finally, I want to thank my family and my close, respectful friends for their support, love, patience and encouragement over years. Especial thanks go to my dear nieces (Zoja and Aglaja) and nephew (Anton), which gave me the mood in the difficult writing phases, to complete this thesis.

²² www.caos-project.de

Contribution

This dissertation includes data gathering by TERENO scientist (Thomas Grau, PhD student at Helmholtz Centre for Environmental Research – UFZ Leipzig) at the soil moisture hillslope in Schaeferthal. It concerns the data set of groundwater table with five wells collecting during the time from February 24, 2014 to February 26, 2014. The Figure 3-4 shows the data of the ground water table for the north-facing hillslope.

Affidavit

I, the undersigned Dipl.-Geophys. (KIT) Tatiana Feskova, affirm that my monograph dissertation with the title “System-oriented approach for catchment characterization in terms of typical landscape subunits based on the geophysical models” is result of my own work, and is done to the best of my information, knowledge, and belief. All sources and materials applied are listed and referenced in the dissertation.

I also affirm that this monograph dissertation has not been submitted as part of another examination processes.

Berlin,
Place,

30.06.2015
Date


Tatiana Feskova

Biographical sketch

Tatiana Feskova was born in Kaliningrad, in USSR/Russia, in 1978. After she graduated from the school in Kaliningrad in 1995, she started studying at the University of Kaliningrad in 1996 and received in 2001 the Diploma in Geography with minor in Oceanology. During her time at the University of Kaliningrad, she worked at Department of Oceanology in Kaliningrad and was interested in coast dynamics and landscape developing at the Baltic coast. She also studied intensively Russian landscape concepts. In October 2004, Tatiana began to study at Karlsruhe Institute of Technology (KIT) in Germany and received the Diploma degree in Geophysics focusing in Seismology and with minors Meteorology and Geodesy in 2010. During the time at KIT, she worked as the student assistance in the working group “Rock physics” and was interested in the simulation of elastic waves in heterogeneous media with ray tracing. After finishing her study at KIT, Tatiana worked in an engineer-geological office in Karlsruhe in the framework of a German-Russian project for preparation for Winter Olympic Game 2014 in Sochi where she improved knowledge and received experience in seismic data interpretation, especial hybrid seismic surveying. Tatiana also worked as research assistance in the Department of Applied Geoscience in working group “Structural geology” at KIT in Karlsruhe and gained her knowledge in Sweden Caledonian and geological mapping with the program ArcGIS. In March 2012, Tatiana began her PhD program in the framework of CAOS project (Catchment As Organised Systems) in the Department of Monitoring and Exploration Technologies at Helmholtz Centre for Environmental Research – UFZ Leipzig in the working group “System analysis and Geotechnics”. I have been PhD student in Department of Mathematic and Applied Geoscience at the Eberhard Karls University of Tübingen, in Germany since February 2015.